Regulation of neural differentiation in mouse embryonic stem cells using small molecules

This dissertation is submitted for the degree of

Doctor of philosophy at Cardiff University

Shun Ming Yuen

Supervisor:

Nicholas Allen

2013

Abstract

Embryonic stem (ES) cells are a potential source of neural derivatives that can be used in stem cell-based therapies. To generate specific cell types in a predictable manner, a detailed understanding of cell fate specification is required. To address this, this study employed mouse ES cells as a model to explore how neural identity was acquired and how regional identities were specified in ES cell-derived neural progenitor cells (NPCs).

Chemical inhibitors are more stable than recombinant proteins, hence they give more reproducible biological responses. This is crucial when generating specific cell types from ES cells for large-scale analysis. This study explored the effect of two newly discovered small molecule inhibitors of BMP signalling, dorsomorphin (DM) and LDN193189 (LDN) on the neural induction of ES cells, and compared their capabilities with those of recombinant noggin. Both DM and LDN treatments increased the expression of neural markers to levels that were comparable to that achieved by noggin treatment, suggesting that both LDN and DM can potentially substitute recombinant noggin in the generation of NPCs *in vitro*.

Retinoic acid (RA) is an important regulator of regional specification *in vivo*, but the underlying mechanisms for giving region-specific response are unclear. Here, early and late NPCs were exposed to RA at specific periods and were analysed for neural and positional markers. Results showed that region-specific responses were produced by RA at specific periods, indicating that NPCs display temporal changes in patterning responsiveness to morphogenic cues.

The ability of morphogens to impose positional response is lost in late cultures. Since Sox1 expression is associated with a naïve neural progenitor state and neural commitment, the expression of Sox1 was examined over time to test whether it was associated with the responsiveness to patterning cues. Both caudal and ventral markers were induced by RA and, because it plays an essential role in ventral patterning, Hedgehog (Hh) agonist purmorphamine respectively in early NPCs but not in late NPCs in both Sox1 positive and negative populations. This suggested that the expression of positional markers was not dependent on a temporally-defined Sox1 progenitor state.

Acknowledgements

To undertake research in this area of study is to be amazed and challenged by its complexity and beauty. I am so grateful for having been given the opportunity to do so within this department and under the direction of my supervisor, Nicholas Allen, who has provided assistance and guidance with this project since its conception.

The completion of much of the experimental work would not have been possible without the invaluable support of many. To Alysia Battersby and Susan Hunter for sharing their expertise in cell cultures; to Siân Rizzo and Katrin Buerger for their thoughtful help with PCR and immunocytochemistry analyses; to Ken Ewan for his unfailing technical skill with the Wst-1 and Beta-Glo assays; to Andrew Hollins for his insight into trouble-shooting Western blotting analyses and to Kirsty Richardson for her understanding of FACS analyses I express my most grateful thanks.

Submitting this thesis has been a social as well as a scientific experience. I am now privileged to count many past and present members of the laboratory as my friends. I must mention, João Bigares, Charlie Geater, Amanda Redfern, Rachel Steeg and Hsiu-Er Tsang: their kindness has done much to make my lab experience enjoyable. My special thanks go to Shona Joy, Susannah Williams, Sali Bagabir and Emma Cope for their constant encouragement. The patience shown to me by the office staff - Natalie Connor-Robson, Emma Davis, Jun Han, Rosalind John, Charmmy Lio, Owen Peters, Sophie Precious, Jitka Soukupova and Sophie Wang – as well as their practical advice – has benefited me enormously.

I would also like to express my gratitude for the encouragement received from people outside the department, especially to Phil and Angharad Ellis, Alice Chan, Shaunki Hettiarachchi and Jovita Wong. They have been such a help to me in meeting the various demands and challenges which are part and parcel, I suppose, of any lengthy period of research commitment.

Last but not least, I would like to thank all my family members back home for their love and loyalty throughout my study!

Abbreviations

AME	**anterior mesendoderm**
AMPK	**5' AMP-activated protein kinase**
ANOVA	**Analysis of variance**
AP	**Anterior-posterior**
APC	**Adenomatous polyoposis coli**
AVE	**Anterior visceral endoderm**
bHLH	**Basic helix-loop-helix**
BLBP	**Brain lipid binding protein**
BMP	**Bone morphogenetic protein**
bp	**Base pair**
BrdU	**Bromodeoxyuridine**
CDM	**Chemically defined medium**
Chd	**Chordin**
ChIP	**Chromatin immunoprecipitation**
Ci	**Cubitus interruptus**
CNS	**Central nervous system**
CRBP	**retinol-binding protein**
CRM	**Cis-regulatory modules**
DM	**Dorsomorphin**
DV	**Dorsal-ventral**
dpc	**Days post coitum**
E	**Embryonic day**
EB	**Embryoid bodies**
EC	**Embryonnic carcinoma**
EDTA	**Ethylene diamine tetra acetic acid**
EGF	**Epidermal growth factor**
Eomes	**Eomesodermin**
Erk1/2	**Extracellular signal-regulated kinase 1/2**
ES	**Embryoinic stem**
FBS	**Foetal bovine serum**
FGF	**Fibroblast growth factor**
FSC	**Forward scatter**

GABA	**Gamma-amino butyric acid**
GFAP	**Glial fibrillary acidic protein**
GFP	**Green fluorescent protein**
Gli	**Glioma-associated oncogene homolog**
GMP	**Good manufacturing practice**
GSK	**Glycogen synthase kinase**
Hh	**Hedgehog**
Hox	**Homeobox**
Id1	**Inhibitor of differentiation**
iPS	**Induced pluripotent stem**
KSR	**Knock-out serum replacement**
LDN	**LDN193189**
Lef	**Lymphocyte enhancer factor**
LGE	**Lateral ganglionic eminence**
LIF	**Leukaemia inhibitory factor**
MAPK	**mitogen-activated protein kinase**
MFI	**Geomtric mean fluorescent intensity**
MGE	**Medial ganglionic eminence**
Ngn	**Neurogenin**
Nog	**Noggin**
NPC	**Neural progenitor cell**
NSC	**Neural stem cell**
Oct4	**Octamer-binding protein 4**
PBS	**Phosphate buffered saline**
PFA	**Paraformaldehyde**
PI3 Kinase	**Phosphatidylinositol-3-ol kinase**
Ptc1	**Patch-1**
r	**rhombomere**
RA	**Retinoic acid**
RALDH2	**Retinaldehyde dehydrogenase 2**
RAR	**Retinoic acid receptor**
RARE	**Retinoic acid response element**
RoDH	**Retinol dehydrogenase**
RT-PCR	**Reverse transcription-polymerase chain reaction**

RXR	**Retinoid X receptor**
S.D.	**Standard derivation**
SFRP2	**Secreted frizzled-related protein-2**
SH2	**Src homology 2**
Shh	**Sonic hedgehog**
siRNA	**Small interfering RNA**
Smad	**Mothers against decapentaplegic homolog**
Smo	**Smoothened**
Sox	**SRY (sex-determining region Y) HMG box**
SSC	**Side scatter**
STAT	**Signal transducer and activator of transcription**
STEP	**striatal-enriched tyrosine phosphatase**
SVZ	**Subventricular zone**
Tcf	**T-cell factor**
TGFβ	**Transforming growth factor β**
TH	**Tyrosine hydroxylase**
Tnc	**Tenascin C**
VZ	**Ventricular zone**
Wnt	**Wingless**

CONTENT

LIST OF FIGURES

LIST OF TABLES

CHAPTER 1:

GENERAL INTRODUCTION

1.1 Background of stem cells

Recent decades have seen an upsurge in the field of stem cell research. It has captured the public imagination, awakening hopes of life-changing applications to previously untreatable medical conditions. Unsurprisingly, several definitions of stem cells have emerged. For the purposes of this thesis, however, stem cells are to be understood in broad terms as master cells which have yet to assume particular characteristics but which are capable of self-generation and of differentiation into a wide variety of cells as found in living organisms (McCulloch and Till, 2005, Friel et al., 2005). They are cells which, under suitable conditions, are able to play a part in generating more specific cell-types relevant, for example, to the healing or restoration of previously weakened or damaged tissue.

Embryonic stem (ES) cells, the particular focus of this study, are key to the generation of other cell types found in adult organisms. As their name suggests, ES cells have great potential: they are at a point where development into more functionally-specific cell types has not yet taken place, whereas adult stem cells can only give rise to a limited range of cell types associated with organs from which they originated. It is for this reason that they have proved such an attractive and fruitful field of research.

1.1.1 The discovery of embryonic stem cells

The identification of mouse ES cells was one of the most critical discoveries of the 20th century (Evans and Kaufman, 1981, Martin, 1981). It was based on an important finding that teratocarcinomas (gonadal tumours) possess a unique type of stem cell, embryonic carcinoma (EC) cells, that can generate all cell types found in teratocarcinomas when grafted to extra-uterine sites (Stevens, 1970, Solter et al., 1970). EC cells were found to be pluripotent and able to generate all cell types found in the three germ layers (ectoderm, endoderm and mesoderm) (Kleinsmith and Pierce, 1964, Martin and Evans, 1975) and can be

propagated in cultures (Martin and Evans, 1975). However, most EC cells are aneuploid. They are unable to produce gametes and produce tumours when injected into the mouse blastocysts (Papaioannou et al., 1978, Rossant and McBurney, 1982). These limitations therefore led to the development of ES cells, which were derived from the inner cell mass of mouse blastocyst-stage embryos (E3.5) (Evans and Kaufman, 1981, Martin, 1981). Like EC cells, ES cells are pluripotent (Doetschman et al., 1985) and self-renew. This means that they remain pluripotent after prolonged propagation (Fig. 1.1). In contrast to EC cells, they maintain a diploid karyotype (Evans and Kaufman, 1981), able to produce gametes in chimaeras and to integrate into embryos, producing normal, fertile chimeras (Bradley et al., 1984). The identification of these characteristics of ES cells was crucial: it formed the basis of our ability to genetically modify mice in order to study gene function.

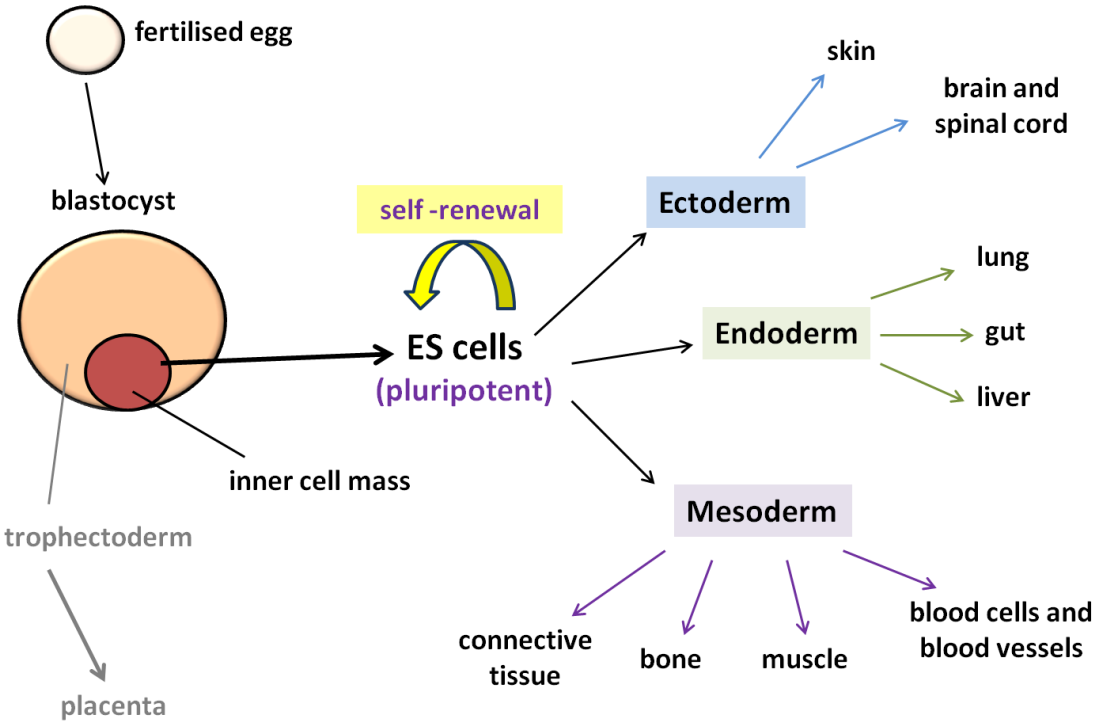

Figure 1.1 Lineages derived from mouse ES cells

The pluripotency of mouse ES cells means that they are responsive to the full range of developmental cues, giving rise to all cell types found in the three germ layers.

1.1.2 The use of mouse ES cells as a model to study neural development

Mouse ES cells were maintained on layers of mitotically inactivated mouse fibroblasts (also known as 'feeders') in fetal bovine serum (FBS) to provide trophic factors for the growth of ES cells (Evans and Kaufman, 1981). More recently other factors (e.g. BMP, LIF, 2i) (Ying et al., 2008, Ying et al., 2003a, Williams et al., 1988) have been identified (see Section 1.2) and have replaced these culturing conditions. In their absence, mouse ES cells differentiate into all the lineages that make up the adult animal (Solter, 2006). Primarily, ES cells will undergo neural specification in the absence of extrinsic factors (Smukler et al., 2006, Tropepe et al., 2001). The detection of this default neural pathway provided an important tool for our understanding of neural development *in vivo* through directing differentiation down specific neuronal lineages.

The directed neural differentiation of mouse ES cells, then, is the subject of this thesis. It seeks to analyse the mechanisms governing the process of neural specification and how neural progenitors behave following neural specification. This has been done by addressing three questions. Firstly, what is the effect of two newly discovered inhibitors, dorsomorphin (DM) and LDN 193189 (LDN) on the generation of neural progenitors (Chapter 3)? Secondly, how is the developmental potential in neural progenitors changed temporally (Chapter 4)? And finally, how relevant is the expression of a particular gene, Sox1, in determining the ability of stem cells to respond to developmental cues (Chapter 5). The relevance of these three lines of inquiry to the question of neural specification is described in Section 1.8.

The isolation of human ES cells from human blastocysts (Thomson et al., 1998) was another important step in stem cell history: it meant that the benefits of stem cell research were not limited to understanding embryonic development but could also be extended to therapeutic applications. They could be used to provide a source of cells that could be implanted into the nervous system to replace cells whose function is lost providing they

faithfully recapitulate the developmental programme that allows them to survive and fully integrate into the neural circuit (Price et al., 2011). Thus, they have opened up possibilities for tackling some currently incurable neurodegenerative diseases (e.g. Parkinson's disease) (Thomson et al., 1998). Furthermore, they can be directed to a particular phenotypes for disease modelling and for identifying new targets for drug screening (Eglen et al., 2008).

To develop ES cells for replacement therapy, ultimately we need to understand neural development using human ES cells. However, as an initial step, mouse ES cells provide an important tool and possess many benefits over human ES cells. The protocols relating to the cultivation of mouse ES cells are well established and do not raise any of the ethical issues which, in the minds of some, remain, and which are not overcome even by the use of existing human ES cell lines. Some of these issues, and problems arising from the rejection of tissue are now being addressed by the use of induced pluripotent stem (iPS) cells, which are produced by reprogramming adult fibroblast cells to an embryonic-like state using Oct4, Sox2, Klf4 and c-Myc (Takahashi and Yamanaka, 2006, Takahashi et al., 2007), mouse cell-based research still has much to offer. In practical terms, while the difference between the doubling times for undifferentiated mouse and human ES cells cannot be ignored, it is nevertheless not substantial (～16 hours for mouse ES cells and ～36 hours for human ES cells (Buecker et al., 2010). On the other hand, the doubling times for ES cell-derived neural stem cells are on a bigger time scale (～24 hours for mouse ESC-derived NSC and 5-10 days for human ESC-derived NSC) (Conti et al., 2005). Again, on a practical level, mouse ES cells can be maintained more effectively as they can be passaged as single cells by trypsin digest. Most human ES cell lines cannot grow from a single cell, and therefore they have to be passaged as small clumps of cells (Buecker et al., 2010). In addition, because they come from diverse sources (Thomson et al., 1998), human ES cell lines vary in the efficiency of their differentiation into particular lineages (Silva and Smith, 2008). Additionally, at the present moment, mouse ES cell research provides a more fully documented basis for research in

comparison to human ES cell research. The ready availability of resources like knock-out and knock-in reporter mouse ES cell lines, for example, has made gene function study more practicable. Fundamental to all of this is the fact that, within a range of prescribed limits, research on mouse ES cells offers a high degree of transferability to work on human ES and iPS cells.

1.2 Self-renewal of mouse ES cells

Once it was established that the use of mouse ES cells would provide a meaningful model for the analysis of neural specification, it became necessary to understand the interplay between extrinsic and intrinsic factors in the ES cells' capacity for self-renewal. It is on these factors that determine whether these cells remain self-renewing or undergo differentiation depends.

1.2.1 Extrinsic factor 1: the role of LIF in maintaining pluripotency of ES cells

Early ES cell work indicated that the undifferentiated state of ES cells was supported by a trophic factor produced by feeder cells. It was later discovered that the feeders could be replaced by conditioned media from buffalo-rat liver cells (Smith and Hooper, 1987). Subsequently, the critical factor that was found to be required for ES cells to remain undifferentiated was the leukaemia inhibitory factor (LIF) (Williams et al., 1988, Smith et al., 1988). ES cells that are grown in feeders that lack a functional LIF gene are unable to propagate effectively (Stewart et al., 1992). The effect of LIF is primarily mediated through the Janus kinases / signal transducer and activator of transcription 3 pathway (JAK/STAT3 pathway). Study has shown that LIF can also activate the phosphatidylinositol-3-ol kinase (PI3K)-Akt and mitogen-activated protein kinase (MAPK) pathways (Paling et al., 2004). For the JAK/STAT3 pathway, the binding of LIF with the receptor complex results in either the heterodimerisation of low-affinity LIF receptor (LIFRβ) and gp130 or the homodimerisation of the gp130 cell surface receptor complex (Nakamura et al., 1998). This then triggers the activation of Jaks and the subsequent tyrosine phosphorylation of LIFRβ and gp130, creating docking sites for Src homology 2 (SH2) domain-containing signalling molecules such as STAT1 and STAT3 (Stahl et al., 1995). In ES cells, only STAT3 but not STAT1 has an effect on self-renewal. This is because co-expression of wild-type STAT3 but not STAT1 can restore

self-renewal in ES cells that express a dominant negative form of STAT3 (Niwa et al., 1998). The STAT proteins are then phosphorylated by JAKS on their tyrosine residues, which then leads to their dimerization and translocation to the nucleus to regulate specific gene transcription (Darnell, 1997).

1.2.2 Extrinsic factor 2: the role of BMP in maintaining pluripotency of ES cells

Initially, it was thought that LIF alone can inhibit the differentiation of ES cells, but soon it was realised that culturing ES cells in LIF alone did not inhibit neural differentiation in serum-free conditions when ES cells were plated at high cell densities (Ying et al., 2003a). To prevent neural differentiation in such conditions, bone morphogenic protein 4 (BMP4) was introduced. Both BMP4 and serum acted through R-Smad to induce expression of the inhibitor of the differentiation gene (Id). It was found that the forced expression of Id genes enabled ES cells to self-renew in the absence of BMP or serum. Id proteins were seen to promote cell growth and prevent neural differentiation by inhibiting the action of basic helix-loop-helix (bHLH) transcription factors e.g. Neurogenin2 (Ngn2) (Miyazono and Miyazawa, 2002, Ying et al., 2003a). They had little or no effect on mesoderm and endoderm commitment. Therefore, it was deduced that BMP4 in isolation promoted the expression of endodermal and mesodermal genes, but that this expession was suppressed by LIF. This indicated that both STAT3 and the Id gene have to be activated to keep ES cells pluripotent. BMP4 did not increase STAT3 activity, and therefore there appeared to be no cross-regulation between the two pathways. The resultant activity seemed to be dependent on the existence of an appropriate balance between the input of both pathways (Ying et al., 2003a).

1.2.3 Extrinsic factor 3: the role of Wnt in maintaining pluripotency of ES cells

A further pathway was reported to facilitate pluripotency: Wnt signalling. Wnt proteins were observed to signal via the Frizzled receptor and destabilize the β-catenin degradation complex. This complex consists of Axin, adenomatous polyoposis coli (APC) and glycogen synthase kinase 3 (GSK3). The inhibition of GSK3 activity resulted in the translocation of β-catenin to the nucleus where it engages with DNA binding factors of the T-cell factor/ lymphocyte enhancer factor (Tcf/Lef) family to regulate the transcription of target genes (Reya and Clevers, 2005).

Stimulation with Wnt3a (Sato et al., 2004) and the pharmacological inhibition of GSK3 using BIO (Sato et al., 2004) or CHIRON99021 (Ying et al., 2008) were reported to maintain human and mouse ES cells in a pluripotent state. Furthermore, mouse ES cells responded to Wnt ligands (Wnt5a and Wnt6) produced by mouse feeder cells by upregulating STAT3 expression. Such expression is a downstream effector of LIF (Niwa et al., 1998). This indicated that the anti-differentiation effect of Wnt is partly due to the synergistic effect of JAK/STAT3 and Wnt signalling (Hao et al., 2006).

Further work was undertaken on the anti-differentiation effect of Wnt. It was seen to be explained by an upregulation of BMP4 expression - a result of the accumulation of active β-catenin in the nucleus. This accumulation had been induced by APC mutation or the overexpression of transgenic β-catenin. As a result, the number of ES cells committing to the neural lineage was reduced, as revealed by a decreased number of Sox1-expressing cells (Haegele et al., 2003). Conversely, inhibition of Wnt signalling by secreted Frizzled-related protein-2 (SFRP2) (Rattner et al., 1997) was shown to promote neural differentiation of ES cells (Aubert et al., 2002). Thus LIF, BMP4 and Wnts were all identified as being involved in regulating the pluripotency of ES cells.

1.2.4 Intrinsic factors: their role in determining pluripotency and lineage specification

It was identified that the pluripotency of ES cells is regulated by a network of transcription factors. The three most-studied intrinsic regulatory factors are: octamer-binding protein 4 (Oct4), SRY (sex-determining region Y) HMG box 2 (Sox2) and Nanog (Chambers and Smith, 2004, Niwa, 2007). The expression of some regulatory factors was understood to be influenced by the presence of extrinsic factors (Loh and Lim, 2011). For instance, the expression of Sox2 and Nanog is indirectly regulated by LIF through the JAK/STAT3 pathway and PI3-Akt pathway respectively (Niwa et al., 2009). Oct4 is not a direct downstream target of LIF or STAT3 (Matsuda et al., 1999), but its expression was shown to be maintained by Sox2 (Masui et al., 2007).

Customarily, it was held that each pluripotency factor inhibits ES cell differentiation by suppressing genes that are involved in cell differentiation (Silva and Smith, 2008). Although this model can explain how ES cells remain undifferentiated, it failed to account for the multilineage differentiating potential of ES cells (Loh and Lim, 2011). More recent findings showed that these intrinsic regulatory factors can also function as lineage specifiers in that they can direct the differentiation of pluripotent cells into specific lineages (Thomson et al., 2011). Oct4 promoted mesodermal differentiation (Niwa et al., 2000, Thomson et al., 2011), while Sox2 promoted neuroectodermal differentiation (Kopp et al., 2008, Thomson et al., 2011). Nanog directs endodermal differentiation in human ES cells by binding to and upregulating expression of the master gene that governs definitive endodermal differentiation, namely Eomesodermin (Eomes) (Teo et al., 2011). Nanog was found to block BMP-induced mesodermal differentiation by interacting with Smad1 (Suzuki et al., 2006). Since many different lineage specifiers with mutually exclusive lineages are expressed at the same time in ES cells, they have to inhibit each other's lineage-inducing activities in order to maintain pluripotency (Loh and Lim, 2011). For instance Oct4 represses neuroectodermal

differentiation by binding to a region of the promoter Sox2, and Sox2 represses the mesodermal lineage by binding to the promoter region of brachyury (Thomson et al., 2011). Therefore, the pluripotency of ES cells appeared to be safeguarded by maintaining equilibrium between the expression of pluripotency factors (Loh and Lim, 2011).

1.2.5 Extrinsic factor 4: FGF signalling in regulating lineage specification

Even when ES cells were undifferentiated, they continuously produced the differentiating signal fibroblast growth factor 4 (FGF4) (Kunath et al., 2007) under the influence of Oct4 and Sox2 (Yuan et al., 1995). This autocrine mechanism was seen to enable ES cells to respond to differentiating signals. $FGF4^{-/-}$ ES cells had a lower expression of early neural markers (Sox1 and nestin) and the neuronal marker β-III-tubulin than did wide-type ES cells (Kunath et al., 2007). Blocking FGFR using PD173074 (Mohammadi et al., 1998) inhibited the expression of the mesodermal marker Brachyury (Kunath et al., 2007). FGF4 signalled via the mitogen-activated protein kinase (Erk1/2) (Stavridis et al., 2007), and similar results were obtained in $Erk2^{-/-}$ ES cells. This indicated that cells that are deficient in Erk1/2 signalling are less effective in lineage commitment (Kunath et al., 2007). Therefore, inhibiting Erk1/2 signalling using 2i (SU5402 (Mohammadi et al., 1997) and PD184352 (Davies et al., 2000)) enhanced the expression of Oct4 and Nanog. Because of this Ying et al. proposed that extrinsic signals are dispensable for maintaining self-renewal in ES cells (Ying et al., 2008). However, their model failed to take into account that ES cells are also continuously producing BMP4 to support their own self-renewal (Ying et al., 2003a). Therefore it seemed that suppressing differentiating signals in itself is not enough to maintain self-renewal in ES cells (Loh and Lim, 2011).

1.3 Generation of neural progenitors and neuronal cells from ES cells

Section 1.2 has sought to outline what progress has been made in understanding the mechanisms which govern the pluripotency of ES cells. This provides an important context for considering advances made in developing new strategies for the generation of neural progenitors. There follows an account of a range of approaches which have come to play a part in these advances over the last two decades, later to be summarised as table 1.1.

1.3.1 Differentiating ES cells as embryoid bodies

The earliest method of initiating neural differentiation was to differentiate ES cells into what were known as either as floating spheres or, more commonly, embryoid bodies (EBs) (Doetschman et al., 1985). The central relevance of EBs to the study of the generation of neural progenitors lies, as their name implies, in the fact that they are capable of recapitulating embryonic development (ten Berge et al., 2008). Differentiating ES cells as EBs generated a variety of cell types (Zhuang et al., 1992). However, only a minority of cells showed neuron-like morphology. Later, it was discovered that the performance of EB cells in terms of producing neuron-characterised cells could be enhanced by treating EBs with retinoic acid (RA) (0.5 μM). Differentiated cells generated 38% of neuron-like cells in the presence of RA. They produced neuritic outgrowth, expressed β-III-tubulin and NF-M proteins and had voltage-gated K^+, Na^+ and Ca^{2+} channels (Bain et al., 1995). RA also suppressed the expression of mesodermal genes (brachyury, cardiac actin, and zeta-globin) (Bain et al., 1996).

A recent study revealed that a dual mechanism is at work when RA induces neural differentiation in ES cell cultures. It works by first stimulating Erk activity through rapid FGF8 induction while the expression of FGF4 is still high. At a point when cells acquire a primitive ectoderm-like state, RA inhibits Erk activity through the downregulation of FGF4. This was

confirmed by using a FGFR inhibitor (PD173074) (Mohammadi et al., 1998) which mimics the action of RA in promoting neural differentiation. Once ES cells have sufficient Erk signalling, it was noted that they cannot return to the undifferentiated ES state even when Erk signalling is inhibited (Stavridis et al., 2010).

1.3.2 Differentiating ES cells by co-culturing with stromal cells

Although differentiating ES cells as EBs using RA generated cells with neural character, it was difficult to analyse the regulatory steps involved in neural specification because EBs contain different kinds of cells including mesodermal and endormal cells (Maye et al., 2000). Additionally, RA itself is a strong teratogen (Soprano and Soprano, 1995), which might have unwanted side-effects when employed at non-physiological concentrations. Alternatives needed to be found. Other methods of differentiating ES cells in the absence of RA or serum were explored by co-culturing them on a monolayer of bone marrow-derived stromal cells (PA-6 cells). The active component of PA-6 cells is referred to as stromal cell-derived inducing activity (SDIA). Using this approach, neural progenitors were generated at over 90% efficiency, with no significant generation of mesodermal cells. A percentage of 30 ± 4% of TH-positive midbrain dopaminergic neurons was generated from β-III-tubulin positive neurons on day 12 by means of SDIA, while the percentage of neurons generated following the treatment of EBs with FGF8, Shh and ascorbate (33.9 ± 5.5%) was at a comparable level (Lee et al., 2000). Crucially, neurons induced by stromal cells were able to restore TH expression when transplanted into the mouse striatum treated with 6-hydroxydropamine (6-OHDA) for depleting dopaminergic projections (Kawasaki et al., 2000). It was also observed that SDIA only acts at an early stage of ES cell differentiation, because re-plating day 7-cultures which were Sox1-positive on laminin generated a number of TH positive neurons similar to that produced when cultures were plated on PA-6 cells (Parmar and Li,

2007). The disadvantage of this approach was that the molecular mechanisms involved in neurogenesis were unclear (Kawasaki et al., 2000).

1.3.3 Differentiating ES cells as adherent monolayer culture

Although differentiating ES cells as EBs had considerable value, nevertheless some limitations, especially in terms of heterogenicity and the reproducibility of results (Morshead et al., 2002) remained. These limitations, combined with the difficulties associated with co-culturing, as already described, underlined the desirability of an additional approach. Consequently, Ying and co-workers attempted to circumvent these problems by developing the adherent monolayer protocol (Ying et al., 2003b). In their approach, ES cells were differentiated on gelatin-coated plastic in the absence of serum and LIF in chemically defined medium (CDM) (N2B27). They generated 60% of Sox1-expressing cells, Sox1 being the earliest neural marker for neuroectoderm in mouse embryos (Pevny et al., 1998). The neurons generated were immunopositive for γ-aminobutyric acid (GABA) and TH from day 6 to day 8 of differentiation after replating on fibronectin-coated plates. Differentiating cells as monolayer had the advantage of the easy visualization and manipulation of cell colonies. More homogenous cell colonies could also be achieved because colonies had better exposure to growth factors (Ying et al., 2003b).

1.3.4 Differentiating ES cells using chemically defined medium (CDM)

Further steps to eliminate problems related to the consistency of results involved the use of chemcally defined medium (CDM). Early studies that had reported the use of RA in generating neurons with voltage-dependent channels were mainly performed in a serum-supplemented medium (Strubing et al., 1995, Fraichard et al., 1995). Although a serum-supplemented medium produced functional neurons, serum contains a variety of poorly-characterised factors that made it difficult to analyse the growth factors involved in the neural conversion process (Wiles and Johansson, 1999). In order to have full control over the generation of specific neurons it was necessary to develop protocols that could direct the neural differentiation of ES cells in a defined way. Differentiating ES cells in serum-free CDM proved to be a better alternative than serum-supplemented medium because all the components in CDM are defined (Bouhon et al., 2005).

The first study on the use of CDM reported that cells differentiated as EBs showed a 10-fold increase in the neuroectodermal marker Pax6 after 5 days and no expression of mesodermal marker brachury (Wiles and Johansson, 1999). Ying et al. used the first commercially available serum-free supplement B27 and developed a variant forumation (N2B27) to differentiate ES cells as adherent cultures and generated neuronal and glial cells (Ying et al., 2003b) (see section 1.3.3). After that, Bouhon et al. reported differentiating ES cells as EBs using a different formulation (DMEM/F12). This showed that cells expressed early neural markers (nestin, RC2 and Sox1) on day 4. Replating cells on laminin-coated coverslips on day 8 generated β-III-tubulin positive cells after 4 days of differentiation. Only a minority of cells expressed astrocyte marker (GFAP) and oligodendrocyte marker (NG2) on day 14. No non-neural lineage marker such as muscle marker desmin or epithelial marker pan-cytokeratin was detected which showed that cells were mostly directed towards the neural lineage (Bouhon et al., 2005).

Differentiation method	Results	Reference
Embryoid bodies (EB)	Differentiated cells generated 38 % of neuron-like cells in the presence of RA. They produced neuritic outgrowth, , expressed β-III-tubulin and NF-M proteins and had voltage-gated K^+, Na^+ and Ca^{2+} channels	(Bain et al., 1995)
Differentiation of EBs in CDM	10-fold increase of Pax6 expression was observed on day 5 of differentation with undetectable Brachury expression	(Wiles and Johansson, 1999)
Co-culturing ES cells with stromal cells	30% of TH-positive midbrain dopaminergic neurons were generated from day 12 to day 14	(Kawasaki et al., 2000)
Adherent monoculture	Cells generated 60% of Sox1 positive cells on day 4 of differentiation, and were immunopositive for β-III-tubulin , γ-aminobutyric acid (GABA) and TH from day 6 to day 8	(Ying et al., 2003b)

Table 1.1 Strategies developed for directing neural differentiation of mouse ES cells.

1.4 Inhibition of BMP signalling in neural specification

This development of CDM-based neural differentiation protocols was vital. It made possible the analysis of the signals involved in converting ES cells to neural progenitor cells. A central requirement in understanding this process has been the study of the role of BMP inhibition in neural induction. There follows an account of the stages involved in that study.

1.4.1 Neural induction: the default model

The investigation of what drives neural induction *in vivo* began in the 1920s through the work of Hans Spemann and his student Hilde Mangold. They discovered that when the dorsal lip of the bastopore (the opening formed during gastrulation by the invagination of cells to form the mesoderm and endoderm) was transplanted into the ventral mesoderm of a gastrula- stage Salamander embryo, then a second body axis is formed. This axis led to the generation of almost all of the central nervous system (except the floor plate) (Spemann and Mangold, 1924). Since the second body axis was derived from the host and not from the donor tissue, this led to a hypothesis that the dorsal lip of the blastopore (otherwise known as the 'organizer') is a region that releases neural inducing signals. Soon after, regions that have similar functions as the organizer were found in other vertebrates: Hensen's node in chicks (Waddington, 1933) and the node in mammals (Waddington, 1936).

The discovery of organizer was followed by decades of research to identify the molecules responsible for inducing neural development. Further progress was made in the late 1980s. It was discovered that when the *Xenopus* gastrula animal cap explant was cultured in isolation, it gave rise to epidermis. However, if the animal cap was split up into into single cells, they became neural tissue (Grunz and Tacke, 1989). It was then observed that overexpressing a dominant negative transforming growth factor β (TGF-β) receptor (Activin receptor) in the animal cap generated ectopic neural tissue (Hemmati-Brivanlou and

Melton, 1994), indicating that a TGF-β-related signal is involved in inhibiting neural specification. Subsequently, this signal was identified as BMP, on the basis that even a very low dose of BMP4 can convert dispersed animal cap cells back into epidermis (Wilson and Hemmati-Brivanlou, 1995). Later, it was found that genes expressed in the organizer including noggin (Lamb et al., 1993, Smith and Harland, 1992, Smith et al., 1993), follistatin (Hemmati-Brivanlou and Melton, 1994) and chordin (Sasai et al., 1994) are BMP inhibitors and can convert ectoderm into neural tissue. These findings led to the development of what was known as the 'default model of neural induction'. This proposed that in the absence of BMP signalling. Uncommitted ectodermal cells acquire neural identity by default. On the other hand, If BMP signalling is active, ectodermal cells are prevented from forming neuroectoderm and instead become epidermis (Hemmati-Brivanlou and Melton, 1997).

1.4.2 The use of BMP inhibitors in generating neural progenitors from ES cells

Active BMP signalling does not only prevent neural specification in ecotodermal cells (see section 1.4.1). It also has the effect of maintaining self-renewal in ES cells by preventing neural differentiation (Ying et al., 2003a) (see section 1.2.2). Therefore, in order to initiate neural differentiation in ES cell cultures, BMP signalling would need to be inhibited.

The generation of particular neural and neuronal subtypes from ES cells is influenced by the introduction of exogeneous factors. Historically, neural specification has been facilitated by using recombinant proteins. But they have disadvantages: a short shelf-life, high cost, and instability (Burton et al., 2010). Therefore, the potential for the use of modulators which are chemically based has attracted much attention. They are stable, cost-effective and consistent. They can therefore be used to generate large, homogenous populations of ES cell-derived neural progenitors for drug screening studies and cell-based therapy for neurodegenerative diseases (Hong and Yu, 2009).

Dorosmorphin (DM) (6- [4- (2-Piperidin-1-ylethoxy) phenyl] -3-pyridin-4-ylpyrazolo [1,5-a] pyrimidine), is also referred to as compound C. It acts as an inhibitor of AMP activated protein kinase (AMPK) (Zhou et al., 2001). It has been reported to inhibit PI3K and p38 MAPK phosphorylation and NFκB activity in human umbilical vein endothelial cells in an AMPK-independent manner (Kim et al., 2011). But, significantly, it has also been identified for its BMP inhibition function. It was recently found to be an inhibitor of the BMP signalling pathway when a phenotypic screen was used to identify compounds that disrupt the formation of the zebrafish dorsoventral axis. DM specifically inhibits BMP type I receptors and blocks BMP mediated Smad1/5/8 phosphorylation but not MAPK p38 phosphorylation. Noggin, conversely, blocks the activation of both pathways in cultured mouse pulmonary artery smooth muscle cells (Yu et al., 2008). The use of DM thus could provide a useful tool for studying the effect of BMP inhibition on neural induction in ES cell cultures.

Because of the off-target effects observed in DM, it was necessary to design a more specific compound. LDN193189 (LDN) (4- (6- (4- (piperazin-1-yl) phenyl) pyrazolo [1,5-a] pyrimidin-3-yl) quinoline hydrochloride) is a more recently discovered small molecule for inhibiting the BMP pathway. It is produced by replacing the pendent-4-pyridine ring with 4-quinoline (Cuny et al., 2008), and is a more effective tool than DM as it can be used more specifically in the precise study of BMP inhibition in ES cells (Vogt et al., 2011).

1.4.3 The activity of BMP inhibitors in the BMP signalling pathway

The way in which BMPs can be controlled within the process of neural induction needs to be properly understood. BMPs comprise the largest group of the TGFβ superfamily of extracellular signalling molecules (Wozney and Rosen, 1998). During active BMP signalling, BMPs signal through type I and II receptors, each of which contains serine/threonine kinase at their C-termini. The binding of BMPs stabilises type I and type II receptor interaction and permits efficient transphophorylation of the type I receptor by the type II receptor. Active type I receptor kinase domain then phosphorylates cytoplasmically localised BMP-responsive effectors. Receptor- associated Smads (R-Smads) including Smads 1, Smad5 and Smad8 then bind to Co-Smad (also known as Smad4). The co-Smad-R-smad protein complex then translocates to the nucleus and binds to DNA to regulate gene expressions (Chen et al., 2004, Blitz and Cho, 2009)

The BMP antagonists, noggin and chordin, inhibit BMP signalling by binding to BMP ligands and prevent them from binding to their receptors (Sasai and DeRobertis, 1997). On the other hand, DM and LDN antagonise BMP signalling by inhibiting the function of BMP receptor type I. This findng is based on the evidence that the phosphorylation of Smad 1/5/8 can be inhibited by DM in cells transfected with constitutively active forms of BMP type I receptors (Alk2, Alk3 and Alk6) (Yu et al., 2008). A schematic illustration of the BMP pathway can be found in Fig 1.2.

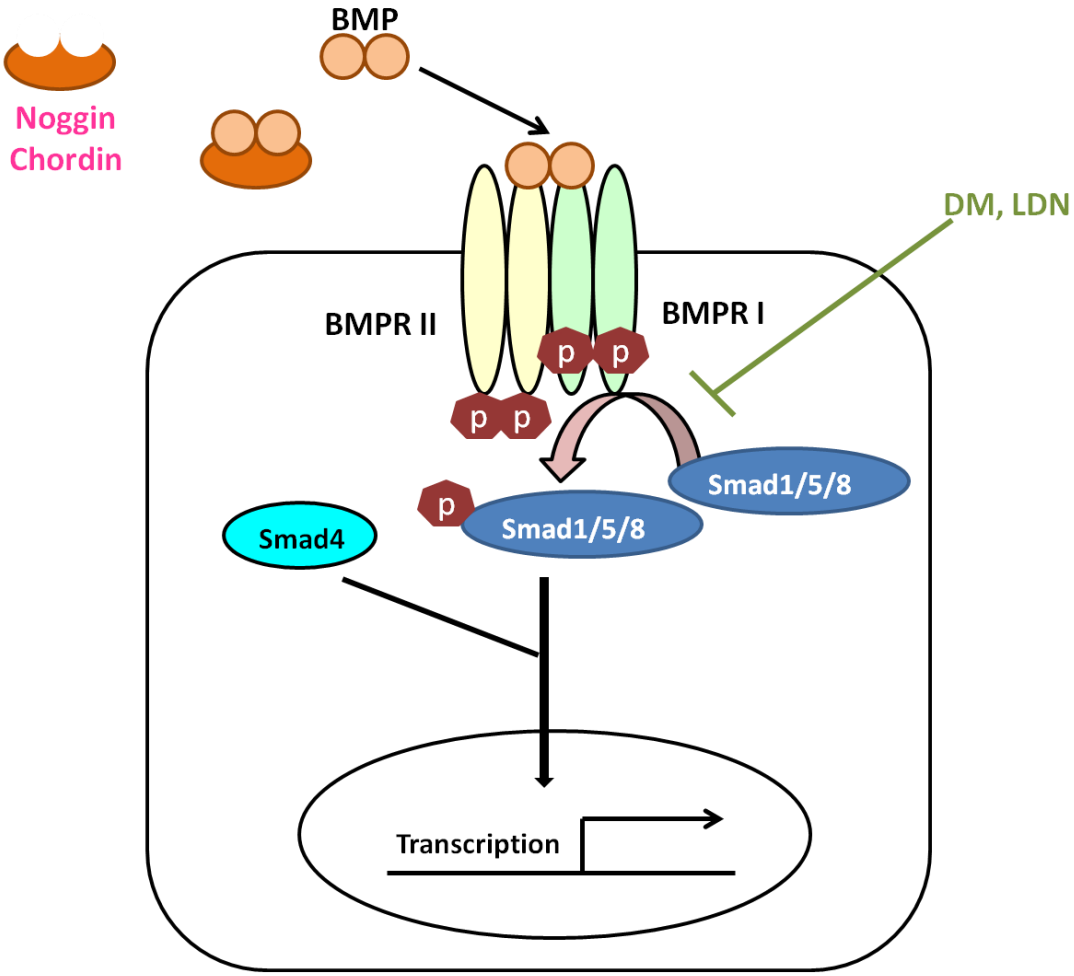

Figure 1.2 The BMP signalling pathway

Binding of BMP ligand causes homomeric or heteromeric dimerization of BMP receptors, which then phosphorylates Smad 1/5/8. They bind to Smad4 (co-Smad) to form a complex, which then enters into the nucleus to activate transcription of target genes. This signalling pathway can be further modulated by BMP inhibitors (e.g. noggin and chordin) which prevent the BMP ligands from binding to the receptors or DM and LDN which inhibit BMP receptor I (Chen et al., 2004, Yu et al., 2008).

1.5 Regional specification *in vivo*

This study is concerned with the question of the regulation of regional specification in ES cells. This section, therefore, offers an anatomically-related framework for the later discussion of how structures are developed.

After neural induction, the ectodermal cells are committed to become neuroectoderm. The earliest neural tissue is believed to be anterior in character and is associated with the forebrain. This is based on evidence that the expression of Otx2 is observed throughout the epiblast (formed shortly after the mouse embryo implants into the mother) during pre-streak stage (E6.0) and is restricted to the anterior part of the embryo between early- and late-streak stages (E6.5 to E7.5) (Ang et al., 1994). The anterior character is maintained by signals released from four regions: the anterior visceral endoderm (AVE), the node, the gastrula organiser and the anterior mesendoderm (AME). The AVE expresses Lefty (a Nodal inhibitor) and Cerberus (a combined BMP and Wnt inhibitor) to inhibit posteriorizing signals (Belo et al., 1997, Meno et al., 1997). The node and the gastrula organiser (the predecessor of the node) release noggin and chordin (Bachiller et al., 2000, Kinder et al., 2001) to induce the development of anterior neural tissue. The posterior neural tissue is induced by posteriorizing signals such as RA which is synthesized by Raldh2 expressed in the node (Ribes et al., 2009) to form more posterior structures including midbrain, hindbrain and spinal cord (Durston et al., 1989). By E7.5, the neuroectoderm is thickened and forms the neural plate. The neural plate folds inward to form the neural groove, rolls up and joins dorsally to form the neural tube in a process of neurulation (E8.5). The AME (which is a derivative of the node) that lies underneath the neural tube releases chordin and noggin for the maintainenance of the forebrain character (Anderson et al., 2002). The overall body plan of an organism is illustrated in Fig 1.3. A summary of the development of the mouse nervous system from E6.0 to E8.5 is given in Fig. 1.4.

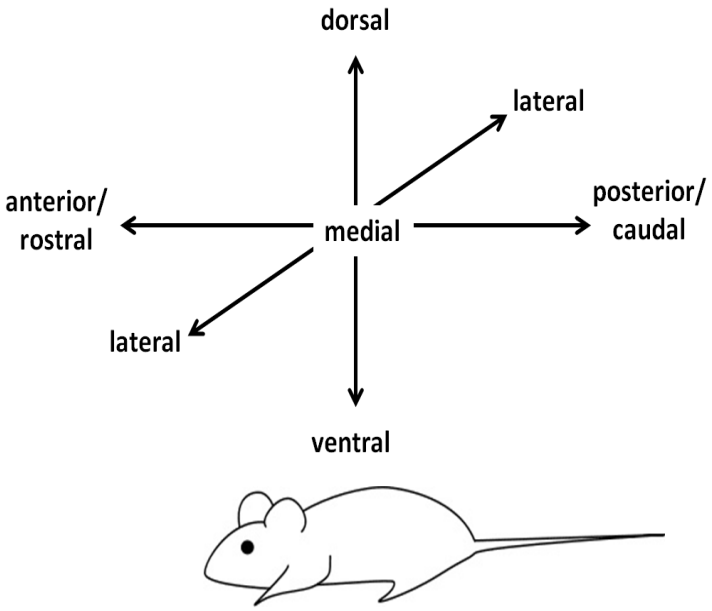

Figure 1.3 Anatomical terms used to describe locations in embryos

Anatomical terms are used to describe how different parts of developing organisms are located relative to each other. The end of an embryo where the head is found is referred as anterior, and its opposite end is referred as posterior. Anterior can also be described as rostral and posterior can be described as caudal. The axis running through from the anterior end to the posterior end is referred as the anteroposterior (AP) axis. The axis that runs perpendicular to the AP axis is called the dorsoventral (DV) axis. It runs from the dorsal side (the back where the spinal cord develops) to the ventral side (the side towards the chest). The remaining axis runs from medial (towards the midline) to lateral (away from the midline) and is perpendicular to the AV and DV axes (Price et al., 2011).

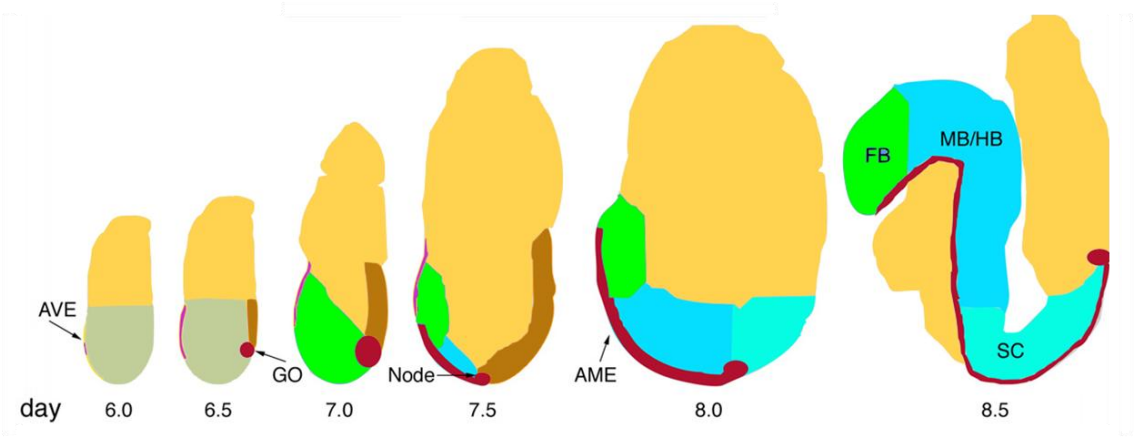

Figure 1.4 Neural induction and regional specification in the mouse embryo from day 6.0 to day 8.5

The epiblast (grey) is formed shortly after the mouse embryo is implanted into the mother. It exists in a pre-anterior state from E6.0 to E6.5. The anterior visceral endoderm (AVE) (purple) is formed at the anterior region of the epiblast and releases signals that antagonise posterior signals. When gastrulation begins (E6.5), the posterior end of the embryo forms the primitive streak (brown) which expresses posteriorizing signals including Wnts, Nodal and FGFs. The early gastrular organiser (GO) (maroon) is formed at the anterior end of the primitive streak and is responsible for inducing anterior neural development. By mid-streak stage (E7.0), the anterior neural precursors (green) shift towards the anterior region and lie side-by-side with the AVE. The node formed at late-streak stage (E7.5) is responsible for releasing both anteriorising and posteriorizing signals. By E8.5, and the neural tube is now specified into the forebrain (FB), midbrain (MB), hindbrain (HB) and spinal cord. The anterior mesoendoderm (AME) is formed underneath the neural tissue for its maintenance. This diagram (Levine and Brivanlou, 2007) has been adapted and is not drawn to scale.

Distinct neuronal subtypes are generated from discrete progenitor domains along the neural tube. The neural progenitor domains are characterized by restricted expression of transcription factors (Campbell, 2003). It is the unique combination of these transcription factors that determines the spatial organisation and specification of a neuronal subtype (Price et al., 2011, Allen, 2008). The expression domains of some of these transcription factors in the forebrain, hindbrain and spinal cord are described below.

1.5.1 Organisation of telencephalic progenitors

The telencephalon, the most rostral region of the forebrain, can be divided into the pallium (or dorsal telencephalon) and the subpallium (ventral telencephalon) (Wilson et al., 2000). The pallium develops into cerebral cortex while the subpallium develops into basal ganglia which includes the striatum and the globus pallidus (Gerfen, 1992). Distinct populations of neurons of the basal ganglia come from ganglionic eminences of the subpallium including the medial ganglioinic eminence (MGE) and lateral ganglinoic eminence (LGE) (Sousa and Fishell, 2010).

The expression of Foxg1 was found in the telencephalic epithelium (Xuan et al., 1995). The neuroepithelium of the cortex was observed to express Pax6 (Stoykova and Gruss, 1994), whereas that of the subpallium (especially in the LGE) expresses Gsh2 (Hsieh-Li et al., 1995, Toresson et al., 2000) . Nkx2.1 is specifically expressed in the MGE, but not in the LGE (Sussel et al., 1999). Early-born neurons derived from the pallium expressed Tbr1 (Bulfone et al., 1995), whereas neurons derived from the subpallium express Dlx2 (Bulfone et al., 1993, Porteus et al., 1994, Anderson et al., 1997, Long et al., 2009). Ngn2 and Mash1 are bHLH transcription factors that regulate neurogenesis in the pallium and subpallium respectively (Nieto et al., 2001, Casarosa et al., 1999). The majority of subpallium-derived neurons are GABAergic (Stuhmer et al., 2002) whereas those derived from the pallium are glutamatergic (Hevner et al., 2001).

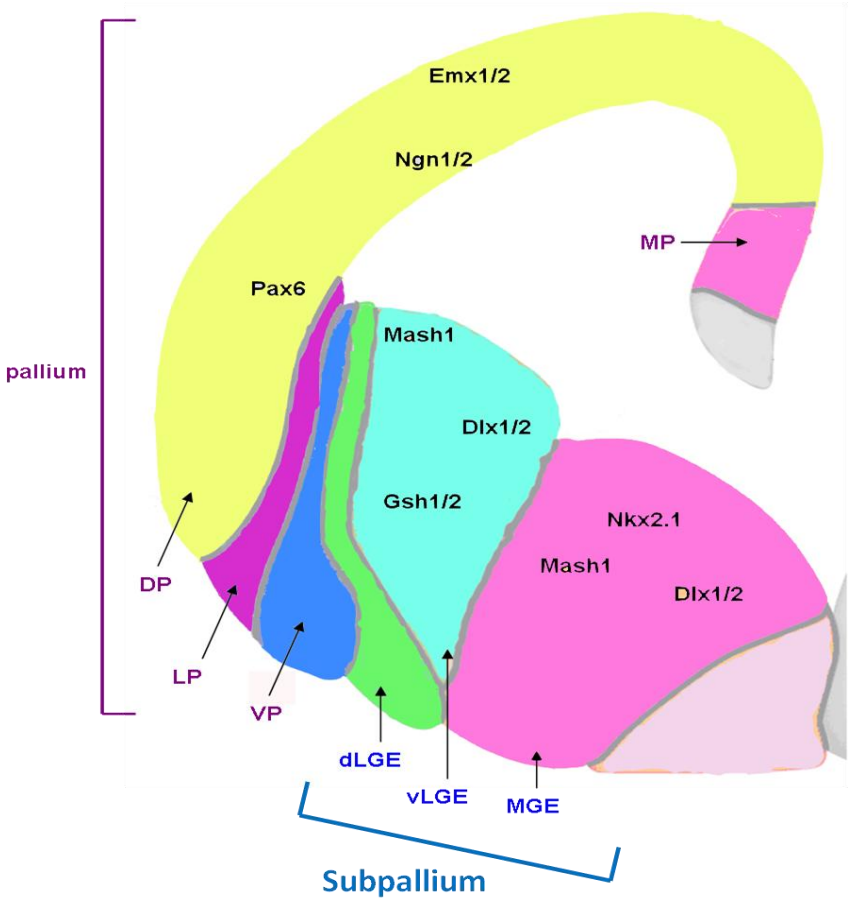

Figure 1.5 Schematic coronal section through the telencephalic vesicles at E14

Expression domains of dorsal telencephalic progenitor (Emx1/2, Ngn1/2 and Pax6) and ventral telencehaplic subdomains (Mash1, Dlx1/2, Gsh1/2 and Nkx2.1) are shown. Morphologically defined structures in the pallium and subpallium were labelled in purple and blue respectively. dLGE, dorsal LGE; DP, dorsal pallium; LP, lateral pallium; MP, medial pallium; vLGE, ventral LGE; VP, ventral pallium. Figure has been adapted (Schuurmans and Guillemot, 2002, Wilson and Rubenstein, 2000).

1.5.2 Specification of hindbrain rhombomeric progenitors

As hindbrain structure differs from that of the forebrain, hindbrain patterning merits separate discussion. The vertebrate hindbrain is patterned via the generation of eight neuroepithelial compartments called 'rhombomere' (r). Distinct neuronal subtypes are generated from each rhombomere. The identity and patterning of rhombomere is mediated by the transcription factor of the Hox gene family, whose expression is under the control of RA (Glover et al., 2006) and will be described further in section 1.6. The Hox genes in turn are regulated by two transcription factors Krox20 (direct target for Hoxa2 and Hoxb2) (Nonchev et al., 1996) and Kreisler (direct target for Hoxa3 and Hoxb3) (Manzanares et al., 1999). Some of the Hox genes are direct targets of RA because they contain RA response element (RARE) in their promoters and they include Hoxa1 (Frasch et al., 1995), Hoxb1 (Marshall et al., 1992, Studer et al., 1998) and Hoxb4 (Gould et al., 1998) (Fig. 1.6).

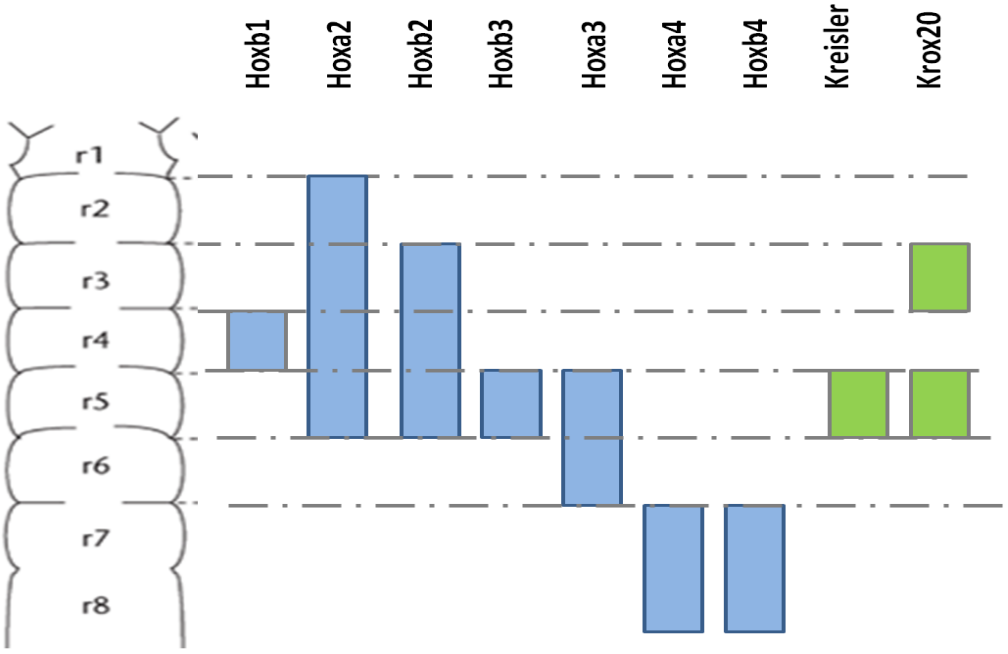

Figure 1.6 Expression pattern of Hox genes, Kreisler and Krox20 in the vertebrate hindbrain

This diagram shows the expression patterns of genes involved in rhombomere specification. The figure has been adapted (Guthrie, 2007).

1.5.3 Specification of ventral progenitors

The specification of neuronal subtypes in the spinal cord has been identified with the appearance of distinct cell types found at defined positions along the dorsoventral axis of the neural tube. From ventral to dorsal, there are p3, pMN, p2, p1 and p0 progenitors. The homeodomain proteins expressed by the progenitors can be subdivided into two groups on the basis of their mode of regulation by sonic hedgehog (Shh) signalling. The expression of class I proteins are repressed by Shh signalling whereas the expression class II proteins requires exposure to Shh (Jessell, 2000) (Fig. 1.7).

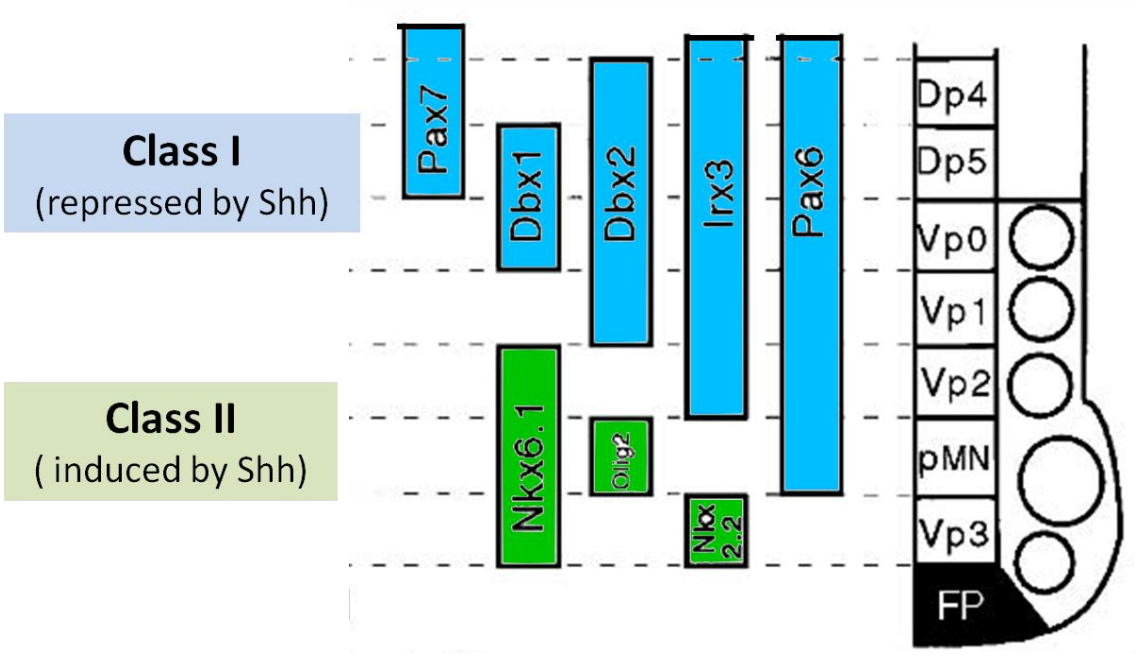

Figure 1.7 Expression pattern of homeodomain transcription factors along the DV axis of the spinal cord

Class I progenitor homeodomains are repressed by Shh whereas class II progenitor homeodomains are activated by Shh. FP, floorplate. Figure has been adapted (Wijgerde et al., 2002).

1.5.4 Neurogenesis and gliogenesis

A further stage in neural development, following on from the establishment of the progenitor domains, comes when neurons are generated in a process called neurogenesis. Initially, new neural progenitors are generated from neuroectodermal cells through symmetrical division on the inner side of the neural tube closest to the lumen. In the brain, the proliferative zone for the neuroectodermal/neuroepithelial cells is found in the inner side of the neural tube and is known as the ventricular zone (VZ). During the onset of neurogenesis (E12), some of these neurepithelial cells downregulate certain epithelial features such as protein for the tight junction (occludin) (Aaku-Saraste et al., 1996) and generate radial glial cells through asymmetrical division. Radial glial cells are so called because they have cellular and molecular characteristics such as expression of astrocyte-specific glutamate transporter (GLAST) (Shibata et al., 1997) and brain lipid binding protein (BLBP) (Feng et al., 1994) that are similar to astroglia, but they also maintain neuroepithelial properties such as expression of nestin (Hartfuss et al., 2001). They divide asymmetrically to give rise to neurons and self-renewing radial glial cells. Radial glial cells are present throughout the whole process of neurogenesis and the remaining radial glial cells that are still present by the end of neurogensis are transformed into astrocytes (Noctor et al., 2004). They also undergo molecular change such as downregulation of neurogenic factors such as Pax6 (Heins et al., 2002) and subsequently replace neuroepithelial cells (Gotz and Huttner, 2005). Besides radial glial cells, another cell type generated from neuroepithelial cells and radial glial cells through asymmetrical division during neurogenesis at VZ is called the basal progenitor cell. Basal progenitors are different from radial glial cells because they express Tbr2 but do not express Pax6 and GLAST (Englund et al., 2005, Malatesta et al., 2003). These cells undergo symmetrical division to generate two daughter neurons (Haubensak et al., 2004). At a later stage of neurogenesis (E13 for ventral telencephalon, E15

for dorsal telencephalon), these basal progenitors are numerous enough to form a visible secondary proliferative layer that is basal to VZ. This layer is called the subventricular zone (SVZ) (Gotz and Huttner, 2005). In addition, a subpopulation of basal progenitors express epithermal growth factor receptors (EGFRs) that are asymmetrically distributed. This results in differing levels of EGFR expression in the daughter cells and the subsequent generation of astrocytes and oligodendrocytes (Sun et al., 2005). Thus early SVZ cells are mostly neurogenic whereas late SVZ cells are mostly gliogenic. The population of basal progenitors that are committed to be neurons exit the cell cycle and migrate towards the outside of the neural tube to a region called the mantle zone where they accumulate and differentiate into mature neurons (Gotz and Barde, 2005) (Fig. 1.8).

The decision whether to exit the cell cycle and undergo differentiation or to remain as progenitors is partly determined by negative regulator Hes genes and positive regulator proneural genes. Proneural genes (e.g. Ngn2 and Mash1) encode transcription factors of the bHLH class that initiates neurogenesis by directing the exit from the cell cycle and by promoting the expression of proteins that are found in post-mitotic neurons (Ma et al., 1996, Guillemot, 1999). Within the neural cells (i.e., those that are committed to undergoing neurogenesis), the proneural factor triggers the expression of those Notch ligands known as Delta genes (Kunisch et al., 1994). Delta molecules interact with the Notch receptors of the neighbouring progenitors. This leads to an activation of Notch signalling in the neighbouring progenitors. This in turn results in the production of Hes proteins including Hes1 and Hes5 (Akazawa et al., 1992, Jarriault et al., 1995, Ohtsuka et al., 1999), which are transcriptional repressors. They inhibit neurogenesis by repressing the expression of the bHLH factors of the recipient cells (Ohtsuka et al., 1999), thus reducing their neural competence (Price et al., 2011). Therefore, proneural genes serve to trigger neural commitment while Notch signalling maintains the population of progenitor cells. Proneural genes have also been

reported to direct neurogenesis by downregulating the expression of SoxB1 genes (Sox1-3), which are crucial for maintaining neural stem cell population (Bylund et al., 2003).

While SoxB1, Hes and proneural genes regulate the neural commitment of progenitor cells, different neuronal subtypes are generated from a common progenitor pool with specific temporal patterns (Mizutani and Gaiano, 2006). The temporal regulation of neurogenesis in the neocortex, for example, leads to the generation of six main layers of neurons. The neurons of each layer have distinct morphologies and functional identities (Mizutani and Gaiano, 2006). The preplate is generated first. The preplate is then separated into marginal and subplate layers by cortical neural progenitors. These are generated in the VZ and migrate outwards to create successive neuronal layers. Neurons destined for deep layers 6 and 5 are produced first, followed by those that were destined for more superficial layers 4, 3 and 2 (Price et al., 2011). (Fig. 1.9) Crucially, the sequential generation of neurons destined for different neocortical layers is programmed intrinsically (Shen et al., 2006). Isolated progenitor cells when grown at clonal density first generate Cajal-Retzius neurons (found at the marginal zone or layer 1) (Hevner et al., 2003b). These progenitor cells then express Foxp2 and Tle4 markers such as is found in layer 6 (Ferland et al., 2003, Yao et al., 1998), then a marker such as is found in layer 5 (neuronal marker ERG81) (Hevner et al., 2003a) and then eventually a marker such as found in layer 4 (neuronal marker Cux1) (Nieto et al., 2004). The order and timing of the generation of the neuronal subtype *in vitro* follows the order and timing of the generation of the neuronal subtype *in vivo*. In addition, the ability of late-stage progenitors to produce earlier neuronal subtypes is more restricted as this development progresses. Isolated progenitor cells first lose the capability to generate Cajal-Retzius neurons, followed by deep layer cortical neurons. This indicates that late-stage progenitors produce a narrower range of neuronal subtypes than early-stage progenitors. Although investigation has not ruled out the possibility that extrinsic factors might be involved, it has been observed that exposing developing clones to media conditioned by

high-density neocortical cultures of various ages or by co-culturing developing clones with neocortical progenitors which are of different ages did not significantly alter the neuronal composition. This indicated that the supposed extrinsic factors seemed to be overridden by the intrinsic factors programmed within each individual progenitor (Shen et al., 2006). Further discussion of these issues lies outside the scope of this study, it is nevertheless interesting to note that though the exact mechanism for the molecular regulation of the neuronal birth date is yet to be elucidated, it has been thought to be partly regulated by Foxg1 expression. For example, decreasing Foxg1 expression to about 50% of its normal level significantly enhanced the generation of Cajal-Retzius neurons from progenitors even at stages when such an increase would not normally be expected (Shen et al., 2006).

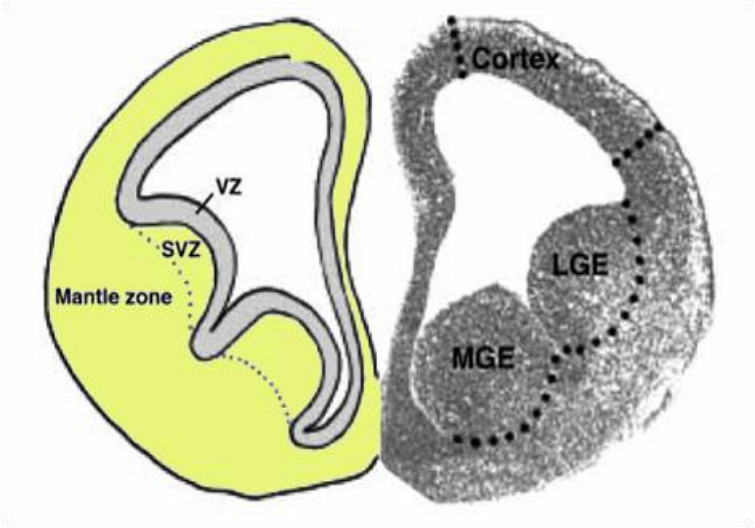

Figure 1.8 Schematic coronal section through the telencephalic vesicles at E12.5

Ventricular zone (VZ), subventricular zone (SVZ) and mantle zone in the telencephalon are shown. The VZ extends along the DV axis and contain proliferative radial glial cells. The SVZ zone contains intermediate progenitor cells that undergo symmetrical division. The mantle zone is the region where neural progenitor cells undergo neurogenesis. Figure adapted from (Toresson et al., 1999).

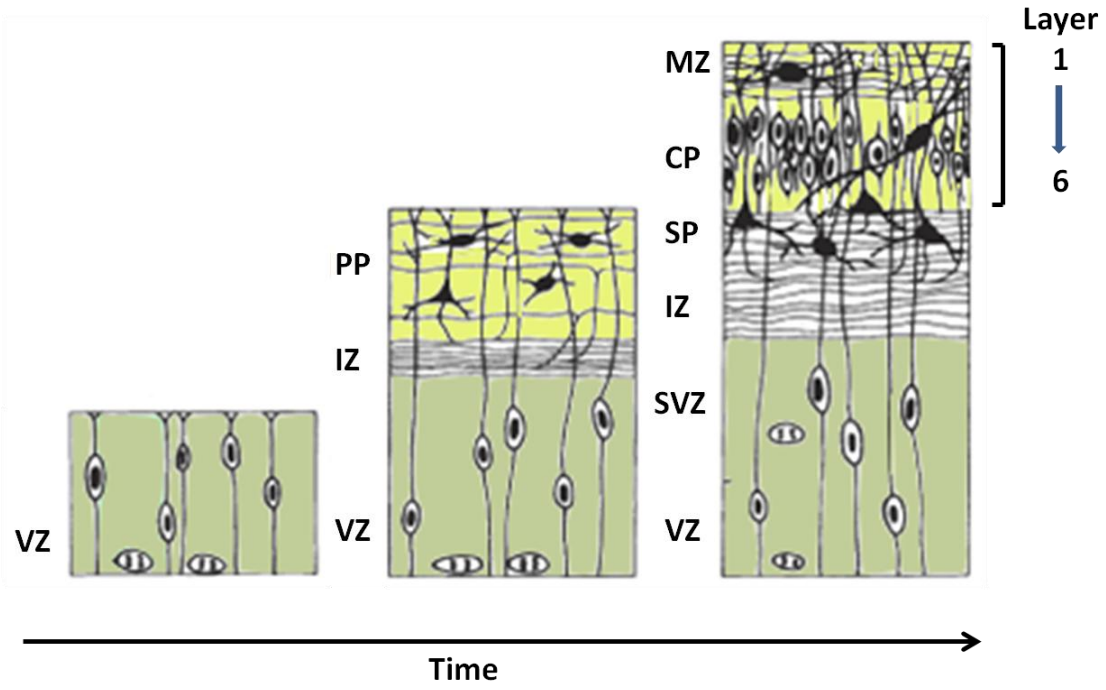

Figure 1.9 Layers in the developing cerebral cortex

These panels show the cross-section of the cerebral cortex at different stages of development. During the early stages (left), progenitor cells undergo proliferation in the ventricular zone (VZ). At the beginning of corticogenesis (middle), postmitotic neurons migrate to the outer surface of the cerebral wall and become the preplate (PP). The intermediate zone (IZ) forms in between the PP and the VZ. At later stages (right), neurons generated from the VZ migrate outwards to create successive neuronal layers between the outer part, the marginal zone (MZ) and the lower part, the subplate (SP). The subventricular zone (SVZ), where most of the glial cells are generated, is formed at this stage. Figure has been adapted (Parnavelas, 2000).

1.6 Regulation of regional specification *in vivo*

Successful manipulation of the cell fates of ES cell-derived NPCs, a basic requirement to the aims of this study, depends on an understanding of the regulation of fate specification *in vivo*.

During vertebrate development, signals are generated in specific locations. Many of these signals act in a graded fashion and give positional information in such a way that the distance of a cell from the signal source determines the concentration of signal to which it is exposed, and in turn influences the fate of the responding cell. Signals that have direct concentration-dependent and distance-related effects are called morphogens (Wolpert, 1996, Lawrence and Struhl, 1996).

Several morphogens including the members of the hedgehog (Hh) and TGFβ families, have all been shown to play a role in specifying developing tissues (Lander, 2007). Much of our understanding of the effects of morphogens on regional specification in the CNS is based on studies of the effect of Hh signalling on the specification of progenitor domains in spinal cord tissue where partially overlapping patterns of transcription factors are found (Jessell, 2000). Similar concepts can be applied to the development of other tissues. This thesis will focus on the patterning effects mediated by Hh and RA signalling.

1.6.1 The establishment of progenitor homeodomains by graded signalling

1.6.1.1 Effect of Shh on establishing progenitor domains In the spinal cord

Shh is released from the floor plate and underlying notochord (Marti et al., 1995b, Echelard et al., 1993, Marti et al., 1995a). A gradient of Shh activity is known to exist in the ventral part of the spinal cord, with the highest Shh activity found at the ventral end (Echelard et al., 1993). The fact that the progenitor identities are governed by the Shh gradient is a significant finding. As mentioned in section 1.5.3, the expression of class I

proteins is repressed by Shh signalling (Ericson et al., 1997). The more ventral the boundary of progenitor domain, the higher the concentration of Shh required for the repression of protein expression (Ericson et al., 1997). For instance, the repression of Irx3 requires ～3 nM of recombinant Shh, a concentration higher than that required for the repression of Pax7 (～2 nM) (Briscoe et al., 2000), but lower than that required for complete repression of Pax6 (～4 nM) (Ericson et al., 1997). The expression of class II proteins is induced by Shh signalling (Briscoe et al., 1999). Induction of Nkx6.1 requires ～0.25 nM of recombinant Shh whereas induction of Nkx2.2 requires 3-4 nM of Shh-N (Ericson et al., 1997, Briscoe et al., 2000).

1.6.1.2 Effect of RA on the development of hindbrain

Much evidence suggest RA acts like a morphogen and regulates anteroposterior patterning in a concentration-dependent manner (White et al., 2007). The level and distribution of RA is determined by the availability of retinol, RA carrier proteins (CRABPs) which control the movement of RA from one cellular compartment to the other (Giguere et al., 1990, Smith et al., 1991), the local availability of RA receptors (RARα, β, γ and RXRα, β, γ) (Leroy et al., 1991, Kamei et al., 1993), and a combination of synthesis and degradation by two RA metabolic enzymes: Raldh2 which converts retinaldehyde into RA and Cyp26s which converts RA into inactive products (Fujii et al., 1997, Duester, 1998, White et al., 1996). Both metabolic enzymes have been suggested to be responsible for setting up the RA gradient along the AP axis (Swindell et al., 1999). A schematic illustration of the RA signalling diagram can be found in Fig. 1.10.

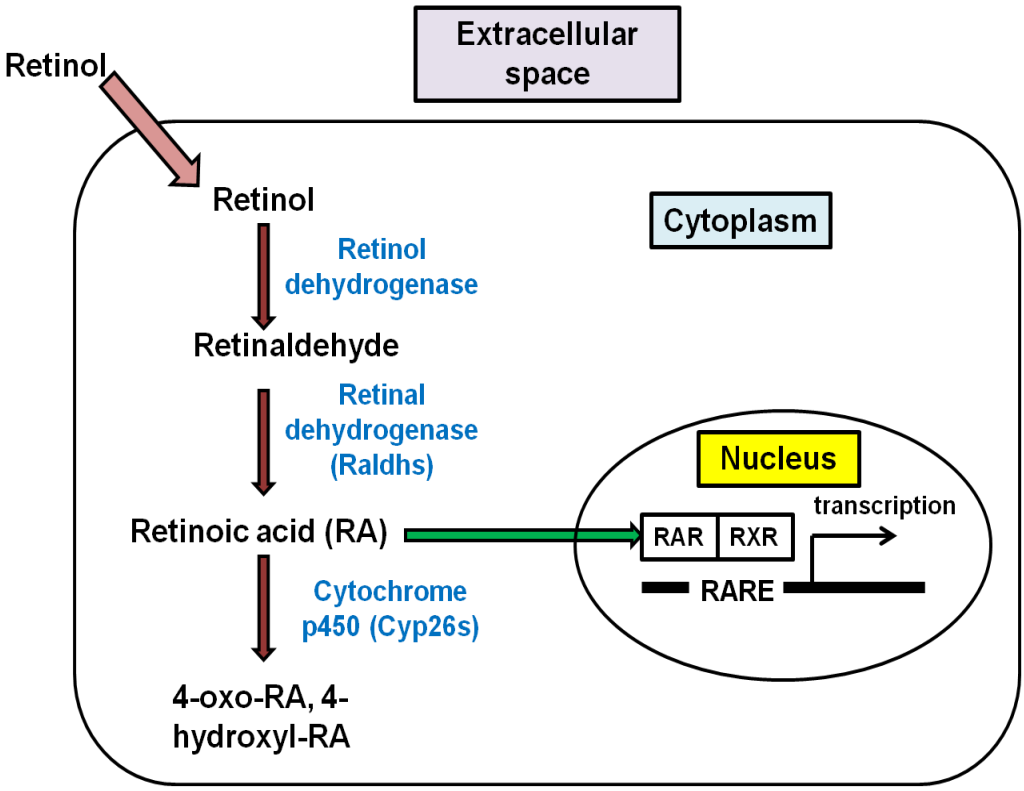

Figure 1.10 The RA signalling pathway

Retinol circulates in blood and binds to cellular retinol-binding protein (CRBP) in the cytoplasm. It is then metabolized by retinol dehydrogenase (RoDH) to retinal, which is then converted to RA by retinaldehyde dehydrogenases (Raldhs). RA then enters the nucleus and binds to the RA receptors (RARs) and the retinoid X receptors (RXRs). RARs and RXRs heterodimerize and bind to DNA which contains the RA-response element (RARE) sequence and activates the transcription of target genes (Maden, 2002). Excess RA can then be metabolised into products such as 4-oxo-RA, 4-hydroxyl-RA by P450 cytochrome enzymes including CYP26A1, CYP26B1 and CYP26C1 to ensure appropriate RA signalling in specific tissues (Reijntjes et al., 2005).

One of the earliest experiments about the effect of RA gradient on regional specification conducted on *Xenopus* along the AP axis made it clear that RA treatment (10^{-5} M) inhibits the formation of anterior structures such as the forebrain and stimulates the formation of posterior structures such as the hindbrain. The higher the concentration of RA treatment, the more dramatic the effect of regional transformation (Durston et al., 1989). Consistent results were found in mouse study which confirm that RA treatment at mid-late streak stage downregulated expression of forebrain markers (Otx1, Otx2, Emx1, Emx2 and Dlx2) and induced rostral extension of the Hoxb1 domain (Simeone et al., 1995).

More examples to demonstrate the effect of RA gradient can be found in hindbrain patterning. For instance, treating chick embryos with a decreasing concentration of RA receptor (RAR) antagonist (BMS493) (Wendling et al., 2000) resulted in the progressive establishment of more posterior rhombomeres (Dupe and Lumsden, 2001), and a similar observation was also found in Zebrafish embryos (Maves and Kimmel, 2005). Loss of function mutants in the RA synthetic enzyme Raldh2 in mice displayed anterior expansion as shown by the downregulation of the Kreisler gene in posterior rhombomeres (r5-r6) and an ectopic expression of Hoxb1 (normally expressed in r4) and Meis2 (normally expressed in r2-3) in r5-r6 (Niederreither et al., 2000). The opposite effect was found when there is loss of Cyp26a1 function mutants in mice: they displayed posterior transformation of r2-4, revealed by the ectopic expression of Hoxb1 in r2 (Abu-Abed et al., 2001, Sakai et al., 2001).

1.6.2 The defining of progenitor boundaries by cross-repressive interactions

1.6.2.1 In the spinal cord

The ventral to dorsal gradient of Shh activity establishes the progenitor domains in the spinal cord but the clear boundaries found between each progenitor domain require an additional mechanism to establish and maintain them. For example, misexpression of Nkx2.2 in regions dorsal to the p3 domain resulted in the lack of expression of Pax6. Similarly, misexpression of Pax6 ventral to its normal limit resulted in the lack of expression of Nkx2.2, indicating that Pax6 acts by repressing the expression of Nkx2.2 in the p3 domain and sharpens the pMN/p3 boundary through cross-repressive interaction with Nkx2.2. Similar cross-repressive interaction exists between class I Dbx2 protein and class II Nkx6.1 protein, both proteins having complementary expression domains at the p1/p2 boundary (Briscoe et al., 2000) (see diagram 1.7).

1.6.2.2. In the brain

Similar examples of cross-repressive interactions can also be found within the telencephalon. There the pallio-subpallial boundary is maintained by cross-repressive interactions between dorsal Pax6 and ventral Gsh2 (Yun et al., 2001, Carney et al., 2009), and the complementary expression domains found between dorsal Ngn2 and ventral Mash1 ensure that the correct neuronal subtypes are generated (Fode et al., 2000) (see diagram 1.5). The interaction between Pax6 and Pax2, for example, defines the forebrain-midbrain boundary (Matsunaga et al., 2000), and the interaction between Otx2 and Gbx2 delineates the midbrain-hindbrain boundary (Simeone, 2000).

1.6.3 The temporal control of cell fate specification

So far we have considered in what ways the establishing of progenitor homeodomains is affected by morphogen gradients and cross-repressive interactions. No discussion of regional specification, however, can fail to take into account the question of temporal control.

1.6.3.1 Regulation of cell fates by changing Shh duration in the spinal cord

Although more ventral cell types can be generated with increasing concentrations of recombinant Shh (see section 1.6.1), distinct neuronal subtypes cannot be generated by simply increasing the concentration of recombinant Shh. Exposing chick neural explants to 0.05 nM to 0.4 nM of Shh produced a mixture of V0 to V2 neurons, indicating that incremental differences in Shh concentration were insufficient to generate distinct neuronal subtype from each progenitor homeodomain. If however chick explants were exposed to a fixed concentration of recombinant Shh (0.5 nM) but over lengthier time periods, distinct neuronal subtypes were generated progressively: 12 hours of Shh exposure generated V2 neurons with a marked reduction in V0 neurons whereas 24 hours of Shh exposure generated pMN neurons with a reduction of V2 and V0 neurons. Accordingly, the expression of more ventral markers of the progenitor domains also can be induced by increasing the duration of Shh exposure from 0 hour to 24 hours. This led to the conclusion that in addition to the concentration of morphogens, the actual length of the duration of morphogen exposure was also important in specifying cell fates (Dessaud et al., 2010). Continued Shh signalling was necessary for maintaining the ventral identities of progenitors even after the progenitor identities were established. If Shh signalling was interrupted by administering Shh antagonist cycloplamine (Incardona et al., 1998) after all the progenitor domains were

established in chick embryos, some ventral markers are downregulated and cells adopted a more dorsal character (Dessaud et al., 2010).

1.6.3.2 Regulation of cell fate by changing FGF8 duration at isthmic organiser

Further experimentation has investigated cell fate regulation at the boundary between the midbrain and hindbrain border. This border, the isthmus, is a key organizing centre. FGF8 is expressed in the isthmus (Crossley and Martin, 1995) and plays an important role in directing the development of the tectum (developed from dorsal midbrain) and cerebellum (developed from anterior hindbrain) (Chi et al., 2003). It was reported that the variation in the duration of FGF8 exposure influenced the development of the tectal-isthmo-cerebellum region in mouse. The formation of Isthmus requires the longest duration of FGF signalling. Progressively shorter durations of signalling are required for the development of more posterior tectal structures, and for regions from medial to lateral of the cerebellum (Sato and Joyner, 2009).

1.6.3.3 Temporal change in RA levels by Cyp26s in hindbrain patterning

More recent studies of Cyp26 genes have shed light on the temporal control of RA in hindbrain patterning. Based on the finding that RA generated by Raldh2 forms an anterior boundary r2/r3 (next to the r2 border of Cyp26a1 expression) at E7.5 and then at r4/5 (next to the r4 border of Cyp26c1 expression) at E8.5, Sirbu et al. suggested that the boundaries of expression of rhombomere-specific genes are determined by RA-catabolizing enzymes that shift over time. Furthermore, they showed that the duration of RA exposure is crucial for rhombomere specification because a longer period of RA activity was found in r5-r8 than in r3-r4 (Sirbu et al., 2005). Consistent results were found in an independent study carried out in zebrafish and therefore a model was proposed stating that the differential responsiveness to RA along the hindbrain AP axis is entirely determined by the dynamic expression of Cyp26

genes, and hence that rhombomeres can be specified in a 'gradient-free' manner. Their results placed temporal control at the centre of hindbrain patterning (Hernandez et al., 2007). However, Maves and Kimmel argued that the expression of more posterior genes does not depend on the duration of RA exposure. They observed that when zebrafish embryos were treated with RALDH-inhibiting DEAB, a uniform concentration of RA (1 nM) was necessary for r5-r6 specification at a stage later than that needed for r7 specification (Russo et al.,1988). Therefore, they suggested that the sequential expression of more posterior genes required a higher level of RA than that of the anterior genes, and, deduced that this expression was achieved by gradually increasing the RA gradient over time (Maves and Kimmel, 2005). White et al. then reconciled these observations above by proposing that both RA and FGF act collaboratively in shaping the RA gradient. They showed that FGF signalling acts indirectly by inhibiting RA-mediated expression of Cyp26a1, thus explaining the anterior to posterior decline in the expression of Cyp26a1 when the level of RA could be expected to increase. These observations were further studied by computer analysis. This showed that RA gradients are shaped by interaction beween feedback (RA degradation induced by RA signalling) and feedforward (RA degradation repressed by FGF signalling). This integrated morphogen system enables RA gradients to be remain stable during fluctuations in RA synthesis and over an expanding field of cells (White et al., 2007).

1.6.4 The spatial control of responsiveness

1.6.4.1 Spatial difference in RA responsiveness in the forebrain

Within the forebrain, most sites of RA signalling (detected by examining RARE-lacZ reporter mice) and RA synthesis (detected by examining the expression of Raldh1, Raldh2 and Raldh3) did not co-localise, suggesting that different regions of the forebrain can have different competences of RA signalling (Luo et al., 2004). Ventral telencephalon was reported to be more competent in retinoid signalling than dorsal telencephalon because the induction of RA responsive gene striatal-enriched tyrosine phosphatase (STEP) (Lombroso et al., 1991) in LGE and MGE explants was higher than that found in dorsal telencephalon. The induction was mediated by RARβ since the expression of STEP was reduced in RARβ$^{-/-}$ mutant mice. Hence it was suggested that RARβ plays a key role in regulating retinoid signalling competence in the developing telencephalon (Liao et al., 2005b). Furthermore, the various expression patterns of different isoforms of RARβ were detected at E13.5 LGE. RARβ1/3 expression is found in the caudal and dorsolateral domains whereas expression of RARβ2 mRNA was detected in the rostral and ventromedial domains. Interestingly, RARβ2 mRNA was expressed in a decreasing gradient in the developing striatum along the AP axis, but no such gradient was found for the other two isoforms of RARβ (RARβ1/3 and RARβ3). The authors suggested that the spatial arrangement of different isoforms in different domains is what in fact forms the basis of differential gene control regulated by RA signalling through RAR. (Liao et al., 2005a). It could probably also explain the expression of STEP when RARβ2 (but not other isoforms of RARβ) was ectopically expressed in the dorsal telencephalon (Liao et al., 2005b).

1.6.5 The modulation of the signal transduction in response to morphogens

1.6.5.1 Shh in the spinal cord

Progress also has been made in understanding the molecular mechanisms of how cells respond to changes in the concentration and duration of Shh in the ventral neural tube. The binding of of Shh (a homolog of Hh) ligand to a transmembrane protein receptor Patch-1 (Ptc1) results in the release of the repression of the transmembrane protein smoothened (Smo) (Stone et al., 1996, Taipale et al., 2002). This then transduces the Shh signal to the cytoplasm and subsequently regulates the expression of the glioma-associated oncogene homolog (Gli) family of zinc transcription factors (Gli1, Gli2 and Gli3) producing a net increase in their transcriptional activator function through proteolytic cleavage (Sasaki et al., 1999) (Fig. 1.11).

Studies of the chick neural explants revealed that Gli activity remains unchanged at a low concentration of recombinant Shh (1 nM) but decreases in response to a high concentration of Shh (≥4 nM) during the first 12 hours of exposure. This suggested that adjusting Gli activity allows cells to become desensitized to Shh in response to ongoing exposure to Shh. After 12 hours, Gli activity was sustained at high concentrations of Shh but was reduced rapidly at low concentrations. This adaptation mechanism appears to be important for the discrimination of Olig2 and Nkx6.1 expression and involves the regulation of Ptc1. If the expression of Ptc1 is silenced by small interfering RNA (siRNA), the expression of both Olig2 and Nkx6.1 was found even at a concentration that would normally only induce Olig2 (1 nM). This indicated that the upregulation of Ptc1 is involved in transforming extracellular concentrations of morphogen into time-limited periods of signal transduction. In the case of ventral tube patterning, this occurred through adjusting the period of Gli activity (Dessaud et al., 2007).

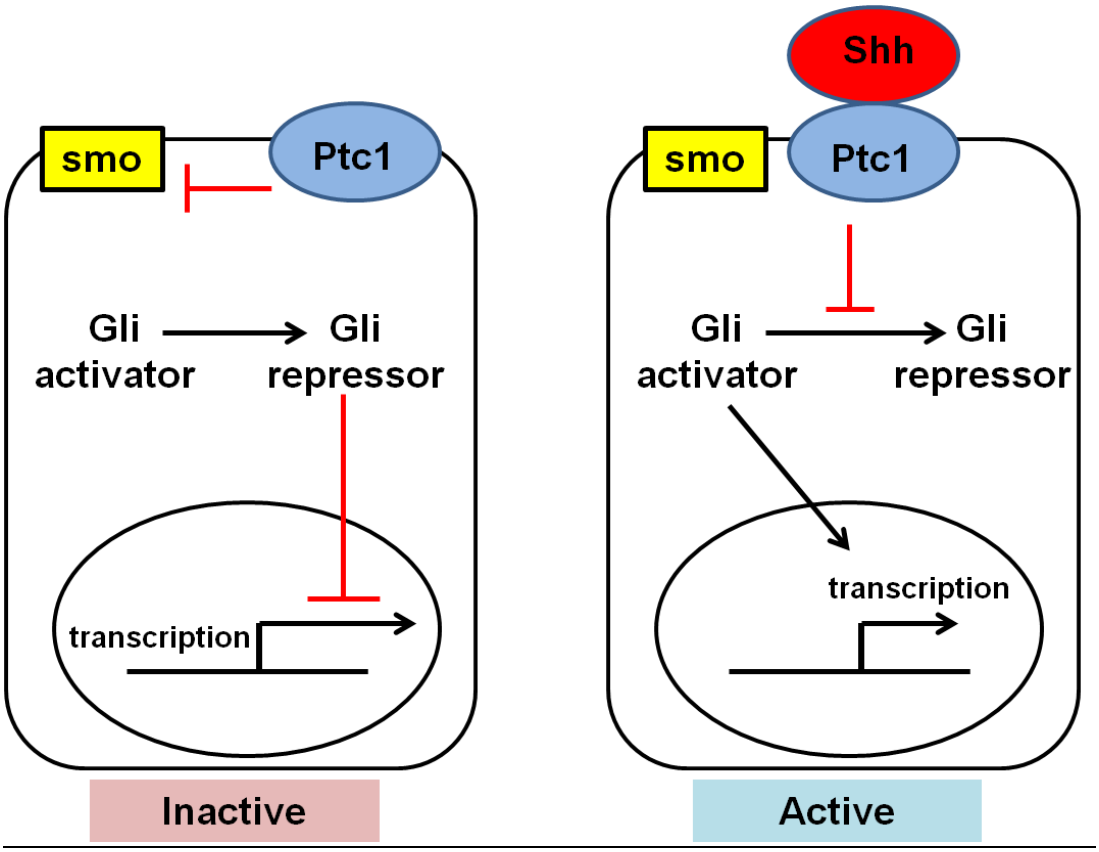

Figure 1.11 The Hh signalling pathway

The cell surface receptor for Shh is a transmembrane protein receptor Patch-1 (Ptc1). In the absence of Hh, Ptc1 prevents the binding of another transmembrane protein Smoothened (Smo) from reaching the cell surface. Upon Hh binding, the Ptc1 receptor is downregulated, and allows Smo to move towards the cell surface. This prevents the protease from cleaving Gli protein, which acts as a repressor in cleaved form in the absence of Hh or Shh signal. The uncleaved form of Gli protein acts as an activator and enables the subsequent change in expression of target genes (Bai et al., 2004, Pan et al., 2006).

1.7 Cell fate specification of ES cell - derived NPCs

This introduction has sought to indicate how temporal and spatial considerations, together with morphogen concentrations, can regulate regional specification *in vivo*. The strategies that manipulate the cell fates of ES cell-derived NPCs using morphogens involved altering one or a combination of the following parameters: the choice of morphogens, their concentration and the period of exposure (Irioka et al., 2005). By its very nature, a spatial perspective cannot be adopted in order to control cell fate: cell-cell interactions are changed each time when the cells are passaged. Despite this limitation to the parameters available for generating neural progenitors *in vitro*, studies have shown that neural progenitors with specific regional characters can nevertheless be generated.

1.7.1 The influence of morphogen concentration on regional identities

1.7.1.1 The effect of RA and Shh on the generation of pMN progenitors in the spinal cord

Crucially, studies have demonstrated that those morphogens involved in generating neural progenitors with regional identities in animal studies can direct ES cells to form specific classes of neurons (Wichterle et al., 2002). This transferability, with its potential for the bio-medical application of findings to other spheres, provides a model for the investigation of the molecular processes involved in cell fate specification. Both RA and Shh are involved in spinal progenitor specification *in vivo* (Briscoe et al., 2000, Ericson et al., 1997, Pierani et al., 1999), and both signals have been shown to induce ES cells to generate spinal progenitor cells and subsequently differentiate into motoneurons (Wichterle et al., 2002). Cells exposed to the caudalising signal RA (2 µM) in isolation displayed characteristics of progenitor cells located in the dorsal and intermediate spinal cord as most cells expressed Pax7, Pax6, Irx3 and Dbx1 and few cells expressed Nkx6.1, Olig2 and Nkx2.2 (Wichterle et al., 2002). Joint exposure of RA and a low concentration of Shh agonist, Hh-Ag1.3 (0.01 µM)

(Frank-Kamenetsky et al., 2002) ventralized neural progenitors. This was indicated by an increased number of Pax6- and Irx3- positive cells, and a reduction in the number of Dbx1-positive cells together with the induction of a few Nkx6.1- and Olig2-positive cells. Joint exposure of RA and a high concentration of Shh agonist, Hh-Ag1.3 (1 μM), resulted in the elimination of Dbx1 expression, the reduction of Pax6 and Irx3 expression and a marked increase in Nx6.1 and Olig2 expression (Wichterle et al., 2002). Both Nkx6.1 and Olig2 are closely linked with the generation of spinal motor neurons *in vivo* (Mizuguchi et al., 2001, Sander et al., 2000, Novitch et al., 2001). The dorsal-to-ventral shift in the expression profile of transcription factors in response to increasing levels of Hh signalling resembled the behaviours of neural tube progenitors *in vivo* (Briscoe et al., 2000, Ericson et al., 1997) (see Fig. 1.12). This indicated that signalling factors that operate along the DV axis of the neural tube *in vivo* can be made use of *in vitro* to direct the differentiation of ES cells into specific neural progenitors (Wichterle et al., 2002).

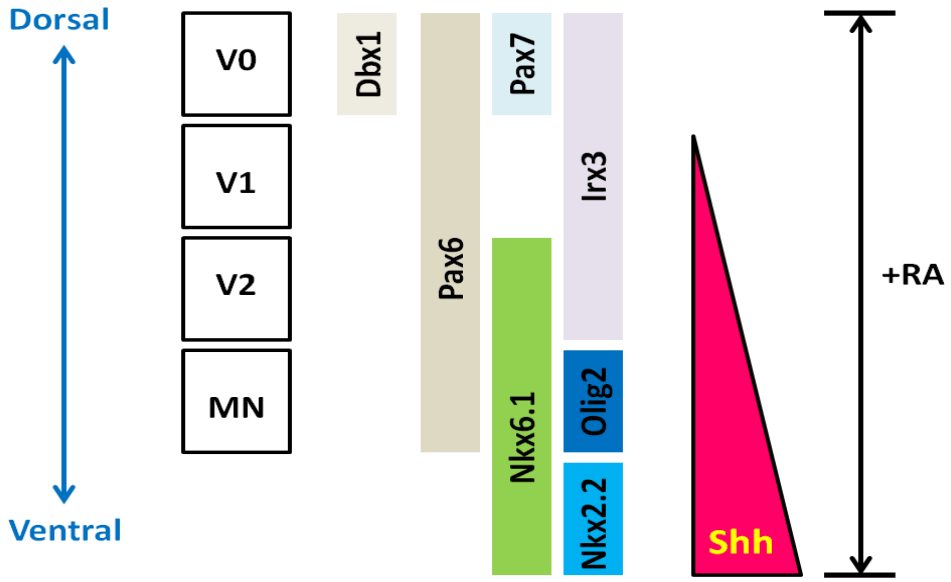

Figure 1.12 Specification of dorsoventral identities of ES cell- derived NPCs is dependent on the concentration of Shh

ES cell-derived NPCs are ventralised by Shh in a concentration-dependent manner. Cells treated with caudalizing signal RA alone expressed markers that are found in the V0, V1 domains (Pax7, Pax6, Irx3 and Dbx1); cells treated with a low concentration of Shh agonist expressed markers specific to the V1, V2 domains (Pax6, Irx3); cells treated with a high concentration of Shh agonist expressed markers specific to the MN domain (Nkx6.1 and Olig2). This diagram has been adapted (Wichterle et al., 2002).

1.7.1.2 The use of recombinant Shh in the generation of region-specific telencephalic progenitors

The way in which altering the concentration of Shh results in the generation of telencephalic progenitors is another example of the part played by concetration levels. In the absence of extrinsic Shh signal or when Hh signalling was inhibited by Hh antagonist cyclopamine, telencephalic progenitors (Foxg1 positive) preferentially gave rise to pallial progenitors and express Pax6 and Tbr1 (Danjo et al., 2011, Eiraku et al., 2008). A moderate dose of recombinant Shh (10 nM) strongly suppressed the expression of pallial markers and induced the expression of LGE marker Gsh2. A high dose of Shh (30 nM) results in the induction of the expression of MGE marker Nkx2.1 in neural progenitors on day 12 of differentiation (Danjo et al., 2011). This is further evidence that the regional specification of ES cells is influenced by the concentration of morphogens.

1.7.1.3 The effect of changes in the concentration of RA on AP and DV patterning of NPCs

The generation of spinal motor neurons from ES cells through systematic variation in the identity and concentration of patterning signals has provided a general strategy for generating other defined progenitors (Wichterle et al., 2002). Similarly, the anteroposterior identities of NPCs can be manipulated by changing the concentration of RA. In the absence of RA, EBs expressed genes that are specific to the forebrain but not the hindbrain or the spinal cord on both day 4 and day 6 of differentiation. A low concentration of RA (0.01 μM), on the other hand, induced the expression of midbrain-to-hindbrain markers but not the spinal cord markers. A high concentration of RA (1 μM) induced the expression of hindbrain and rostral spinal cord markers but reduced the expression of forebrain and midbrain markers (Okada et al., 2004, Okada et al., 2008) (Fig. 1.13). Consistent results were obtained in another independent study using SDIA-treated ES cells (Irioka et al., 2005), indicating that

the effect of changing RA concentration on regional specification is not restricted to EBs and can be transferable to other methods of inducing neural differentiation in ES cells. The concentration of RA also has an effect on the dorsoventral identities of NPCs. Both class I and class II genes were induced by low RA concentration (Okada et al., 2004), but only class I genes were induced by a high concentration of RA, indicating that high concentrations of RA promote dorsal specification and disrupt the ventral specification of NPCs (Okada et al., 2004, Irioka et al., 2005).

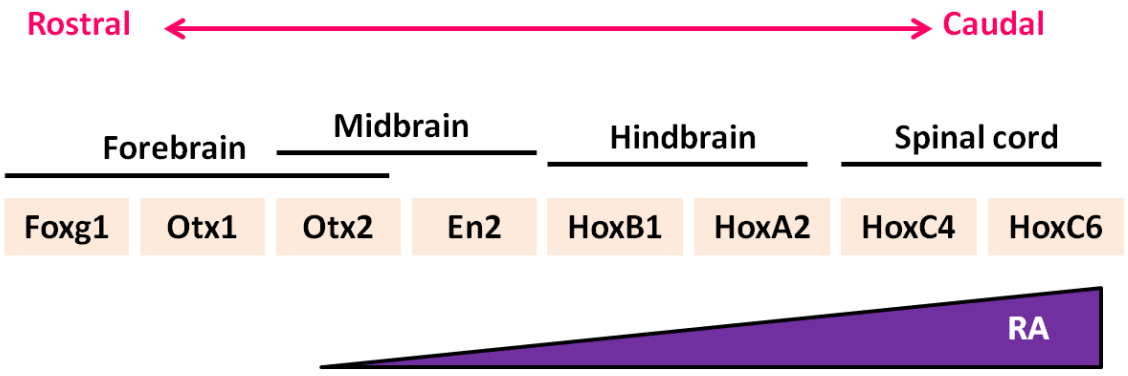

Figure 1.13 Specification of rostrocaudal identities of ES cell-derived NPCs is dependent on the concentration of RA

ES cell-derived NPCs are caudalized by RA in a concentration-dependent manner. Cells that received no RA treatment expressed markers that are specific to the forebrain (Foxg1, Otx1). Cells treated with low concentrations of RA expressed midbrain to hindbrain markers (En2, HoxB1, HoxA2), and a reduced expression of forebrain markers. Cells treated with high concentrations of RA expressed spinal cord markers (HoxC4 and HoxC6), with reduced expression of forebrain and midbrain markers.

1.7.2 The temporal regulation of cell fate specifcation

1.7.2.1 The use of recombinant Shh in the generation of subpallial progenitors

The acquisition of cell fates in ES cell-derived NPCs is not influenced only by the concentration of the morphogens. The timing of morphogen treatment is equally important. For instance, the expression of subpallial markers Gsh2 and Dlx2 in telencephalic progenitors was strongly induced by Shh treatment on day 3 but not on day 7. Pallial markers Pax6 and Tbr1 expression was suppressed by Shh treatment between day 3 to day 4 but not on day 6.

Furthermore, the temporal duration of Shh treatment also plays a critical role in specifying the identities of telencephalic progenitors. To direct telencephalic progenitors to a subpallial fate requires continuous Shh exposure (10 nM) until day 9. If, however, the period of exposure is between day 3 to day 8, telencephalic cells give rise to pallial fate. Interestingly, treating telencephalic progenitors with a high concentration of Shh (30 nM) from day 9 onwards inhibited LGE differentiation (Danjo et al., 2011). It can be observed, therefore, that the timing of morphogen treatment plays an important role in determining the identities of neural progenitors.

1.7.2.2 The effect of RA exposure on AP patterning

The period of RA exposure also has an impact of the specification of the regional identities of neural progenitors. Expression of caudal markers (Hoxb4 and Hoxb9) was found in SDIA-treated ES cells by a 1-day exposure of RA (2 µM) at any point between day 3 and day 8. On the other hand, the expression of forebrain markers (Foxg1 and Otx2) was strongly suppressed by 1-day or 2-day exposure of RA from day 3 to day 6, but the suppression was not found when RA was added after day 6. This indicated that different positional markers have different temporal windows of expression in response to RA treatment (Irioka et al., 2005).

1.7.3 Temporal changes in responsiveness to morphogens

The temporal control of the expression of regional markers in response to morphogens was further studied by Bouhon et al. They demonstrated that the ability of morphogens to impose regional identities is only found in early NPCs (from day 8 cultures). Late NPCs (from day 20 cultures) are refractory to RA and Shh signals and display constitutive expression of Olig2, Mash1, EGFR and vimentin, a phenotypic profile that is associated with putative gliogenic radial glia with lower neurogenic potential (Bouhon et al., 2006). The underlying mechanism for the change in responsiveness to morphogen is not clear. This indicates that although ES cells provide a valuable source for generating specific neuronal subtypes to be used for regenerative medicine and drug research, much remains to be clarified in terms of how time-related considerations govern their response to morphogens in acquiring specific regional identities, a process which can subsequently influence the generation of specific neuronal subtypes.

1.8 Aims and objectives of the study

My interest lay in understanding the mechanisms governing the generation of neural progenitors from ES cells and in discovering to what extent the acquisition of positional identities of neural progenitors is influenced by a number of related factors: BMP inhibition, temporal changes in responsiveness and gene expression.

BMP inhibition is essential for neural induction. Generating homogenous populations of NPCs using recombinant proteins for comparative studies or large-scale analyses has proved challenging: recombinant proteins, such as noggin, usually have a short shelf-life and there are batch-to-batch differences. Chemical alternatives have been developed in an attempt to find more stable and reliable inhibitors. Therefore, the first aim of this study is:

-To examine to what extent the use of two newly discovered BMP chemical inhibitors, DM and its derivative LDN enhance neural induction in ES cell cultures and to discover whether they can be used to replace recombinant noggin (chapter 3).

Much work has been carried out on the study of the caudalization of neural progenitors by RA at their early stages (Wichterle et al., 2002, Okada et al., 2004, Okada et al., 2008, Irioka et al., 2005). A later stage has also received attention (Bouhon et al., 2006). However, the temporal stage-specific effects of RA on regional specification of NPCs have not been established. Therefore this study also seeks:

-To examine how temporal considerations influence the responsiveness of NPCs to RA thus determining the expression profile of different positional and neural markers in early and late neural cultures (chapter 4).

The ability of ES cell-derived NPCs to respond to morphogens in a predictable manner can only be found in early NPCs but not in late NPCs (Bouhon et al., 2006). The exact explanation for the change in responsiveness has not yet emerged. Therefore, since Sox1 expression is associated with a naïve neural progenitor state and neural commitment, the final part of the study undertakes

- *To examine whether Sox1 expression is associated with the change in responsiveness to morphogens in late NPCs (chapter 5).*

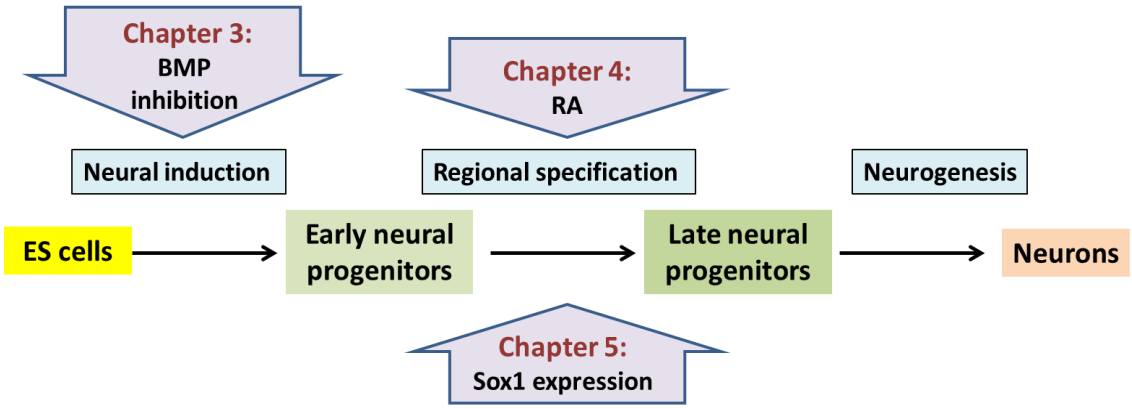

Figure 1.14 **Diagram showing the major steps involved in neural differentiation of ES cells and showing the correspondence between the research chapters and the major steps involved in the neural differentiation of ES cells.**

The specification of neuronal fate can be considered in three sequential steps:

1) the neuralisation of ES cells to produce neural progenitors;

2) the regional specification of neural progenitor cells and

3) the generation of neurons from neural progenitors through cell cycle exit.

Chapter 3 investigates the effects of newly discovered BMP inhibitors LDN193189 (LDN) and dorsomorphin (DM) and compares the action of LDN and DM to that of recombinant noggin in order to assess the feasibility of using LDN and DM as substitutes for recombinant noggin.

NPCs can be specified regionally in response to morphogens. Since RA plays a major role in regulating regional identities in NPCs (Okada et al., 2008, Okada et al., 2004), the question of temporal responsiveness to RA in early and late NPCs is investigated in Chapter 4.

Chapter 5 investigates whether Sox1 expression is related to the responsiveness to patterning cues found in NPCs because Sox1 is associated with a naïve neural progenitor state and neural commitment.

CHAPTER 2:

MATERIALS AND METHODS

2.1 *In vitro* methods

2.1.1 Mouse embryonic stem cell lines

Two mouse ES cell lines were used for most studies. The previously described Foxg1Z cell line was generated by replacing most of the coding sequence of *Foxg1* with *LacZ* and a neomycin cassette (Xuan et al., 1995). The expression of β-galatosidase is therefore under the control of the *Foxg1* promoter and this allows the expression of Foxg1 to be monitored by the expression of β-gatatosidase that can be measured using Beta-Glo assay (session 2.1.4) and Xgal staining (session 2.1.9). Another previously described cell line was 46C. This was generated by replacing *Sox1* with the coding sequence of GFP and also an internal ribosome entry site (IRES)-linked to the puromycin resistance gene (Ying et al., 2003b). This enables the expression of Sox1 in ES cells to be observed by fluorescence microscopy (session 2.1.10) and purified by fluorescence activated cell sorting (FACS) (session 2.1.5). Both cell lines were gifted historically to Nicholas Allen.

2.1.2 General culture conditions

2.1.2.1 ES media

Mouse ES cells were maintained in ES cell culture medium which consisted of knockout Dulbecco's modified eagle medium (D-MEM) (*Gibco, Invitrogen, Paisley, Scotland, UK*), supplemented with 15% knockout serum replacement (KSR) (*Gibco*), 1% penicillin/streptomycin (PS) (*Gibco*), non-essential amino acids (NEAA) (1 mM) (*Gibco*), L-glutamine (2 mM) (*Gibco*), β-mercaptoethanol (0.1 mM) (*Sigma, Gillingham, Dorset, UK*) and leukaemia inhibitory factor (LIF) (see section 2.1.3 for the preparation of LIF).

2.1.2.2 Chemically defined medium

Chemically defined medium (CDM) was used to generate neural progenitors from ES cells. It consisted of advanced DMEM/F-12 (ADF) (*Gibco*), 1× lipid concentrate (*Gibco*), 1% PS, glutamine (2 mM), 18 µg/ml transferrin (*Roche Applied Science, West Sussex, UK*), 14 µg/ml insulin (*Sigma*).

2.1.2.3 Splitting cells

Culture medium was aspirated off and cells were washed with Ca^{2+} and Mg^{2+} free phosphate buffered saline (PBS) pH 7.2 (*Gibco*). They were then lifted off the plate by adding accutase (*PAA laboratories, Farnborough, Hampshire, UK*) and left at 37°C for 15 minutes. The enzymatic action of accutase was slowed down by adding an equal volume of PBS. Cells were harvested from the culture dishes by centrifugation at 1000 rpm for 3 minutes.

2.1.2.4 Freezing cells

Cells were split as described in section 2.1.2.3 and re-suspended in freezing media which was made up of 10% dimethyl sulfoxide (DMSO) (*Sigma*) in ES cell culture medium. Cells were aliquoted at 2 x 10^6 cells per ml in cryovials (*Nunc*) and placed into a cryochamber with isopropanol at -80°C. After 24 hours, cryovials of cells were removed from the isopropanol and stored at liquid nitrogen cell storage tank.

2.1.2.5 Thawing cells

Cells were removed from -80°C and thawed in a water-bath at 37°C for 2-3 minutes before being transferred to ES cell culture medium and centrifuged at 1000 rpm for 3 minutes. The pellet was re-suspended in fresh ES cell culture medium and the cells were plated on gelatin-coated dishes.

2.1.2.6 Maintaining ES cells

ES cells were maintained on petri-dishes (*Nunc, Thermo Fisher Scientific, Loughborough, Leicestershire, UK*) coated with 0.1% gelatin in Ultrapure water (*Chemicon International, Walford, UK*). The medium was changed daily and cultures were split every 2-3 days as described in section 2.1.2.3 when they reached sub-confluency. After centrifugation, the pellet was re-suspended in ES cell culture medium and re-plated at 1.5 x 10^6 cells per 10 cm plate. Cell counts were performed by transferring 10 µl of cell suspension to a haemocytometer and viewed under a microscope. The number of cells per milliliter was determined by the average number of cells in four different squares on the haemocytometer.

2.1.2.7 Generating neural progenitors from ES cells

Neural differentiation of ES cells was induced by splitting ES cells as described in section 2.1.2.3. After centrifugation, the resulting pellet was plated onto gelatin-coated petri-dish (*Nunc*) at 1.17 × 10^4 cells per cm^3 in ES medium overnight. The following day, after 2 washes of Ca^{2+} and Mg^{2+} free PBS, ES cell culture medium was replaced with chemically defined medium (CDM). Medium was changed every 2 days. When cells needed to be differentiated for 20 days, they were split on day 6, day 10, day 14 and day 18 as described in section 2.1.2.3. The resulting pellet was plated on poly-L-ornithine (PLO) (*Sigma*) coated plates (*Nunc*) at 7 x 10^4 cells per cm^3 in CDM. Details of the growth factors and small molecules used for inducing neural differentiation in this study can be found in table 2.1.

Small molecules/growth factors	Suppliers	Stock solution
All-trans-RA	Sigma, UK	absolute ethanol
BMP4	Peprotech, *,USA*	0.1% BSA
Dorsomorphin (DM)	Sigma, UK	absolute ethanol
FGF2	Peprotech, *USA*	0.1% BSA
LDN193189 (LDN)	Stemgent,*, USA*	absolute ethanol
Noggin	Peprotech, *USA*	0.1% BSA
Purmorphamine	Calbiochem, *UK*	DMSO

Table 2.1 Suppliers and stock solutions of growth factors and small molecules

2.1.3 Preparation of LIF plasmid DNA for transfection

The LIF expression vector was kindly donated by Prof Vladimir Buchman. The expression vector (ampicillin resistant) was transformed into TOP 10 *E. coli* chemically competent cells (*Invitrogen*) and left on ice for 20 minutes. It then underwent a heat shock at 42°C for 1 minute and was transferred to ice for a further 2 minutes before 1 ml cultivation medium (*Invitrogen*) was added. The bacterial suspension was then transferred to a bacteriological tube (*Falcon, Becton Dickinson Labware, New Jersey, USA*) and left to shake at 37°C for 30 minutes. Subsequently, 100 µl bacterial suspension was streaked onto a selective agar and left at 37°C overnight.

An individual colony was selected using an inoculation loop, and transferred to a bacteriological tube containing 5 ml of Luria-Bertani (LB) media (*DIFCO; Becton Dickinson)* and ampicillin (150 µg/ml) (*Sigma*), and left to shake at 37°C overnight. A glycerol stock was made from the bacterial suspension by combining 600 µl of the bacterial suspension with 400 µl LB media: glycerol (1:1). The remainder of the bacterial suspension was centrifuged and maxi prep was performed on the resulting pellet, following instructions using the Qiagen endofree plasmid Maxi kit (*Qiagen, West Sussex, UK*). A sample of the resulting DNA was run on a 0.8% agarose gel and visualised with Safeview. The DNA was stored at -20°C in Tris-EDTA (TE) at 200 ng/µl.

For transfecting LIF plasmid DNA, COS (monkey renal epithelial) cells were used. Cells were maintained on T25 tissue culture treated flasks in COS culture medium which contains Glutamax DMEM (*Gibco*) supplemented with 10% fetal calf serum (FCS) (*Invitrogen*), L-glutamine (2 mM) and 1% PS. Medium was changed every 2-3 days and cells were passaged at 70-80% confluence. For passaging, medium was aspirated off, cells were washed in PBS, 0.1% trypsin-EDTA (*Gibco*) was added and cells were incubated at 37°C for 2-3 minutes. Cells were harvested, resuspended in COS culture medium and centrifuged at 1000

rpm for 3 minutes. The pellet was resuspended in COS culture medium and replated according to the desired ratio for splitting, usually 1.5 x 10^6 cells per T25 flask. Cells were transfected at 70% confluence using Lipofectamine transfection reagent (*Invitrogen*). After 24 hours, the transfection mix was removed and ES cell culture medium without LIF or PS was added and incubated at 37°C overnight. After a further 24 hours, the medium was collected into a 50 ml falcon tube and stored at 4°C. Another volume of ES cell culture medium without LIF or PS was added and incubated at 37°C overnight. After 24 hours, the medium was collected and combined with the medium collected 24 hours previously, the resulting 'LIF-conditioned media was stored at -20°C.

To determine the optimal concentration of LIF-conditioned medium for maintaining ES cell cultures. Cells were seeded at 2.5 x10^5 cells per cm^3 and 5 x 10^4 cells per cm^3 on gelatin-coated 6cm dishes (*Nunc*) with ES cell culture medium. LIF condition media at concentrations of 1:2000, 1:1000, 3:20000 and 1:500 were added into the ES cell culture medium. LIF prepared by Dr Sophie Precious was used as a positive control and medium with no LIF was used as a negative control. Medium was changed daily with replacement of the appropriate concentration of LIF conditioned medium. Each day, the cultures were checked microscopically and the concentration of LIF conditioned media that produced cells with comparable morphology with the positive control was chosen.

2.1.4 Beta-Glo assay

This assay quantified the activity of beta-galatosidase based on the principle that β-galactosidase cleaves the luciferin-galactoside substrate (6-O-β-galactopyranosyl-luciferin) in the assay to form luciferin. This in turn reacts with luciferase which produces oxyluciferin. Oxyluciferin emits a luminescent signal measurable by a plate reader. Foxg1Z ES cells were plated on 96-well plate as 2000 cells per well on day 6, day 10, day 14 and day 18. On the day of analysis, cells were lysed with the addition of 30 µl of reporter lysis buffer (*Promega, Southampton, UK*) onto each well for 15 minutes at room temperature. The lysate was then mixed with 30 µl of Beta-Glo reagent (prepared as described by manufacturer's instructions) (*Promega*). After 30 minutes, the plate was scanned by a scanning multiwell plate reader (Fluro *Optima, BMG labtech, Buckinghamshire, UK*) at 420 nm. 46C cells were used as a control for negative background luminescence and the readings recorded from these cells were subtracted from all those from Foxg1Z cells.

2.1.5 FACS analysis

2.1.5.1 Principles of a flow cytometer

Sox1/GFP expression of 46C cells was measured by a flow cytometer approach as this allowed rapid quantification of a large number of cells. When cell samples were introduced into a flow cytometer, they were ordered through a fluidic system, which consisted of a central channel containing the cell samples enclosed by an outer sheath fluid. The pressure of the flowing sheath fluid against the cells in the narrowing central channel created a velocity gradient in the flow front, forming a parabolic flow front and the greatest velocity was found at the centre while zero velocity was found at the wall. As a result, cells flowed in single file. This effect is called hydrodynamic focusing (Fig 2.1(a)). To obtain information on

the flowing cell samples, each single cell was analysed by lasers, which produced light at different frequencies. Light scattered in a forward direction is collected by a lens known as the forward scatter channel (FSC). This provided information about cell size as well as viable cells and cell debris. Light scattered perpendicular to the laser was collected by the side scatter channel (SSC), which provided information about granular content and cytoplasmic complexity of a cell (Fig. 2.1(b)). GFP was excited at 488 nm and detected by a number of fluorescence channels called photomultiplier. The specificity of detection was controlled by the use of optical filters which only permit passage of light with specific wavelengths (Carter and Ormerod, 2005).

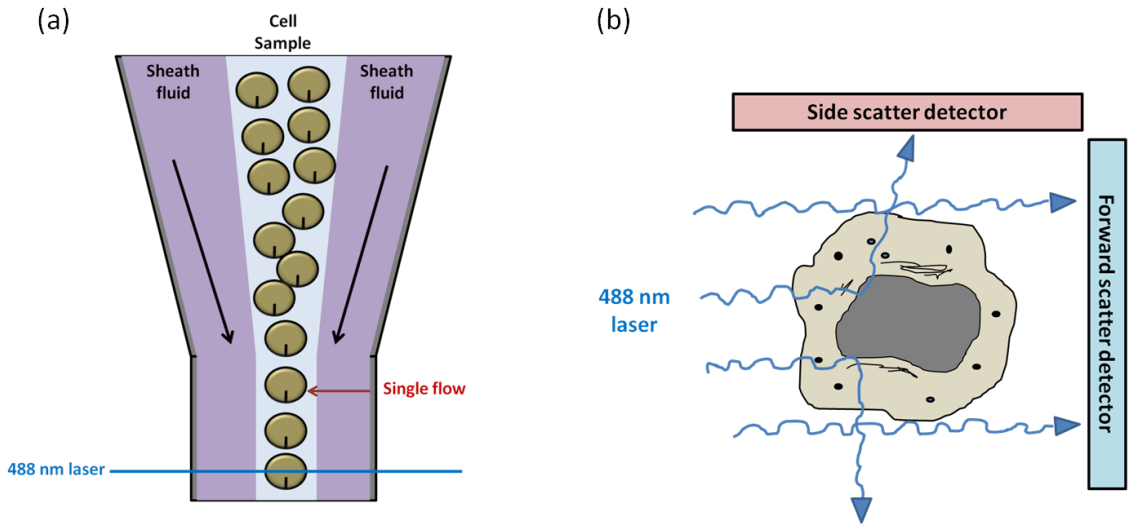

Figure 2.1 Cell flow in a flow cytometer

(a) Cell samples are focused hydrodynamically to produce a single stream of cell particles and are analysed by the 488 nm laser. Black arrows denote the direction of sheath flow.

(b) Light scattered in a forward direction is detected by the forward scatter channel which provides information about cell size; light scattered perpendicular to the laser is detected by the side scatter channel which provides information about granularity and cytoplasmic complexity.

2.1.5.2 Detection of fluorescence intensity

Colonies were dissociated as described in section 2.1.2.3. The resulting pellet was re-suspended in 1 ml of Ca^{2+} and Mg^{2+} free PBS and all samples were stored at 4°C until required. To detect fluorescence intensity, cells were passed through 30 µm filters (*Celltrics, Partec, UK*) into 12 mm FACS tubes (*Falcon, Becton Dickinson (BD) Biosciences, Oxford, UK*) and viewed on a BD FACS Canto flow cytometer (*BD Biosciences*). The BD FACS Canto is a dual laser bench top flow cytometer equipped with 633 nm and 488 nm lasers and BD FACS Diva software (v 5. 0. 3). Single colour analysis was performed on 46C cells that express GFP.

To control for GFP expression, undifferentiated 46C cells were used in chapter 3 and Foxg1Z cells were used in chapter 5.

2.1.5.3 Cell sorting

Cells were prepared as previously described for the flow cytometry analysis. Cells were analysed using a three-laser BD FACS Aria (*BD Biosciences*), equipped with 633 nm, 488 nm and 370 nm lasers and BD FACS Diva software (v 5. 0. 3) for FSC and SSC as described previously. Foxg1Z cells were used to set background fluorescent levels. Bimodal and trimodal distributions were observed in each case and the brightest subpopulation was denoted GFP positive. Cells that were less intensely fluorescent were denoted GFP negative. All data collected was analysed by FlowJo 7.6.4 software. Both populations were sorted and total RNA isolated using RNeasy Mini kit (*Qiagen*).

2.1.6 Immunocytochemistry

Immunochemistry was performed in order to detect specific protein antigens in cell cultures. On the day of analysis, medium was discarded, cells washed with PBS and fixed with 4% paraformaldehyde (PFA) at 4°C for 15 minutes followed by 3 washes with PBS. Information about the concentration of primary and secondary antibodies can be found in table 2.3.

To prevent unspecific antibody binding, blocking solution which included 2% goat serum (*Dako, Cambridgeshire, UK*) and 3% BSA in PBS solution was added for 2 hours at room temperature. Cells were then incubated overnight at 4°C with primary antibody in blocking solution. If double staining was performed, both antibodies raised in different species were added at the same time. Primary antibodies were removed and after 3 washes in PBS, cells were incubated with secondary antibody in blocking solution for 1 hour at room temperature. Secondary antibodies were removed and 3 washes with PBS carried out.

Hoescht nuclear stain was applied for 1 hour at room temperature. After 3 washes of PBS, cover-slips were mounted onto glass microscope slides using PBS : glycerol (1:1) and sealed with clear nail varnish and stored at 4°C.

Fixative (4% paraformaldehyde)
4 g PFA
100 ml of 1X PBS
Heat with addition of NaOH
Titrate until pH7-8

Table 2.2 Preparation of 4% paraformaldehyde

Primary antibody	Species	Supplier	Cat. No.	Dilution
Foxg1	Rabbit	Abcam	Ab18259	1:2000
GFAP	Rabbit	Abcam	Ab7260	1:2000
HoxB4	Mouse	DSHB	CloneI12	1:5
nestin	Mouse	DSHB	Clone Rat-401	1:5
p75	Rabbit	Promega	G3231	1:500
Pax6	Mouse	DSHB	Clone 1-223	1:5
β-galactosidase	Mouse	DSHB	Clone 40-1a	1:5
β-III-tubulin	Rabbit	Abcam	Ab18207	1:1000

Secondary antibody	Supplier	Cat. No.	Dilution
anti-rabbit α 594	Invitrogen	A11037	1:200
anti-mouse α 594	Invitrogen	A11032	1:200
anti-mouse α 488	Invitrogen	A10667	1:200

Table 2.3 Information about antibodies used in fluorescence immunocytochemistry

2.1.7 Wst-1 mitochondrial activity assay

Cell proliferation reagent WST-1 (*Roche*) was used to determine the relative number of metabolically active cells. The assay works by measuring the amount of formazan produced by metabolically active cells in the culture. The formazan produced is dark red in colour and can be measured at 450 nm. The readings obtained at 450 nm was normalised by absorbance at 590 nm. Cells were grown on a 24-well plate and Wst-1 reagent was added at 1:25 dilution on day 6 of differentiation. After 3-4 hours of incubation at 37°C, 100 µl of each sample was transferred to a 96-well plate and scanned by a scanning multiwall spectrophotometer (*Fluro Optima, BMG Labtech*).

2.1.8 Western blotting

2.1.8.1 Protein extraction from cells in monolayer culture

Western blotting was performed to detect phosphorylation of Smad1/5/8 and expression of β-actin. Confluent 6 cm dishes were washed with cold PBS and placed on ice. Ice-cold lysis buffer (300 µl) (RIPA buffer from *Sigma*) which contained phosphatase inhibitor (*Sigma*) and protease inhibitor (*Roche*) was added. Cells were incubated for 30 mins at 4°C with intermittent agitation after which they were centrifuged for 20 mins at 4 °C at 12,500 rpm. The supernatant was transferred to a fresh tube and the pellet was discarded. Samples were stored as aliquots at -80 °C.

2.1.8.2 Determination of protein concentration

A standard was prepared using a dilution series of BSA ranging from 25 µg per ml to 2 mg per ml, and 25 µl of each standard was triplicated, alongside 25 µl of the samples. The bicinchonnic acid (BCA) working reagent from the Pierce BCA Protein Assay kit (Cat No. 23227, Thermo Scientific) was prepared as recommended by the manufacturer and 200 µl of working reagent was added to each sample and mixed thoroughly on a plate shaker for 30

seconds. The plate was incubated at 37°C for 30 minutes and cooled to room temperature. The absorbance was read at 590 nm using a scanning multiwall spectrophotometer (*Fluro Optima, BMG Labtech*).

2.1.8.3 Western blot

A polyacrylamide resolving gel (10%) was prepared and left to set with distilled water layered on the surface. The water was removed and replaced with a stacking gel and left to set with the correct comb size. Laemellis loading buffer (*Sigma*) was added to the protein at a 1:1 ratio and incubated at 95°C for 5 minutes to denature the protein samples. Samples were loaded alongside a full range rainbow ladder (*GE Healthcare, UK*) and run at 50 mA until the dye front reached the bottom of stacking gel followed by a current of 100 mA until the dye front reached the base of the resolving gel.

The protein bands were then transferred to a membrane by electroblotting. To carry this out, Hybond ECL membrane (*GE Healthcare*) was soaked in distilled water briefly and then in transfer buffer (TBS) for 10 minutes. After that, the gel and the membrane were layered between two sponges and pieces of filter paper and soaked in transfer buffer. The transfer was carried out at 50mA for 1 hour at room temperature. The membrane was then carefully removed, rinsed in TBS-Tween (TBST) and blocked with 1% (w/v) milk (*Marvel, UK*) for 1 hour, followed by incubation with 1:1000 dilution of rabbit polyclonal Smad1/5/8 antibody (*Cell Signaling Technologies, Boston, USA*) or 1:10000 dilution of rabbit monoclonal antibody (*Cell Signaling Technologies*) in 1% milk in TBST. The membrane was then washed three times with TBST at room temperature. This was then followed by incubation with a 1:10000 dilution of goat anti-rabbit IgG, horseradish peroxidase-conjugated secondary antibody (*Cell Signaling Technologies*) in 1% (w/v) milk in TBST for 1 hour at room temperature. The membrane was then washed three times with TBST for 20 minutes each. Information about making polyacrylamide resolving gel and TBS can be found in table 2.4.

Detection was performed by placing the membrane in a developing cassette and coating the membrane with 0.5 ml of SuperSignal West Dura Stable peroxide buffer (*Thermo Scientific, Massachusetts, USA*) mixed as directed by manufacturer's instructions. The solution was poured off and Chemiluminescent film (*Roche*) was placed over the membrane and exposed for various time intervals. Band intensity was quantified by QuantiScan (*Bio Soft, Cambridgeshire, UK*).

Polyacrylamide resolving gel		Transfer buffer (TBS)	
Acrylamide	10%	Tris base	0.25 M
Tris pH 8.8	0.37 M	Glycine	1.92 M
SDS	0.1%	Methanol	20%
Ammonium persulphate	0.1%		
TEMED	0.6%		

Table 2.4 Preparation of polyacrylamide resolving gel and transfer buffer

2.1.9 X-gal staining

5-Bromo-4-chloro-3-indolyl galactopyranoside (X-gal) staining was performed to visualize positive population of Foxg1/LacZ cells as β-galatosidase cleaves X-gal and yields a blue product. To perform the assay, cells were washed with PBS (with Ca^{2+} and Mg^{2+}) (*Gibco*) and fixed with 1% formalin for 5 minutes at 4°C. Cells were then washed with PBS (with Ca^{2+} and Mg^{2+}) and incubated with X-gal staining solution (5 µl of X-gal was used in every 1 ml of Ferro/Ferri-cyanide solution) at 37°C overnight in the dark. X-gal staining solution was removed and the cells were fixed in 4% formalin for 15 minutes after 3 PBS (with with Ca^{2+} and Mg^{2+}) washes. Information about making X-gal and ferro/ferri-cyanide solution can be found in table 2.5.

X-gal		Ferro/Ferri-cyanide solution	
X-gal	0.5 g	Ferricyanide	0.825 g
N,N-dimethylformamide	0.5 ml	$MgCl_2$	0.2 g
		PBS	495 ml
		(stored at 4°C in the dark)	

Table 2.5 Preparation of X-gal reagents

2.1.10 Microscopy

For immmunocytochemistry, cells were visualized under UV fluorescence using the Leitz microscope and Olympus BX61 microscopes at different wavelengths (560 nm-red; 494 nm-green; 346 nm-blue). Images were processed using Optronics magnaFire Software and Adobe Photoshop.

2.2 Molecular methods

2.2.1 RNA extraction

Cells were washed with Ca^{2+} and Mg^{2+} free PBS and RNA was extracted using Qiagen RNeasy Mini Kit, RNase-free Dnase set and QiaShredder (*all from Qiagen, West Sussex, UK*). After RNA is extracted, the amount of RNA was measured by NanoDrop ND1000 spectrophometer (*Labtech International*), which measures RNA concentration at 260 nm. Purity of RNA was assessed by the absorbance at 260 nm and 280 nm.

2.2.2 cDNA synthesis

For first strand synthesis, Dnase-treated RNA was incubated with random primers (*Invitrogen*) and 10 mM dNTP mix for 5 minutes at 65°C. After it had been ice-chilled, 5X first strand buffer, 0.1 M DTT and RNase Out Rnase Inhibitor (*all from Invitrogen*) were added and incubated for 2 minutes at 25°C. Superscript II (*Invitrogen*) was then added and incubated for 10 minutes at 25°C, followed by incubations at 42°C for 50 minutes and 70°C for 15 minutes. cDNA produced in this process was used for RT-PCR analysis.

2.2.3 RT-PCR: Reverse Transcription-Polymerase Chain Reaction

Reverse transcription-polymerase chain reaction (RT-PCR) was used to amplify DNA sequences. Each 50 µl reaction contained Go Taq DNA polymerase (*Promega*), 5X green flexi buffer (*Promega*), 25 mM $MgCl_2$ solution (*Promega*), 10mM dNTP, oligo pairs at 10 pmol each and water (*Qiagen*). Each PCR cycle included an initial denaturation step at 94°C for 30 seconds, an annealing step at 55°C for 30 seconds and an extension step at 72°C for 2 minutes. PCR products were analysed by electrophoresis on a 1.8% agarose gel with

Safeview (*NBS Biologicals, Cambridgeshire, UK*) added to visualise the products. The gel was run at 80 V for 40 minutes in 1 mM TAE buffer which consisted of Tris base, acetic acid and ethylene diamine tetra acetic acid (EDTA). To normalize variations in the quantities of input cDNA, the amount of transcript was normalized against the level of GAPDH. Band intensity of the PCR products was measured by Gel Doc 2000 (*Bio-Rad Laboratories, Hertfordshire, UK*).

2.2.4 Primer sequences

Primer pairs were generated using *Mouse Genome Informatics* and *Ensembl* for sequence information, and *Primer 3 Input for primer design*. All primer sequences are listed in table 2.6. They are of 19-25 base pairs (bp) in length and generate transcripts of 200 to 600 bp.

primer	forward sequence	reverse sequence	Product size (bp)
CK18	agattgccagctctggattg	gttctccaagttgatgttctgg	287
Emx2	gacctcagacgattaaaagtcc	gcatttgactgacagctcc	406
En2	gactcggacagctctcaagc	acactggccttttgttcacg	510
Foxg1	gggcaacaaccactccttctccac	gacccctgattttgatgtgtgaaa	396
GAPDH	accacagtccatgccatcac	tccaccaccctgttgctgta	452
HoxB3	tggaaaggaatccacagc	gcagaaaaccaaccgtagg	407
Mash1	cgtcctctccggaactgat	tcctgcttccaaagtccatt	482
Nestin	agtcagagcaagtgaatgg	agaaacaagatctcagcagg	600
Ngn2	gatgccaagctcacgaagat	ggagacgagagagggagacc	387
Nkx2.1	gtcgatgagtccaaagcaca	cgatgttccgcatggtgtc	320
Oct4	cgcgttctctttggaaaggtgttc	ctcgaaccacatccttctct	313
Pax6	ctgtaccaacgataacatacc	cccttcgattagaaaacc	455
Ptc1	ctccgcacagagtatgacc	agtcactgtcaaatgcatcc	598

Table 2.6 Primer sequences used for RT-PCR analysis

2.3 Statistical analysis

Statistical analyses were performed using Minitab 16 statistical software. Parametric data was analysed using a paired t-test, the two-sample t-test and the Tukey-Kramer test for *post-hoc* comparisons after one-factor analysis of variance (ANOVA) was performed. For non-parametric data, the Mann-Whitley *U* test was performed for paired comparisons and the Krustal-Wallis test was carried out.

CHAPTER 3:

INVESTIGATION OF THE PHARMACOLOGICAL INHIBITION OF BONE MORPHOGENIC PROTEIN SIGNALLING IN EMBRYONIC AND NEURAL PROGENITOR CELLS

3.1 Introduction

This chapter examines whether two newly discovered BMP chemical inhibitors, Dorsomorphin (DM) and its derivative LDN193189 (LDN), can replace recombinant noggin in the neural induction of mouse ES cell cultures. Noggin inhibits the BMP signalling pathway by binding to the BMP ligands and preventing them from binding to their receptors (Sasai and DeRobertis, 1997). *In vivo*, noggin is released from the organiser (Lamb et al., 1993, Smith and Harland, 1992, Smith et al., 1993) in *Xenopus* or the node in mouse (Bachiller et al., 2000). It promotes neural specification of ectodermal cells (Hemmati-Brivanlou and Melton, 1994, Reversade et al., 2005), regulates the BMP levels during neural tube closure (Ybot-Gonzalez et al., 2007) and the development and patterning of the ventral neural tube (McMahon et al., 1998).

In vitro, BMP inhibition has been demonstrated to enhance the neural induction of ES cells. Previous studies showed that the number of neural colonies generated from ES cell increased by at least 50% in the presence of noggin (Tropepe et al., 2001, Okada et al., 2008) or 3-4 folds from Smad4$^{-/-}$ ES cells (Tropepe et al., 2001). When Smad4$^{-/-}$ ES cells were encouraged to undergo neuronal differentiation by plating onto poly-L-orithine coated plates, they generated 13% more nestin positive cells and 16% more β-III-tubulin positive cells than wild-type control ES cells (Tropepe et al., 2001), and similar results were obtained with noggin treated-ES cells (Okada et al., 2004). Smad4$^{-/-}$ cells differentiated as embryoid bodies (EBs) gave a higher expression of tyrosine hydroxylase (TH), which is expressed in dopaminergic neurons (Sonntag et al., 2005) . This indicated that BMP inhibition can effectively enhance neural induction of ES cells.

Since evidence has shown that BMP inhibition can enhance the generation of neural and neuronal cells, recombinant noggin was used in to promote differentiation of mouse ES cells towards the neural lineage to generate motoneurons (Wu et al., 2012) and GABAergic

neurons (Okada et al., 2008). However, recombinant proteins usually have a short shelf-life and batch-to-batch differences (Burton et al., 2010). This can affect the reproducibility of results. In order to reproducibly generate neural progenitor cells and also for scaling up cultures, replacing the expensive and unstable recombinant noggin with chemical inhibitors would provide a great advantage because of the potential for cost effectiveness, reproducibility and scalability (Burton et al., 2010).

Dorsomorphin (DM) is the first reported chemical inhibitor that inhibits BMP signalling and caused severe dorsalization in zebrafish. DM specifically inhibits BMP type I receptors and blocks BMP mediated Smad 1/5/8 phosphorylation (Yu et al., 2008). Hence, this chemical compound can be used to study the effect of BMP inhibition on the neural induction of mouse ES cells. LDN193189 (LDN) was a more recently developed chemical compound for inhibiting the BMP pathway and was designed to be more stable and potent than DM by altering the pendent-4-pyridine ring to 4-quinoline (Cuny et al., 2008). The half maximal inhibitory concentration (IC_{50}) of DM and LDN for BMP receptor type-I activin receptor-like kinase 2 (ALK2/BMPR1) is 148.1 nM and 40.7 nM respectively, indicating that the LDN is more potent than DM and has a greater specificity for BMPR1 (Hao et al., 2010).

The similarity in the inhibitory actions of DM, LDN and noggin found in *in vivo* models suggested that they could be used as substitutes for recombinant noggin in neural differentiation protocols. Hence, this chapter deals with the actions of DM and LDN on the neural differentiation of mouse ES cells and compared their actions with those of recombinant noggin. The ES cell line used in this study was 46C and is a Sox1 reporter cell line. The open reading frame of Sox1 of this cell line has been replaced with the coding sequence of green fluorescence protein (GFP) and an internal ribosome entry site (IRES)-linked puromycin resistance gene (Ying et al., 2003b), thus allowing easy measurement of Sox1 locus expression using flow cytometry and fluorescence microscopy. The 46C ES cell line was first used in Ying et al.'s study and they generated 60% of

Sox1-positive cells on day 4 of differentiation (Ying et al., 2003b). Sox1 expression represents the generation of neural progenitors because it is one of the earliest neural markers expressed when ES cells undergo neural differentiation (Ying et al., 2003b, Bouhon et al., 2005). In mouse, Sox1 was reported to be involved in directing the acquisition of neural fate in the ectoderm (Pevny et al., 1998) and is important for maintaining stem cell character of neural progenitor cells (Bylund et al., 2003). To ensure cells had more uniform exposure to DM, LDN and noggin treatments, ES cells were differentiated as adherent monolayer, based on the adherent monolayer protocol developed by Ying and co-workers (Ying et al., 2003b). Modification of the adherent protocol was made by plating ES cells in ES medium with LIF overnight rather than plating them directly in CDM to allow for better plating efficiency. ES cells were differentiated in chemically defined media (CDM) described in Bouhon et al. 's study to minimize the influence of exogenous signals (Bouhon et al., 2005).

3.2 Results

3.2.1 Phosphorylation of Smad 1/5/8 of undifferentiated ES cells treated with DM, LDN and noggin

Before examining the effect of DM and LDN on the neural specification of ES cells, it was necessary to check whether DM and LDN acted as BMP inhibitors in undifferentiated ES cells and antagonised phosphorylation of Smad1/5/8. The pluripotency of undifferentiated mouse ES cells is maintained through active autocrine BMP signalling by the expression of both BMP4 and BMP receptors (Ying et al., 2003a, Bertacchi et al., 2013). The antagonism of Smad phosphorylation by LDN and DM could thus be tested directly. Strong Smad 1/5/8 phosphorylation was found in untreated ES cells, confirming that BMP signalling was active in the undifferentiated ES cells (Lane 7 in Fig. 3.1(a) and Lane 1, Fig. 3.2(a)). To test the effects of DM and LDN, cells were treated with increasing doses of LDN and DM for 24 hours maintained in the presence of LIF. The results showed that phosphorylation of Smad1/5/8 was reduced in LDN-treated samples and DM-treated samples in a dose-dependent manner. LDN was more potent than DM in antagonising BMP signalling in undifferentiated ES cells, because higher doses of DM were required to reduce phosphorylation to a level comparable with that observed in noggin treatment (Figs. 3.1 and 3.2).

(a)

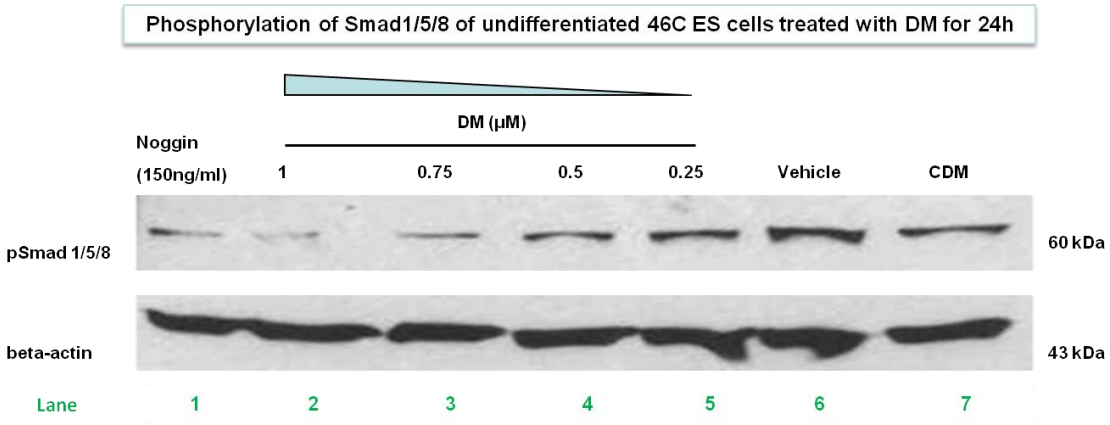

(b)

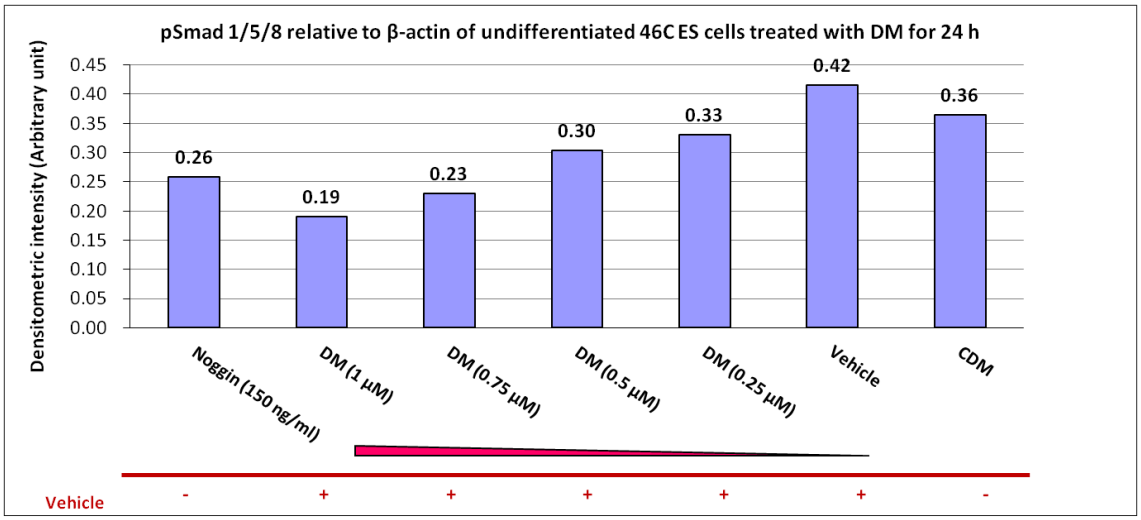

Figure 3.1 Western blotting of undifferentiated 46C ES cells treated with DM and noggin

(a) Undifferentiated 46C ES cells were treated with DM (0.25 μM, 0.5μM, 0.75μM, 1μM) for 24 hours in CDM in the presence of LIF. Protein was extracted and phosphorylation of Smad 1/5/8 was detected by Western blotting. Ethanol (0.1 %) was used as a vehicle control for DM. Noggin (150 ng/ml) was used as a positive control for phosphorylated Smad1/5/8 inhibition. Equal loading was confirmed by β-actin.

(b) Band intensity of phosporylated Smad1/5/8 was quantified by QuantiScan and was expressed as a value relative to β-actin expression (n=1).

(a)

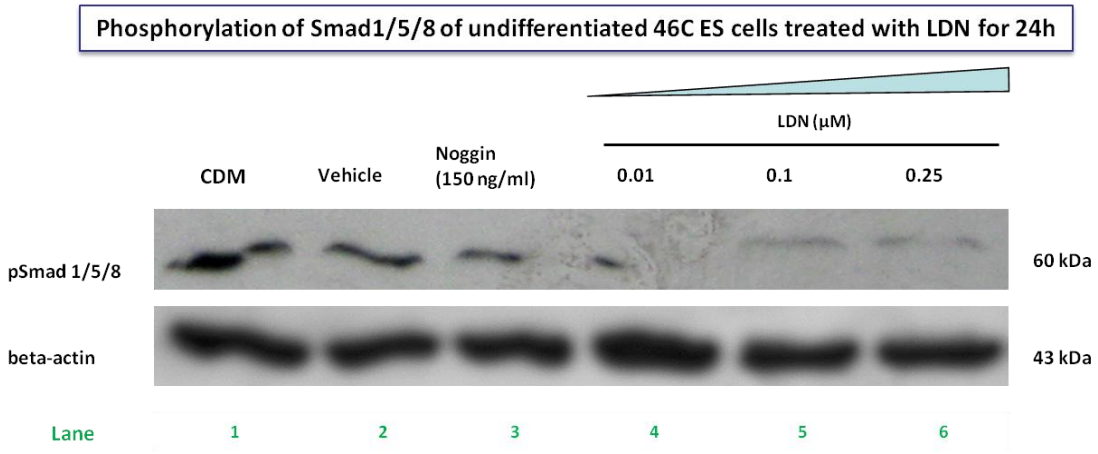

(b)

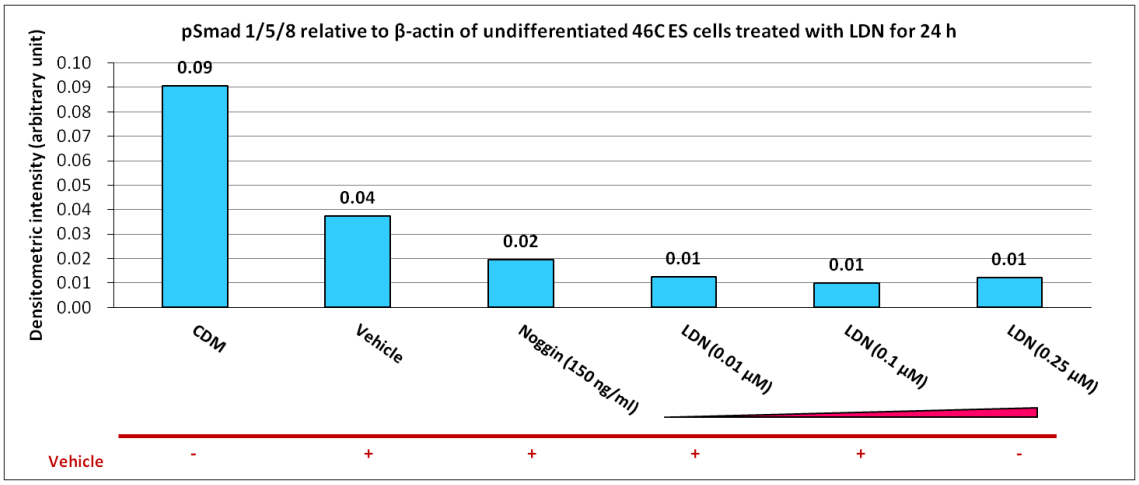

Figure 3.2 Western blotting of undifferentiated 46C ES cells treated with LDN and noggin

(a) Undifferentiated 46C ES cells were treated with LDN (0.01 μM, 0.1 μM, 0.25 μM) for 24 hours in CDM in the presence of LIF. Protein was extracted and phosphorylation of Smad 1/5/8 was detected by Western blotting. Ethanol (0.1 %) was used as a vehicle control for LDN. Noggin (150 ng/ml) was used as a positive control for phosphorylated Smad1/5/8 inhibition. Equal loading was confirmed by β-actin.

(b) Band intensity of phosporylated Smad1/5/8 was quantified by QuantiScan and was expressed as a value relative to β-actin expression (n=1).

3.2.2 Effect of cell plating density on neural differentiation

Studies in the past have shown that ES cells undergo neural differentiation at optimal cell plating densities. For instance, Tropepe et al. found that if the cell plating density was increased from 10 cells/µl to 50 cells/µl, the percentage of nestin immolabelled cells would be decreased from 82% to 40% after 24 hours of plating (Tropepe et al., 2001). In another study, Watanabe et al. showed that the percentage of Sox1 positive cells increased from 60% to 85% when the cell plating density was increased from 0.5 x 10^4 cells/ml to 5 x 10^4 cells/ml, and the percentage of Sox1 positive cells decreased from 85% to 55% when the cell plating density was decreased from 5 x 10^4 cells/ml to 50 x 10^4 cells/ml after 2 days of plating (Watanabe et al., 2005). In view of this, it was necessary to find out what is a suitable plating density for ES cells for generating neural progenitors.

To determine the effect of cell plating densities on the generation of neural progenitors, ES cells were plated from 500 cells/cm^2 up to 5000 cells/cm^2 and differentiated in CDM. On day 6 of the differentiation, cells were dissociated into single cell suspension and the percentage and intensity of Sox1/GFP-expressing cells were analysed by flow cytometry.

Cells introduced in a flow cytometer were analysed for forward scatter (FSC) and side scatter (SCC). FSC is a measure of relative cell size while SSC is a measure of relative cellular granularity. Density dotplots of SSC against FSC were generated, and voltages for SSC and FSC were adjusted so that all the recorded cell events were shown on the density plots. A gate (G1) was generated to exclude cell debris (which usually has low SSC and low FSC values) and cell aggregates (which usually have high SSC and high FSC values) (Fig. 3.3 (a)). The subpopulation that was included in the G1 gate was analysed for Sox1/GFP expression. Single parameter histograms were generated to show the relative fluorescence intensity on the x-axis and cell count on the y-axis, and the voltage was adjusted so that the negative control sample for GFP expression (i.e. undifferentiated 46C ES cells) was set to the second logarithmic decade (Fig 3.3 (b)).

For each analysis, a histogram of undifferentiated ES cell samples was overlaid with histogram of the treated cell samples. Sox1/GFP expression for each treated sample was assessed according to fluorescence intensity and the percentage of expressing cells. If the treated sample displayed a unimodal distribution of fluorescence intensity, the intensity of Sox1/GFP expression was determined by comparing the geometric mean fluorescence intensity (MFI) of the treated cells with that of undifferentiated ES cells. The percentage of Sox1/GFP expression was considered to be 100% if the entire population of the treated samples shifted and had higher GFP intensity than undifferentiated samples (Fig. 3.3 (c)). If the treated sample displayed a bimodal distribution of fluorescence intensity, the population was divided into positive and negative subpopulations, and was defined by placing a delineator at the limit of the undifferentiated sample (between 0.5% to 1%). Cells that were found above this level were considered to be positive. The fluorescence intensity of Sox1/GFP was determined by comparing the MFI of positive subpopulation with that of negative subpopulation. The percentage Sox1/GFP expression was determined by the positive subpopulation (Fig. 3.3 (d)) (Richardson, 2011).

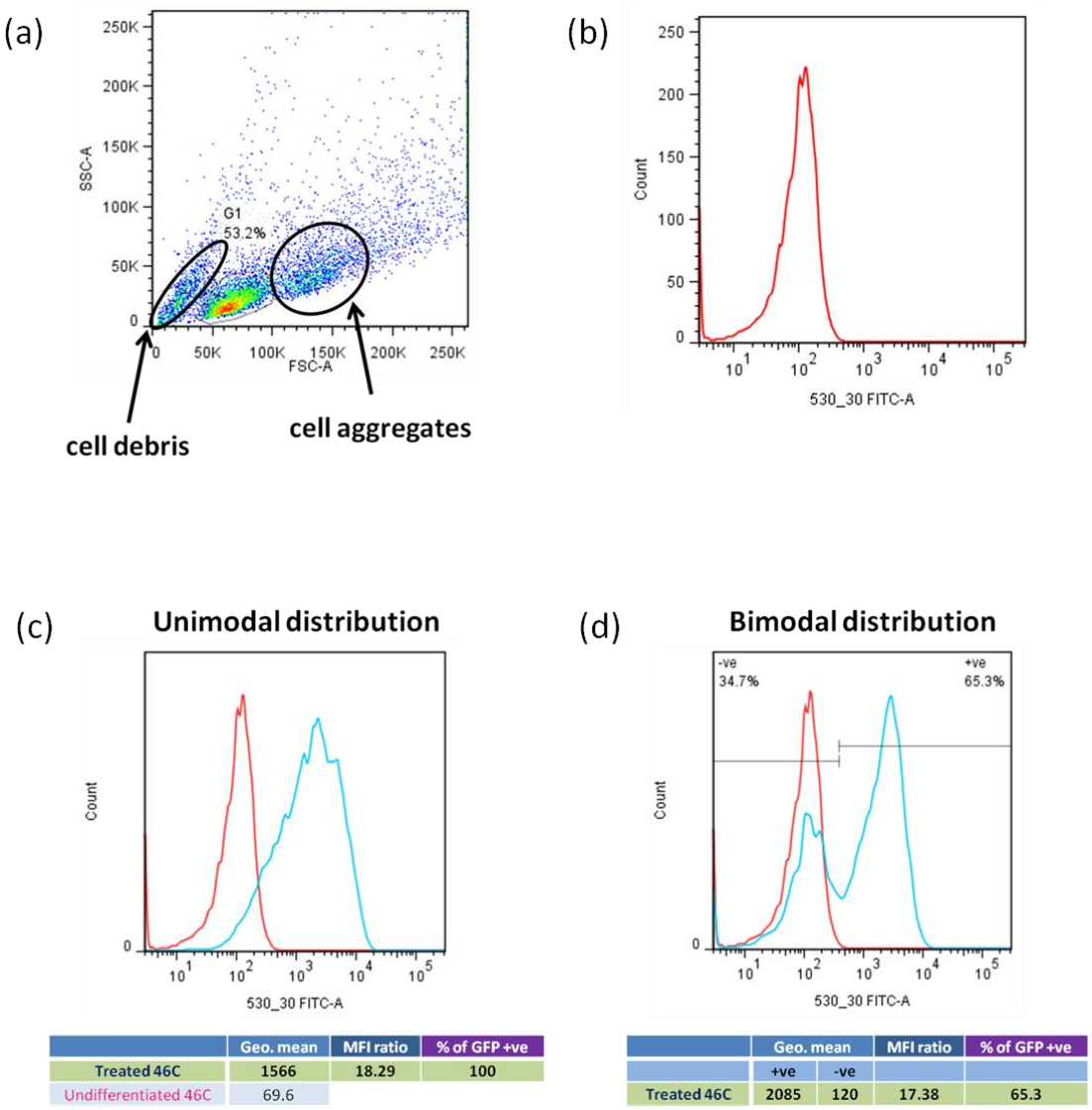

	Geo. mean	MFI ratio	% of GFP +ve
Treated 46C	1566	18.29	100
Undifferentiated 46C	69.6		

	Geo. mean		MFI ratio	% of GFP +ve
	+ve	-ve		
Treated 46C	2085	120	17.38	65.3

Figure 3.3 Gating strategies for flow cytometry analysis

(a) A density dotplot of side scatter (SSC) against forward scatter (FSC) illustrating cell population included in gate (G1) for Sox1/GFP expression analysis. Cell debris (low SSC and low FSC) and cell aggregates (high SSC and high FSC) were not included in the G1 gate. Red pixels represent the population with the highest cell density and blue pixels represent the population with the lowest cell density.

(b) A histogram showing cell count against fluorescent intensity for the negative control sample (undifferentiated 46C ES cells) for GFP expression. Voltages were adjusted so that the median fluorescence was close to the second logarithmic decade.

(c) A histogram showing the fluorescence intensity of the negative control sample (red line) and treated sample that displays unimodal distribution (blue line). Geometric mean (Geo. mean) fluorescence value, MFI ratio and percentage of GFP expression of the corresponding sample are shown on the table.

(d) A histogram showing the fluorescence intensity of a negative control sample (red line) and a treated sample that displays bimodal distribution (blue line). Geo. mean fluorescence value, MFI ratio and percentage of GFP expression of the corresponding sample are shown in the tables.

The MFI values of Sox1/GFP expressing cells plated at different cell densities were normally-distributed and displayed equal variance, hence parametric one-way ANOVA statistical analysis was performed. The effect of cell plating density on MFI was significant overall (one-way ANOVA, $F_{3,8} = 5.21$, $P = 0.028$). A significant difference was found between the lowest and the highest cell plating densities (500 cells/cm^2 and 5000 cells/cm^2) when the Tukey-Kamer test was performed ($P < 0.05$). The Tukey-Kamer test is a post-hoc statistical test for determining individual significance between samples after performing an ANOVA test. Cells plated at 2500 cells/cm^2 and 5000 cells/cm^2 that were Sox1/GFP negative, and hence neither of these cell plating densities were used in subsequent differentiation experiments. Cells plated at 500 cells/cm^2 and 1250 cells/cm^2 generated 100% of Sox1/GFP positive cells. Although the mean MFI value was higher at 500 cells/cm^2, very few colonies were found at this plating density, which could be a problem if cells were subjected to further treatments. Therefore, the second lowest cell plating density of 1250 cells/cm^2 was used in the subsequent experiments (Fig. 3.4).

(a)

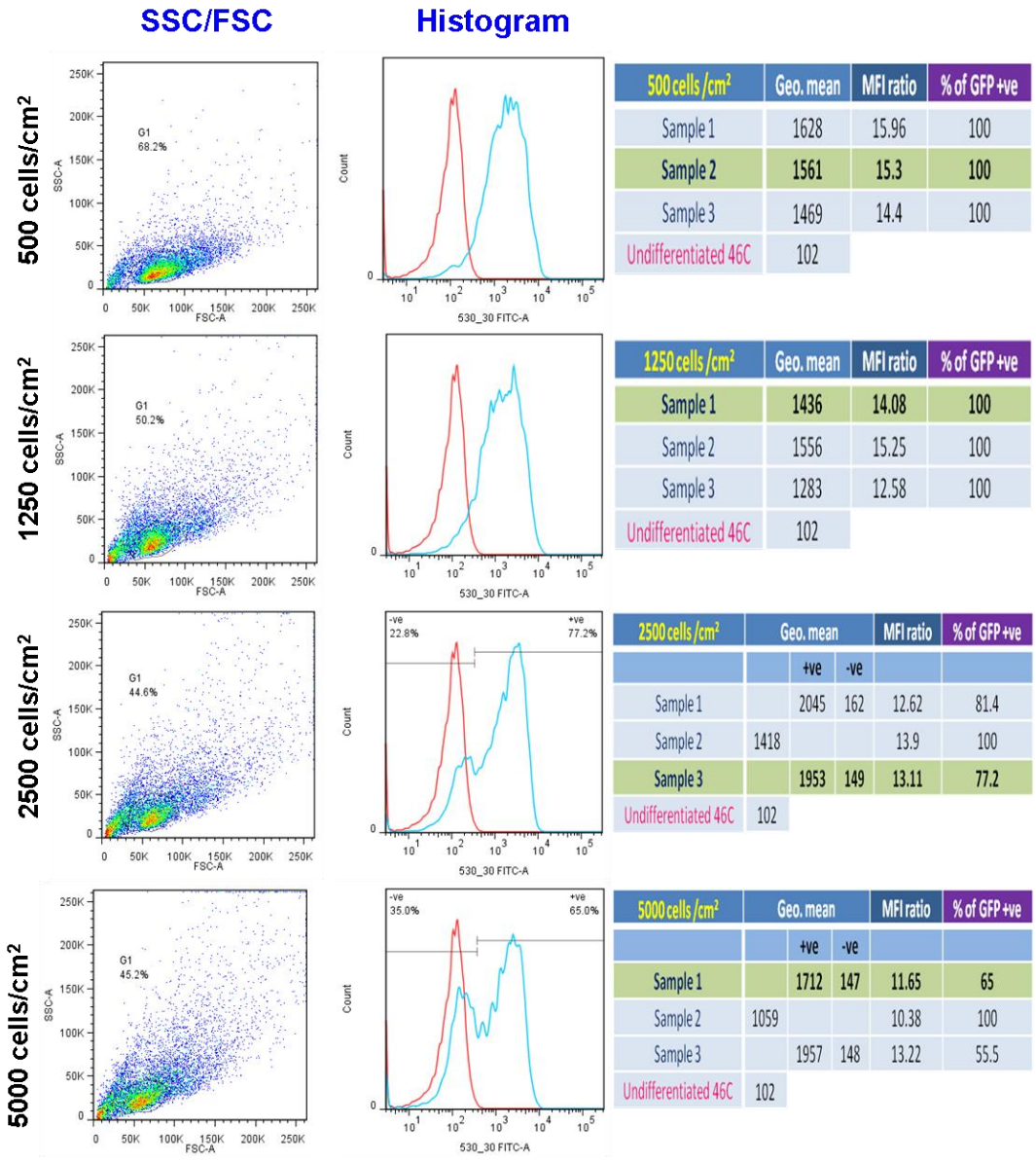

500 cells /cm²	Geo. mean	MFI ratio	% of GFP +ve
Sample 1	1628	15.96	100
Sample 2	**1561**	**15.3**	**100**
Sample 3	1469	14.4	100
Undifferentiated 46C	102		

1250 cells /cm²	Geo. mean	MFI ratio	% of GFP +ve
Sample 1	**1436**	**14.08**	**100**
Sample 2	1556	15.25	100
Sample 3	1283	12.58	100
Undifferentiated 46C	102		

2500 cells /cm²	Geo. mean		MFI ratio	% of GFP +ve
		+ve	-ve		
Sample 1		2045	162	12.62	81.4
Sample 2	1418			13.9	100
Sample 3		**1953**	**149**	**13.11**	**77.2**
Undifferentiated 46C	102				

5000 cells /cm²	Geo. mean		MFI ratio	% of GFP +ve
		+ve	-ve		
Sample 1		**1712**	**147**	**11.65**	**65**
Sample 2	1059			10.38	100
Sample 3		1957	148	13.22	55.5
Undifferentiated 46C	102				

Figure 3.4 Mean fluorescence intensity (MFI) and percentage of Sox1/GFP expression of 46C cells plated at different cell densities

(a) 46C ES cells were plated at different cell plating densities (500 cells/cm^2, 1250 cells/cm^2, 2500 cells/cm^2, 5000 cells/cm^2) and differentiated in CDM for 6 days. Cells were dissociated and analysed by flow cytometry. Cells were gated in G1, excluding clumped cells and debris. The percentage of cells included in the G1 gate is shown on the SSC/FSC plots. The fluorescent intensity of undifferentiated 46C ES cells (red line) and differentiated 46C cells (blue line) is shown on the histograms. The bimodal distribution is divided into +ve and -ve cell populations. Tables show the percentage of Sox1/GFP expressing cells, the geometric mean (geo. mean) fluorescence value and MFI ratio of each sample acquired. The highlighted regions (in green) indicate the samples represented in the SSC/FSC plots and the histograms.

(b)

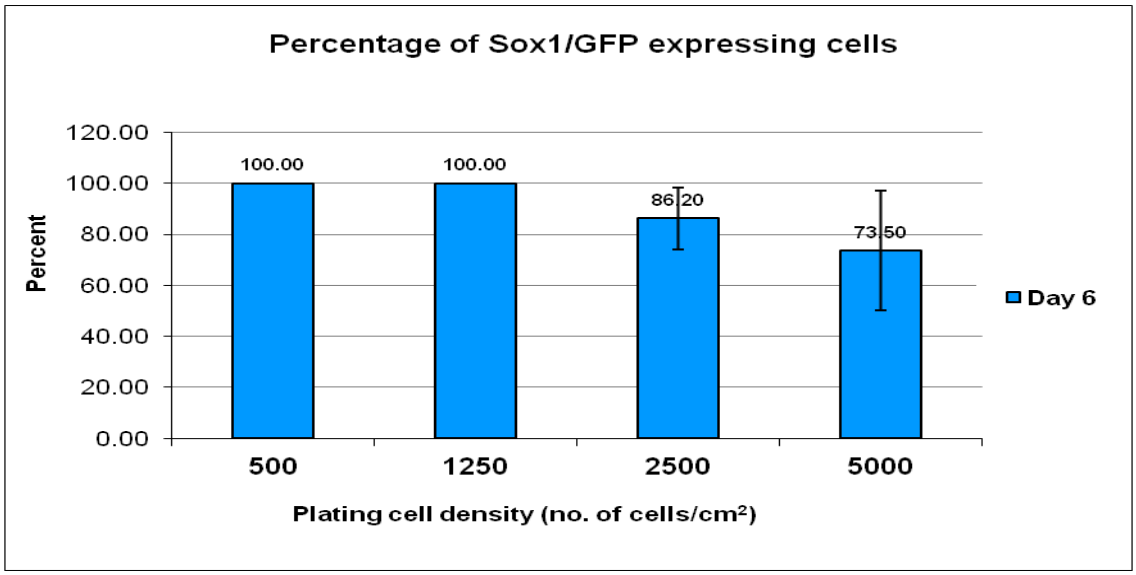

(c)

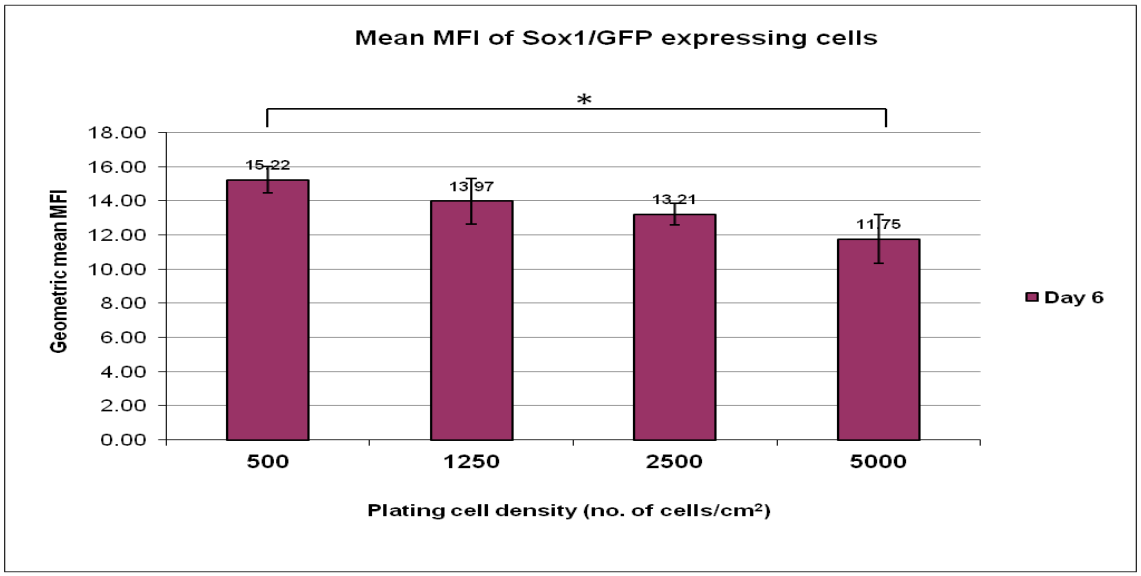

(b) The graph illustrates the mean percentage of Sox1/GFP expressing cells on day 6 of neural differentiation for each plating cell density. Bars represent the mean ± standard deviation (S.D.) of three independent experiments. (Krustal-Wallis test, $P = 0.273$)

(c) The graph illustrates the mean MFI ratio of Sox1/GFP expressing cells on day 6 of neural differentiation for each plating cell density. Bars represent the mean ± S.D. of three independent experiments. Significant *post-hoc* difference is indicated with bracket. (Tukey-Kramer test, $*P < 0.05$)

3.2.3 Effect of DM and LDN treatments of Sox1/GFP expression

Next, the effect of two doses of DM and LDN on Sox1/GFP expression in cultures was investigated. Cells were differentiated in CDM with LDN (0.1 µM and 0.25 µM) or DM (0.25 µM and 0.5 µM) for 6 days. DM and LDN can be dissolved in ethanol (0.1%) therefore it was used as the vehicle control for LDN and DM treatments. All treatments except that of BMP4 induced over 90% of Sox1/expression (Fig. 3.6 (b)). Both LDN and DM treatments produced higher mean MFI values than those in CDM control cultures. Although LDN produced higher mean MFI values than DM, the differences between the tested doses were not significant when a non-parametric Mann-Whitney *U* test was performed (Mann-Whitley *U* test, $P > 0.05$). A Mann-Whitney *U* test was performed because the data were normally-distributed but did not display equal variance, hence the data did not satisfy the requirements for performing parametric statistical analysis (Fig. 3.6 (c)).

Because Sox1/GFP expression was too high on day 6 and the differences between the tested doses of LDN and DM treatments were small and insignificant, additional flow cytometry analysis was carried out on day 4. Similarly, all treatments induced over 90% of Sox1/GFP expression on day 4 as determined by the unimodal right-shift in the FACS analysis (Fig. 3.5 (b)). Similar to day 6, treatments with LDN produced higher MFI values than treatments with DM but the differences between the tested doses were not obvious. This might suggest that undifferentiated cells exhibit a high background of Sox1/GFP expression or that differentiated cells were unable to respond to BMP modulators. The second possibility was unlikely because differentiated cells responded to BMP4 treatment by reducing Sox1/GFP expression substantially from over 90% to 0% by comparing CDM treatment with BMP4 treatment (Fig. 3.5 (b))

(a)

Day 4 | SSC/FSC | Histogram

CDM

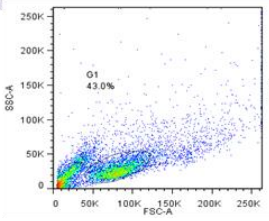

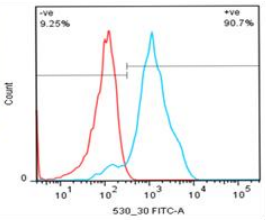

CDM	Geo. mean		MFI ratio	% of GFP +ve
	+ve	-ve		
Sample 1	1361	143	9.52	90.7
Sample 2	**1432**	**144**	**9.24**	**90.7**
Sample 3	1582	183	8.64	94.8

Vehicle

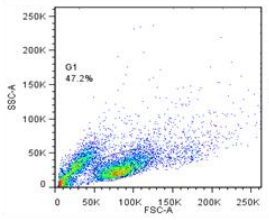

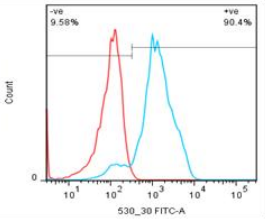

Vehicle	Geo. mean		MFI ratio	% of GFP +ve
	+ve	-ve		
Sample 1	**1455**	**133**	**10.86**	**94.1**
Sample 2	1508	148	10.19	92.4
Sample 3	1822	154	11.83	90.4

LDN (0.1 µM)

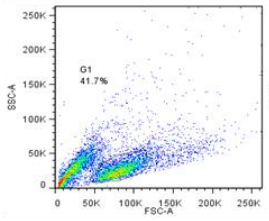

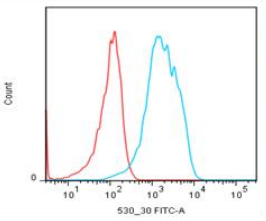

LDN (0.1 µM)	Geo. mean			MFI ratio	% of GFP +ve
		+ve	-ve		
Sample 1	**1666**			**23.94**	**100**
Sample 2		1890	183	10.33	93.9
Sample 3	1981			28.46	100
Undifferentiated 46C	69.6				

LDN (0.25 µM)

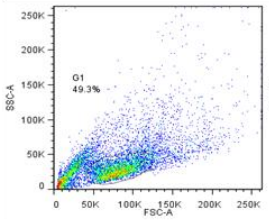

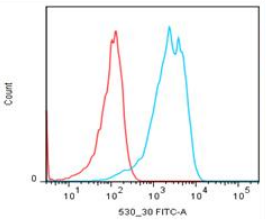

LDN (0.25 µM)	Geo. mean			MFI ratio	% of GFP +ve
		+ve	-ve		
Sample 1		1860	159	11.70	93.5
Sample 2	**1705**			**24.50**	**100**
Sample 3	2059			29.58	100
Undifferentiated 46C	69.6				

DM (0.25 µM)

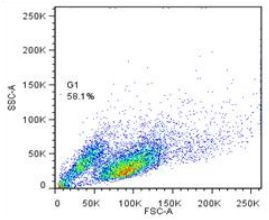

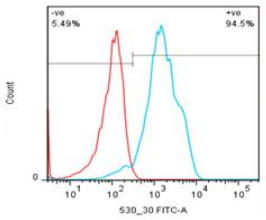

DM (0.25 µM)	Geo. mean			MFI ratio	% of GFP +ve
		+ve	-ve		
Sample 1		**1652**	**146**	**11.32**	**94.5**
Sample 2		1460	140	10.43	95.3
Sample 3	1664			23.91	100
Undifferentiated 46C	69.6				

DM (0.5 µM)

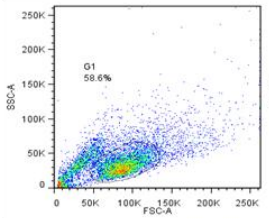

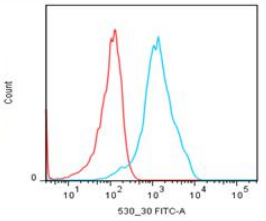

DM (0.5 µM)	Geo. mean	MFI ratio	% of GFP +ve
Sample 1	**1268**	**18.22**	**100**
Sample 2	1164	16.72	100
Sample 3	1619	23.26	100
Undifferentiated 46C	69.6		

BMP4 (2 ng/ml)

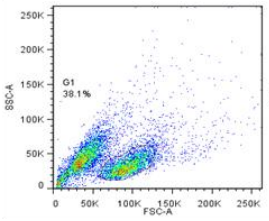

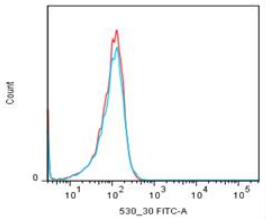

BMP4 (2ng/ml)	Geo. mean	MFI ratio	% of GFP +ve
Sample 1	104	1.49	0
Sample 2	**103**	**1.48**	**0**
Sample 3	99.6	1.43	0
Undifferentiated 46C	69.6		

(b)

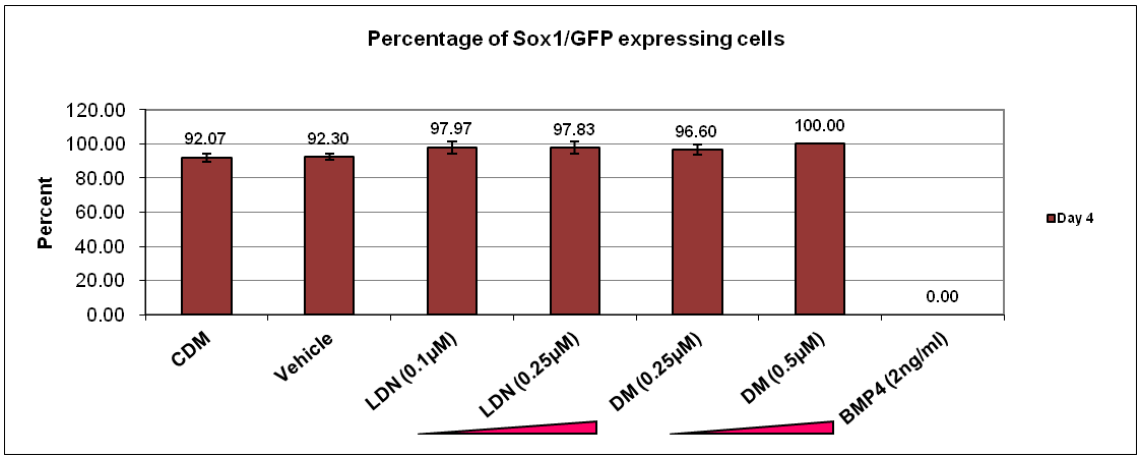

(c)

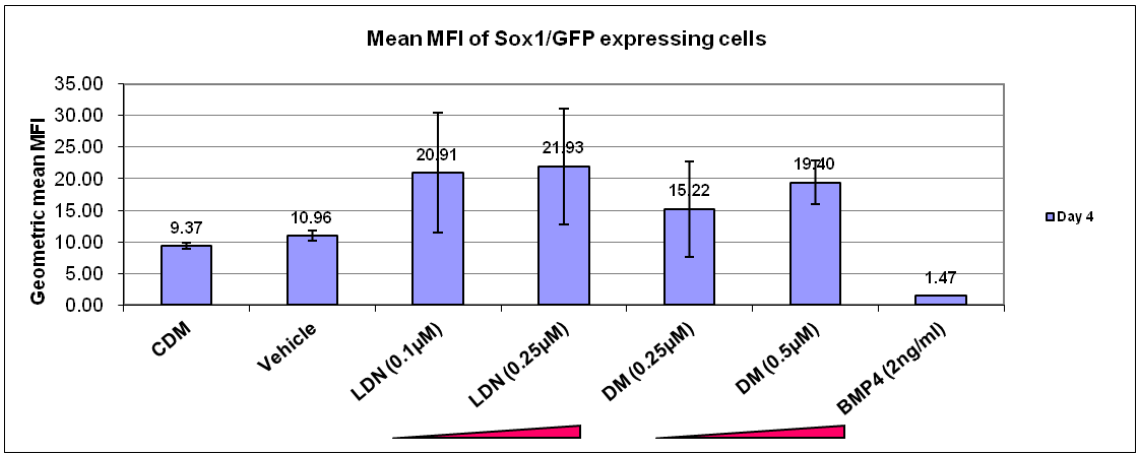

Figure 3.5 Flow cytometry analysis for Sox1/GFP expression of 46C cells treated with LDN, DM and BMP4 on day 4

(a) 46C cells were treated with LDN (0.1 µM and 0.25 µM), DM (0.25 µM and 0.5 µM) and BMP4 (2 ng/ml) for 4 days. Cells were dissociated and analysed by flow cytometry for Sox1/GFP expression. Ethanol (0.1%) was used as a vehicle control for LDN and DM. Cells were gated in G1, excluding clumped cells and debris. The percentage of cells included in the G1 gate is shown on the SSC/FSC plots. The fluorescent intensity of gated control samples (undifferentiated 46C ES cells) (red line) and gated treated samples (blue line) is shown on the histograms. The bimodal distribution is divided into +ve and -ve cell populations. Tables show the percentage of Sox1/GFP expressing cells, the geometric mean (geo. mean) fluorescence value and MFI ratio of each sample acquired. The highlighted regions (in green) indicate the samples represented in the SSC/FSC plots and the histograms.

(b) The graph illustrates the mean percentage of Sox1/GFP expressing cells on day 4 of neural differentiation for each treatment. Bars represent the mean ± S.D. of three independent experiments.

(c) The graph illustrates the mean MFI ratio of Sox1/GFP expressing cells on day 4 of neural differentiation for each treatment. Bars represent the mean ± S.D. of three independent experiments. (Mann-Whitley *U* test for all comparisons, $P > 0.05$)

(a)

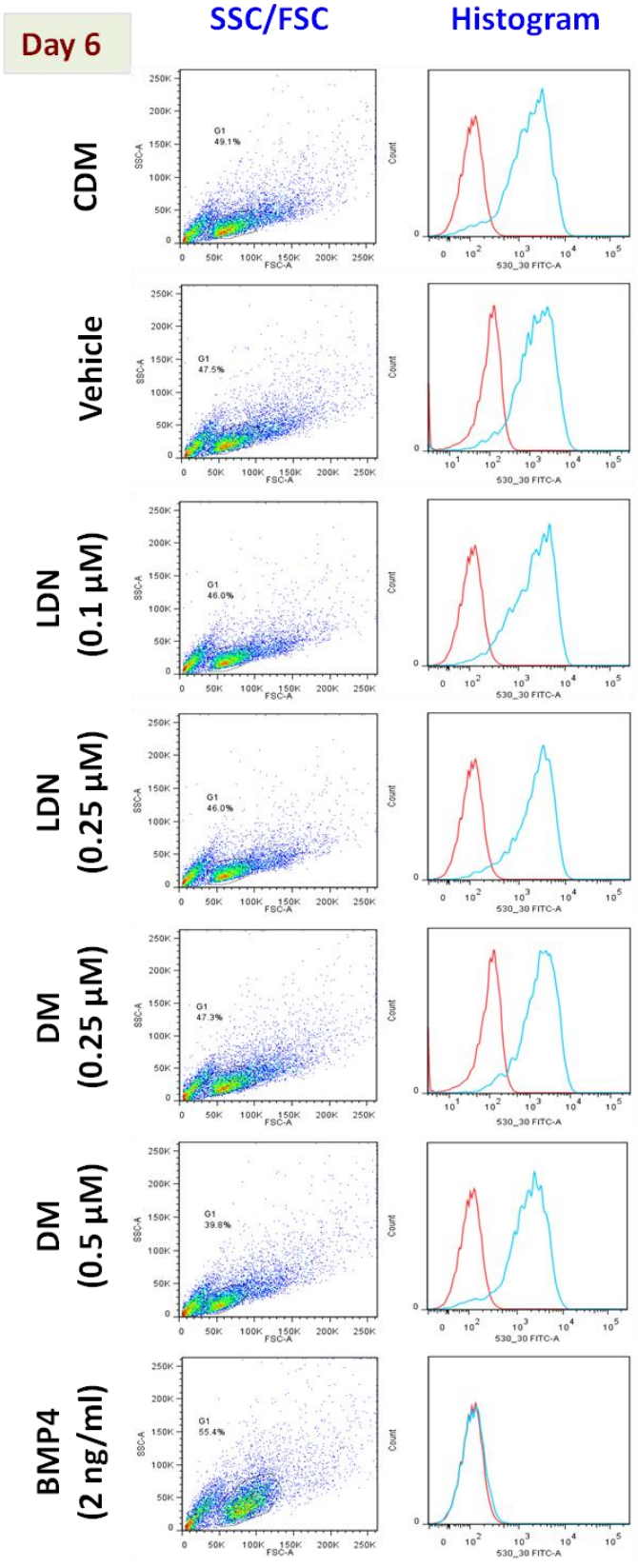

CDM	Geo. mean			MFI ratio	% of GFP +ve
		+ve	-ve		
Sample 1	1471			21.14	100
Sample 2	**1271**			**18.26**	**100**
Sample 3		1674	155	10.8	94.8
Undifferentiated 46C	69.6				

Vehicle	Geo. mean			MFI ratio	% of GFP +ve
		+ve	-ve		
Sample 1	1295			18.61	100
Sample 2	**1267**			**18.20**	**100**
Sample 3		1807	135	13.39	93.6
Undifferentiated 46C	69.6				

LDN (0.1 µM)	Geo. mean	MFI ratio	% of GFP +ve
Sample 1	**1762**	**25.32**	**100**
Sample 2	2052	29.48	100
Sample 3	1364	19.60	100
Undifferentiated 46C	69.6		

LDN (0.25 µM)	Geo. mean	MFI ratio	% of GFP +ve
Sample 1	**1886**	**27.1**	**100**
Sample 2	1140	16.38	100
Sample 3	2153	30.93	100
Undifferentiated 46C	69.6		

DM (0.25 µM)	Geo. mean			MFI ratio	% of GFP +ve
		+ve	-ve		
Sample 1	1716			24.66	100
Sample 2	**1557**			**22.37**	**100**
Sample 3		1853	136	13.63	93.6
Undifferentiated 46C	69.6				

DM (0.5 µM)	Geo. mean	MFI ratio	% of GFP +ve
Sample 1	1350	19.40	100
Sample 2	1571	22.57	100
Sample 3	**1467**	**21.08**	**100**
Undifferentiated 46C	69.6		

BMP4 (2ng/ml)	Geo. mean	MFI ratio	% of GFP +ve
Sample 1	104	1.49	0
Sample 2	109	1.57	0
Sample 3	**105**	**1.51**	**0**
Undifferentiated 46C	69.6		

(b)

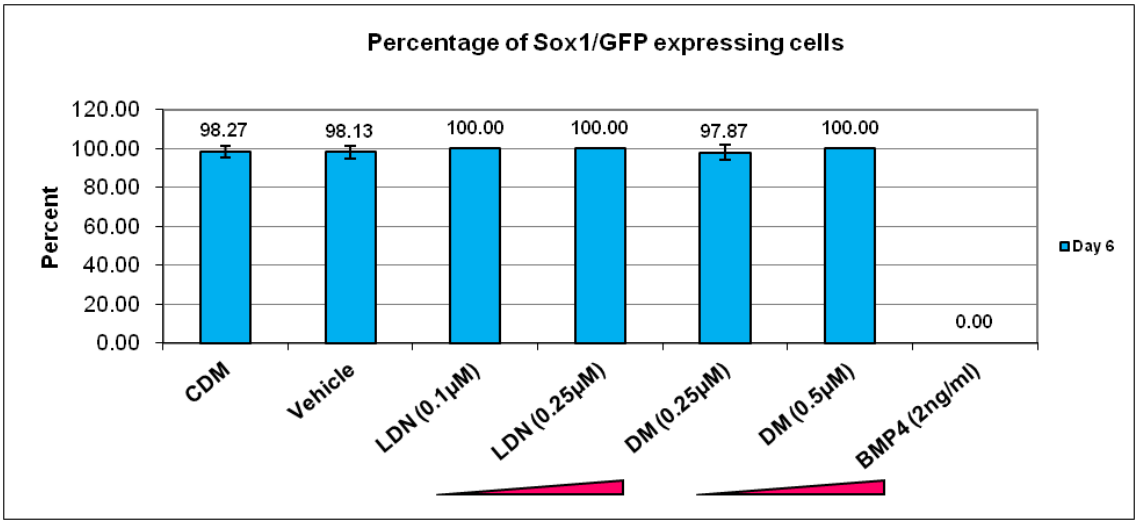

(c)

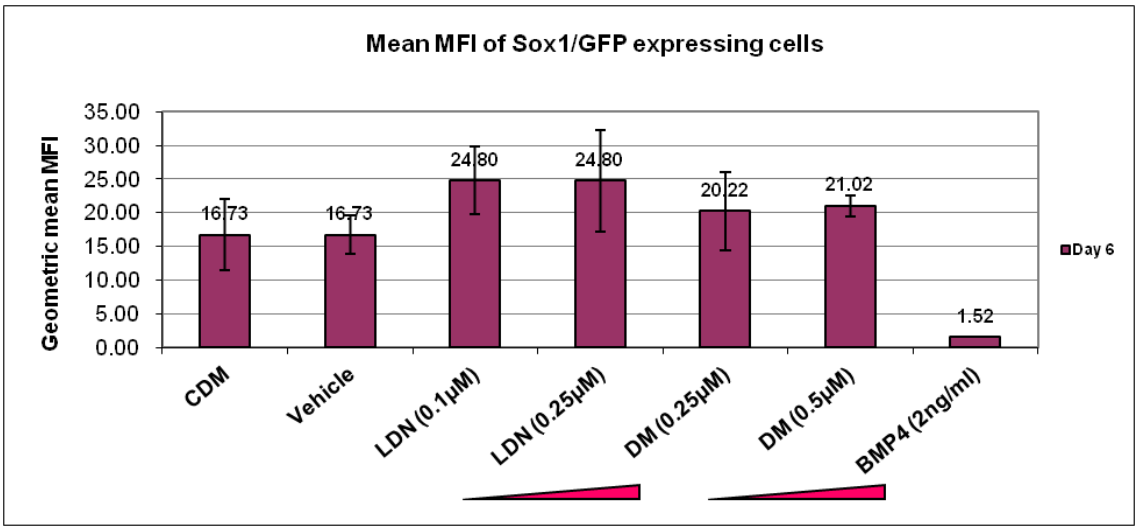

Figure 3.6 Flow cytometry analysis for Sox1/GFP expression of 46C cells treated with DM, LDN, noggin and BMP4 on day 6

(a) 46C cells were treated with LDN (0.1 µM and 0.25 µM), DM (0.25 µM and 0.5 µM) and BMP4 (2 ng/ml) for 6 days. Cells were dissociated and measured by flow cytometry for Sox1/GFP expression. Ethanol (0.1%) was used as a vehicle control for LDN and DM. Cells were gated in G1, excluding clumped cells and debris. The percentage of cells included in the G1 gate is shown on the SSC/FSC plots. The fluorescent intensity of gated control samples (undifferentiated 46C ES cells) (red line) and gated treated samples (blue line) is shown on the histograms. The bimodal distribution is divided into +ve and -ve cell populations. Tables show the percentage of Sox1/GFP expressing cells, the geometric mean (geo. mean) fluorescence value and MFI ratio of each sample acquired. The highlighted regions (in green) indicate the samples represented in the SSC/FSC plots and the histograms.

(b) The graph illustrates the mean percentage of Sox1/GFP expressing cells on day 6 of neural differentiation for each treatment. (Krustal-Wallis test, $P = 0.217$)

(c) The graph illustrates the mean MFI ratio of Sox1/GFP expressing cells on day 6 of neural differentiation for each treatment. Bars represent the mean ± S.D. of three independent experiments. (Krustal-Wallis test, $P = 0.055$)

3.2.4 Effect of BMP4 on Sox1/GFP expression

CDM alone seemed to have produced a 'ceiling effect' on the percentage of Sox1/GFP expressing cells on day 4 and day 6, and LDN and DM treatments appeared to have little or no further effect on the percentage of Sox1/GFP expressing cells. Therefore, it was necessary to bring down the Sox1/GFP level before the effect of LDN and DM could be determined and compared. BMP4 has been shown to suppress neural cell fate specification and direct cells towards epidermal cell fate (Ying et al., 2003b, Kunath et al., 2007). BMP4 was therefore added to reduce the Sox1/GFP expression. Because the previous experiment has shown that 2 ng/ml BMP4 reduced Sox1/GFP expression from 90% to 0% (Fig. 3.5 (b), Fig. 3.6 (b)), a BMP4 dose that would yield a percentage that reduced Sox1/GFP expression but not did not completely abrogate Sox1/GFP expression was decided upon. To examine the dose response of BMP4, cells were treated with BMP4 ranging from 0 ng/ml to 2 ng/ml. As shown by Fig. 3.7(b), the percentage of Sox1/GFP expressing cells was reduced by BMP4 in a dose-dependent manner, indicating that cells were responsive to BMP4 treatment.

BMP4 at 0.5 ng/ml was chosen for subsequent comparison of the effect of selected LDN and DM doses. The lowest dose of BMP4 (0.1 ng/ml) was not chosen because LDN and DM would probably overcome the effect of BMP4 completely; likewise, higher doses of BMP4 (1 ng/ml, 1.5 ng/ml and 2 ng/ml) were not chosen because the effect of LDN and DM antagonism might not be obvious enough to detect. The percentage of Sox1/GFP expression was 37.33 % at 0.5 ng/ml of BMP4 treatment (Fig 3.7 (b)), and this concentration of BMP4 was used for the next experiment to compare the effect of BMP antagonism on treatments with LDN and DM.

(a)

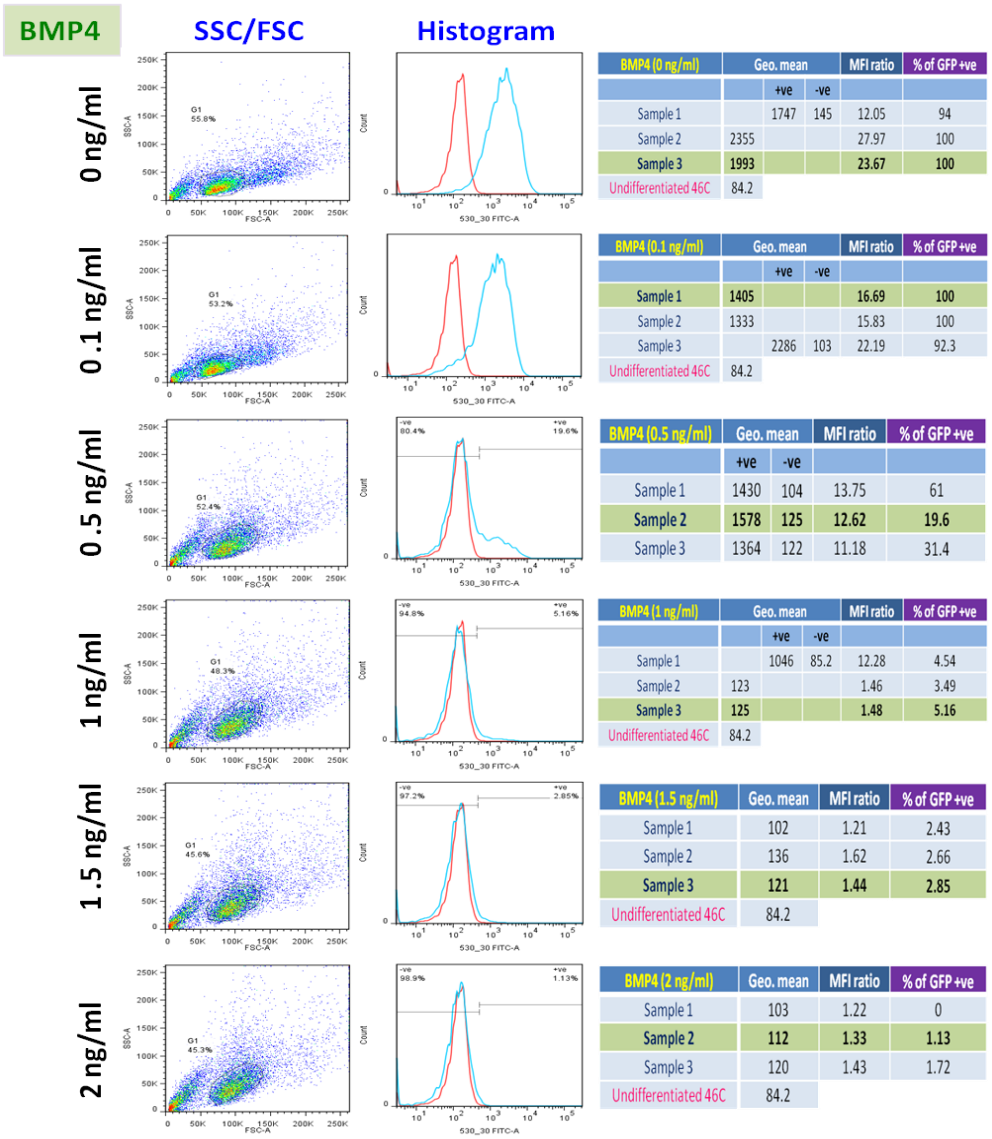

BMP4 (0 ng/ml)	Geo. mean			MFI ratio	% of GFP +ve
		+ve	-ve		
Sample 1		1747	145	12.05	94
Sample 2	2355			27.97	100
Sample 3	**1993**			**23.67**	**100**
Undifferentiated 46C	84.2				

BMP4 (0.1 ng/ml)	Geo. mean			MFI ratio	% of GFP +ve
		+ve	-ve		
Sample 1	**1405**			**16.69**	**100**
Sample 2	1333			15.83	100
Sample 3		2286	103	22.19	92.3
Undifferentiated 46C	84.2				

BMP4 (0.5 ng/ml)	Geo. mean		MFI ratio	% of GFP +ve
	+ve	-ve		
Sample 1	1430	104	13.75	61
Sample 2	**1578**	**125**	**12.62**	**19.6**
Sample 3	1364	122	11.18	31.4

BMP4 (1 ng/ml)	Geo. mean			MFI ratio	% of GFP +ve
		+ve	-ve		
Sample 1		1046	85.2	12.28	4.54
Sample 2	123			1.46	3.49
Sample 3	**125**			**1.48**	**5.16**
Undifferentiated 46C	84.2				

BMP4 (1.5 ng/ml)	Geo. mean	MFI ratio	% of GFP +ve
Sample 1	102	1.21	2.43
Sample 2	136	1.62	2.66
Sample 3	**121**	**1.44**	**2.85**
Undifferentiated 46C	84.2		

BMP4 (2 ng/ml)	Geo. mean	MFI ratio	% of GFP +ve
Sample 1	103	1.22	0
Sample 2	**112**	**1.33**	**1.13**
Sample 3	120	1.43	1.72
Undifferentiated 46C	84.2		

Figure 3.7 Flow cytometry analysis of 46C cells treated with BMP4

(a) 46C cells were treated with BMP4 (0.1 ng/ml, 0.5 ng/ml, 1 ng/ml, 1.5 ng/ml and 2 ng/ml) for 6 days. Cells were dissociated and analysed by flow cytometry for Sox1/GFP expression. Cells were gated in G1, excluding clumped cells and debris. The percentage of cells included in the G1 gate is shown on the SSC/FSC plots. The fluorescent intensity of gated control samples (undifferentiated 46C ES cells) (red line) and gated treated samples (blue line) is shown on the histograms. The bimodal distribution is divided into +ve and -ve cell populations. Tables show the percentage of Sox1/GFP expression, the geometric mean (geo. mean) fluorescence value and MFI ratio of each sample acquired. The highlighted regions (in green) indicate the samples represented in the SSC/FSC plots and the histograms.

(b)

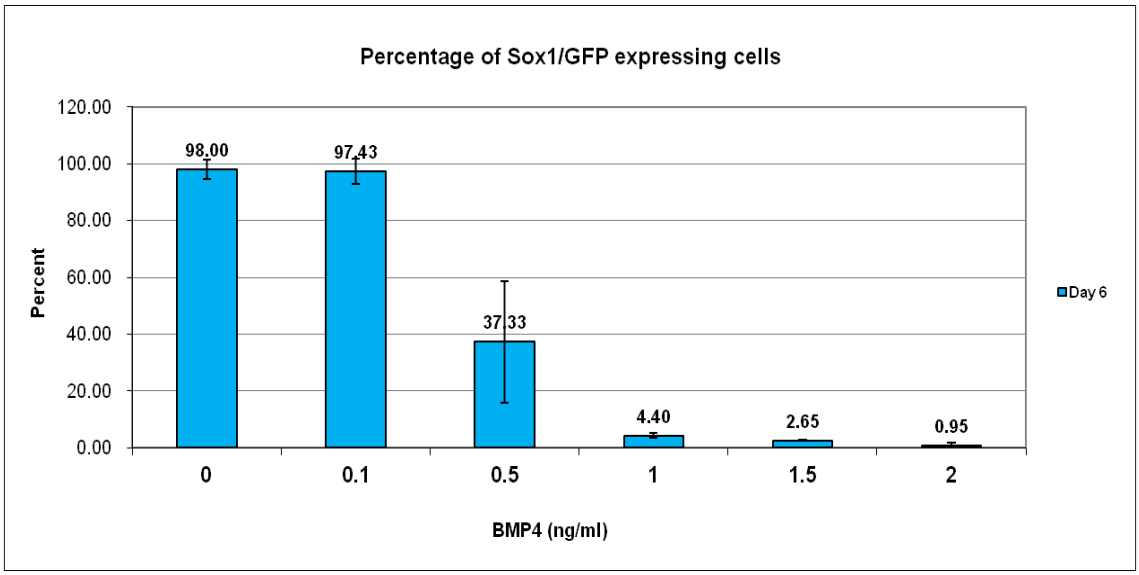

(c)

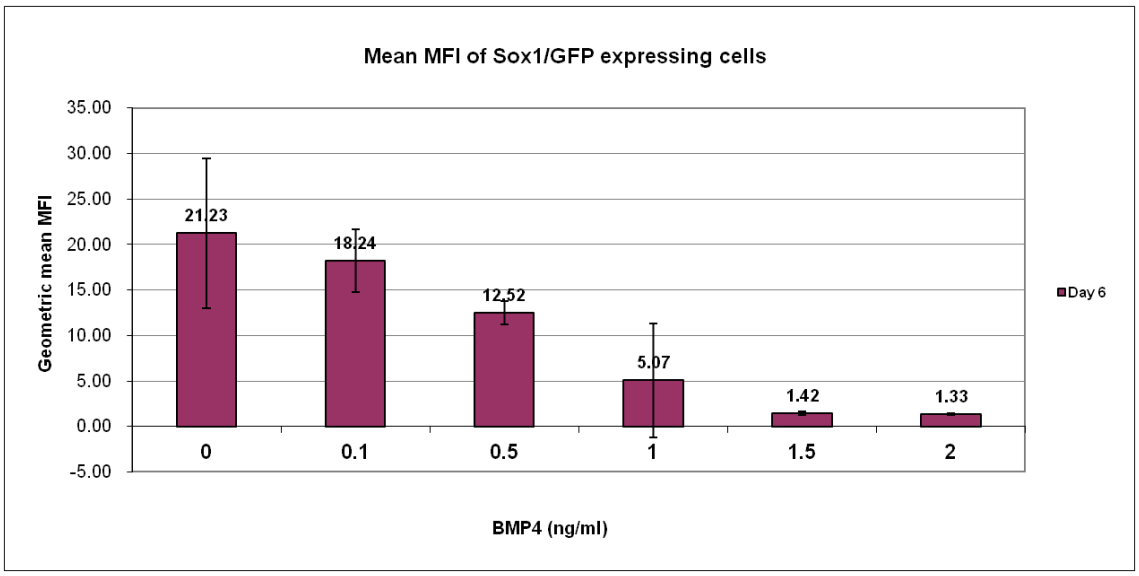

(b) The graph illustrates the mean MFI ratio of Sox1/GFP expressing cells on day 6 of neural differentiation for each BMP4 concentration. Bars represent the mean ± S.D. of three independent experiments. (Mann-Whitley *U* test for all comparisions, $P > 0.05$)

(c) The graph illustrates the mean MFI ratio of Sox1/GFP expressing cells on day 6 of neural differentiation for each BMP4 concentration. Bars represent the mean ± S.D. of three independent experiments. (Mann-Whitley *U* test for all comparisons, $P > 0.05$)

3.2.5 Effects of DM and LDN on Sox1/GFP expression in the presence of BMP4

The high percentage of Sox1/GFP expressing cells found in CDM alone in cultures makes it difficult to compare the effect of DM, LDN (Figs. 3.5 and 3.6). Therefore 0.5 ng/ml of BMP4 was added into the cultures in order to determine the ability of LDN and DM to induce neural differentiation.

In analysing the MFI values on day 4, significant differences were found across all samples (one-way ANOVA test, $F_{6,14} = 64.11$, $P < 0.0001$) (Fig. 3.8 (c)). LDN (0.1 µM and 0.25 µM) had significantly higher MFI values than vehicle control (ethanol 0.1%), DM (0.25 µM and 0.5 µM) and BMP4 treatments (Tukey-Kramer test, $P < 0.05$). The difference in MFI value between DM treatments and the vehicle control was not significant, suggesting that LDN was more effective than DM in antagonising BMP4 to induce Sox1/GFP expression. No significance difference was found in the percentage of Sox1/GFP expression for all treatments (Fig. 3.8 (b)).

On day 6, no significant difference was found in MFI values and the percentage of Sox1/GFP expression between individual samples (Mann-Whitney *U* test, $P > 0.05$) (Fig. 3.9(b), (c)). LDN treatments induced a higher percentage and mean MFI values of Sox1/GFP expression on day 6 than day 4. In contrast, it appeared that the mean MFI values of DM treatments only started to increase on day 6 (compare Fig 3.8 (c) and Fig. 3.9 (c)). The reason for the slight delay before the differentiation of ES cells becomes positive for Sox1/GFP expression in response to treatment with DM compared to LDN is not clear. Although the percentage of Sox1/GFP positive cells was much lower in DM treatments than LDN treatments on day 4 and 6, it was still higher than vehicle control (ethanol 0.1%) which contains BMP4 (0.5 ng/ml) (compare Fig 3.7(b) and Fig. 3.8 (b)).

Combining the data collected on day 4 and day 6, it appeared that LDN and DM were both able to overcome BMP4-induced suppression of neural differentiation. LDN was more potent than DM because higher percentage and mean MFI values of GFP expression were found. In the absence of BMP4, DM treatments induced strong expression of Sox1/GFP, though not as strong as LDN treatments (compare Fig 3.6 (b), (c) and Fig. 3.9 (b), (c)), suggesting that the induction of Sox1/GFP in DM treatments might require other mechanisms in the absence of BMP4.

(a)

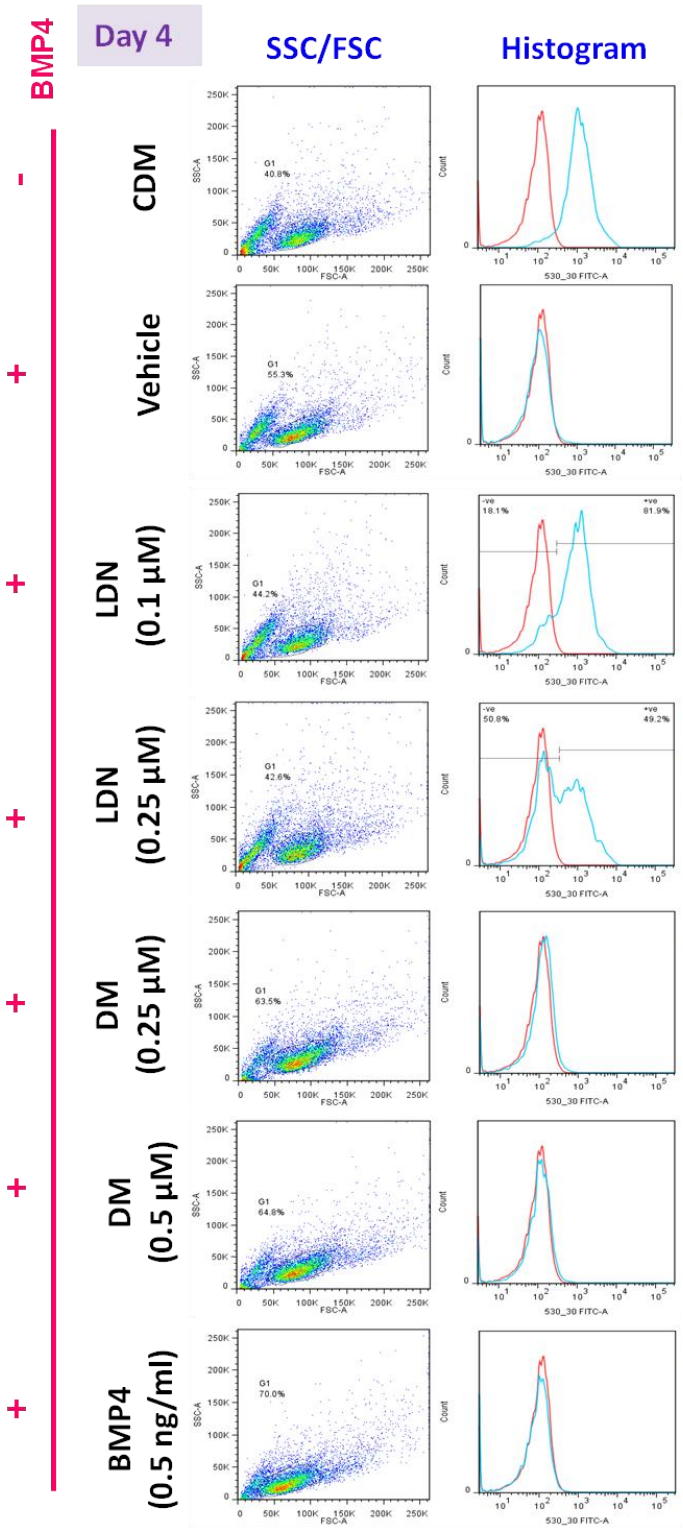

CDM	Geo. mean			MFI ratio	% of GFP +ve
		+ve	-ve		
Sample 1	1060			15.23	100
Sample 2	1147			16.48	100
Sample 3		1418	156	9.09	94
Undifferentiated 46C	69.6				

Vehicle	Geo. mean	MFI ratio	% of GFP +ve
Sample 1	105	1.51	0
Sample 2	91.6	1.32	0
Sample 3	94.2	1.35	0
Undifferentiated 46C	69.6		

LDN (0.1 µM)	Geo. mean		MFI ratio	% of GFP +ve
	+ve	-ve		
Sample 1	903	131	6.89	43.6
Sample 2	862	109	7.91	49.5
Sample 3	1052	143	7.36	81.9

LDN (0.25 µM)	Geo. mean		MFI ratio	% of GFP +ve
	+ve	-ve		
Sample 1	1074	128	8.39	49.2
Sample 2	1063	104	10.22	62.3
Sample 3	1297	170	7.63	100

DM (0.25 µM)	Geo. mean	MFI ratio	% of GFP +ve
Sample 1	122	1.75	0
Sample 2	99.6	1.43	0
Sample 3	163	2.34	18.1
Undifferentiated 46C	69.6		

DM (0.5 µM)	Geo. mean	MFI ratio	% of GFP +ve
Sample 1	113	1.62	0
Sample 2	109	1.57	0
Sample 3	198	2.84	24.5
Undifferentiated 46C	69.6		

BMP4 (0.5ng/ml)	Geo. mean	MFI ratio	% of GFP +ve
Sample 1	93.5	1.34	0
Sample 2	95.6	1.37	0
Sample 3	86.6	1.24	0
Undifferentiated 46C	69.6		

(b)

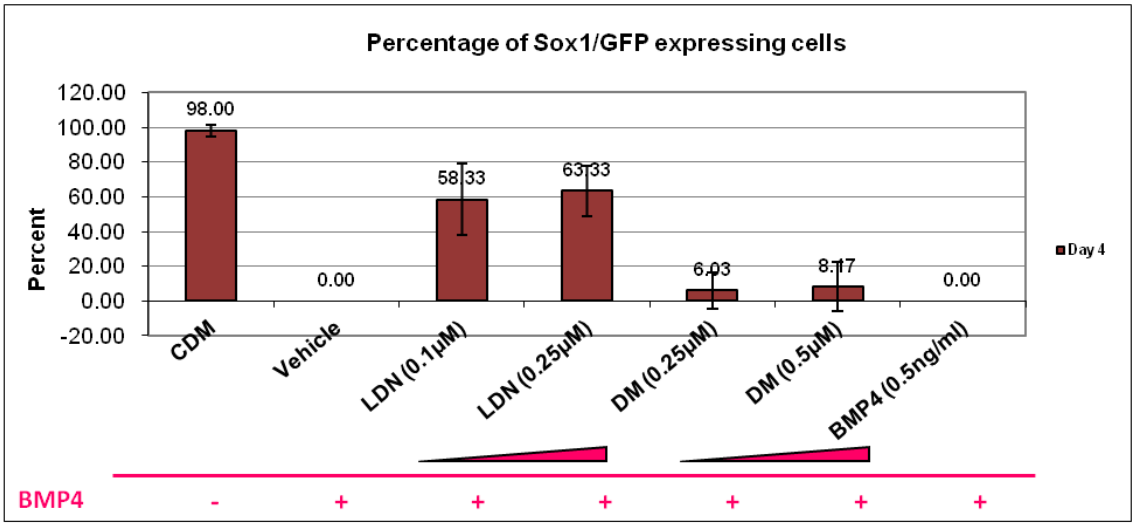

(c)

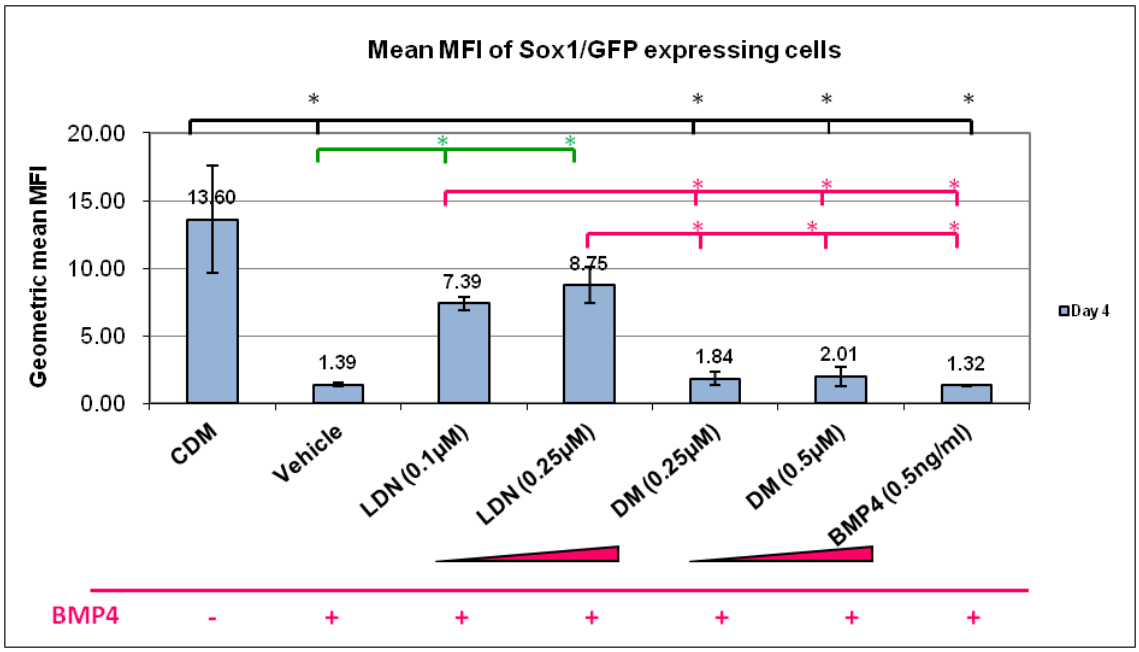

Figure 3.8 Flow cytometry analysis of 46C cells treated with LDN, DM in the presence of BMP4 on day 4 of neural differentiation

(a) 46C cells were treated with LDN (0.1 µM and 0.2 5µM), DM (0.25 µM and 0.5 µM) in addition to BMP4 (0.5 ng/ml) for 4 days. Cells were dissociated and analysed by flow cytometry for Sox1/GFP expression. Ethanol (0.1%) was used as a vehicle control for LDN and DM. Cells were gated in G1, excluding clumped cells and debris. The percentage of cells included in the G1 gate is shown on the SSC/FSC plots. The fluorescent intensity of gated control samples (undifferentiated 46C ES cells) (red line) and gated treated samples (blue line) is shown on the histograms. The bimodal distribution is divided into +ve and -ve cell populations. Tables show the percentage of Sox1/GFP expression, the geometric mean (geo. mean) fluorescence value and

MFI ratio of each sample acquired. The highlighted regions (in green) indicate the samples represented in the SSC/FSC plots and the histograms.

(b) The graph illustrates the mean percentage of Sox1/GFP expressing cells on day 4 of neural differentiation for each treatment. Bars represent the mean ± S.D. of three independent experiments. (Mann-Whitley *U* test for all comparisons, $P > 0.05$)

(c) The graph illustrates the mean MFI ratio of Sox1/GFP expressing cells on day 4 of neural differentiation for each treatment. Bars represent the mean ± S.D. of three independent experiments. Significant *post-hoc* differences are indicated with brackets. (Tukey-Kramer test, $*P < 0.05$)

(a)

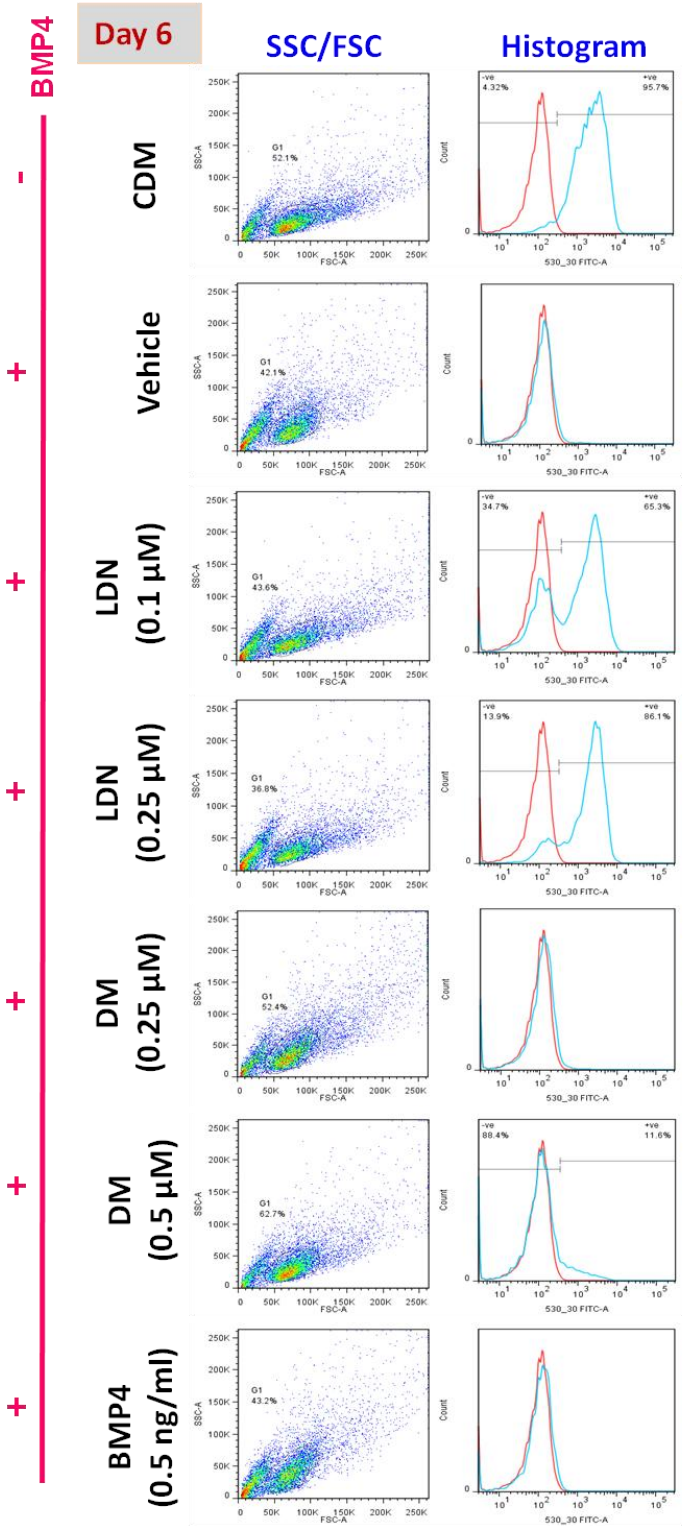

CDM	Geo. mean			MFI ratio	% of GFP +ve
		+ve	-ve		
Sample 1	1577			22.66	100
Sample 2		1734	120	14.45	91.7
Sample 3		**2209**	**150**	**14.73**	**95.7**
Undifferentiated 46C	69.6				

Vehicle	Geo. mean	MFI ratio	% of GFP +ve
Sample 1	116	1.67	0
Sample 2	141	2.03	0
Sample 3	**116**	**1.67**	**0**
Undifferentiated 46C	69.6		

LDN (0.1 µM)	Geo. mean		MFI ratio	% of GFP +ve
	+ve	-ve		
Sample 1	2180	124	17.58	76.8
Sample 2	**2085**	**120**	**17.38**	**65.3**
Sample 3	2403	145	16.57	86.8

LDN (0.25 µM)	Geo. mean		MFI ratio	% of GFP +ve
	+ve	-ve		
Sample 1	**2403**	**145**	**16.57**	**86**
Sample 2	2053	126	16.34	80.7
Sample 3	2748	155	17.34	84.7

DM (0.25 µM)	Geo. mean			MFI ratio	% of GFP +ve
		+ve	-ve		
Sample 1	105			1.51	0
Sample 2	**119**			**1.71**	**0**
Sample 3		1222	116	10.53	14.6
Undifferentiated 46C	69.6				

DM (0.5 µM)	Geo. mean			MFI ratio	% of GFP +ve
		+ve	-ve		
Sample 1		**977**	**104**	**9.39**	**11.06**
Sample 2	119			1.71	0
Sample 3		1443	120	12.03	26.2
Undifferentiated 46C	69.6				

BMP4 (0.5ng/ml)	Geo. mean	MFI ratio	% of GFP +ve
Sample 1	110	1.58	0
Sample 2	**116**	**1.67**	**0**
Sample 3	127	1.82	0
Undifferentiated 46C	69.6		

(b)

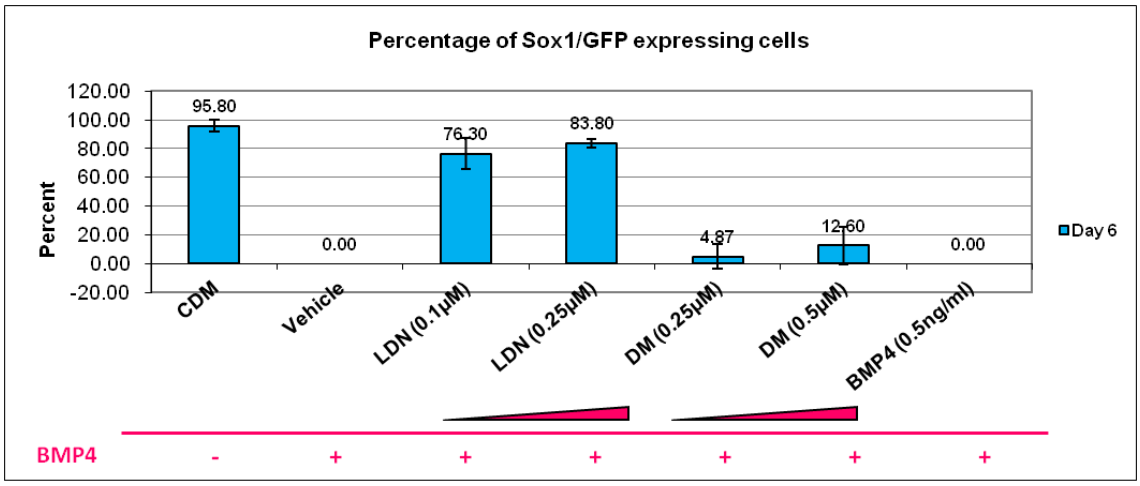

(c)

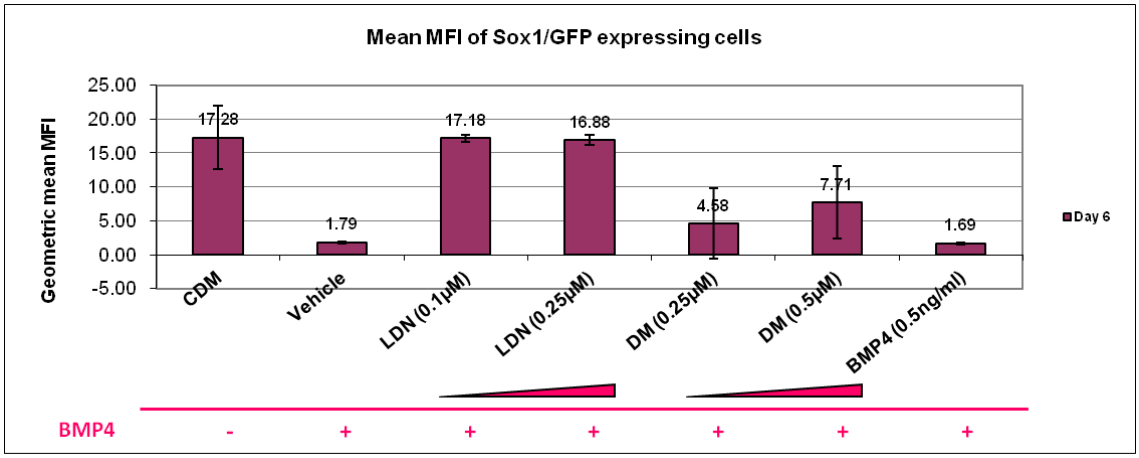

Figure 3.9 Flow cytometry analysis of 46C cells treated with LDN, DM in the presence of BMP4 on day 6 of neural differentiation

(a) 46C cells were treated with LDN (0.1 µM and 0.25 µM), DM (0.25 µM and 0.5 µM) in addition to BMP4 (0.5 ng/ml) for 6 days. Cells were dissociated and analysed by flow cytometry for Sox1/GFP expression. Ethanol (0.1%) was used as a vehicle control for LDN and DM. Cells were gated in G1, excluding clumped cells and debris. The percentage of cells included in the G1 gate is shown on the SSC/FSC plots. The fluorescent intensity of gated control samples (undifferentiated 46C ES cells) (red line) and gated treated samples (blue line) is shown on the histograms. The bimodal distribution is divided into +ve and -ve cell populations. Tables show the percentage of Sox1/GFP expression, the geometric mean (geo. mean) fluorescence value and MFI ratio of each sample acquired. The highlighted regions (in green) indicate the samples represented in the SSC/FSC plots and the histograms.

(b) The graph illustrates the mean percentage of Sox1/GFP expressing cells on day 6 of neural differentiation for each treatment. Bars represent the mean ± S.D. of three independent experiments. (Mann-Whitley *U* test for all comparisons, $P > 0.05$)

(c) The graph illustrates the mean MFI ratio of Sox1/GFP expressing cells on day 6 of neural differentiation for each treatment. Bars represent the mean ± S.D. of three independent experiments. (Mann-Whitley *U* test for all comparisons, $P > 0.05$)

3.2.6 Comparing the effect of LDN and DM with noggin on Sox1/GFP expression

The effect of two doses of LDN and DM on Sox1/GFP expression was examined in the previous section. This section looked at whether the effect of LDN and DM was comparable to recombinant noggin. Cells were treated with LDN (0.25 µM), DM (0.5 µM) and noggin (150 ng/ml). Significant differences were found in the percentage of Sox1/GFP expressing cells across all samples on day 4 (one-way ANOVA test, $F_{6,14} = 74.91$, $P < 0.0001$). Both LDN and DM treatments induced a significantly higher expression of Sox1/GFP than the vehicle control (Tukey-Kamer test, $P < 0.05$). The difference in the percentage of Sox1/GFP expression of LDN and DM was not significant when compared to noggin treatment (Fig. 3.10 (b)). Although DM treatment produced lower mean MFI value, it induced Sox1/GFP expression in 100% of cells, an effect that was also found in LDN and noggin treatments (Fig. 3.10 (b)). Interestingly, both LDN and DM had a lower percentage of Sox1/GFP expressing cells on day 6 than day 4. Whether the decrease was due to the way cells were gated or whether cells had undergone phenotypic changes will require further studies to confirm. DM treatment induced much higher mean MFI value on day 6 than day 4 (Fig. 3.11 (c)). A similar observation was also found in the flow cytometry analyses shown in Figs. 3.8 and 3.9.

Cells displayed different levels of responsiveness to recombinant BMP4. In the previous experiment, 0.5 ng/ml of BMP4 reduced the percentage of Sox1/GFP-expressing cells to 0% whereas in this experiment, 0.5 ng/ml of BMP4 only reduced this percentage to 40-60% of Sox1/GFP -expressing cells on day 4 and 6 (compare Figs. 3.8 and 3.10 or Figs 3.9 and 3.11). This difference could be due to batch-to-batch differences in recombinant BMP4 or to different response mechanisms found in different batches of 46C cells.

(a)

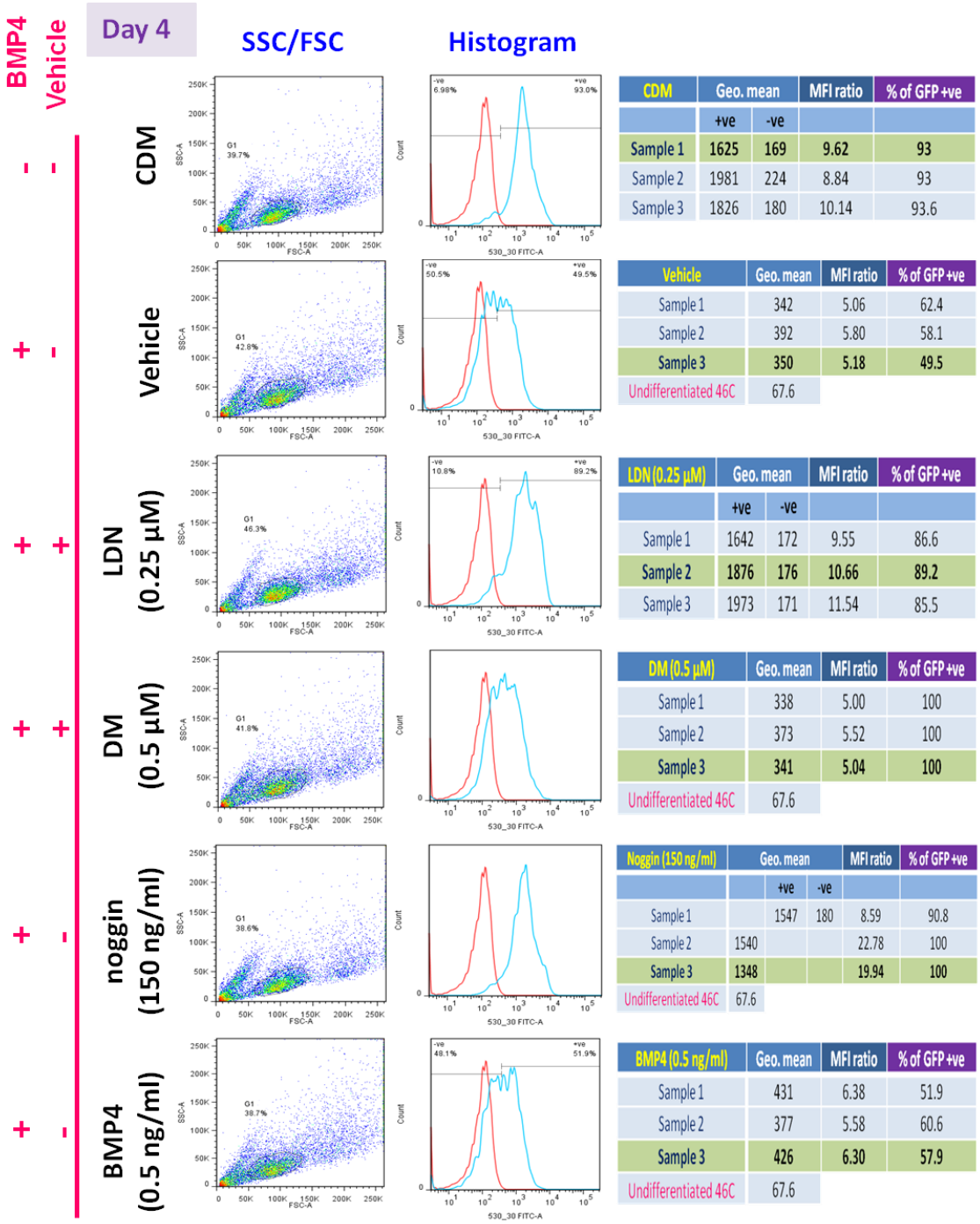

CDM	Geo. mean		MFI ratio	% of GFP +ve
	+ve	-ve		
Sample 1	1625	169	9.62	93
Sample 2	1981	224	8.84	93
Sample 3	1826	180	10.14	93.6

Vehicle	Geo. mean	MFI ratio	% of GFP +ve
Sample 1	342	5.06	62.4
Sample 2	392	5.80	58.1
Sample 3	350	5.18	49.5
Undifferentiated 46C	67.6		

LDN (0.25 µM)	Geo. mean		MFI ratio	% of GFP +ve
	+ve	-ve		
Sample 1	1642	172	9.55	86.6
Sample 2	1876	176	10.66	89.2
Sample 3	1973	171	11.54	85.5

DM (0.5 µM)	Geo. mean	MFI ratio	% of GFP +ve
Sample 1	338	5.00	100
Sample 2	373	5.52	100
Sample 3	341	5.04	100
Undifferentiated 46C	67.6		

Noggin (150 ng/ml)	Geo. mean		MFI ratio	% of GFP +ve
	+ve	-ve		
Sample 1	1547	180	8.59	90.8
Sample 2	1540		22.78	100
Sample 3	1348		19.94	100
Undifferentiated 46C	67.6			

BMP4 (0.5 ng/ml)	Geo. mean	MFI ratio	% of GFP +ve
Sample 1	431	6.38	51.9
Sample 2	377	5.58	60.6
Sample 3	426	6.30	57.9
Undifferentiated 46C	67.6		

(b)

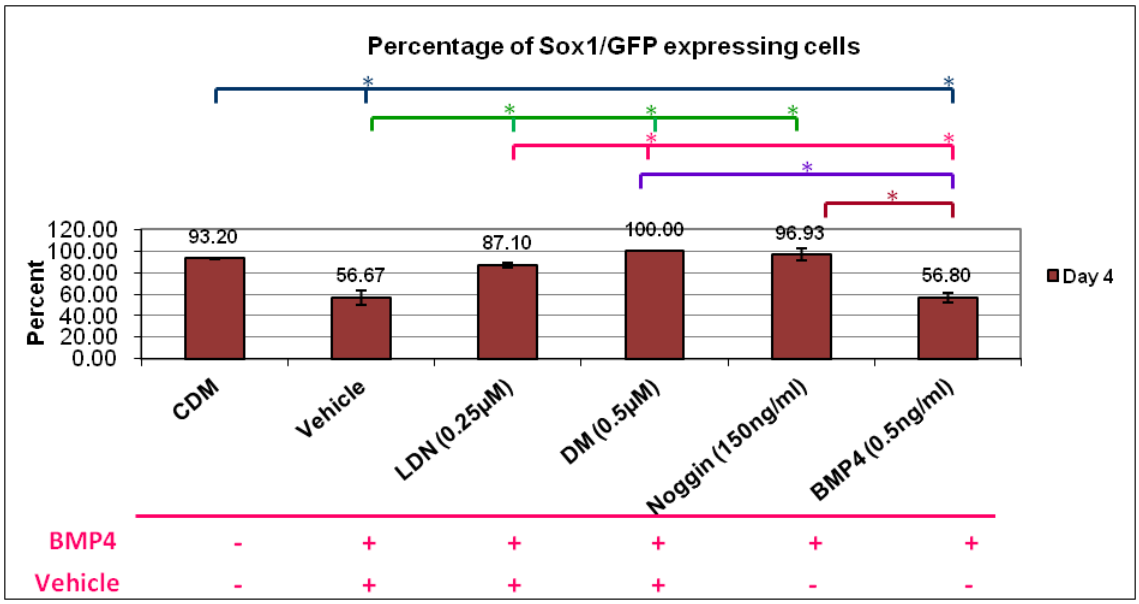

(c)

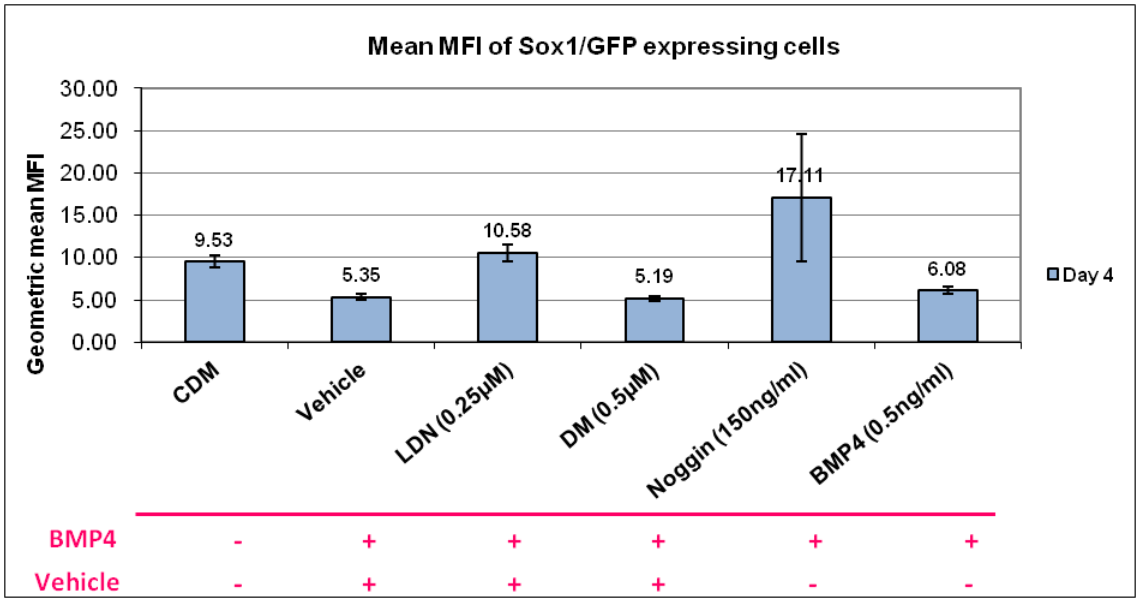

Figure 3.10 Flow cyotmetric analysis of 46C cells treated with LDN, DM and noggin in the presence of BMP4 on day 4 of neural differentiation

(a) 46C cells were treated with LDN (0.25 µM), DM (0.5 µM) and noggin (150 ng/ml) in addition to BMP4 (0.5 ng/ml) for 4 days. Cells were dissociated and analysed by flow cytometry for Sox1/GFP expression. Ethanol (0.1%) was used as a vehicle control for LDN and DM. Cells were gated in G1, excluding clumped cells and debris. The percentage of cells included in the G1 gate is shown on the SSC/FSC plots. The fluorescent intensity of gated control samples (undifferentiated 46C ES cells) (red line) and gated treated samples (blue line) is shown on the histograms. The bimodal distribution is divided into +ve and -ve cell populations. Tables contain the

percentage of Sox1/GFP expression, the geometric mean (geo. mean) fluorescence value and MFI ratio of each sample acquired. The highlighted regions (in green) indicate the samples represented in the SSC/FSC plots and the histograms.

(b) The graph illustrates the mean percentage of Sox1/GFP expression on day 4 of neural differentiation for each treatment. Bars represent the mean ± S.D. of three independent experiments. (Tukey-Kramer test, $*P < 0.05$)

(c) The graph illustrates the mean MFI ratio of Sox1/GFP expression on day 4 of neural differentiation for each treatment. Bars represent the mean ± S.D. of three independent experiments. Significant *post-hoc* differences are indicated with brackets. (Mann-Whitley *U* test for all comparisons, $P > 0.05$)

(a)

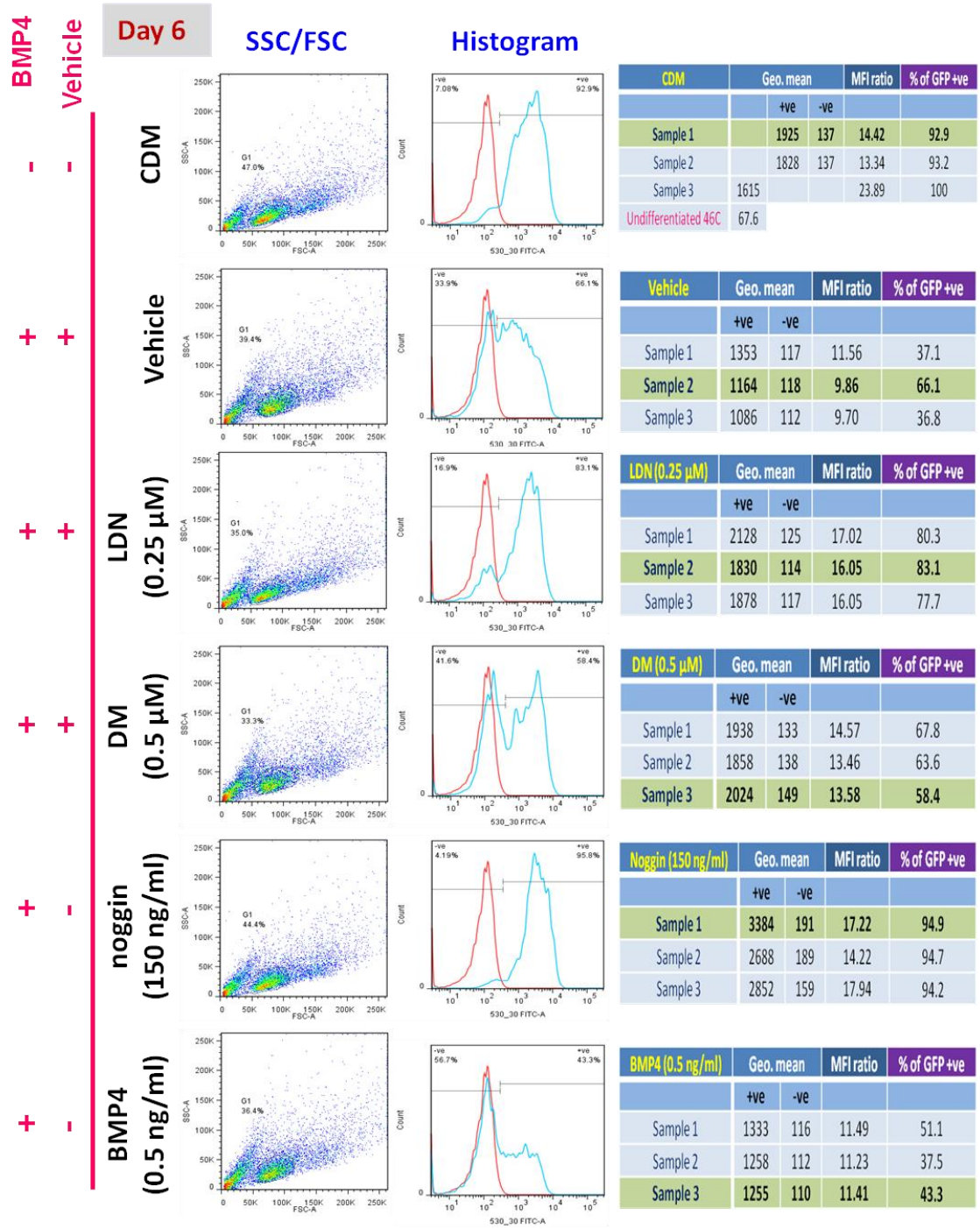

CDM	Geo. mean		MFI ratio	% of GFP +ve
	+ve	-ve		
Sample 1	1925	137	14.42	92.9
Sample 2	1828	137	13.34	93.2
Sample 3	1615		23.89	100
Undifferentiated 46C	67.6			

Vehicle	Geo. mean		MFI ratio	% of GFP +ve
	+ve	-ve		
Sample 1	1353	117	11.56	37.1
Sample 2	1164	118	9.86	66.1
Sample 3	1086	112	9.70	36.8

LDN (0.25 µM)	Geo. mean		MFI ratio	% of GFP +ve
	+ve	-ve		
Sample 1	2128	125	17.02	80.3
Sample 2	1830	114	16.05	83.1
Sample 3	1878	117	16.05	77.7

DM (0.5 µM)	Geo. mean		MFI ratio	% of GFP +ve
	+ve	-ve		
Sample 1	1938	133	14.57	67.8
Sample 2	1858	138	13.46	63.6
Sample 3	2024	149	13.58	58.4

Noggin (150 ng/ml)	Geo. mean		MFI ratio	% of GFP +ve
	+ve	-ve		
Sample 1	3384	191	17.22	94.9
Sample 2	2688	189	14.22	94.7
Sample 3	2852	159	17.94	94.2

BMP4 (0.5 ng/ml)	Geo. mean		MFI ratio	% of GFP +ve
	+ve	-ve		
Sample 1	1333	116	11.49	51.1
Sample 2	1258	112	11.23	37.5
Sample 3	1255	110	11.41	43.3

(b)

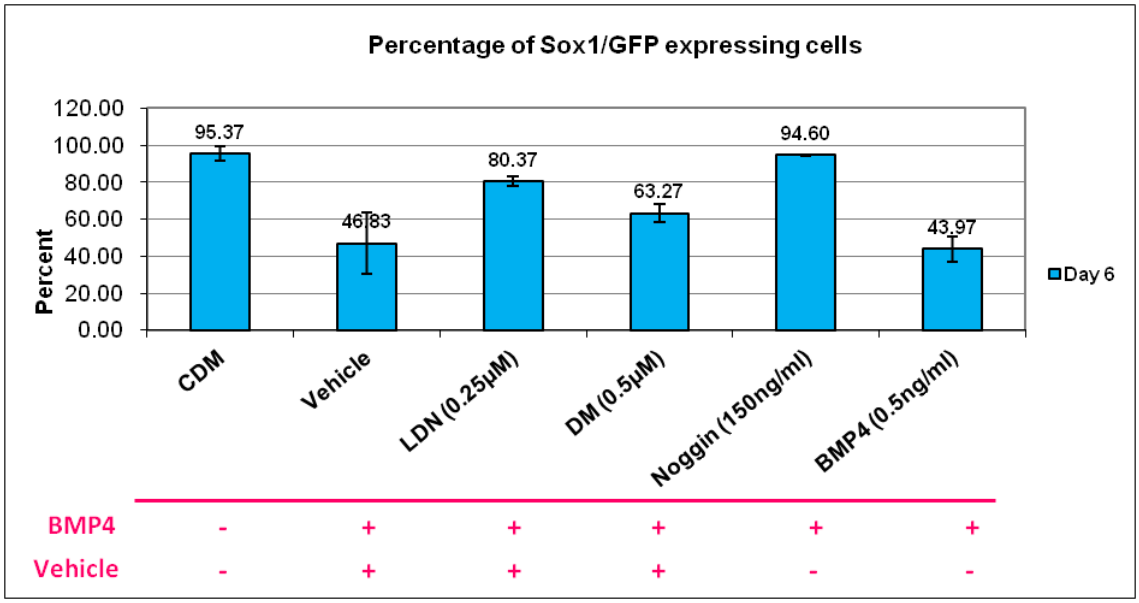

(c)

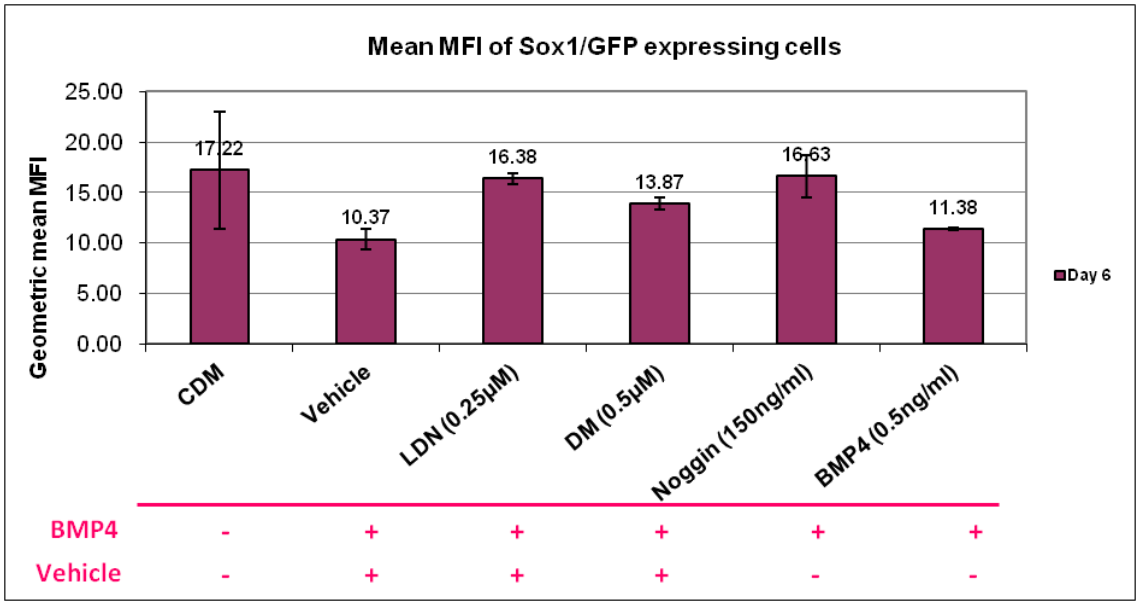

Figure 3.11 Flow cytometry analysis of 46C cells treated with LDN, DM and noggin in the presence of BMP4 on day 6 of neural differentiation

(a) 46C cells were treated with LDN (0.25 µM), DM (0.5 µM) and noggin (150 ng/ml) in addition to BMP4 (0.5 ng/ml) for 6 days. Cells were dissociated and analysed by flow cytometry for Sox1/GFP expression. Ethanol (0.1%) was used as a vehicle control for LDN and DM. Cells were gated in G1, excluding clumped cells and debris. The percentage of cells included in the G1 gate is shown on the SSC/FSC plots. The fluorescent intensity of gated control samples (undifferentiated 46C ES cells) (red line) and gated treated samples (blue line) is shown on the histograms. The bimodal distribution is divided into +ve and -ve cell populations. Tables contain the

percentage of Sox1/GFP expression, the geometric mean (geo. mean) fluorescence value and MFI ratio of each sample acquired. The highlighted regions (in green) indicate the samples represented in the SSC/FSC plots and the histograms.

(b) The graph illustrates the mean percentage of Sox1/GFP expression on day 6 of neural differentiation for each treatment. Bars represent the mean ± S.D. of three independent experiments. (Mann-Whitley *U* test for all comparisons, $P > 0.05$)

(c) The graph illustrates the mean MFI ratio of Sox1/GFP expression on day 4 of neural differentiation for each treatment. Bars represent the mean ± S.D. of three independent experiments. (Mann-Whitley *U* test for all comparisons, $P > 0.05$)

3.2.7 Effect of LDN and DM on cell lineage marker expression

Besides examining the expression of Sox1, it was necessary to examine the expression of other neural and non-neural lineage markers after treatment with LDN, DM and noggin in order to determine the extent they can be used as substitutes for noggin. Cells were subjected to immunocytochemistry analysis for neural and neural crest expression. Background staining was detected by treating the samples following the immunocytochemistry protocol described in section 2.1.8, omitting primary antibodies and incubating cells with appropriate secondary antibodies. Immunostaining for control samples in Fig. 3.12 which shows that the background staining was almost undetectable.

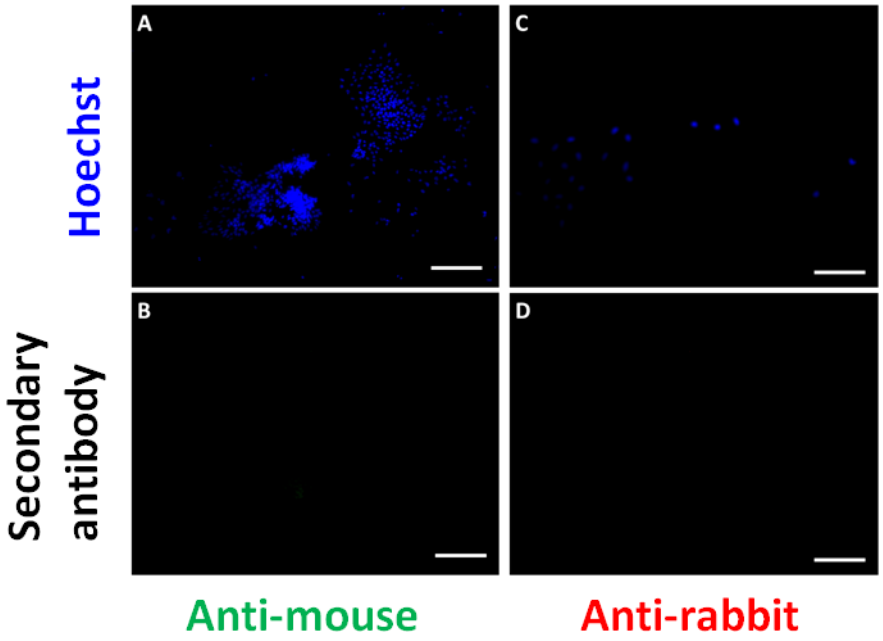

Figure 3.12 Fluorescent immunocytochemistry analysis of control samples

Background staining from the secondary antibodies used for the immunocytochemistry analysis was detected by treating samples without adding primary antibody. The primary antibodies used in this study were either raised in mouse or rabbit. Cells were fixed and also stained with Hoechst nuclear stain to identify cell nuclei (blue). Scale bars = 100 µm.

Nestin is a marker of neural precursor cells in embryonic CNS tissue as it is expressed from E7.5 within the neuroepithelium of the neural plate (Lendahl et al., 1990). On day 6 of neural differentiation, LDN appeared to induce a marginally higher percentage of nestin expression than all other treatments (Fig 3.13).

All treatments appeared to have a similar percentage (between 75% to 90%) of Pax6 expression. *In vivo*, Pax6 expression is found in the ventricular zone of the pallium in mouse embryos (Hill et al., 1991) and is important for establishing and maintaining neural progenitor cell population (Gotz et al., 1998, Quinn et al., 2007). Interestingly, the vehicle control induced strong expression of Pax6 (Fig 3.14).

Examination of the expression of low-affinity neurotrophin receptor p75, a marker for self-renewing neural crest cells (Stemple and Anderson, 1992), shows that it was strongly induced by noggin but not by DM and LDN, suggesting noggin might have an effect on neural crest expression. Neural crest cells are a transient migratory population originating from cells in the dorsal neural folds at the border of the neural plate and epidermal ectoderm and giving rise to neurons and glia of the peripheral nervous system, as well as pigment-producing melanocytes of the skin (Knecht and Bronner-Fraser, 2002, Nieto, 2001) (Fig 3.15).

(a)

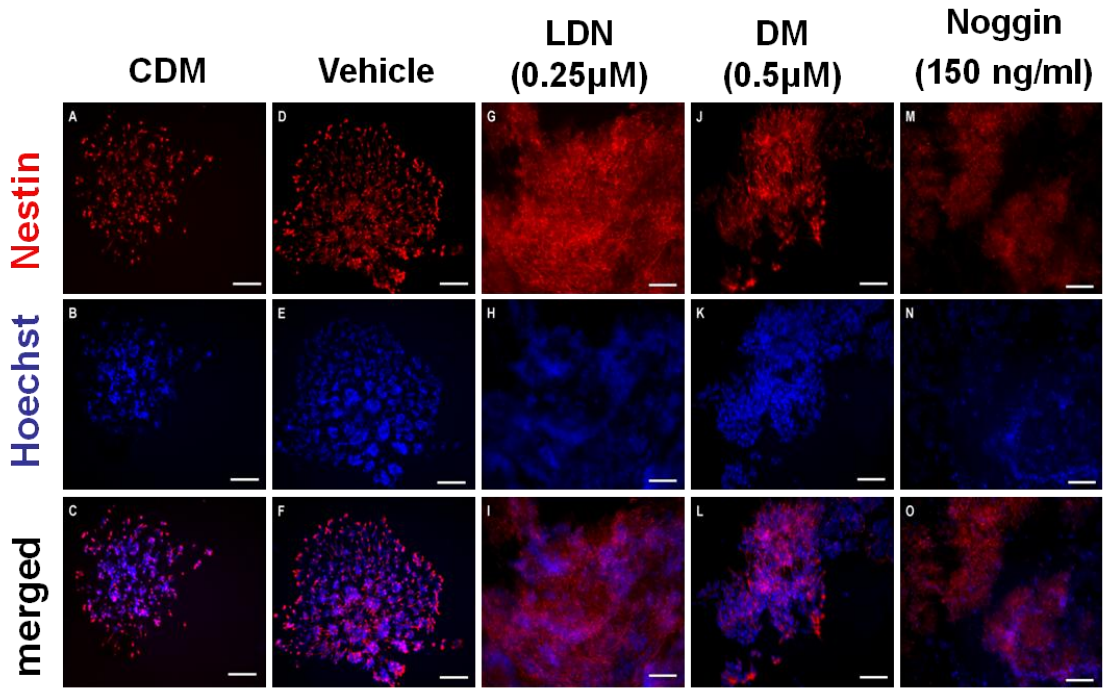

(b)

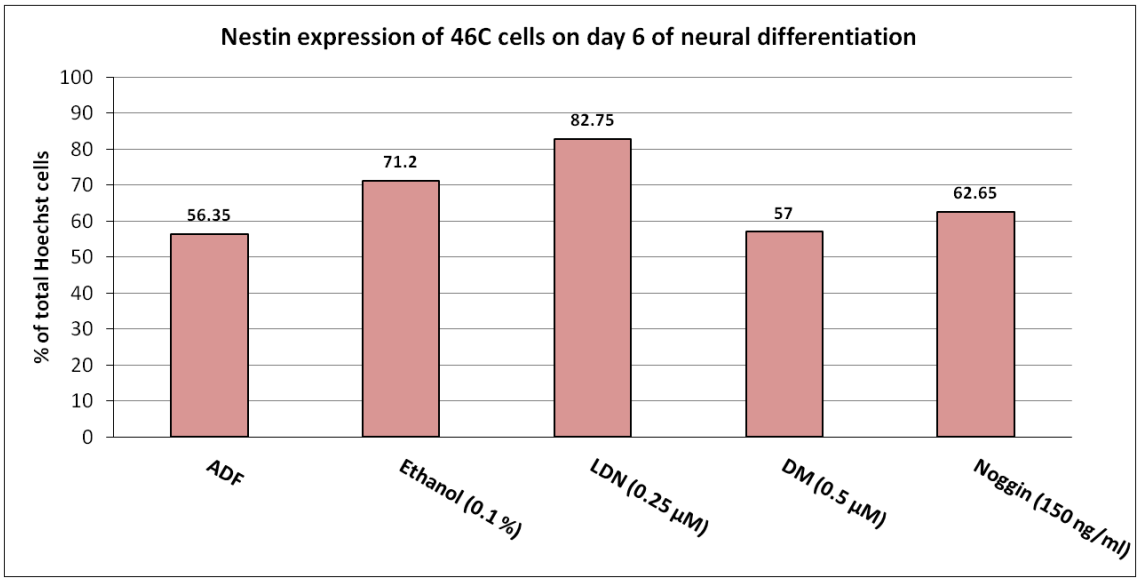

Figure 3.13 Immunocytochemistry analysis of nestin expression

(a) Nestin expression was analysed by fluorescent immunocytochemistry. 46C cells were treated with LDN (0.25 µM), DM (0.5 µM) and noggin (150 ng/ml) for 6 days. Cells were fixed and double-labelled for nestin (red) and Hoechst nuclear stain (blue). Scale bars = 100 µm.

(b) Nestin immuno-positive cells on day 6 were counted and were represented as percentage of total Hoechst cells. Bars represent the mean of the numbers obtained by counting two random fields of one coverslip from one experiment.

(a)

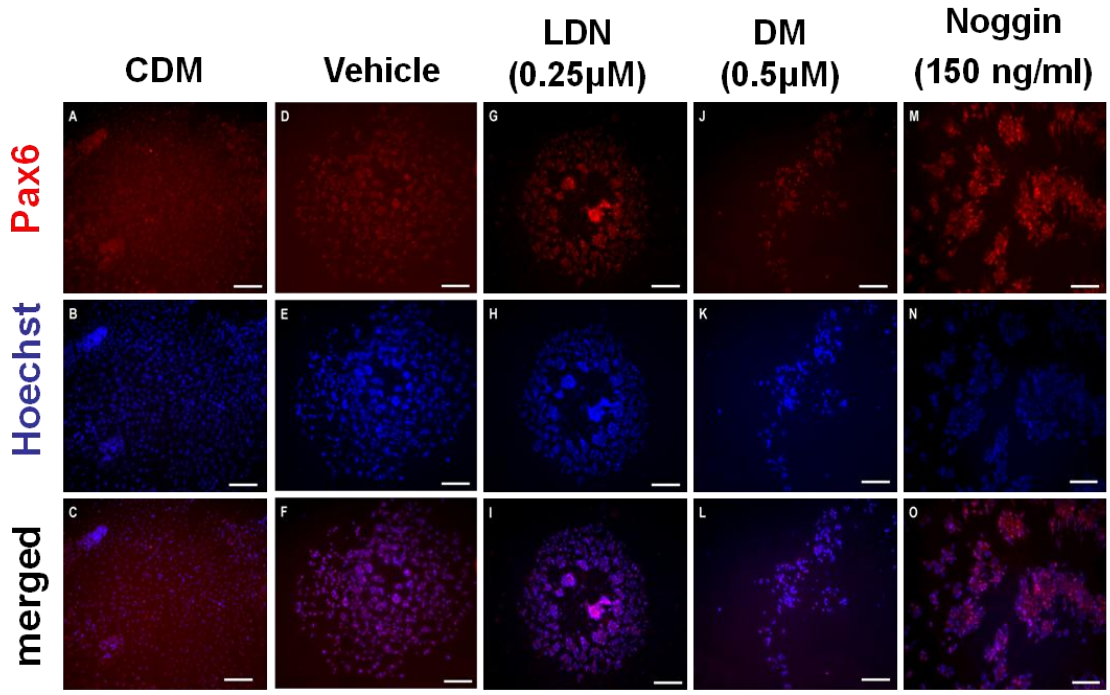

(b)

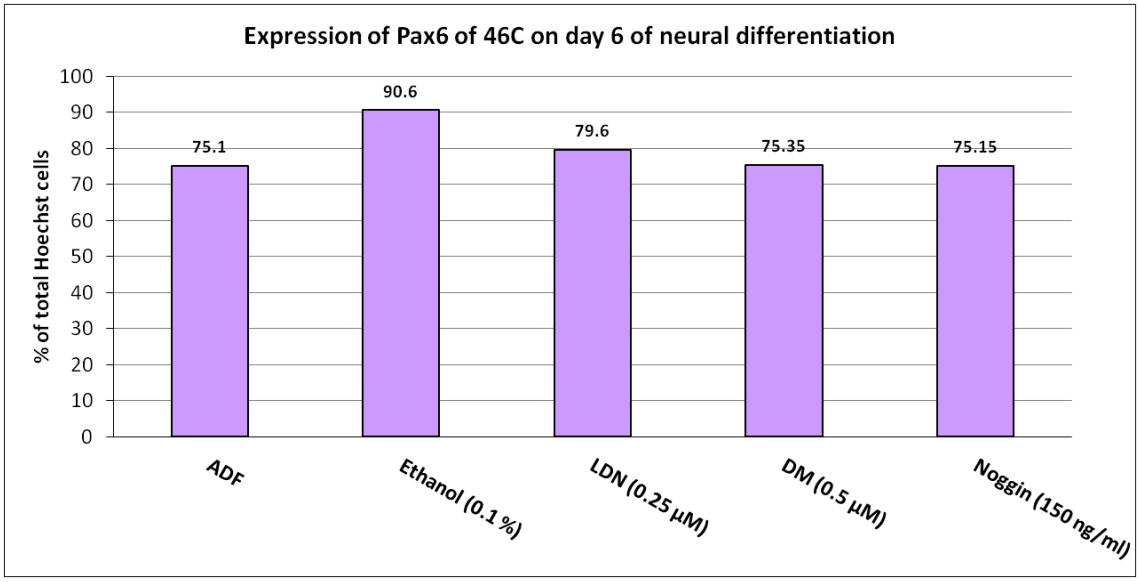

Figure 3.14 Immunocytochemistry analysis of Pax6 expression

(a) Pax6 expression was analysed by fluorescent immunocytochemistry. 46C cells were treated with LDN (0.25 µM), DM (0.5 µM) and noggin (150 ng/ml) for 6 days. Cells were fixed and double-labelled for Pax6 (red) and Hoechst nuclear stain (blue). Scale bars = 100 µm.

(b) Pax6 immuno-positive cells on day 6 were counted and were represented as percentage of total Hoechst cells. Bars represent the mean of the numbers obtained by counting two random fields of one coverslip from one experiment.

(a)

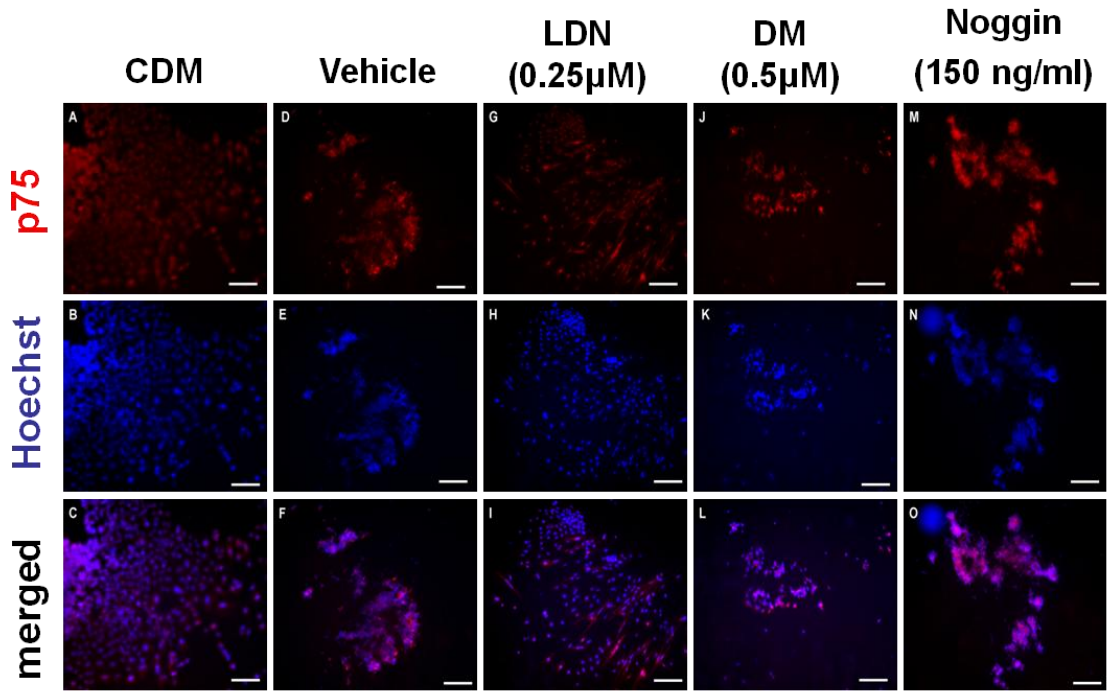

(b)

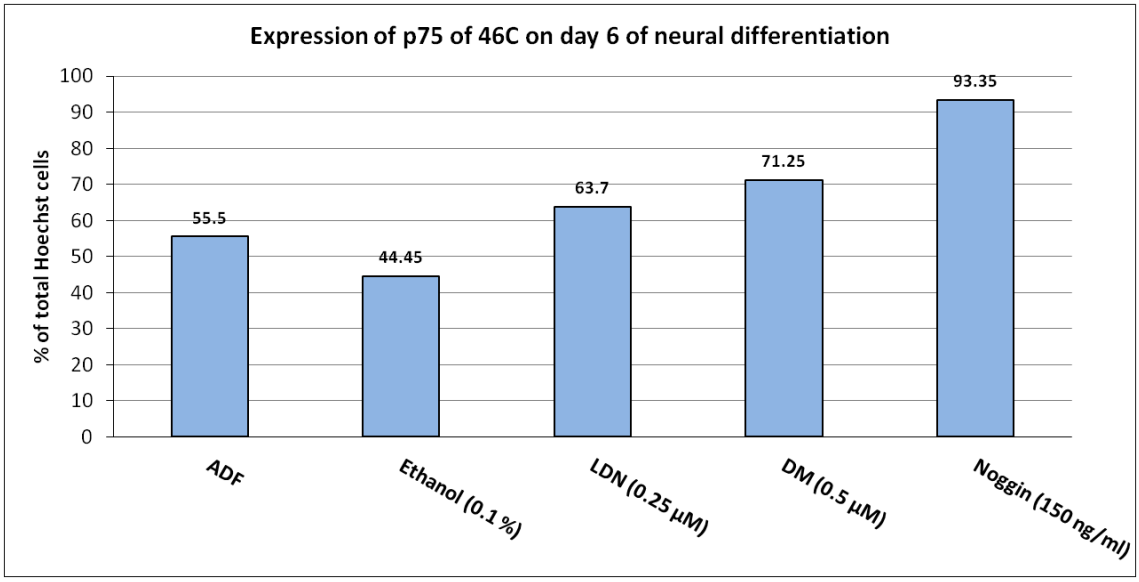

Figure 3.15 Immunocytochemistry analysis of p75 expression

(a) p75 expression was analysed using fluorescent immunocytochemistry. 46C cells were treated with LDN (0.25 µM), DM (0.5 µM) and noggin (150 ng/ml) for 6 days. Cells were fixed and double-labelled for p75 (red) and Hoechst nuclear stain (blue). Scale bars = 100 µm.

(b) p75 immuno-positive cells on day 6 were counted and were represented as percentage of total Hoechst cells. Bars represent the mean of the numbers obtained by counting two random fields of one coverslip from one experiment.

To further examine the lineage commitment of the ES cell-derived neural progenitors, the expression of genes restricted to neural and non-neural lineages was analysed by RT-PCR. It has been shown that Oct4 is essential for the maintenance of pluripotency and is expressed in early pluripotent cells (Niwa et al., 2000) and downregulated upon LIF withdrawal (Faherty et al., 2005). Most cells treated with BMP modulators were committed to other lineages by day 6 of differentiation as strong expression of Oct4 was only found in the undifferentiated ES cells and was lost following differentiation after LIF withdrawal and treatment with either DM, LDN and noggin(Fig. 3.16).

The difference in nestin expression between LDN or DM treatments and the vehicle control (ethanol 0.1%) is small but it appeared that noggin, LDN (0.25 μM) and DM (0.5 μM) -treated cells induced higher Pax6 and nestin expression than CDM control (Fig. 3.16).

The expression of Sox9 was relatively low compared to the expression of Pax6 and nestin. Sox9 is expressed in the dorsal tip of the neural fold and is responsible for specifying neural crest character (Stuhlmiller and Garcia-Castro, 2012, Zhao et al., 1997). The expression of CK18 was also relatively weak across all samples. CK18 is an intermediate filament protein that is expressed in the epithelia (Baribault et al., 1993), indicating that most cells were not directed to the epithelial lineage even in the absence of BMP inhibitors (Fig. 3.16).

The results obtained from RT-PCR and immunocytochemistry analysis showed that the expression of neural markers (Pax6 and nestin) were relatively strong in LDN, DM and noggin treatments, while the expression of neural crest and epithelial markers (p75, Sox and CK18) were relatively weak compared to the expression of neural markers (Pax6 and nestin) for all treatments: this indicated that most cells when differentiated up to day 6, in the presence or absence of LDN or DM, gave rise to cells that have the characteristics of neural progenitor cells.

(a)

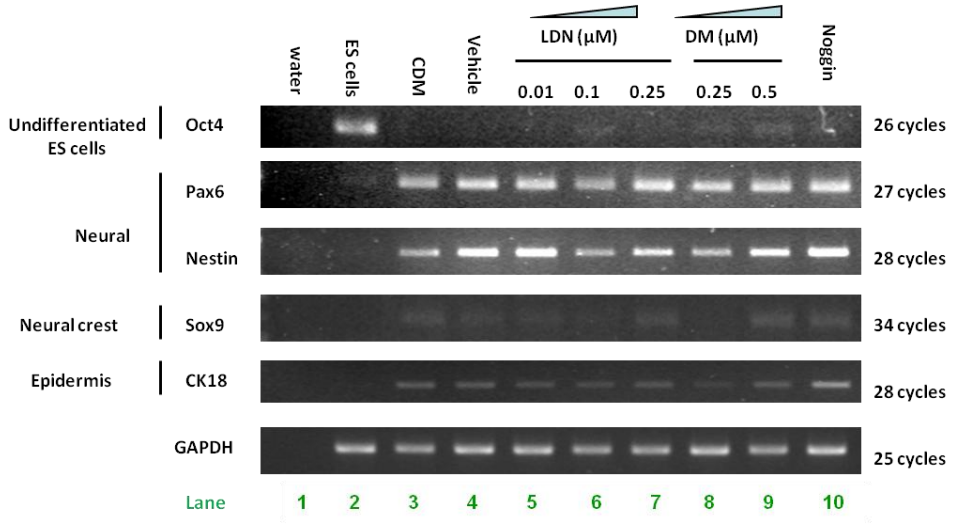
water
ES cells
CDM
Vehicle
LDN (μM)
DM (μM)
Noggin
0.01 0.1 0.25 0.25 0.5
Undifferentiated ES cells
Oct4
26 cycles
Neural
Pax6
27 cycles
Nestin
28 cycles
Neural crest
Sox9
34 cycles
Epidermis
CK18
28 cycles
GAPDH
25 cycles
Lane
1 2 3 4 5 6 7 8 9 10

(b)

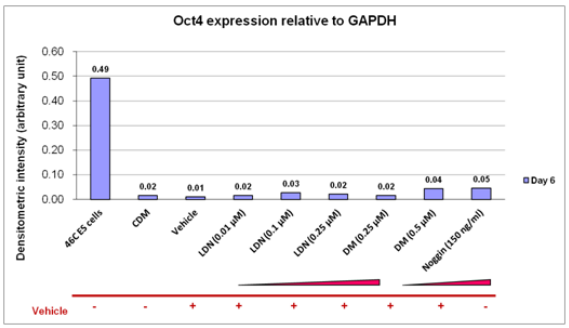
Oct4 expression relative to GAPDH
Densitometric intensity (arbitrary unit)
0.49 0.02 0.01 0.02 0.03 0.02 0.02 0.04 0.05
Day 6
46C ES cells
CDM
Vehicle
LDN (0.01 μM)
LDN (0.1 μM)
LDN (0.25 μM)
DM (0.25 μM)
DM (0.5 μM)
Noggin (150 ng/ml)
Vehicle

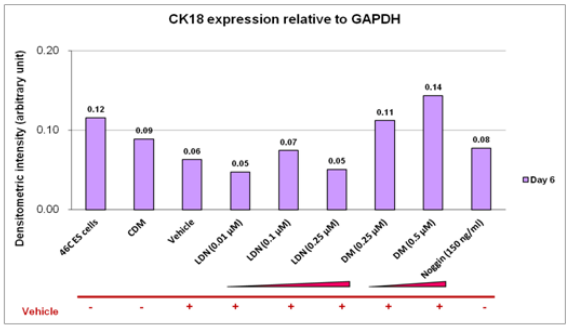
CK18 expression relative to GAPDH
Densitometric intensity (arbitrary unit)
0.12 0.09 0.06 0.05 0.07 0.05 0.11 0.14 0.08
Day 6
46C ES cells
CDM
Vehicle
LDN (0.01 μM)
LDN (0.1 μM)
LDN (0.25 μM)
DM (0.25 μM)
DM (0.5 μM)
Noggin (150 ng/ml)
Vehicle

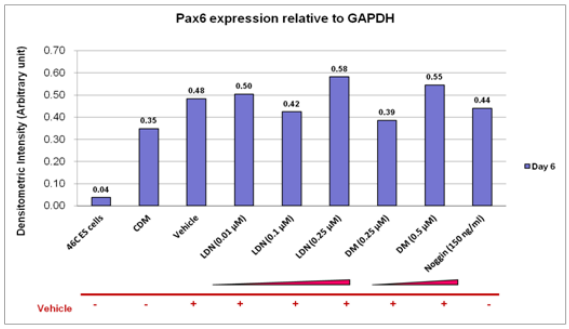
Pax6 expression relative to GAPDH
Densitometric intensity (Arbitrary unit)
0.04 0.35 0.48 0.50 0.42 0.58 0.39 0.55 0.44
Day 6
46C ES cells
CDM
Vehicle
LDN (0.01 μM)
LDN (0.1 μM)
LDN (0.25 μM)
DM (0.25 μM)
DM (0.5 μM)
Noggin (150 ng/ml)
Vehicle

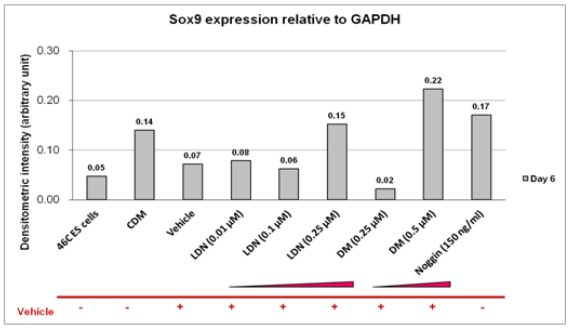
Sox9 expression relative to GAPDH
Densitometric intensity (arbitrary unit)
0.05 0.14 0.07 0.08 0.06 0.15 0.02 0.22 0.17
Day 6
46C ES cells
CDM
Vehicle
LDN (0.01 μM)
LDN (0.1 μM)
LDN (0.25 μM)
DM (0.25 μM)
DM (0.5 μM)
Noggin (150 ng/ml)
Vehicle

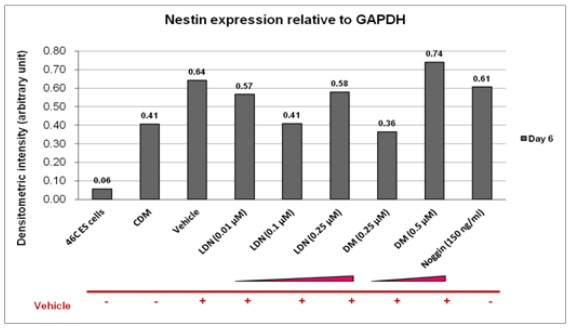
Nestin expression relative to GAPDH
Densitometric intensity (arbitrary unit)
0.06 0.41 0.64 0.57 0.41 0.58 0.36 0.74 0.61
Day 6
46C ES cells
CDM
Vehicle
LDN (0.01 μM)
LDN (0.1 μM)
LDN (0.25 μM)
DM (0.25 μM)
DM (0.5 μM)
Noggin (150 ng/ml)
Vehicle

Figure 3.16 RT-PCR analysis of LDN, DM and noggin treated 46C cells on day 6 of neural differentiation

(a) Gene expression of Oct4, Pax6, nestin, Sox9 and CK18 was determined by RT-PCR analysis on day 6 of neural differentiation. 46C cells were treated with LDN (0.01 μM, 0.1 μM, 0.25 μM), DM (0.25 μM, 0.5 μM). No BMP4 was added in any treatment. Noggin (150 ng/ml) was used as a positive control. Ethanol (0.1%) was used as a vehicle control for LDN and DM.

(b) Band intensity of the PCR products of Oct4, Pax6, nestin, Sox9 and CK18 was quantified by Gel Doc 2000 and was expressed as arbitrary values relative to those obtained for GAPDH.

3.2.8 Phosphorylation of Smad 1/5/8 of neural progenitor cells treated with DM, LDN and noggin

Results obtained from flow cytometry analysis showed that expression of Sox1/GFP was induced by LDN and DM in the presence of BMP4 (0.5 ng/ml) (Figs. 3.6 - 3.9). To confirm that this effect was by BMP antagonism, Western blotting for Smad 1/5/8 phosphorylation was performed at the same time-point (i.e. day 6). The presence of BMP4 induced strong phosphorylation of Smad 1/5 /8 (lane 10, Fig. 3.17 (a), (b)), and this was inhibited by noggin treatment to a level that was similar to that of cultures differentiated in CDM alone (lane 1 and lane 9, Fig. 3.17 (a), (b)). LDN and DM reduced Smad 1/5/8 phosphorylation in a dose-dependent manner (land 3-5 and lane 6-8, Fig. 3.17 (a), (b)). These observations indicate that that LDN and DM antagonise the BMP4 signal through reducing Smad1/5/8 phosphorylation.

Both LDN (0.1 µM) and DM (0.5 µM) treatments showed very similar levels of pSmad 1/5/8 inhibition (lane 4 and 7, Fig. 3.17 (a), (b). However the treatment with LDN (0.1 µM) induced much stronger expression of Sox1/GFP than DM (0.5 µM) treatment (Figs 3.6 and 3.7), suggesting that the level of pSmad 1/5/8 inhibition alone did not determine the level of Sox1/GFP expression.

(a)

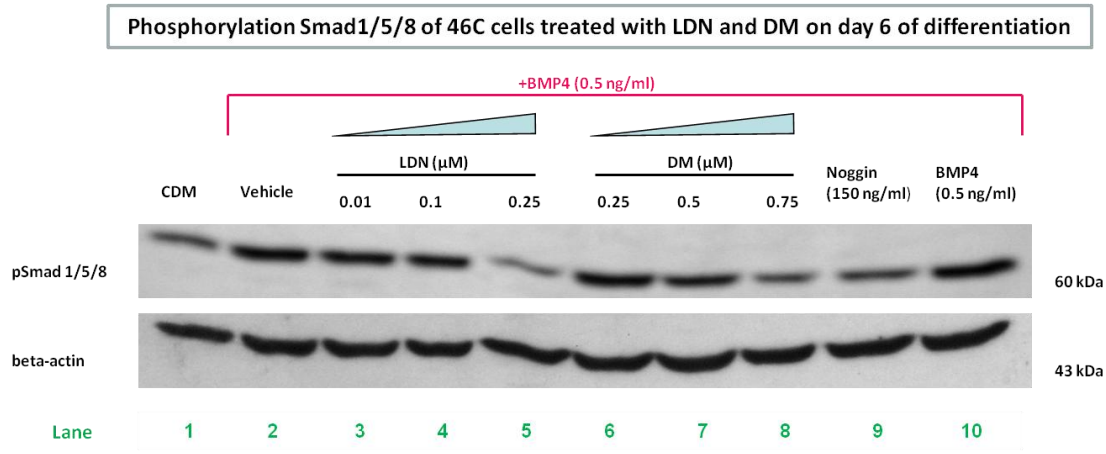

(b)

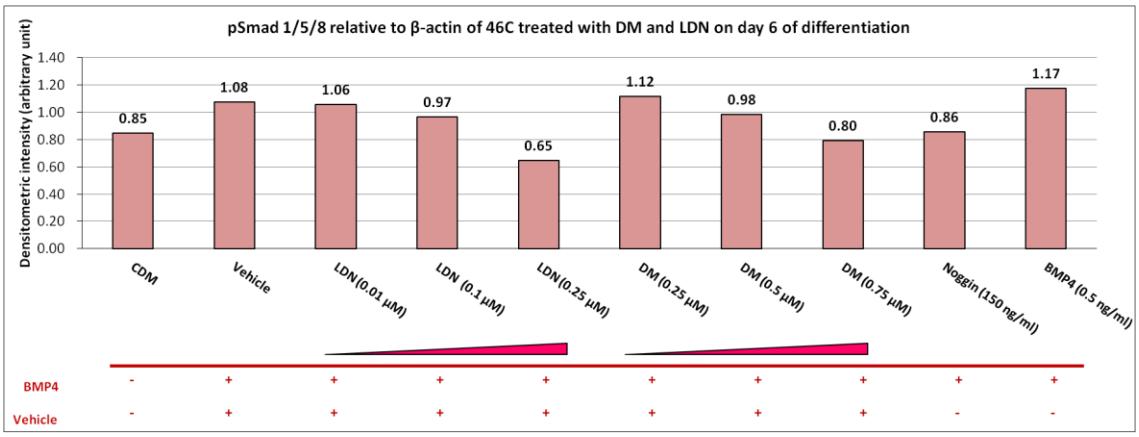

Figure 3.17 Western blotting of 46C cells treated with LDN, DM, noggin and BMP4 on day 6 of neural differentiation

(a) 46C cells were differentiated with LDN (0.01 μM, 0.1 μM, 0.25 μM) and DM (0.25 μM, 0.5 μM, 0.75 μM) for 6 days. Protein was extracted and phosphorylation of Smad 1/5/8 was detected by Western blotting. Ethanol (0.1 %) was used as a vehicle control for LDN and DM. Noggin (150 ng/ml) was used as a positive control for phosphorylated Smad 1/5/8 inhibition. All samples contained BMP4 (0.5 ng/ml) except CDM. Equal loading was confirmed by β-actin.

(b) Band intensity of phosporylated Smad1/5/8 was quantified by QuantiScan and was expressed as a value relative to β-actin expression (n=1).

3.2.9 Effect of DM, LDN and noggin on the metabolic activity

Although DM and LDN enhanced the expression of Sox1/GFP and Pax6 and nestin (Fig. 3.7-3.14), fewer colonies were found at higher doses of LDN and DM when observed under the microscope. Therefore, this raised the question as to whether the treatments with LDN, DM or noggin also had effects on cell vitality. To do this, Wst-1 mitochondrial activity assay was performed to study potential differences in the metabolic rate of cells cultured with increasing concentrations of DM (0.25 µM to 0.75 µM) and LDN (0.01 µM to 0.25 µM). The assay works by measuring the amount of formazan produced by cellular enzymes which cleave tetrazolium salts in Wst-1 reagent. The amount of formazan produced is directly related to the overall activity of mitochondrial dehydrogenases, which in turn correlates to the number of metabolically active cells in the culture.

The absorbance measurements for all treatments measured on day 4 were similar and no significant differences were found (Krustal-Wallis test, $P = 0.384$). On day 6, significant differences were found across all samples (one-way ANOVA test, $F_{8,18} = 66.52$, $P < 0.001$). The metabolic activity was reduced in a dose-dependent manner for DM and LDN treatments, showing that increasing doses of LDN and DM decreased the metabolic activity of the cultures. Significant differences were found between the highest dose and lowest dose of LDN (0.01 µM and 0.25 µM) and DM (0.25 µM and 0.75 µM) (Tukey-Kramer test, $P < 0.05$). This suggested that the metabolic rate and, consequently, the health of the cultures were adversely affected by LDN and DM at higher doses but not at the lower doses. Therefore, the selection of a dose of these compounds for use in differentiation experiments will reflect a compromise between the effectiveness of blockade of BMP signalling and the maintenance of healthy cell cultures (Fig. 3.18).

(a)

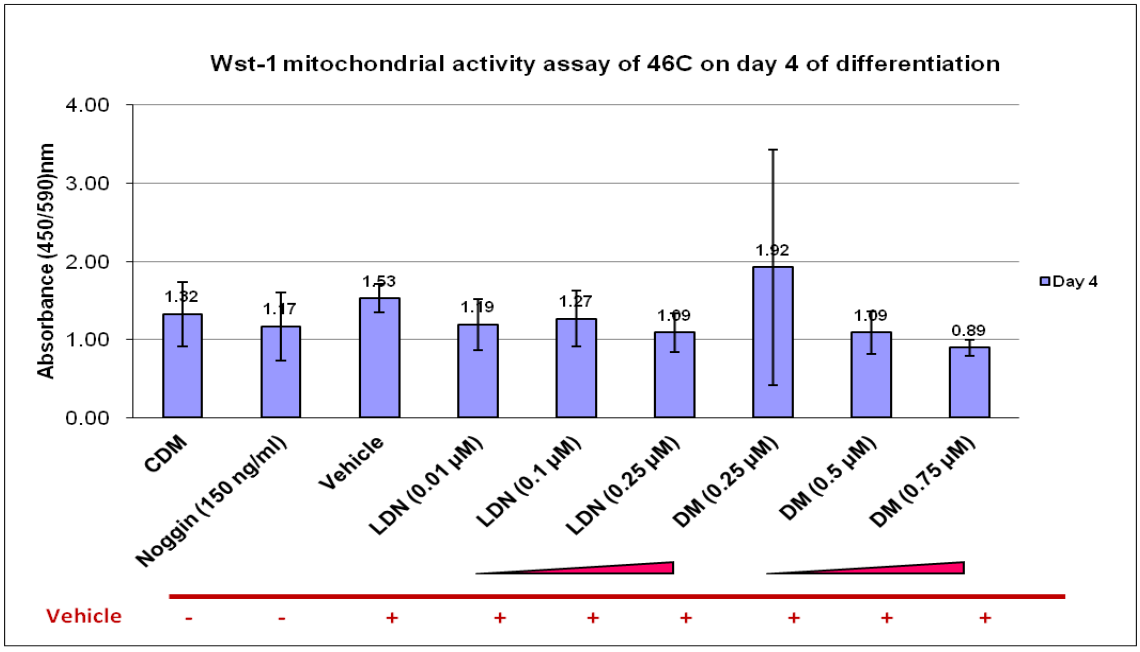

(b)

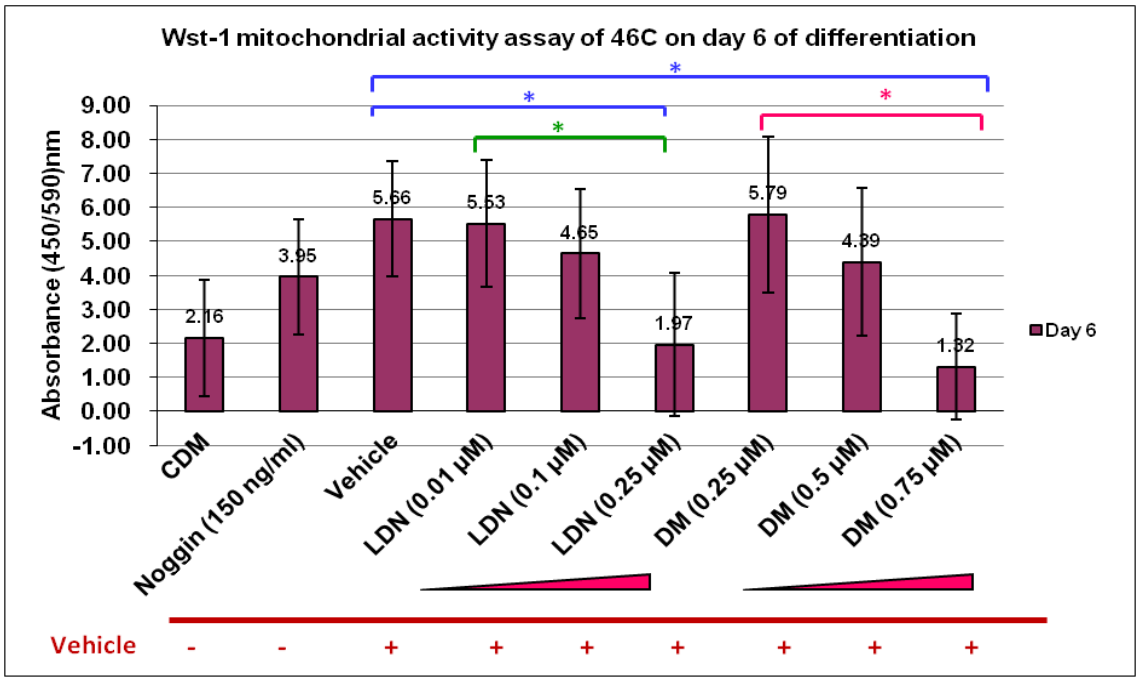

Figure 3.18 Wst-1 mitochondrial activity assay for DM, LDN and noggin treated samples on day 4 and day 6 of neural differentiation

46C cells were treated with LDN (0.01 µM, 0.1 µM, 0.25 µM), DM (0.25 µM, 0.5 µM, 0.75 µM) and noggin (150 ng/ml). Ethanol (0.1 %) was used as a vehicle control for LDN and DM. Cells were differentiated on 96-well plates. The plates were measured at 450 nm normalised absorbance measurements at 590 nm after 2 hours of incubation at 37°C with the Wst-1 reagent. No BMP4 was added in any treatment.

(a) The graph illustrates the mean absorbance on day 4 of neural differentiation for each treatment. Bars represent the mean ± S.D. of three independent experiments. (Krustal-Wallis test, $P = 0.384$)

(b) The graph illustrates the mean absorbance on day 6 of neural differentiation for each treatment. Bars represent the mean ± S.D. of three independent experiments. Significant *post-hoc* differences are indicated with brackets. (Tukey-Kramer test, $*P < 0.05$)

3.3 Discussion

The use of recombinant noggin in inducing the neural differentiation of cell cultures has been shown to enhance neural conversion of ES cells (Tropepe et al., 2001, Okada et al., 2008, Okada et al., 2004, Wu et al., 2012) but with limitations because they have a short shelf-life and have batch-to-batch variation and thus the results might not be always be reproducible (Burton et al., 2010). This study therefore looked at whether LDN and DM could be used as a replacement of recombinant noggin in neural differentiation protocols because they are more stable and cost-effective and therefore can be scaled up effectively for large scale analysis such as drug screening studies.

To investigate the effect of LDN and DM on neural induction of ES cells, 46C Sox1-GRP reporter ES cell line was used to provide assay for neural induction, in particular using flow cytometry analysis to quantify the percentages of cells expressing GFP under different culture treatment regimes. Surprisingly, over 90% of ESC-derived neural progenitor cells expressed Sox1/GFP using CDM as the base differentiation medium in the absence of LDN or DM treatments on day 4 and day 6 of differentiation (Figs. 3.5 and 3.6). Lower percentages of Sox1/GFP expressing cells (60%) were reported by Ying et al.'s study, which describes the first monolayer differentiation protocol. The discrepancy between the findings herein and those of Ying et al's might be due to differences in protocol design. In Ying's protocol, ES cells were plated directly in N2B27 medium, whereas in this study, ES cells were plated in ES medium overnight before differentiation was initiated by changing the medium to CDM. Plating ES cells in ES medium overnight probably produced more optimal cell densities for more effective neural conversion to occur. As revealed by other studies (Watanabe et al., 2005, Tropepe et al., 2001), cell plating densities had a significant effect on the expression of Sox1/GFP on day 4 and day 6 of differentiation. An important factor that regulates differentiation decision between cells is Notch signalling (Lai, 2004). Moderately activated

Notch signalling synchronises the timing of neural induction, homogenizes the level of Sox1 expression between cells and amplifies Sox1 expression (Lowell et al., 2006). It would be valuable to find out whether Sox1 expression found at different cell-plating densities is associated with Notch signalling. The activity of Notch can be detected by generating a reporter cell line for RBPJK protein (which is activated by Notch intracellular domain upon ligand binding (Lai, 2004)) to measure Notch activity at different cell plating densities.

Although it has been shown that noggin treatment can increase the number of neural colonies (Tropepe et al., 2001), this study showed that a high percentage of Sox1-positive cells (>90%) was generated on day 4 and day 6 of differentiation in CDM alone and that DM or LDN treatment did not produce any significant increase in Sox1-positive cells (Fig. 3.5 and 3.6). This raised the question of whether exogenous BMP inhibition is necessary to induce neural differentiation. In fact, certain *in vitro* studies have demonstrated that blocking BMP signalling did not enhance neural conversion. Ying et al. showed that noggin treatment did not increase the level of Sox1/GFP expression in adherent monolayer cultures (Ying et al., 2003b). Kawasaki's study on stromal cell-induced neural differentiation showed that blocking BMP signalling using BMPR-Fc receptobody can reverse the inhibitory effect of BMP4 but had no significant effect on the generation of β-III-tubulin positive colonies (Kawasaki et al., 2000). Furthermore, Smuckler showed that single ES cell differentiated in PBS alone expressed nestin and Sox1 after 4 hours, although nutritive factors were needed for long-term maintenance of neural cultures (Smukler et al., 2006). All this evidence suggested that it might be possible that the high percentage of Sox1/GFP expression found in this study was due to endogenous expression of BMP inhibitors in subpopulations of cells. Therefore it would be worthwhile to find out the expression of BMPs and BMP inhibitors (chordin, follistatin and noggin) of neural progenitors from day 0 to day 6 of differentiation in order to assess the importance of BMP inhibition in neural differentiation.

The first evidence that suggested DM and LDN can enhance neural differentiation was that they induced higher intensity of Sox1/GFP expression than CDM alone. However, since the levels of Sox1/GFP induction were already high in CDM alone, it was difficult to make accurate comparisons of the effects of LDN, DM and noggin. Therefore in order to make these such comparisons on the level of Sox1/GFP induction, neural induction in the base medium CDM was first suppressed by treatment with a low dose of BMP4, thus providing a more sensitive and direct assay to measure the potency of BMP antagonism to the different agents for Sox1/GFP induction. In the presence of BMP4 (0.5 ng/ml), LDN was more effective than DM in overcoming the BMP4 suppression of neural induction as assessed by induction of Sox1/GFP expression. DM induced higher expression of Sox1/GFP than the vehicle control (ethanol 0.1%) but the response was slower than LDN (Figs. 3.8 and 3.9). The difference in the response rate could be due to the difference in chemical groups found in LDN and DM and will require some structure-activity studies to confirm.

In examining the expression of the neural markers Pax6 and nestin, using RT-PCR and immunocytochemistry, noggin led to greater expression than did CDM control. The results obtained from LDN- and DM-treated samples were less conclusive and would require further work to confirm. The data obtained from RT-PCR nevertheless appeared to show that both LDN (0.25 μM) and DM (0.5 μM) treatments induced at least a comparable if not higher level of nestin and Pax6 expression than the vehicle control (Figs. 3.13 and 3.16). These data are consistent with a DM study carried out in human ES cells and human iPS cells. In human ES cells, expressions of Pax6, Sox1 and nestin showed dose-dependent response to DM through downregulation of Smad1/5/8 expression. The level of increase was even greater than noggin treatment alone (Kim et al., 2010). A surprising result in this study was that noggin appeared to induce a higher level of p75 expression. This would suggest an additional effect on promoting neural crest development, however, it is well-established in the developmental biology literature that BMP antagonism acts to suppress neural crest

development (Kanzler et al., 2000, Okada et al., 2008). Therefore, further studies are required to confirm the observation.

Compared to noggin, both DM and LDN had relatively little effect on the expression of the neural crest markers Sox9 and p75 and also the epithelial marker CK18. Differing doses of both compounds were not observed to result in wide variation in neural marker-expression. The vehicle treatment (ethanol 0.1%) seemed to be able to enhance the expression of Pax6 and nestin, which makes it difficult to determine whether LDN and DM have any additional effect in enhancing the expression of the early neural markers. In addition, the vehicle treatment also increased the level of Smad1/5/8 phosphorylation in DM-treated undifferentiated cells (Fig. 3.17) and increased the mitochondrial activity on day 6 of differentiation (Fig. 3.18). The fact that the effect of vehicle control was detected only in some experiments suggests that certain steps involved in neural specification might be more sensitive to ethanol. These observation could probably be explained by a recent study which showed that exposing mouse ES cells at 25 nM to 100 nM of ethanol resulted in an increase in Oct4/Sox2 ratio in a dose-dependent manner during the first 4 days of RA-directed neural differentiation (Ogony et al., 2013). The change in stoichiometry of Oct4 and Sox2 was reported to be able to divert ES cells from neuroetodermal lineage to mesoendodermal lineage (Thomson et al., 2011). As a result cells expressed less β-III-tubulin on day 6 of differentiation (Ogony et al., 2013). And this suggested that ethanol might have an effect on lineage specification through altering the balance of lineage specifiers.

The use of small molecules for inducing neural progenitors from ES cells can be hindered by its off-target effects. One known off-target effect for DM is 5' AMP-activated protein kinase (AMPK) inhibition (Zhou et al., 2001). AMPK plays a key role in energy consumption, including the regulation fatty acid oxidation and glucose transport (Hardie and Carling, 1997, Merrill et al., 1997, Hayashi et al., 1998). A study of AMPK activity in transgenic mice that had kinase dead (KD) mutation of the α2 catalytic subunit of AMPK in

the heart reveals that the loss of AMPK activity is associated with an inability to augment glucose uptake and glycolysis with an increase in apoptotic activity (increased caspase-3 activity and TUNEL staining) during low-flow ischemia (Russell et al., 2004). Data from the Wst-1 mitochondrial activity assays showed that the metabolic activity of NPCs was reduced with increasing doses of DM and LDN. Whether this observation had any association with AMPK inhibition remains unclear, and requires more studies to clarify. Examination of the effect of DM and LDN on the AMPK pathway will give more information about how AMPK might be associated with the metabolic activity in LDN and DM treatments and allow better strategies for neural differentiation to be designed.

The data in this study indicated that both LDN and DM inhibited Smad1/5/8 phosphorylation in undifferentiated ES cells and neural progenitor cells in a dose-dependent manner (Figs 3.1, 3.2, 3.16), and this was in accordance with previous studies that first describe DM and LDN as BMP inhibitors (Yu et al., 2008, Cuny et al., 2008). However, the DM and LDN do not always have the same effect even though they are structurally similar. For instance, DM but not LDN induced the formation of neurite outgrowth through ErK1/2 activation in PC12 cells, a rat cell line isolated from an adrenal medullary pheochromocytoma and used as a model to study neuronal differentiation and neurite outgrowth (Vaudry et al., 2002, Kudo et al., 2011). The exact mechanism of how DM activate Erk1/2 was unclear but the action is cell type specific because Erk1/2 was not activated in C2C12 cells (murine mesenchymal cell line) (Boergermann et al., 2010). On the other hand, Erk1/2 is a key regulator of cell proliferation through induction of positive regulators of the cell cycle (Meloche and Pouyssegur, 2007, Cargnello and Roux, 2011). Thus it would be of interest to test whether DM or LDN treatment had any effect on Erk1/2 activation because this could explain the reduction in metabolic activity of DM-treated samples analysed by the Wst-1 mitochondrial assay (Fig. 3.18).

Data presented here suggests that LDN is more effective than DM and has a similar effect to recombinant noggin in inducing neural differentiation in mouse ES cultures. The reduction of the metabolic activity of DM and LDN was less pronounced at lower doses. Therefore, one possible way to obtain more neural colonies is to use lower doses of DM and LDN accompanied by recombinant noggin. The delayed action of DM in inducing Sox1/GFP expression suggests that it might be possible to retain more colonies by exposing them to recombinant noggin for a short period initially, followed by DM exposure. More specific small molecules that target the BMP-mediated Smad pathway will need to be developed in future in order to restore the metabolic activity of cells treated with small molecules.

3.4 Conclusion

In summary, 46C cells underwent neural differentiation when plated at low density and expressed early neural markers including Sox1, nestin and Pax6. Although the expression of the neural markers was further enhanced by LDN, DM and noggin, partly due to BMP inhibition, the metabolic activity was reduced by LDN and DM in a dose-dependent manner.

CHAPTER 4:

DEFINING TEMPORAL RESPONSIVENESS OF NEURAL PROGENITORS TO THE CAUDALIZING ACTION OF RETINOIC ACID SIGNALLING

4.1 Introduction

Neural progenitor cells (NPCs) are competent to differentiate into a vast number of neurons and glia. Their potential for differentiating into different neuronal subtypes, therefore, brings with it hopes for the treatment of a number of neurological disorders by stem cell replacement therapy. The identity of neuronal subtype generated from NPCs is determined by the regional identities of the NPCs. A key element of regional specification is temporal regulation: this appeared to govern the developmental potential of NPCs (Allen, 2008). This chapter looks at how the regional specification of NPCs is temporally regulated by retinoic acid (RA), an important regulator for the regional patterning of the neural tube *in vivo* (Maden, 2002).

A number of *in vivo* studies have shown that the effect of RA on neural patterning is stage-specific. RA administration at mid-late streak stage (7.2-7.4 days post coitum (dpc) mice resulted in severe brain malformation including truncation of the brain and molecular alterations such as the repression of forebrain markers, Otx2, Emx2, Emx1 and Dlx1. The effect was stage-specific because if RA was administered 6-10 hr earlier or later, the expression of the forebrain markers was preserved, and less severe brain malformation was found (Simeone et al., 1995, Avantaggiato et al., 1996). This suggested that forebrain patterning undergoes a critical period of RA exposure and brain formation can be affected by the level of RA (Luo et al., 2004). The correct level of RA in the anterior region appears to be controlled by RA catabolizing enzyme Cyp26a1, which is expressed transiently at the anterior epiblast at E7 (Fujii et al., 1997, MacLean et al., 2001). RA administration to Cyp26a1$^{-/-}$ embryos caused severe head truncation between E7.5-E8.5, and a more severe effect was found if RA was supplemented between E6.5-E7.5. This also adds further proof that the effect of RA is stage-specific (Ribes et al., 2007).

RA activity is detected as early as in the epiblast stage (Ribes et al., 2009), and has been reported to regulate neural patterning in a region-specific manner (Rhinn and Dolle, 2012). Within the hindbrain, loss-of-function mutants in RA synthesizing enzyme Raldh2 displayed a loss of posterior rhombomeres (r5-7) in the hindbrain and expansion of more anterior ones (r2-4) (Niederreither et al., 2000, White et al., 2000). Several studies have also reported the role of dynamic expression RA catabolizing enzymes Cyp26s in establishing specific rhombomeric territories by modulating the RA gradient or periods of RA exposure (Gavalas, 2002, Sirbu et al., 2005, Hernandez et al., 2007, Maves and Kimmel, 2005, White et al., 2007) (see section 1.6.3.3).

The effect of RA on forebrain development is somewhat less conclusive compared to that of hindbrain development. Niederreither et al. showed that the forebrain development was normal in Raldh2$^{-/-}$ embryos because the expression of forebrain marker (Otx2) was not affected (Niederreither et al., 1999), whereas a recent transcriptomic analysis of Raldh2$^{-/-}$ embryos reported that expression of forebrain marker Emx2 and Foxg1 was downregulated due to RA deficiency (Paschaki et al., 2013). The role of forebrain development appears to be evident because RA activity was detected in the telencephalon between E9.5 to E14.5 examined by RARE-LacZ transgene (Dolle et al., 2010). Disruption of RA signalling by blocking the RAR receptor resulted in the misspecification of Nkx2.1 MGE progenitors and caused them to initiate LGE-specific neuronal differentiation (Rajaii et al., 2008). A number of studies analysing the effect of RA on forebrain development brought to light the importance of RA in regulating neurogenesis in the LGE (Molotkova et al., 2007). The LGE is more competent to respond to RA signalling than the MGE or the cortex, as revealed by higher expression of cellular retinol binding protein (CRBP) at E12.5 (Toresson 1999), and Raldh3 at E11 (Li et al., 2000, Luo et al., 2004). Enhanced RA signalling in the LGE promoted striatal neuronal differentiation, an effect that was not found in MGE cultures (Toresson et al., 1999). In summary, RA is involved in regulating forebrain and hindbrain development as

shown by the expression of RA receptors, RA synthesizing enzymes (Raldhs) and RA catabolizing cytocrhome P450 (CYP26s) enzymes in both regions. However, the exact mechanisms and requirements for RA to generate region-specific responses remain unclear.

In vitro, RA regulates caudalization in early ES cells-derived NPCs in a concentration-dependent manner (Okada et al., 2004, Okada et al., 2008, Irioka et al., 2005), but relatively little is known about the effect of RA on the expression of forebrain markers in ES cell-derived NPCs. It is known that ES cell-derived NPCs display temporal restriction in cell fate specification (Bouhon et al., 2006). The experiments presented in this chapter aimed to determine how the changing temporal windows of competence and responsiveness to RA can affect the regional specification of NPCs. To investigate this, ES cells were differentiated in the presence of FGF2 for 20 days and RA treatment was initiated at regular intervals. Against this background the expression of early forebrain markers, including that of the early telencephalic marker Foxg1 (Xuan et al., 1995), was determined. The cell line Foxg1Z (a gift from J. Quinn and D. Price) was generated by replacing most of the coding sequence of Foxg1, which is contained in a single exon, with LacZ and a neomycin cassette. They were used for most experiments here as a convenient tool for determining Foxg1 expression using X-gal staining and the Beta-Glo assay to detect Foxg1 driven β-galactosidase expression.

4.2 Results

4.2.1 The characterization of Foxg1Z cells

It has been shown that FGF2 upregulated rostral gene expression (Bouhon et al., 2006), and exposure of ESC-derived NPCs to RA promotes caudalization and suppresses rostral gene expression (Wichterle et al., 2002). Therefore, the first investigation examined whether Foxg1 and the lacZ gene are co-expressed in response to morphogens in Foxg1Z cells. Foxg1Z cells were differentiated for 8 days with FGF2 in the presence or absence of RA. Fluorescent immunocytochemistry was performed to examine the expression of Foxg1 and β-galactocidase (expressed by the LacZ gene) of Foxg1Z cells.

Merged images (images C and C') illustrate that the lacZ reporter and wildtype Foxg1 alleles were co-expressed in response to FGF2. This indicated that Foxg1Z cells responded to FGF2 signalling by expressing Foxg1. Furthermore, this experiment demonstrated that when Foxg1Z cells were differentiated in the presence of RA (1 μM), only very weak expression of Foxg1 and β-galactocidase was detectable, thus indicating that RA treatment for 8 days of differentiation inhibited the expression of Foxg1 (Images E-G, E'-G') (Fig. 4.1).

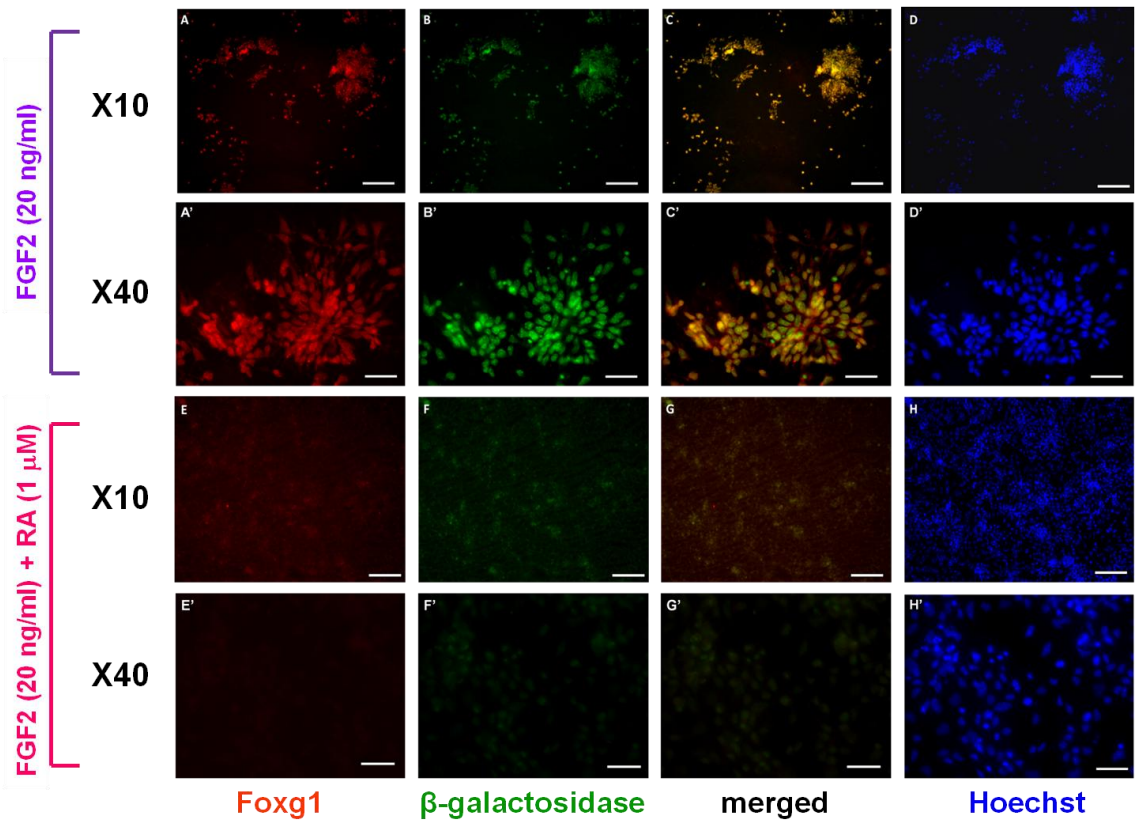

Figure 4.1 **Fluorescent immunocytochemistry analysis of RA treated Foxg1Z cells on day 8 of neural differentiation**

Foxg1Z and β-galactosidase expression was analysed by fluorescent immunocytochemistry on day 8 of differentiation. FGF2 (20 ng/ml) was added from day 4 to day 8, and cells were fixed and triple-labelled for β-galactosidase (green), Foxg1 (red) and Hoechst (blue). Scale bars for x10 images = 100 µm; Scale bars for X40 images = 25 µm.

4.2.2 Investigation of the effect of RA on Foxg1/LacZ expression in early and late neural cell cultures

The last section revealed that the expression of Foxg1/LacZ was strongly reduced after incubating cells with RA (1 μM) for 8 days (Fig. 4.1). The next step was to investigate whether there would be a change in Foxg1 expression when RA was added at different time points. If cells displayed a change in responsiveness to RA, it would be possible that cells might respond to RA by downregulating the expression of hindbrain markers. To investigate this, Foxg1Z cells were maintained in chemically defined medium (CDM) for differentiation for 20 days. FGF2 was added on day 4 to induce Foxg1 expression and to maintain long-term propagation of neural stem cells (Tropepe et al., 2001, Lee et al., 2000, Okabe et al., 1996). FGF2 was added from day 4 and not from day 0 because previously generated data showed that Foxg1Z gave the highest Foxg1 expression on day 8 of differentiation (Precious, 2009) – a phenomenon which could be explained by an *in vivo* finding that neural progenitor cells do not acquire responsiveness to FGF2 before E8.5 (Hitoshi et al., 2004). Starting at day 6 of differentiation, Foxg1Z cells were dissociated into single cells and plated onto poly-L-ornithine coated-tissue culture plastic plates every 4 days thereafter. RA (1 μM) was added at 4-day intervals during the course of differentiation and analyses were carried out on day 8 and day 20 of differentiation. These two time points were chosen because the Bouhon et al. study made it clear that early neural progenitor cells (day 8 cultures) responded to the caudalizing signal RA by displaying differential patterning responses at day 8 and day 20 (Bouhon et al., 2006). A schematic illustration of the differentiation strategy is shown in Fig. 4.2.

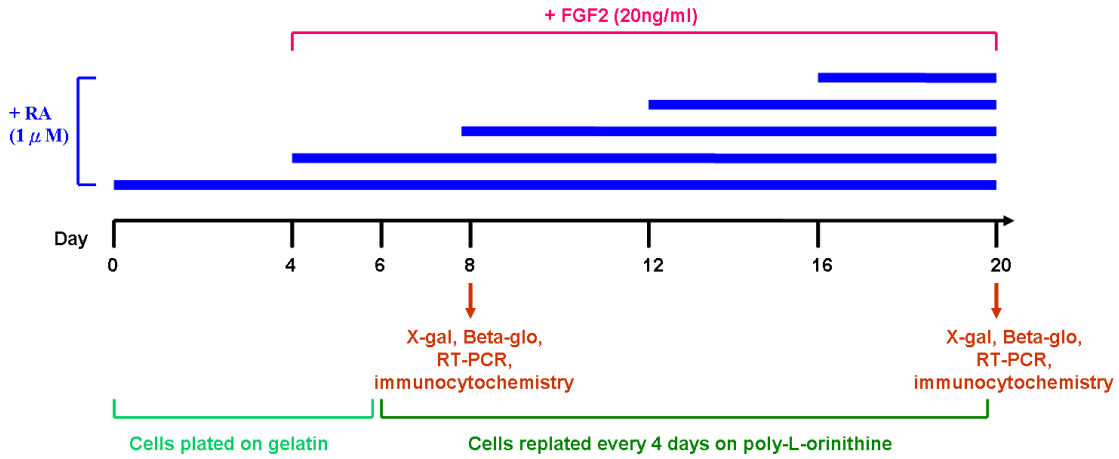

Figure 4.2 Schematic representation of the differentiation protocol used in this study

Foxg1Z cells were differentiated in CDM on gelatin-coated plates for the first 6 days of differentiation and dissociated into single cells and replated onto poly-L-ornithine-coated plates every 4 days. FGF2 (20 ng/ml) was added from day 4 to day 20. RA (1 μM) was added starting at 4-day intervals from day 0 to day 20 and analyses were carried out on day 8 and day 20 of differentiation.

4.2.3 X-gal and Beta-Glo analysis of Foxg1/LacZ expression in early and late neural cultures

The time-window within a 20-day period in which RA had an effect on Foxg1/LacZ expression was examined using 5-Bromo-4-chloro-3-indolyl galactopyranoside (X-gal) staining. X-gal staining measures the activity of beta-galactosidase (encoded by the LacZ gene), This cleaves the β-glycosidic bond in X-gal and gives 5,5'-dibromo-4,4'-dichloro-indigo yielding a blue product. Foxg1/LacZ expression was also quantified using a Beta-Glo assay. To perform the Beta-Glo analysis, Foxg1Z cells were analysed by both the Beta-Glo assay and the Wst-1 assay, and the readings obtained by Beta-Glo assay were normalised by Wst-1 assay. The Beta-Glo assay works by measuring luminescence produced by β-galactosidase which catalyses luciferin-galactoside substrate in the Beta-Glo reagent to produce oxyluciferin. However, the oxyluciferin produced can be misrepresented by the number of metabolically active cells presented because a higher reading can be obtained if more metabolically active cells are present in the sample. To control for this, the number of metabolically active cells was measured by Wst-1 mitochondrial activity assay. This gives readings about the overall metabolic activities of each measured samples.

On day 8, X-gal staining made it clear that the number of Foxg1/LacZ positive cells was highest in the absence of RA (image A, Fig. 4.3 (a)). Almost no Foxg1/LacZ positive cells were found if RA was added on day 0 and only a small number of Foxg1/LacZ positive cells were found when RA was added on day 4 (Images B and C, Fig. 4.3 (a)). Similar results were obtained with the Beta-Glo analysis. That showed that Foxg1/Z cells grown in the control sample (without RA) had the highest Foxg1/LacZ expression. Adding RA (1 μM) on day 0 and day 4 strongly reduced Foxg1/LacZ expression (Fig. 4.3 (b)), indicating that early neural cultures responded to RA primarily by reducing Foxg1 expression.

On day 20, through X-gal analysis, it was seen that the number of Foxg1/LacZ positive cells was relatively similar across all samples, and the day 20 control sample appeared to have a much lower number of Foxg1/LacZ positive cells than the day 8 control sample (Image D, Fig. 4.4 (a)). Adding RA at day 0 gave almost no positive Foxg1/LacZ cells (Image E, Fig. 4.4 (a)). Beta-Glo analysis showed that the expression of Foxg1/LacZ was increased gradually until day 12 and to a level that was comparable to the control sample (Fig. 4.4 (b)), implying that the inhibition of Foxg1 expression by RA was gradually reduced when RA was added at later time points.

In summary, the optimal time point for RA caudalization appears to be at day 0. After this point a diminishing number of cells appear to be receptive to RA signalling (Fig. 4.4 (b)). Although there was no substantial difference between day 0 and day 4 RA additions when Foxg1/LacZ expression was sampled at day 8, Day 0 RA addition was much more effective than day 4 RA addition at reducing Foxg1/LacZ expression when sampled at day 20. At day 16, RA addition also reduced Foxg1/LacZ expression at day 20, indicating that there might be a second time window at which the cells are receptive to caudalization by RA. However, whether NPCs at day 8 are the same as NPCs at day 16 is questionable and the conclusions drawn from time window experiments must be interpreted with this caveat.

(a)

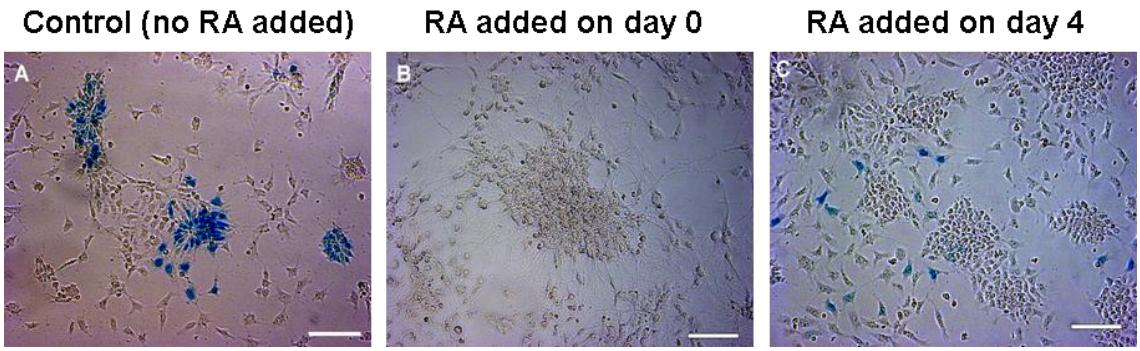

(b)

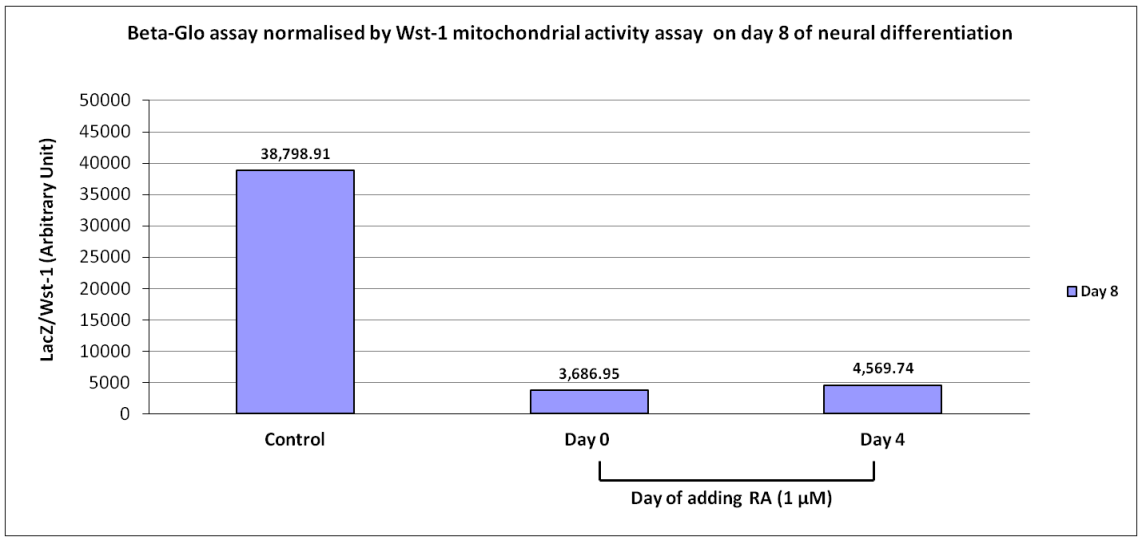

Figure 4.3 Expression of Foxg1/LacZ analysed by Beta-Glo assay and X-gal staining of Foxg1Z cells with RA (1 µM) added at day 0 and day 4

Foxg1Z cells were differentiated in CDM with RA (1 µM) added on day 0 and day 4. FGF2 (20 ng/ml) was added from day 4 to day 8. The expression of LacZ/Foxg1 positive cells was detected by X-gal staining and quantified by Beta-Glo assay on day 8. Bars represent the mean of triplicates of one experiment. Scale bars = 100 µm.

(a)

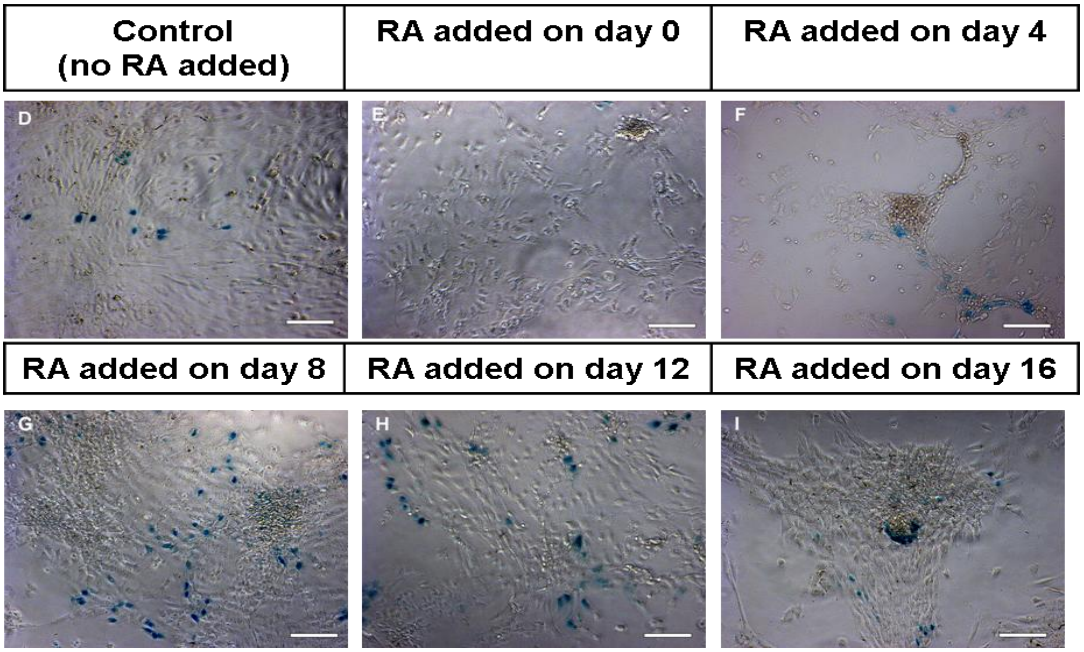

(b)

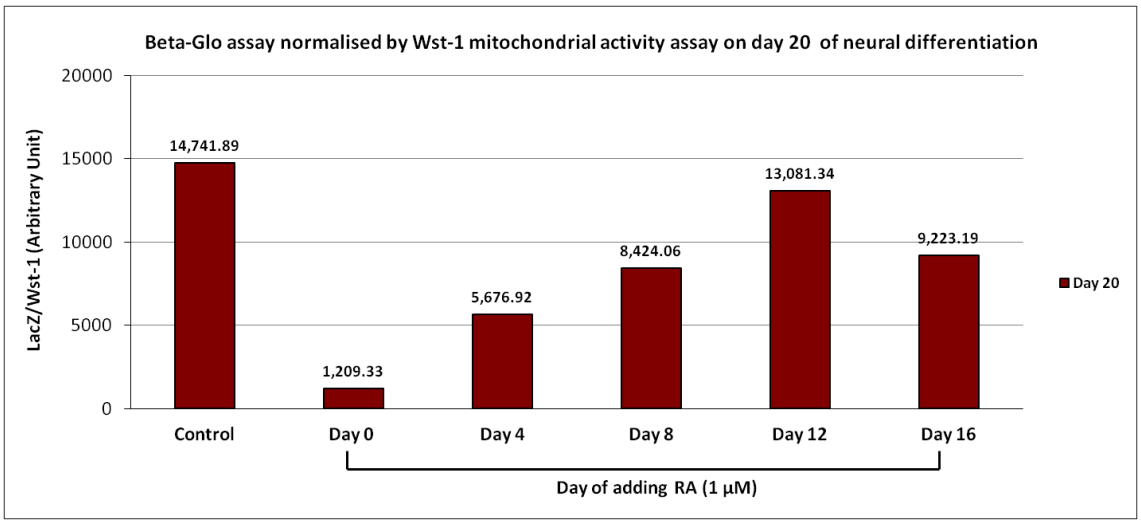

Figure 4.4 Expression of Foxg1/LacZ analysed by Beta-Glo assay and X-gal staining of Foxg1Z cells with RA (1 µM) added at day 0, 4, 8, 12 and 16

Foxg1Z cells were differentiated in CDM with RA (1 µM) added at every 4-day interval from day 0 to day 20. FGF2 (20 ng/ml) was added from day 4 to day 20. The expression of LacZ/Foxg1 positive cells was detected by X-gal staining and quantified by Beta-Glo assay on day 20. Bars represent the mean of triplicates of one experiment. Scale bars = 100 µm.

4.2.4 Effect of RA on anteroposterior patterning of early and late NPCs

The number Foxg1/LacZ-expressing cells was affected by the timing of RA addition and also the duration of RA exposure (Figs. 4.3 and 4.4). The changes in Foxg1/LacZ expression in response to RA suggested that other positional markers might also show differences in expression in early and late cultures. To gain further insight into how RA regulated the specification of rostrocaudal and dorsoventral positional identity in early and late neural cultures, RT-PCR and fluorescence immunocytochemistry of regionally specific markers were performed on the day 8 and day 20 cultures.

Foxg1 expression was strongly suppressed by day 0 RA addition but gradually increased when RA was added from day 4 onwards in early (day 8) and late (day 20) neural cell cultures. This clearly suggests that the optimal time window for caudalization by RA is between day 0 and day 4. LacZ expression also took place, controlled as it is by Foxg1 promoter. The data showed that the expression of LacZ corresponded well with Foxg1 expression in RT-PCR analysis (Fig. 4.5 (a), (b)).

The expression pattern of the protein in question was studied by fluorescence immunocytochemistry. Cells were considered to be immuno-positive if Foxg1 expression overlapped the nuclear stain. The immunocytochemistry data presented in this chapter brings to light an interesting possible trend in the way protein expression might be affected by time and RA treatment. Though their reliability would be enhanced by further work, two independent experiments yielded interesting results. Significant differences were found in Foxg1 expression across all samples (Krustal-Wallis test, $P = 0.002$). As expected, RA reduced Foxg1 expression significantly in early and late cultures (Mann-Whitney U test, $P < 0.05$). It appeared that the difference between the control sample and samples that were treated with RA gradually became less pronounced in late cultures. By the time RA was added on

day 16 in late cultures, the expression level of Foxg1 was about half that which was observed in the control sample in late culture (Fig. 4.6).

RT-PCR analysis of hindbrain marker HoxB3 (Manzanares et al., 1999) in early neural cultures (day 8) showed that the expression was strongly induced by RA. In late neural cultures, strong HoxB3 expression was found when RA was added on day 0, day 4 and day 8 and was gradually diminished when RA was added from day 12 onwards, a time point that coincided with an increased expression of Foxg1/LacZ (Fig. 4.5). Immunocytochemistry shows similar results for another hindbrain marker, HoxB4, expressed in the caudal hindbrain and spinal cord (Nordström et al., 2006). Both early and late NPCs responded to early RA treatment by increasing HoxB4 expression significantly (Tukey Kamer test, $P < 0.05$). The HoxB4 expression appeared to be sustained with late RA treatment. It could be assumed that this was because HoxB4 contains RA response element (RARE) in their promoters (Gould et al., 1998) (Fig. 4.7).

Combining the results obtained by RT-PCR and immunocytochemistry shows that NPCs' competence to respond to RA regional identity cues is restricted temporally. Early RA treatment resulted in strong expression of HoxB3 and HoxB4 and weak expression of Foxg1 in early NPCs; late RA treatment, however, resulted in a weaker upregulation of HoxB3. Late RA treatment also gradually increased the expression of Foxg1 in late NPCs, and the effect appeared to be significant (the difference between the expression level of Foxg1 when RA was added on day 0 and when it was added on day 16 in late NPCs was significant (Mann-Whitney *U* test, $P < 0.05$). Thus, the window of NPCs' competence to respond to the caudalizing signal can be said to occur early, most likely between day 0 and day 4.

(a)

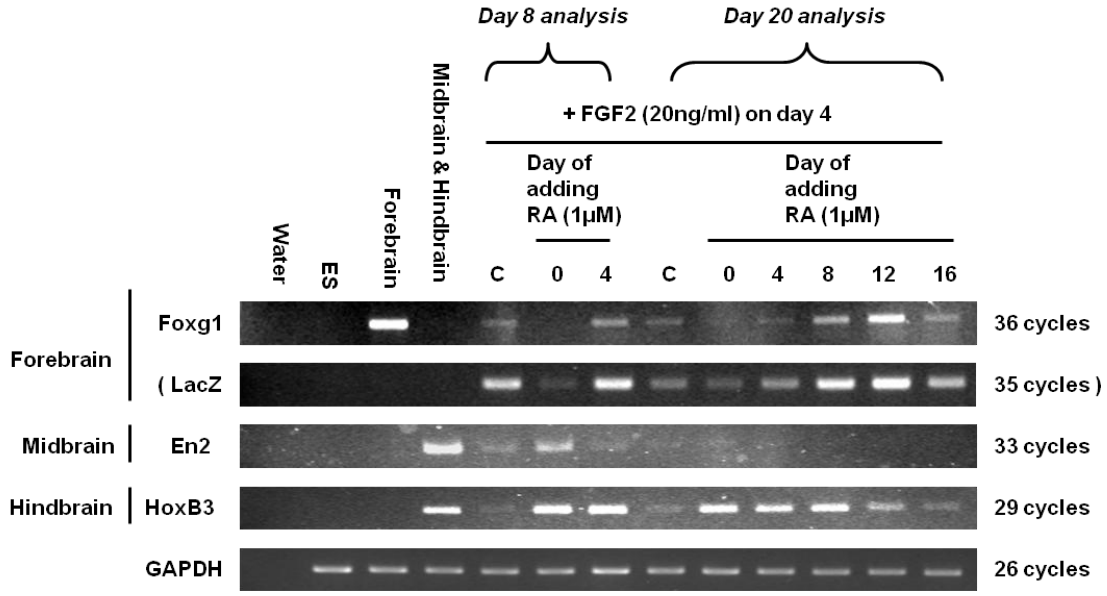

(b)

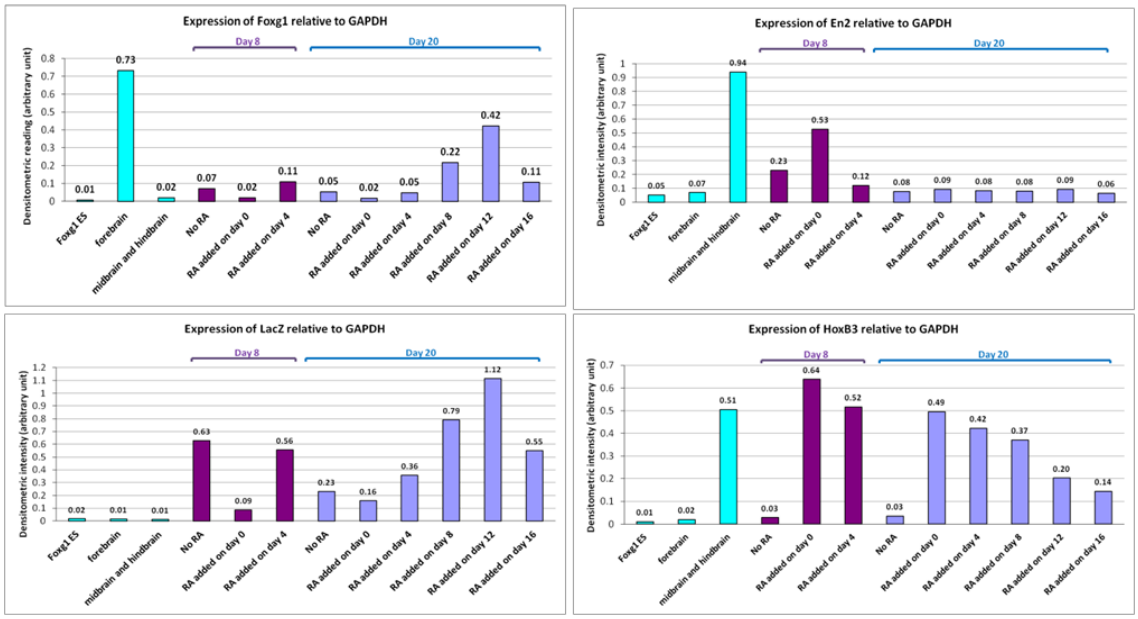

Figure 4.5 **RT-PCR analysis of RA treated samples on day 8 and day 20 of neural differentiation**

(a) Expression of Foxg1, LacZ, En2, HoxB3 was analysed by RT-PCR. RA (1 μM) was added at every 4-day interval from day 0 to day 20. FGF2 (20 ng/ml) was added from day 4 to day 20 in all samples. Control samples (C) contain FGF2 and with no RA. RNA was collected on day 8 and day 20 of neural differentiation. Total RNA from the forebrain, midbrain and hindbrain from E12.5 mouse embryo was used as a positive control. Representative of two independent experiments was shown.

(b) Band intensity of PCR products of Foxg1, LacZ, Emx2, En2 and HoxB4 was quantified by Gel Doc 2000 and was expressed as arbitrary relative values obtained for GAPDH. Bars represent the mean of two independent experiments.

(a)

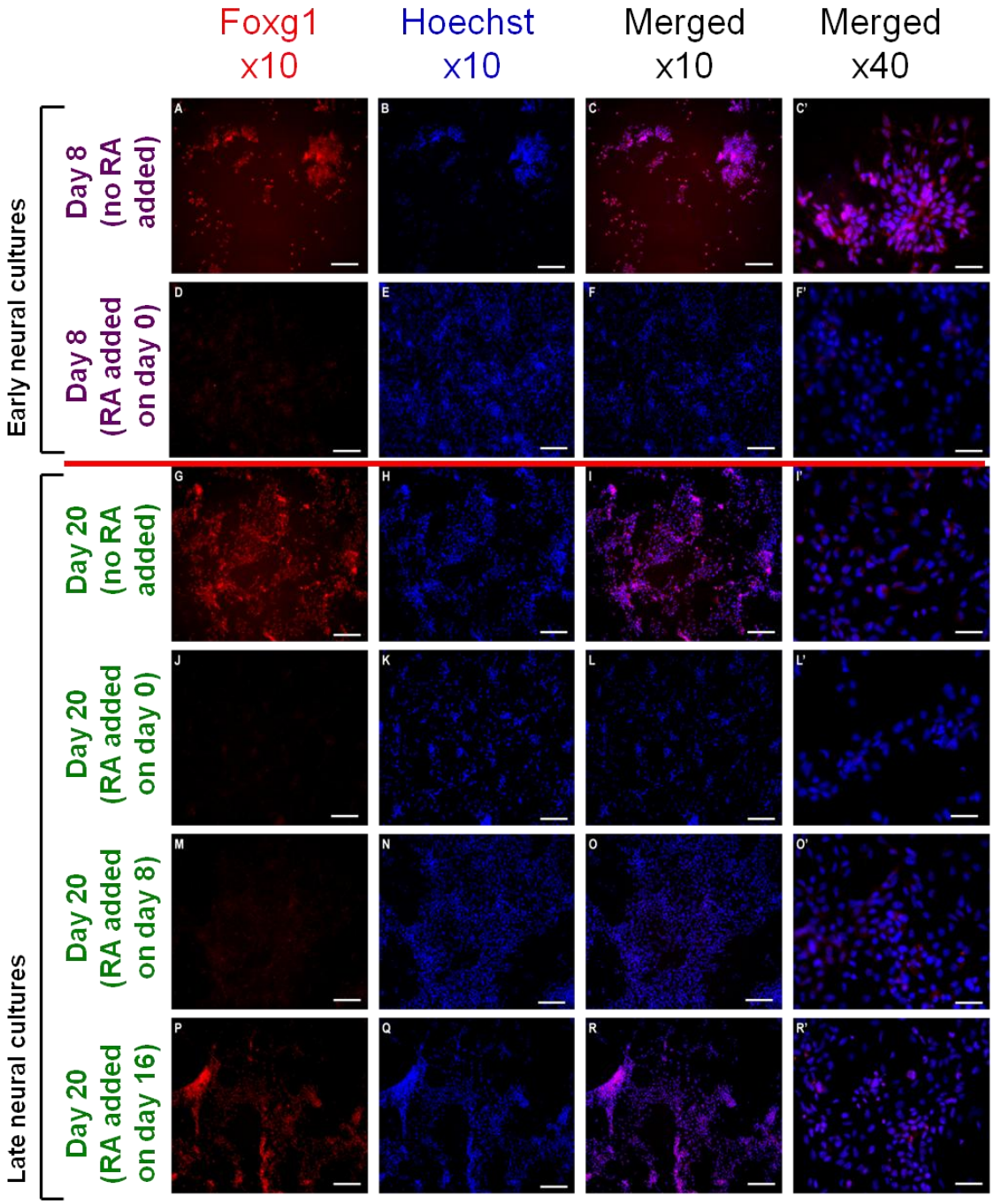
Foxg1 x10
Hoechst x10
Merged x10
Merged x40
Early neural cultures
Late neural cultures
Day 8 (no RA added)
Day 8 (RA added on day 0)
Day 20 (no RA added)
Day 20 (RA added on day 0)
Day 20 (RA added on day 8)
Day 20 (RA added on day 16)
A
B
C
C'
D
E
F
F'
G
H
I
I'
J
K
L
L'
M
N
O
O'
P
Q
R
R'

(b)

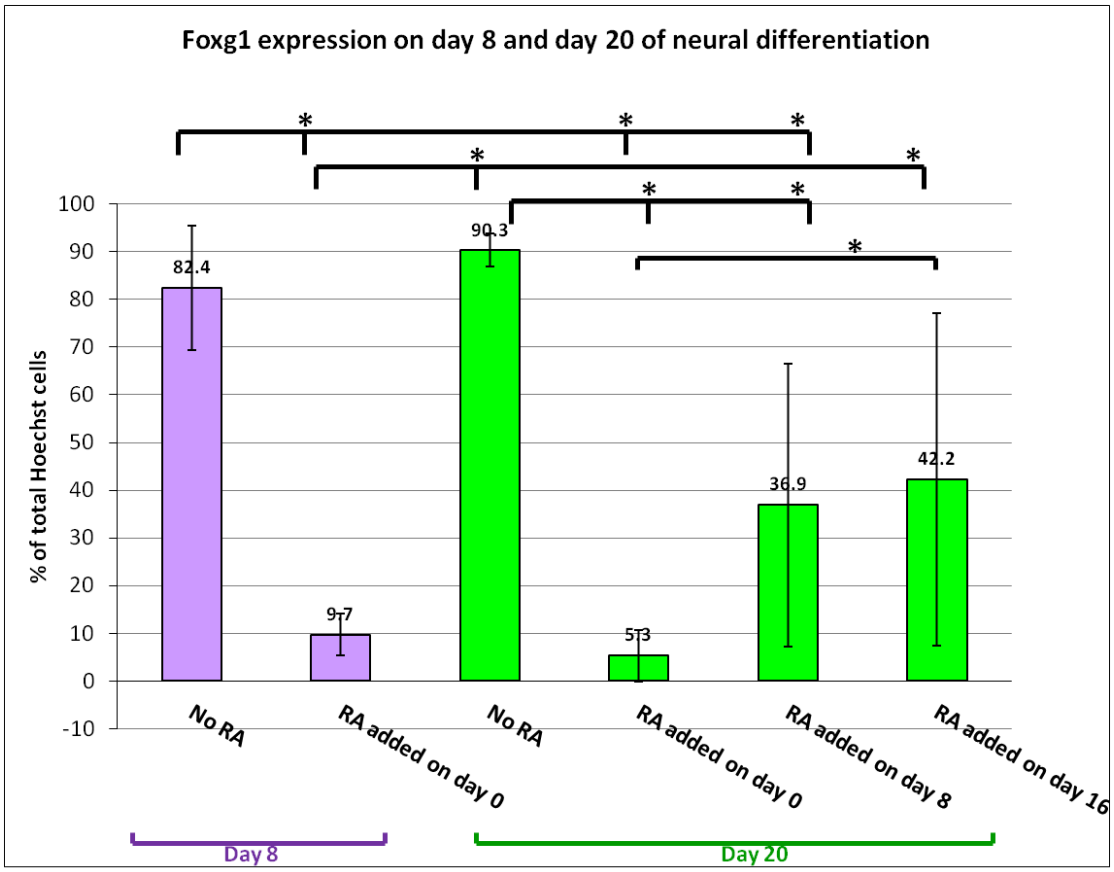

Figure 4.6 Immunocytochemistry analysis of Foxg1 expression of Foxg1Z cells on day 8 and day 20 of differentiation

(a) Foxg1 expression was analysed by fluorescent immunocytochemistry. Foxg1Z cells were treated with RA (1 µM) added on day 0, day 8 and day 16. They were fixed with 4% PFA on day 8 and day 20, double-labelled for Foxg1 (red) and Hoechst nuclear stain (blue). Representative of two independent experiments was shown. Scale bars for x10 images = 100 µm; Scale bars for x40 images = 25 µm

(b) Foxg1 immuno-positive cells on day 8 and day 20 were counted and were represented as percentage of total Hoechst cells. Bars represent the mean of the numbers obtained by counting four random fields of two different coverslips from two independent experiments. Significant *post-hoc* difference is indicated with bracket. (Mann-Whitney *U* test, $*P < 0.05$)

(a)

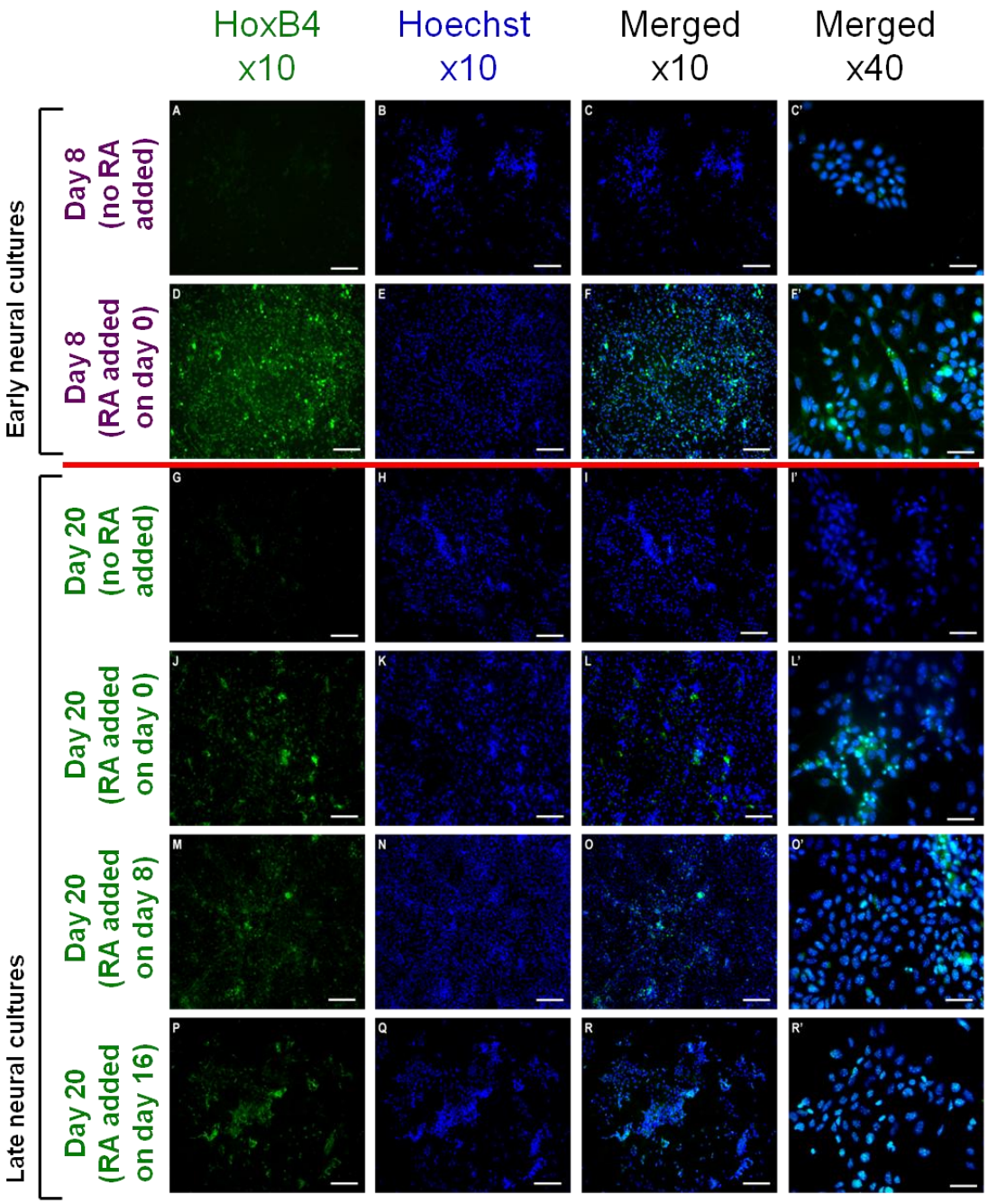
HoxB4 x10
Hoechst x10
Merged x10
Merged x40
Early neural cultures
Day 8 (no RA added)
Day 8 (RA added on day 0)
Late neural cultures
Day 20 (no RA added)
Day 20 (RA added on day 0)
Day 20 (RA added on day 8)
Day 20 (RA added on day 16)

(b)

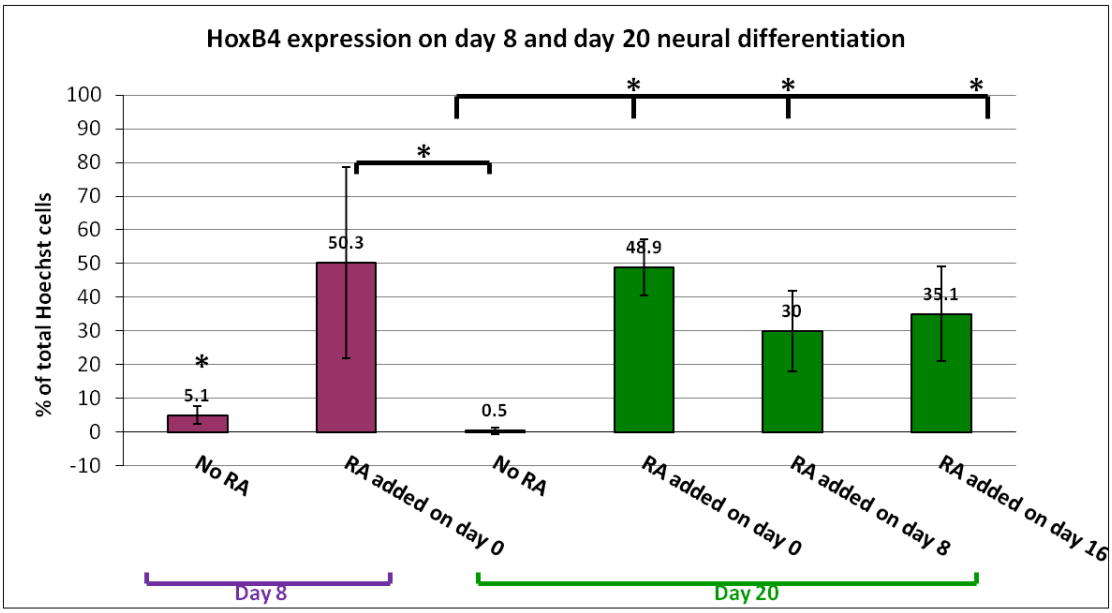

Figure 4.7 Immunocytochemistry analysis of HoxB4 expression of Foxg1Z cells on day 8 and day 20 of differentiation

(a) HoxB4 expression was analysed by fluorescent immunocytochemistry. Foxg1Z cells were treated with RA (1 µM) added on day 0, day 8 and day 16. They were fixed with 4% PFA on day 8 and day 20, double-labelled for HoxB4 (green) and Hoechst nuclear stain (blue). Representative of two independent experiments was shown. Scale bars for x10 images = 100 µm; Scale bars for x40 images = 25 µm

(b) HoxB4 immuno-positive cells on day 8 and day 20 were counted and were represented as percentage of total Hoechst cells. Bars represent the mean of the numbers obtained by counting four random fields of two different coverslips from two independent experiments. Significant *post-hoc* difference is indicated with bracket. (Tukey-Kramer test, $*P < 0.05$)

4.2.5 Effect of RA on dorsoventral patterning of early and late NPCs

The change in the expression of rostral and caudal markers in late NPCs suggested that the expression of dorsal telencephalic and ventral telencephalic markers might be different in late NPCs. To test this, the expression of dorsal telencephalic and ventral telencephalic markers in early and late neural cultures was analysed by RT-PCR and immunocytochemistry. The expression of the dorsal telencaphalic population can be distinguished by the expression of Emx2 (Suda et al., 2010, Gulisano et al., 1996, Simeone et al., 1992), Ngn2 (Imayoshi et al., 2008) and Pax6 (Carney et al., 2009, Stoykova and Gruss, 1994), while the ventral telencephalic population can be distinguished by the expression of Mash1 (Casarosa et al., 1999, Long et al., 2009).

Pax6 expression is found in mitotically active progenitors of the dorsal telencephalon (Puelles et al., 1999). RT-PCR analysis showed that the expression of Pax6 was relatively weak across all samples and therefore it is difficult to draw any conclusion from it. Although no significant difference was found in the number of Pax6-immunopositive cells in both early and late cultures (one-way ANOVA test, $F_{5,18} = 1.92$, $P = 0.141$), it appeared that the expression was reduced slightly by RA treatment in late NPCs (Fig. 4.8, Fig. 4.9). Another dorsal marker Emx2, reported to be downregulated in Raldh2$^{-/-}$ mutants (Paschaki et al., 2013), was induced by RA when added on day 0 in both early and late cultures but its expression was downregulated by RA in late cultures by later RA treatments (Fig. 4.8). Analysis of these two dorsal markers suggests that late RA treatment antagonises the dorsalization in late, but not early NPCs cultures.

Ngn2 and Mash1 are responsible for patterning and regulating neurogenesis in the dorsal and ventral telencephalon respectively (Nieto et al., 2001, Fode et al., 2000). Both markers were induced by RA in early NPCs but only Mash1 in late NPCs when RA was added on day 0. Liao et al. showed that ventral telencephalon is more responsive to RA signalling

than dorsal telencephalon (Liao et al., 2005b), and this probably could explain the strong Mash1 expression induced by RA at day 0 in late culture. However, the expression weakened when RA was added at later time points. Analysis of Mash1 suggests that early RA treatment ventralizes NPCs cultures and here the initial time window for ventralization appeared later (which contrasts with the Emx2 data). From this data, it appears that the time window for ventralization occurs at a later time point than the time window for caudalization, as Mash1 expression was only induced in late cultures (Fig. 4.8).

(a)

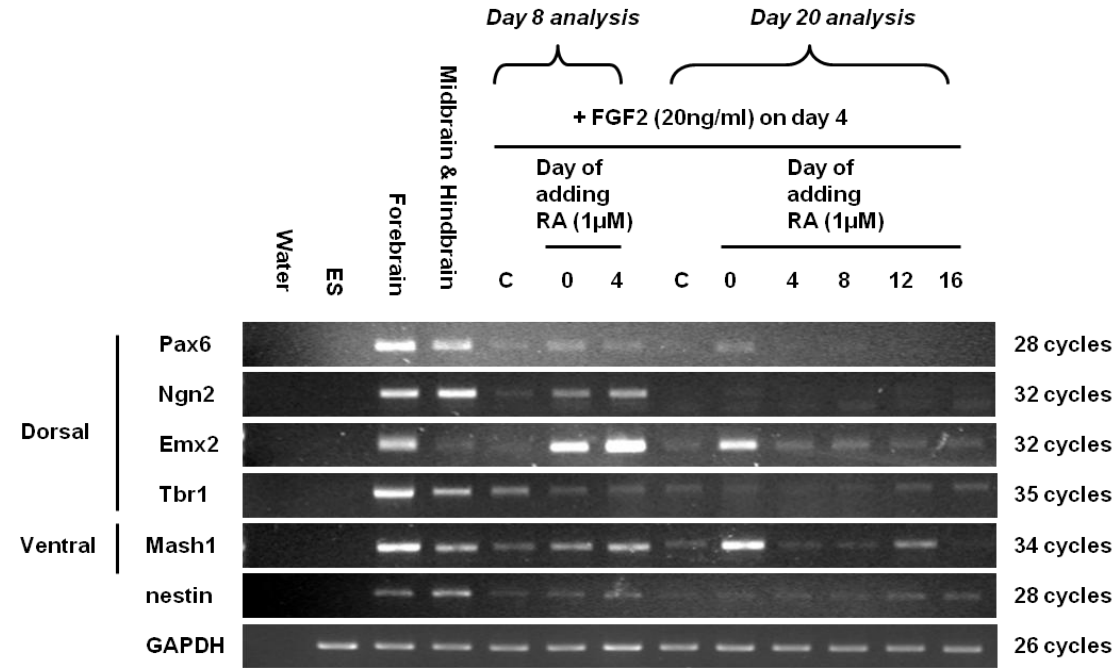

(b)

Figure 4.8 **RT-PCR analysis of RA treated Foxg1Z cells on day 8 and day 20 of neural differentiation**

(a) Expression of Pax6, Ngn2, Emx2, Mash1 and nestin was analysed by RT-PCR. RA (1 μM) was added at every 4-day interval from day 0 to day 20. FGF2 (20 ng/ml) was added from day 4 to day 20. Control samples (C) contain FGF2 and with no RA. RNA was collected on day 8 and day 20 of neural differentiation. Total RNA from the forebrain, midbrain and hindbrain from E12.5 mouse embryo was used as a positive control. Representative of two independent experiments was shown.

(b) Band intensity of PCR product of Pax6, nestin, Ngn2, Tbr1 and Mash1 was quantified by Gel Doc 2000 and was expressed as arbitrary relative values obtained for GAPDH. Bars represent the mean of two independent experiments.

(a)

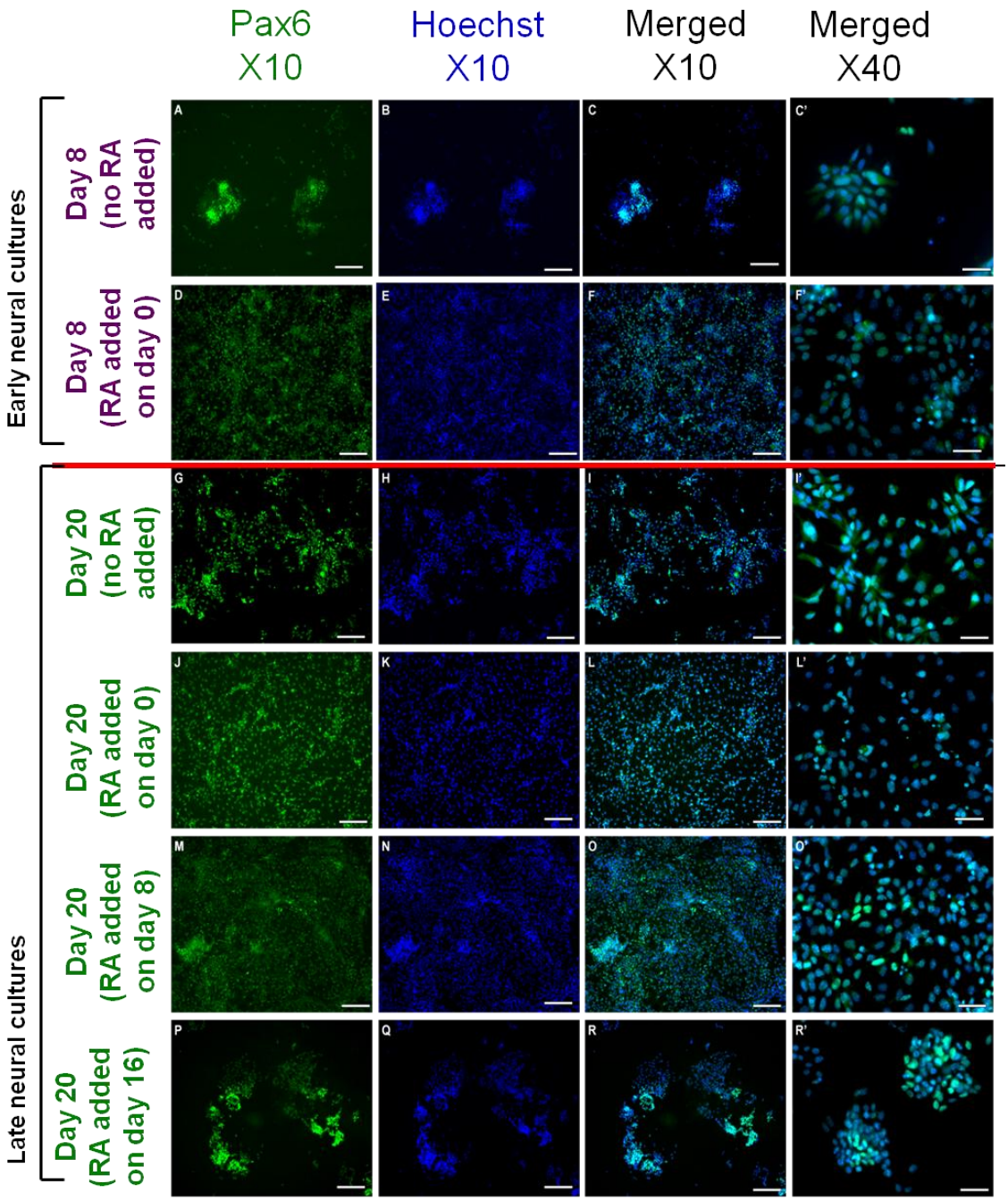
Pax6 X10
Hoechst X10
Merged X10
Merged X40
Early neural cultures
Day 8 (no RA added)
Day 8 (RA added on day 0)
Late neural cultures
Day 20 (no RA added)
Day 20 (RA added on day 0)
Day 20 (RA added on day 8)
Day 20 (RA added on day 16)

(b)

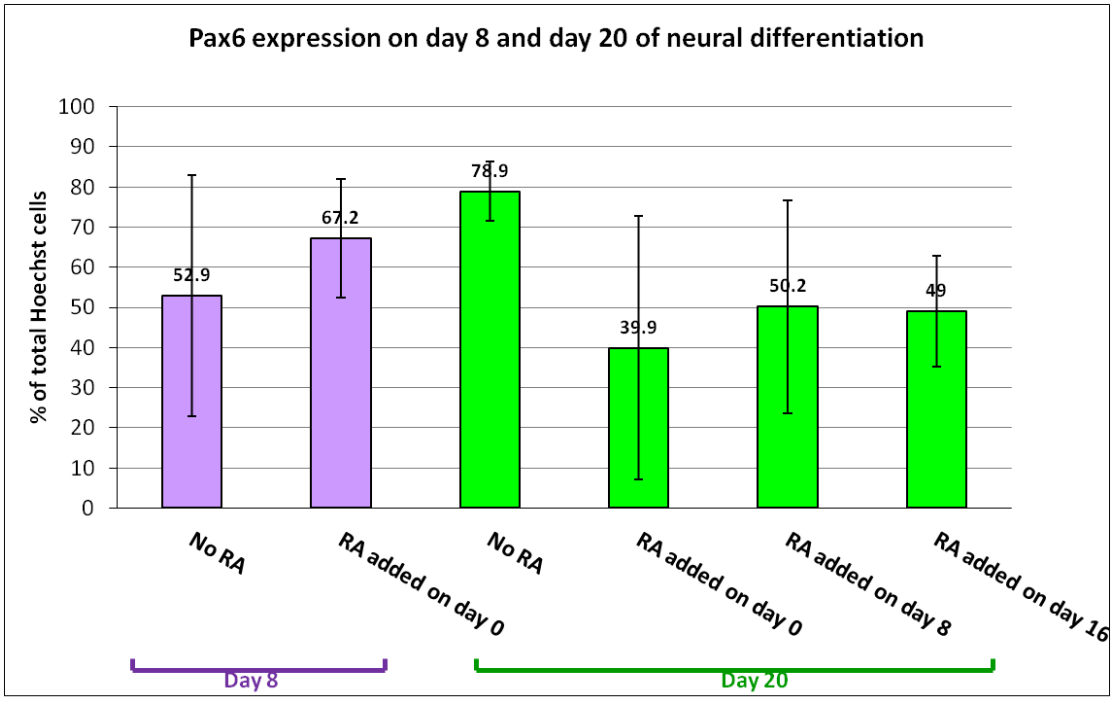

Figure 4.9 Immunocytochemistry analysis of Pax6 expression on day 8 and day 20 of differentiation

(a) Pax6 expression was analysed by fluorescent immunocytochemistry. Foxg1Z cells were treated with RA (1 µM) added on day 0, day 8 and day 16. They were fixed with 4% PFA on day 8 and day 20, double-labelled for Pax6 (green) and Hoechst nuclear stain (blue), Representative of two independent experiments was shown. Scale bars for x10 images = 100 µm; Scale bars for x40 images = 25 µm.

(b) Pax6 immuno-positive cells on day 8 and day 20 were counted and were represented as a percentage of total Hoechst cells. Bars represent the mean of the numbers obtained by counting four random fields of two different coverslips from two independent experiments. (One-way ANOVA test, $P = 0.141$)

4.2.6 Expression of glial and early neuronal markers in early and late neural cultures

To determine whether the progenitor population was maintained in the NPC cultures over the 20 day period (and therefore whether the cells receiving early RA and late RA are NPCs, not differentiated NPCs), the expression of markers for progenitors and differentiated cells was investigated. Nestin is an intermediate filament gene that is expressed by neural stem cells (Lendahl et al., 1990). Nestin expression appeared to be increased by RA treatment, but the expression was similar in both early and late cultures. Immunocytochemistry analysis confirms this, suggesting that the number of neural precursor cells had not decreased in late cultures (Fig. 4.10). Tbr1 is expressed in cortical postmitotic cells (Bulfone et al., 1995, Englund et al., 2005). The expression of Tbr1 was very weak across all samples, indicating that the majority of cells had not undergone neuronal differentiation (Fig. 4.8).

The change in responsiveness to RA could be due to the presence of more mature phenotypes owing to spontaneous differentiation such as β-III-tubulin and GFAP even though NPCs were propagated in the presence FGF2. To investigate this, early and late NPCs were immunostained with early neuronal marker β-III-tubulin and the results show that, in early cultures, weak expression of β-III-tubulin was found. The expression of β-III-tubulin was weak across all samples, except when RA addition on day 8 in late cultures appeared to produce a significant increase in the expression of β-III-tubulin. However, the expression decreased significantly when RA was added on day 16 (Mann-Whitney U test, $P < 0.05$) (Fig. 4.11).

Bouhon et al. demonstrated that late neural cultures express Olig2, Mash1 and EGFR but do not express Ngn1/2, a phenotypic profile that is similar to putative radial glia (Bouhon et al., 2006). To find out whether late cultures of this study displayed a higher gliogenic potential, immunocytochemistry analysis of GFAP was performed. Fig 4.12 illustrates how

only very weak GFAP expression was found in early neural cultures and that the expression increased significantly in late cultures (Tukey-Kamer test, $P < 0.05$) (Fig. 4.12).

(a)

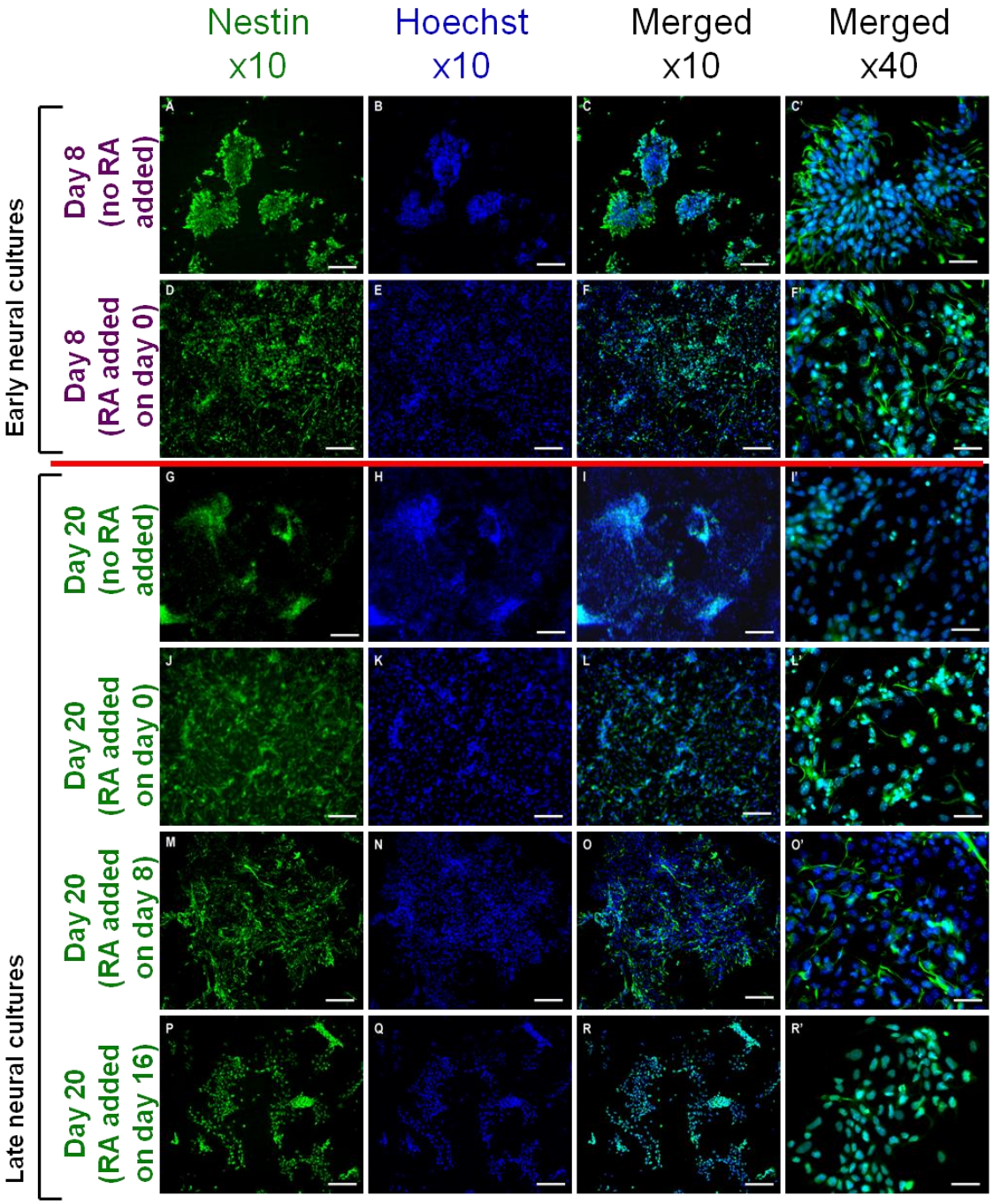
Nestin x10
Hoechst x10
Merged x10
Merged x40
Early neural cultures
Late neural cultures
Day 8 (no RA added)
Day 8 (RA added on day 0)
Day 20 (no RA added)
Day 20 (RA added on day 0)
Day 20 (RA added on day 8)
Day 20 (RA added on day 16)
A
B
C
C'
D
E
F
F'
G
H
I
I'
J
K
L
L'
M
N
O
O'
P
Q
R
R'

(b)

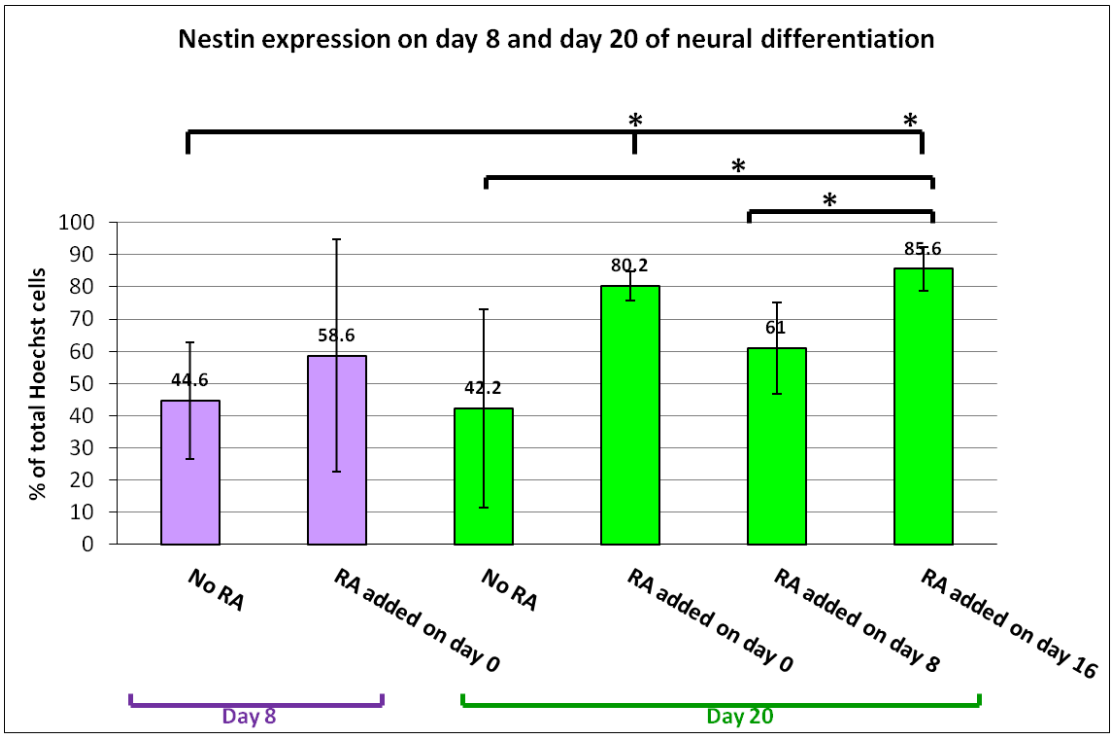

Figure 4.10 Immunocytochemistry of nestin expression on day 8 and day 20 of differentiation

(a) Nestin expression was analysed by fluorescent immunocytochemistry. Foxg1Z cells were treated with RA (1 µM) added on day 0, day 8 and day 16. They were fixed with 4% PFA on day 8 and day 20, and double-labelled for nestin (green) and Hoechst nuclear stain (blue), Representative of two independent experiments was depicted. Scale bars for x10 images = 100 µm; Scale bars for x40 images = 25 µm

(b) Nestin immuno-positive cells on day 8 and day 20 were counted and were represented as a percentage of total Hoechst cells. Bars represent the mean of the numbers obtained by counting four random fields of two different coverslips from two independent experiments. Significant *post-hoc* difference is indicated with bracket. (two sample t-test, $*P < 0.05$)

(a)

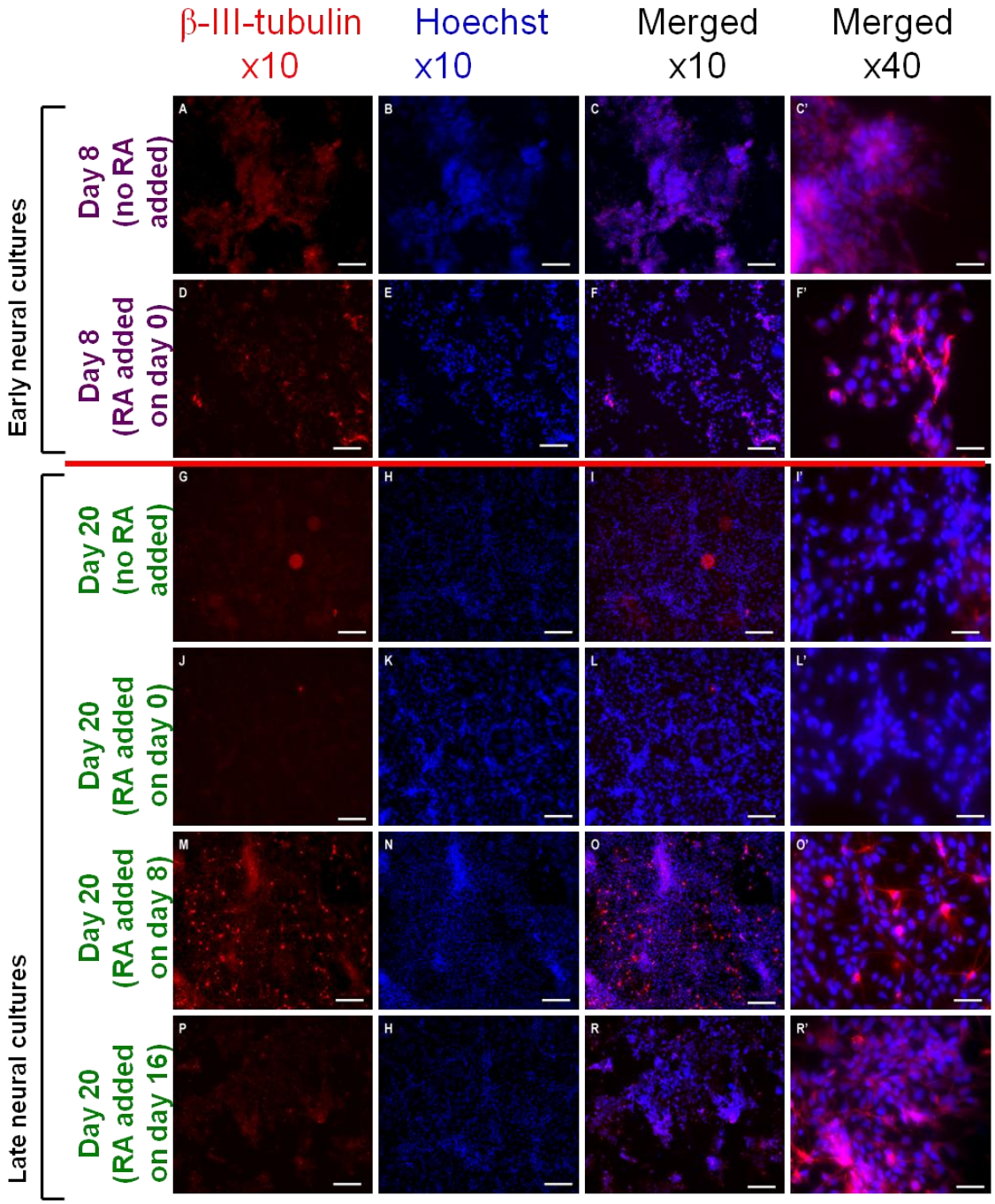
β-III-tubulin x10
Hoechst x10
Merged x10
Merged x40
Early neural cultures
Day 8 (no RA added)
Day 8 (RA added on day 0)
Late neural cultures
Day 20 (no RA added)
Day 20 (RA added on day 0)
Day 20 (RA added on day 8)
Day 20 (RA added on day 16)
A
B
C
C'
D
E
F
F'
G
H
I
I'
J
K
L
L'
M
N
O
O'
P
H
R
R'

(b)

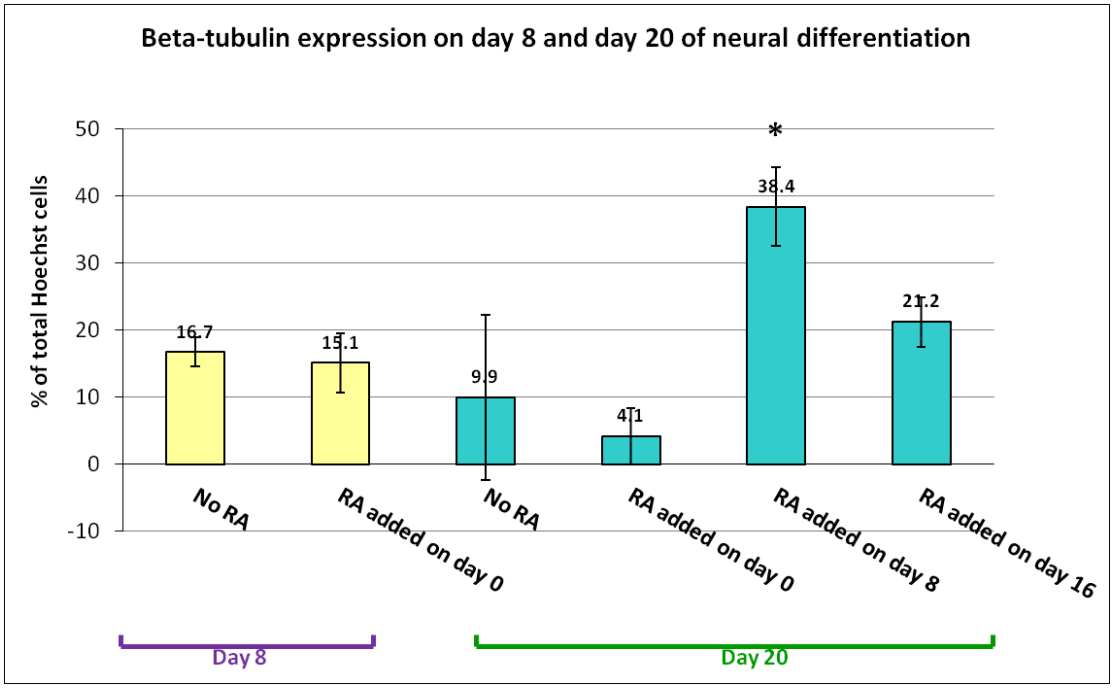

Figure 4.11 Immunocytochemistry analysis of β-III-tubulin expression on day 8 and day 20 of differentiation

(a) β-III-tubulin expression was analysed by fluorescent immunocytochemistry. Foxg1Z cells were treated with RA (1 µM) added on day 0, day 8 and day 16. They were fixed with 4% PFA on day 8 and day 20, double-labelled for β-III-tubulin (red) and Hoechst nuclear stain (blue), Representative of two independent experiments was shown. Scale bars for x10 images = 100 µm; Scale bars for x40 images = 25 µm

(b) β-III-tubulin immuno-positive cells on day 8 and day 20 were counted and were represented as a percentage of total Hoechst cells. Bars represent the mean of the numbers obtained by counting two random fields of four different coverslips from two independent experiments. (Mann-Whitley *U* test, $*P < 0.05$)

(a)

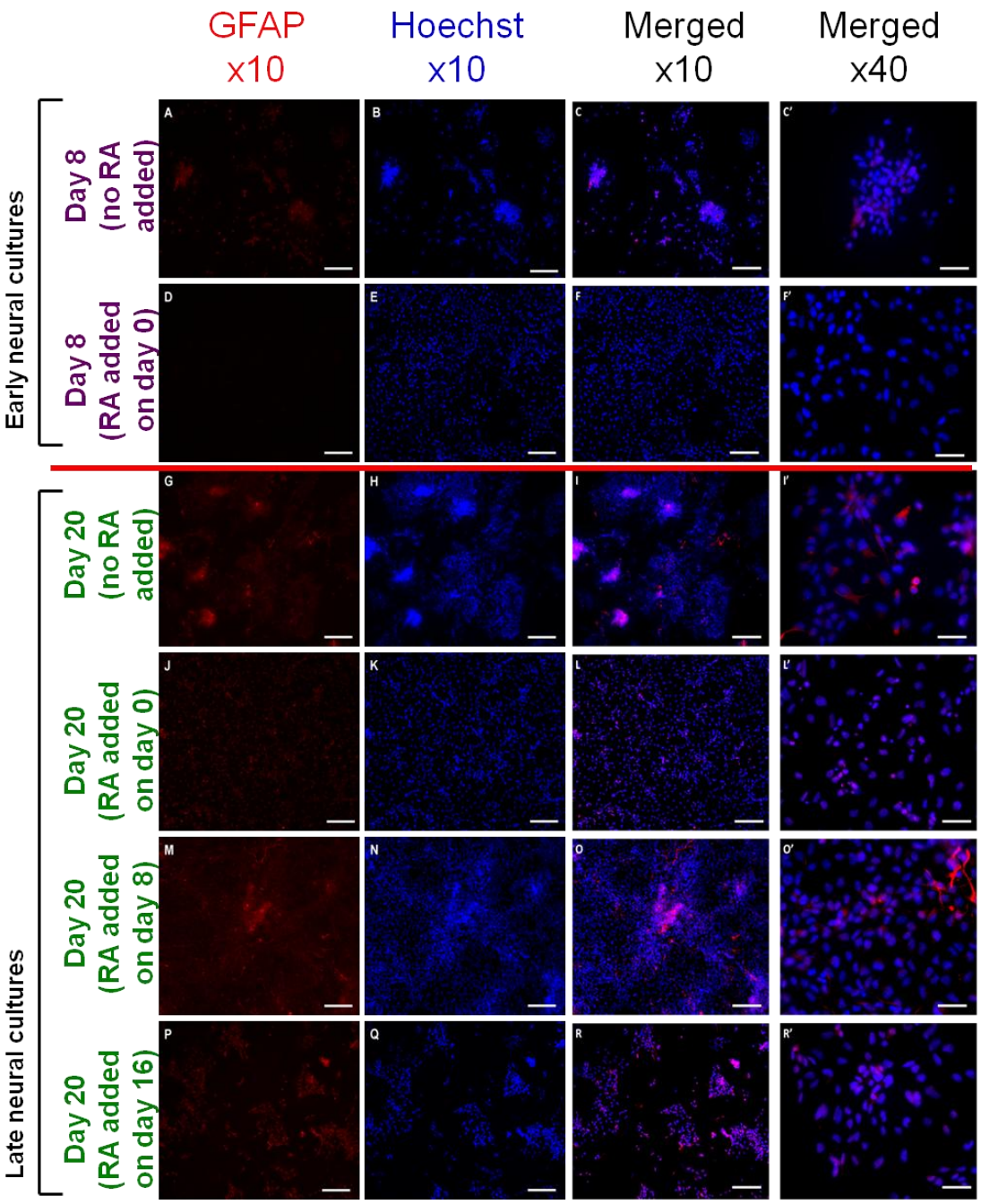
GFAP x10
Hoechst x10
Merged x10
Merged x40
Early neural cultures
Day 8 (no RA added)
Day 8 (RA added on day 0)
Late neural cultures
Day 20 (no RA added)
Day 20 (RA added on day 0)
Day 20 (RA added on day 8)
Day 20 (RA added on day 16)

(b)

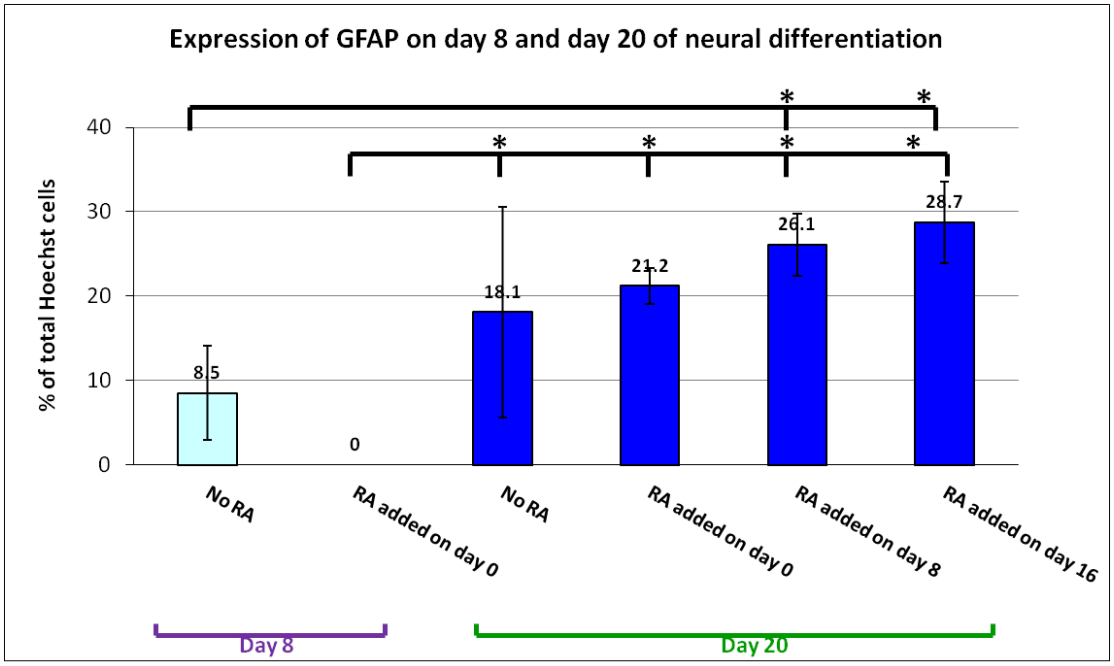

Figure 4.12 Immunocytochemistry analysis of GFAP expression on day 8 and day 20 of differentiation

(a) GFAP expression was analysed by fluorescent immunocytochemistry. Foxg1Z cells were treated with RA (1 µM) added on day 0, day 8 and day 16. They were fixed with 4% PFA on day 8 and day 20, double-labelled for GFAP (red) and Hoechst nuclear stain (blue), Representative of two independent experiments was shown. Scale bars for x10 images = 100 µm; Scale bars for x40 images = 25 µm

(b) GFAP immuno-positive cells on day 8 and day 20 were counted and were represented as a percentage of total Hoechst cells. Bars represent the mean of the numbers obtained by counting four random fields of two different coverslips from two independent experiments. Significant *post-hoc* difference is indicated with bracket. (Tukey-Kramer test, $*P < 0.05$)

4.3 Discussion

During embryogenesis, RA is involved in regulating patterning along the AP and DV axes and subsequently the development of forebrain, hindbrain and the spinal cord (Wilson and Maden, 2005, Maden, 2006, Rhinn and Dolle, 2012). However, how such tissue-specific responses were regulated remained poorly understood. ES cells can be patterned appropriately in response to the right combination of morphogens (Smith, 2001). However, such observation can only be found in early, not late NPCs. This suggested that regional specification in NPCs is regulated by the temporal change in responsiveness to RA (Bouhon et al., 2006). In order to gain full control over the generation of specific neural and neuronal subtypes from ES cells, it was necessary to understand how cells respond to patterning cues over time. This chapter sets out data describing how the temporal change in competence to respond to RA can affect the expression profile of positional markers.

The results in this study showed that the positional identities of ESC-derived NPCs were specified temporally. Adding RA at early time points (day 0 and day 4) generated cells with hindbrain character as confirmed by strong HoxB3 and HoxB4 expression in RT-PCR and immunocytochemistry analysis (Fig. 4.5, 4.6). This observation was consistent with Irioka et al.'s finding that suppression of forebrain gene expression happened in a narrow period during an early phase of differentiation (between day 0 to day 4) *in vitro.* It was also consistent with Okada et al.'s study that Hox genes were induced by RA in ES cell culture in early neural cultures (day 4 and day 6) (Irioka et al., 2005, Okada et al., 2004).

A loss of regional specification was found in late cultures when late NPCs were treated with RA between day 16 to day 20. The expression of all the positional markers tested (Foxg1, HoxB3, En2, Emx2) except those that contain RARE in their promoters (HoxB4 (Gould et al., 1998) and Pax6 (Enwright and Grainger, 2000)) was weak. This is in accordance with Bouhon et al.'s study which shows that late NPCs were unable to acquire anterocaudal or dorsoventral identities in response to late addition of morphogens (Bouhon et al., 2006).

It was observed that different markers had different RA response windows before NPCs lost the competence to be patterned by RA. For instance, in late cultures, the expression of Emx2, Mash1 can only be found with early treatment of RA (day 0) in late culture, but the expression of HoxB3 can be still be induced by RA up to day 8 in late culture (Fig. 4.5 and 4.7). This suggests that NPCs had a wider window of competence to respond to RA induced hindbrain cues. The expression of Foxg1 in late NPCs gradually increased with later periods of RA treatment to a level that was similar to the control as revealed by Beta-Glo analysis or even greater than the control as revealed by RT-PCR analysis (low at RA on day 0 to 4 compared to higher at RA on day 4 to day 12). This indicated that late RA treatment might be needed to sustain Foxg1 expression as a number of *in vivo* studies have reported that RA is essential for ventral forebrain development and that the effect of RA on forebrain development occurs at later time points (Rajaii et al., 2008, Liao et al., 2005b, Liao et al., 2008). It would be interesting to examine the expression of another ventral forebrain marker, Gsh2, which is required for retinoid production in the LGE (Waclaw et al., 2004) to determine whether RA is required for the late expression of ventral forebrain markers.

This study also examined whether the change in responsiveness to RA in late neural progenitor cells was due to NPCs having committed to become neuronal or glial cells. In early cultures, on average about 15% of the cells treated with or without RA expressed β-III-tubulin, while in late cultures, on average about 40% of β-III-tubulin-expressing cells were found when RA was added at day 8 (Figs. 4.11, 4.12). Although the expression of β-III-tubulin was detected in early and late cultures - probably due to spontaneous differentiation as cells were cultured in the presence of FGF2, which maintains cells as neural progenitors (Tropepe et al., 2001, Lee et al., 2000, Okabe et al., 1996) - the comparatively slight increase in β-III-tubulin-expressing cells can probably be explained by a finding that demonstrates that RA treatment speeded up the differentiation process. Cells treated with RA (0.5 μM) from day 4 to 8 in embryoid bodies generated a higher percentage of β-III-tubulin-expressing cells at earlier time points and had fewer precursor cells with lower BrdU incorporation, suggesting that RA treatment can induce an earlier cell-cycle exit and result in neuronal differentiation (Kim et al., 2009). However, considering that nestin expression was found in late NPCs and the expression of Tbr1 was relatively weak across all samples (Fig. 4.8 and 4.10), it seemed unlikely that the change in responsiveness was the result of late NPCs having undergone differentiation.

One important question to ask regarding the weak expression of positional markers (Foxg1, HoxB3, HoxB4,, Emx2, Pax6, Ngn2 and Mash1) with RA treatment between day 16 to day 20 (Figs. 4.5-4.9) is whether these NPCs had lost the competence to respond to RA. This can be answered by examining the expression of RA receptors (RARα, β, γ and RXRα, β, γ). If they were present in response to RA treatment, then it could affirmed that cells still retain the ability to respond to RA signalling (Waclaw et al., 2004). However, the presence of RA signalling machinery such as RA receptors cannot reveal the level of retinoid present in the system. Even though 1 μM of RA was added at every 4-day interval, it is unclear whether late NPCs would respond to the RA treatments by changing the expression of RA catabolizing

enzyme Cyp26s. *In vivo*, temporal expression of Cyp26a1 is involved in regulating the responsiveness of RA in hindbrain patterning (White et al., 2007, Hernandez et al., 2007, Sirbu et al., 2005). Therefore, it would be of interest to examine the expression of Cyp26s in early and late neural cultures to determine whether the level of RA has a role in determining the expression of positional markers.

The change in responsiveness to RA in late cultures could be due to increased repressor activity as a result of more corepressors being recruited by the retinoid receptors. In an independent cell-based study, retinoid receptors acted as repressors by recruiting corepressors in the absence of ligands and as activators by recruiting coactivators when ligands were present (Xu et al., 1999, Glass and Rosenfeld, 2000). Co-activators and co-repressors are proteins that interact with nuclear receptors to regulate gene transcription (Glass and Rosenfeld, 2000). Co-activators for retinoid receptors include steroid receptor coactivator-1 (SRC-1) and P300/CBP-associated factor (P/CAF) (Glass and Rosenfeld, 2000). Co-repressors include the nuclear receptor corepressor (N-CoR) and the silencing-mediator of retinoid and thyroid hormone receptors (SMRT) (Chen and Evans, 1995, Kurokawa et al., 1995, Burke and Baniahmad, 2000). All the four co-activators and co-repressors were expressed at similar levels in the cerebral cortex, the LGE and the MGE in the absence of retinol, but regional differences in repressor activity were found in the telencephalon where repressor activity is higher in the cerebral cortex than in LGE and MGE in the presence of retinol (Liao et al., 2005b). It is possible that the repressor activity is higher in late NPCs when they failed to be patterned by RA. This could be examined in future experiments by comparing the expression of co-repressors and co-activators of RA receptors between early and late NPCs.

4.4 Conclusion

In summary, data presented in this chapter has brought us to a more precise understanding of the effect of RA addition on the acquisition of the regional identities of ES cell-derived NPCs. According to the data presented in this chapter, the most effective time window for RA to caudalize NPCs cultures was between day 0 to day 4 in both early and late cultures. The optimal time point for RA treatment to ventralize NPCs appeared to be at day 0 in late cultures as the induction of ventral forebrain marker can only be found at that time point. RA treatment induced dorsalization in early cultures but not in late cultures. The expression of the tested positional markers was weak with RA treatment between day 16 to day 20 in late cultures. Although conclusive evidence is lacking here, it could well be assumed that it is during this period that late NPCs might have lost the competence to respond to RA signalling.

CHAPTER 5:

INVESTIGATION OF THE RELATIONSHIP BETWEEN SOX1 EXPRESSION AND REGIONAL SPECIFICATION IN RESPONSE TO MORPHOGENS

5.1 Introduction

The previous chapter and Bouhon et al.'s study showed that early ES cell-derived neural progenitor cells (NPC)s were able to respond to RA by expressing caudal markers and a number of other forebrain markers, but the expression of these markers was gradually reduced in late NPCs. This indicated that late NPCs might have a reduced responsiveness to morphogens (Bouhon et al., 2006). As the neurogenic potential of NPCs depends to a certain extent on their competence to respond to morphogens (Gabay et al., 2003, Plachta et al., 2004), this chapter therefore investigates whether the competency to respond to morphogen is related to Sox1 expression.

Sox1 is one of the earliest markers expressed by ES cells-derived NPCs (Ying et al., 2003b, Bouhon et al., 2005). It is a HMG-box transcription factor and belongs to the B1 subgroup of Sox gene family, which includes Sox1, Sox2 and Sox3. Each Sox protein regulates a unique repertoire of genes and plays an important role in the determination of cell fate. It exhibits a domain which is involved in silencing developmental genes in undifferentiated ES cells. The domain is resolved upon differentiation and triggers the activation of lineage-related genes (Kamachi et al., 2000). During neural development, different classes of Sox transcription factors are expressed during neurogenesis and they play important roles in coordinating specific gene expression from early pluripotent stem cell stages to neuronal maturation (Bergsland et al., 2011). SoxB1 proteins are expressed by neural progenitors and SoxC proteins mostly found in post-mitotic neurons (Bergsland et al., 2006, Bylund et al., 2003). Genome wide study of SoxB1 and SoxC proteins revealed that Sox2, Sox3 and Sox11 (belong to SoxC proteins) sequentially bind to a common set of neural genes in mouse ES cells. Sox2 preselects neural lineage-specific genes that will be bound by Sox3 in neural progenitor cells. Neuronal genes that are associated with Sox3 are resolved from bivalent chromatin to a permissive monovalent state upon the binding of Sox11. Sox3 competes for

the binding sites with Sox11 in order to prevent premature Sox11-induced neuronal gene expression. This indicated the importance of SoxB1 proteins in maintaining neural progenitor properties (Bergsland et al., 2011). Moreover, induced expression of Sox1 in P19 embryonal carcinoma cells substituted the requirement of retinoic acid to initiate neural differentiation (Pevny et al., 1998). All of this evidence indicated that Sox1 plays a key role in neural commitment.

In mouse, Sox1 is one of the earliest neural markers expressed in ectodermal cells that are committed to neural cell fate. It is first expressed in neural precursor cells at 7.5 days post coitum (dpc) in the anterior half of late-streak embryo and is maintained in all neuroepithelial cells along the anteroposterior axis until the neural plate bends and fuses to form a neural tube (9.0-9.5 dpc). Downregulation of Sox1 expression is found along the dorsoventral axis and eventually Sox1 expression is restricted to the ventricular zone at 13.5 dpc. This suggested that Sox1 expression is associated with the acquisition of neural fate within the embryonic neural tube but is downregulated when neuroepithelial cells leave the proliferative state and undergo neuronal and glial differentiation (Pevny et al., 1998). The downregulation of Sox1 expression is also found in neural cultures. Conti et al. showed that Sox1 expression is lost after 5 passages In neural stem cells either in the presence of FGF2 alone or with FGF2 and EGF (Conti et al., 2005).

The downregulation of Sox1 found in both *in vivo* and *in vitro* studies and also its role in determining neural commitment suggested that it might be possible that Sox1 was involved in the change in responsiveness of NPCs to morphogens, and consequently led to the loss of regional specification in late NPCs. To investigate this, ES cells-derived NSCs were exposed to RA and sonic hedgehog (Shh) because both morphogens play important roles in regulating AP and DV patterning during the development of the nervous system (Wilson and Maden, 2005).

RA signalling plays an important role in patterning the hindbrain (Gavalas, 2002, Sirbu et al., 2005). The vertebrate hindbrain is arranged as neuroepithelial compartments called 'rhombomere' (r). The identity of rhombomeres is partly conferred by the expression of Homeobox (Hox) genes, which are regulated by RA (Glover et al., 2006). Therefore, any change in competence to respond to RA can be reflected by the change in Hox gene expression.

Hedgehog (Hh) signalling plays an essential role in regulating ventral patterning in the telencephalon (Ericson et al., 1995). Shh (the vertebrate homolog of Hh) is transduced through the transmembrane receptors patched (Ptc1) and smoothened (Smo). The inhibition of Smo by Ptc1 is relieved by Shh, and this allows the transcription of target genes through the Gli transcription factors (Ingham and McMahon, 2001). Three Gli proteins have been identified in vertebrates. Within the telencephalon, Gli2 and Gli3 function as transcriptional repressors in the absence of Hh ligands and as activators when Hh ligands are present. Hh ligands inhibit the repressor form by stopping the proteolytic processing near the DNA binding domain (Pan et al., 2006). Gli1 does not contain any repressor domain and functions as a strong transcriptional activator (Bai and Joyner, 2001, von Mering and Basler, 1999). Misexpression of Shh can result in the induction of ventral forebrain markers in the dorsal forebrain (Rallu et al., 2002).

To understand the expression of Sox1 on the acquisition of positional markers, previously described 46C ES cell line was used in this study. The open reading frame of Sox1 in 46C cells has been replaced with the coding sequence of GFP and an internal ribosome entry site (IRES)-linked puromycin resistance gene (Ying et al., 2003b), and this enables easy visualization and identification of Sox1/GFP expression by fluorescence microscopy and using flow cytometry. Furthermore, cells can also be sorted into Sox1/GFP positive and negative populations using fluorescence activated cell sorting (FACS) to examine the effect of Sox1 on cell fate specification. Knowledge of neural fate specification over time in

response to patterning cues is useful because it enables better strategies to be developed in order to systematically manipulate the cell fate of ES cells-derived NPCs.

5.2 Results

5.2.1 Sox1/GFP expression of 46C cells over time

According to Conti et al. 's study, 46C cells express Sox1 temporarily and the expression is lost after 5 passages using the monolayer protocol described by Ying et al. (Ying et al., 2003b). They show characteristics for neural stem cells because they express RC2 and nestin and are competent for astrocyte and neuronal differentiation (Conti et al., 2005). To find out whether ESC-derived NPCs in early (day 8) and late neural cultures (day 20) had different Sox1 expression, cells were differentiated for 20 days using the same differentiation protocol described in section 4.3.2 (Fig. 4.2) but with no RA added. Since this study deals with the investigation of the effect of Sox1 expression on neural patterning and not neuronal differentiation, ES cells-derived NPCs were cultured in the presence of FGF2 because it has been shown that NPCs can be expanded in FGF2 (Tropepe et al., 2001).

To visualise GFP expression, 46C cells were observed under the fluorescence microscope. Fluorescent images showed that Sox1/GFP expression gradually decreased from day 10 to day 18 but it appeared that a considerable number of cells were still Sox1/GFP positive on day 18 (Fig. 5.1a).

To quantify the expression of Sox1/GFP over time, cells were analysed by flow cytometry. All data were gated and analysed as described in section 2.1.7. Foxg1 cells were differentiated in CDM, the base medium used for differentiation, and were used as the negative control of Sox1/GFP expression for flow cytometry analysis. Differentiated Foxg1Z cells (a Foxg1-LacZ reporter cell line) were used instead of undifferentiated 46C ES cells because the distribution of fluorescence intensity of differentiated Foxg1Z cells changed slightly from day 6 to day 18 (Fig. 5.1 (b)).

The geometric mean fluorescence intensity (MFI) and the percentage of Sox1/GFP expressing cells of 46C cells from day 6 to day 18 were presented in Figs. 5.1(c) and (d). Significant differences were found in the percentage of Sox1/GFP expressing cells over 18 days of differentiation overall (one-way ANOVA test**,** $F_{3,8} = 443.57$, $P < 0.001$), and the percentage of Sox1/GFP expressing cells on day 18 was significantly lower than other time-points (Tukey-Kamer test, $P < 0.05$). Significant differences were also found in the mean MFI values of Sox1/GFP expressing cells over 18 days of differentiation (one-way ANOVA test**,** $F_{3,8} = 35.29$, $P < 0.001$). The mean MFI values on day 14 and day 18 were significantly different from day 6; and the MFI values on day 14 and day 18 were significantly different from day 10 (Tukey-Kamer test, $P < 0.05$). Interestingly, the histogram of day 18 appeared to display two populations of Sox1/GFP positive cells with different fluorescence intensity, and in this case, only the population with the higher fluorescence intensity was considered to be Sox1/GFP positive. It was unclear whether there would be a further change in the population of Sox1/GFP positive cells if cells were cultured for a longer period, but the significant decrease in the percentage of Sox1/GFP expressing cells for the first 18 days enabled further investigation of the effect of the change in Sox1/GFP intensity over time in determining the change in responsiveness to morphogenic cues in late cultures.

(a)

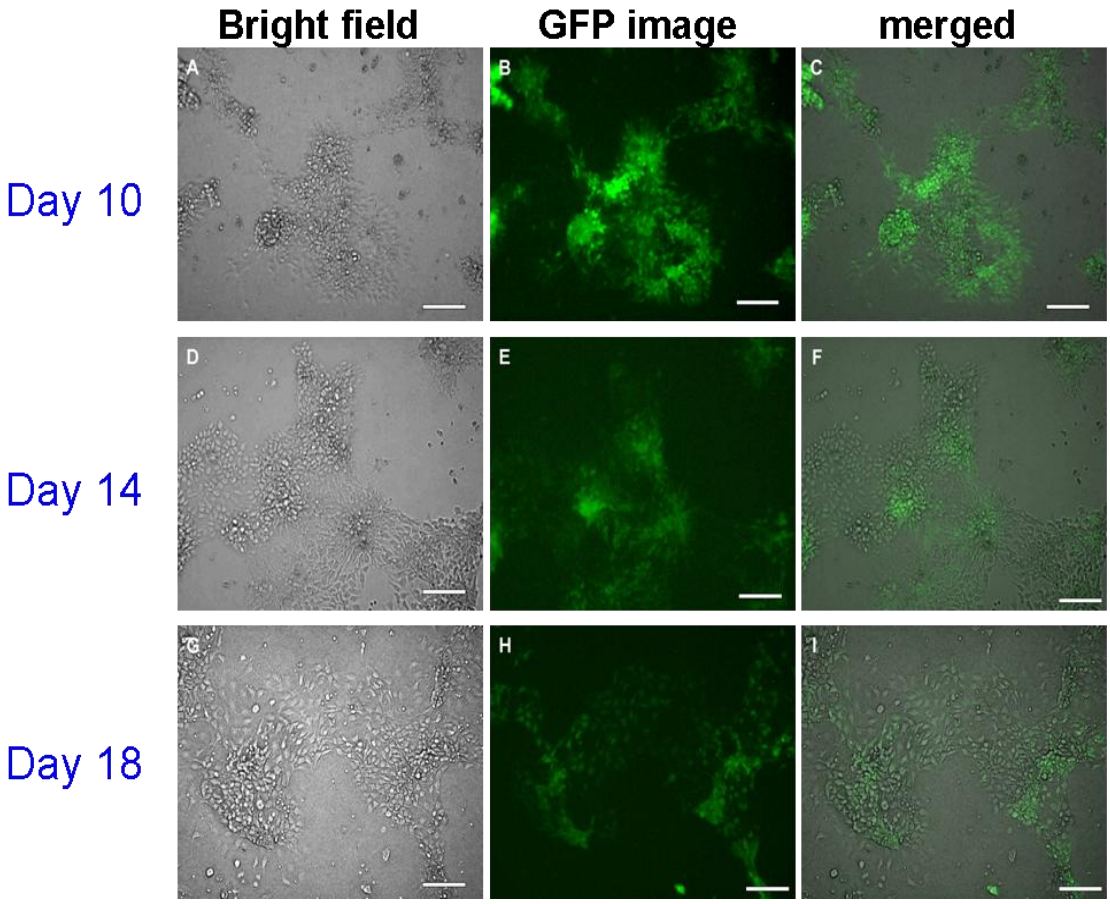

(b)

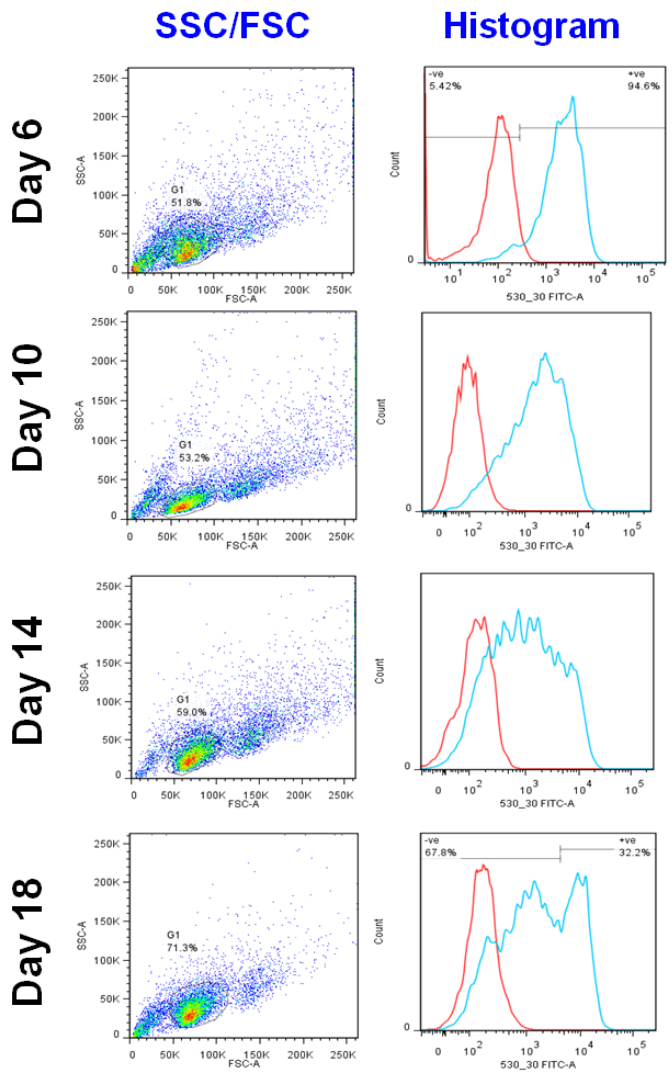

Day 6	Geo. mean		MFI ratio	% of GFP +ve
	+ve	-ve		
Sample 1	2318	169	13.72	92.7
Sample 2	2064		20.83	100
Sample 3	2230	137	16.28	94.6
GFP control	99.1			

Day 10	Geo. mean	MFI ratio	% of GFP +ve
Sample 1	1764	21.08	100
Sample 2	1490	17.80	100
Sample 3	1566	18.71	100
GFP control	83.7		

Day 14	Geo. mean	MFI ratio	% of GFP +ve
Sample 1	970	8.02	100
Sample 2	950	7.85	100
Sample 3	884	7.31	100
GFP control	121		

Day 18	Geo. mean		MFI ratio	% of GFP +ve
	+ve	-ve		
Sample 1	7528	586	12.85	38.5
Sample 2	8680	718	12.09	37.9
Sample 3	8703	687	12.49	32.2

(c)

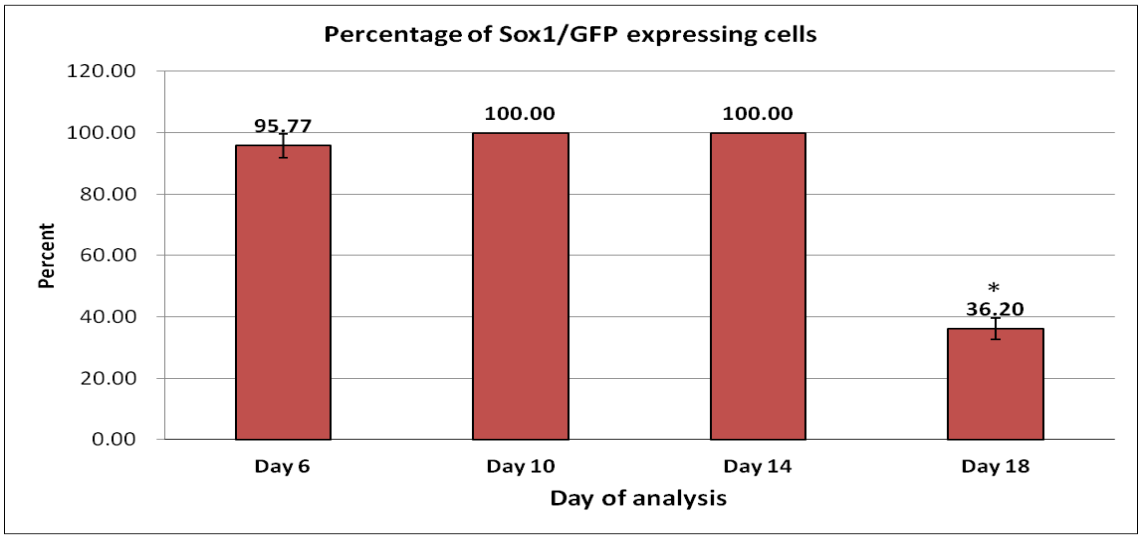

(d)

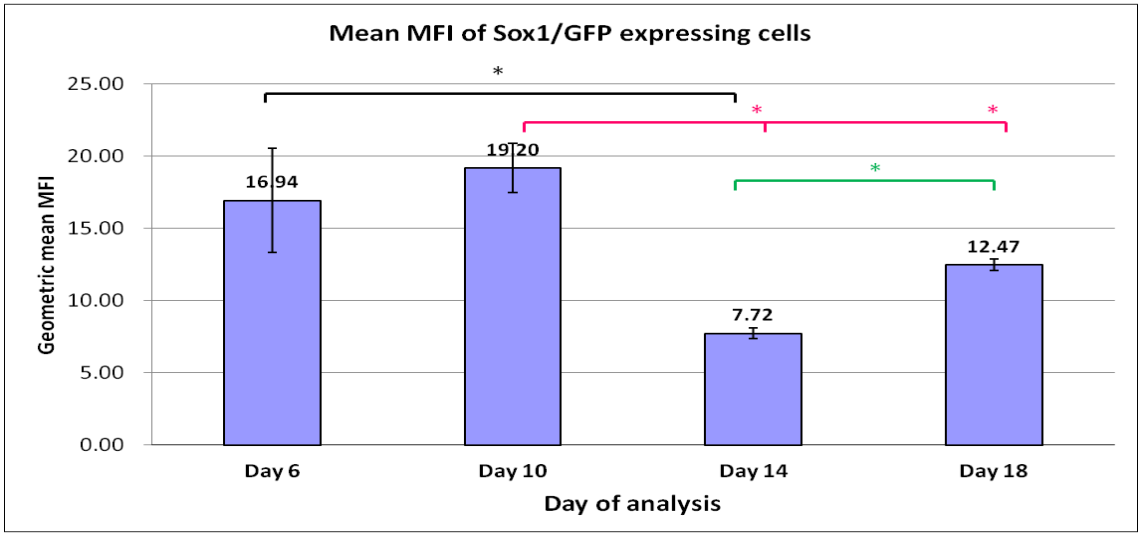

Figure 5.1 Flow cytometry analysis of Sox1 expression over time

(a) 46C cells were differentiated in CDM, FGF2 (20 ng/ml) was added from day 4 to day 18. Bright field and fluorescent pictures of one representative sample on day 10, day 14 and day 18 of neural differentiation are shown. Scale bar = 100 µm

(b) 46C cells were dissociated and measured by flow cytometry on day 6, day 10, day 14 and day 18 for Sox1/GFP expression. Cells were gated in G1, excluding clumped cells and debris. The percentage of cells included in the G1 gate is shown on the SSC/FSC plots. The fluorescent intensity of gated control samples (differentiated Foxg1 cells) (red line) and differentiated samples (blue line) is shown on the histograms. The bimodal distribution on day 18 is divided into subpopulation 1 and 2. Tables show the percentage of Sox1/GFP expression, the geometric mean (geo. mean) fluorescence value and MFI ratio of each sample acquired. The highlighted regions (in green) indicate the samples represented in the SSC/FSC plots and the histograms.

(c) The graph illustrates the mean percentage of Sox1/GFP expressing cells on day 6, day 10, day 14 and day 18 of neural differentiation. Bars represent the mean ± S.D. of three independent experiments. Significant *post-hoc* differences are indicated with an asterisk. (Tukey-Kramer test, $*P < 0.05$).

(d) The graph illustrates the mean MFI ratio of Sox1/GFP expressing cells on day 6, day 10, day 14 and day 18 of neural differentiation. Bars represent the mean ± S.D. of three independent experiments. Significant *post-hoc* differences are indicated with brackets. (Tukey-Kramer test, $*P < 0.05$)

5.2.2 Analysis of Sox1/GFP positive and negative populations treated with RA and purmorphamine on day 8 and day 20 of neural differentiation

The previous section shows that the intensity of Sox1/GFP expression in the absence of any morphogens decreased significantly over 18 days. To find out whether the responsiveness to morphogens was affected by the decrease in the percentage of Sox1/GFP positive cells, 46C cells were differentiated for 20 days and RA (1 μM) was added from day 4 to day 8, when the expression of HoxB3 was strongest; or from day 16 to day 20, when the expression of HoxB3 was weakest according to the results obtained by RT-PCR analysis in section 4.3.4 (Fig. 4.5), and also according to the results from Bouhon et al.'s study which shows that early NPCs can be patterned systematically for the first 4-8 days of cultures while late NPCs were non-responsive to morphogens between day 16 to day 20 and resulted in a loss of regional specification (Bouhon et al., 2006). The effect of Hh signalling on ventral telencephalic expression in early and late neural cultures was studied using a Shh agonist purmorphamine (PM). It was discovered by Wu and co-workers by running a screen of a heterocycle combinatorial library consisting of roughly 50 000 compounds for small molecules that induce the expression of ALP, a marker for osteogenesis. PM produced a significant increase in ALP expression and showed minor toxicity (Wu et al., 2002). Further investigation into this compound indicated that it acts as an agonist for the Hh signalling pathway and increases expression of patched (Ptc) and Gli (Wu et al., 2004). It targets Hh receptor Smoothened (Sinha and Chen, 2006) and has been shown to ventralize diencephalic progenitors in serum-free culture conditions (Wataya et al., 2008) (Fig. 5.2).

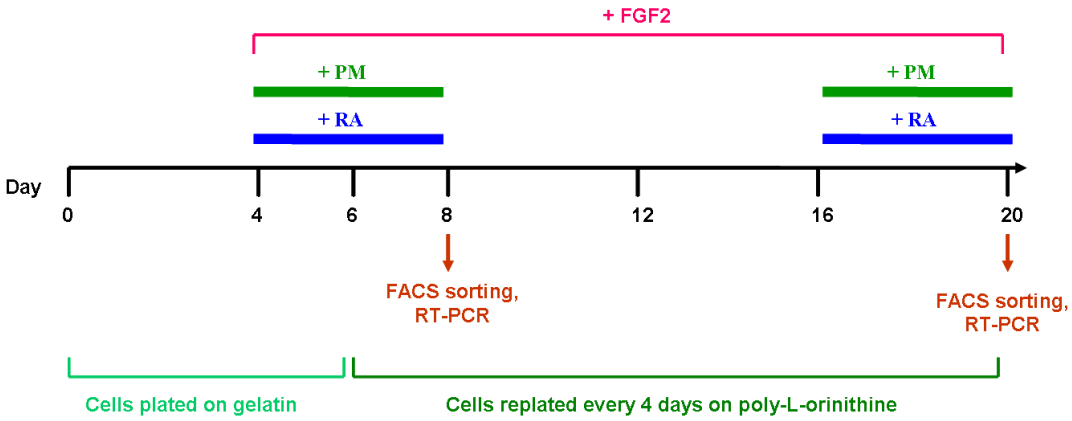

Figure 5.2 Schematic representation of the differentiation protocol used in this study

46C cells were differentiated in CDM for 20 days. FGF2 (20 ng/ml) was added from day 4 to day 20. RA (1 μM) and PM (0.25 μM) was added from day 4 to day 8 and day 16 to day 20. GFP positive and negative populations were sorted by FACS on day 8 and day 20 of differentiation and gene expression was analysed by RT-PCR. ES cells were differentiated on gelatin-coated plates for the first 6 days of differentiation and dissociated into single cells and replated onto poly-L-ornithine-coated plates every 4 days.

The effect of RA and PM on Sox1/GFP expression in 46C cells in early and late neural cultures was examined by fluorescence microscopy and flow cytometry. Fluorescent images of Sox1/GFP showed that more cells expressed GFP in early cultures than in late cultures. It appeared that PM treatment generated more GFP positive cells than CDM and RA treatments in both early and late cultures (Fig. 5.3 (a)).

To understand whether the responsiveness to morphogenic cues was determined by Sox1 expression, 46C cells were sorted by FACS into Sox1/GFP positive and Sox1/GFP negative populations. In early cultures (day 8), the positive and negative populations were defined by placing a delineator at the limit of the control sample fluorescence (between 0.5% to 1%) and cells that were found above this level were sorted as GFP positive. For late cultures (day 20), the delineator was placed at the limit of the negative populations, even though they did not overlap with the negative control samples. In the case of PM treatment where three populations were generated according to the histogram on day 20 (Fig. 5.3 (b)), only the population with the highest GFP intensity was being sorted as GFP positive. RNA was extracted from the GFP positive and GFP negative populations and was then analysed by RT-PCR.

HoxB3 is upregulated in r5 of the hindbrain specifically (Manzanares et al., 1999) and its expression is regulated by RA signalling (Niederreither et al., 2000). Fig. 5.4 showed that HoxB3 expression was strongly induced by RA treatment in early cultures (day 8) but not in late cultures (day 20) in both Sox1/GFP positive and negative populations. Nkx2.1 is a responsive gene of Shh and is expressed exclusively in the MGE and is required in the specification of MGE-derived neurons (Sussel et al., 1999, Butt et al., 2008). Similarly to HoxB3 expression, it was only induced in early cultures.

Interestingly, neither Sox1/GFP positive nor negative populations were permissive for HoxB3 and Nkx2.1 expression on day 20. As the expression pattern was very similar in the Sox1/GFP positive and Sox/GFP negative population in both early and late cultures, this

suggests that the loss of expression of the positional markers in late cultures was not due to a decline in Sox1 progenitor population, and hence the responsiveness to morphogenic cues in neural cultures was not associated with Sox1 expression.

The downregulation of HoxB3 and Nkx2.1 expression in late cultures could be due to an inactivation of Hh signalling. Therefore Ptc1 expression in early and late cultures was examined because it is a direct target of active Hh signalling (Marigo and Tabin, 1996). RT-PCR analysis showed that Ptc1 expression was induced by PM in both Sox1/GFP positive and negative populations and in both early and late neural cultures. This suggested that the lack of Nkx2.1 expression in late neural progenitors was not due to downregulation of Shh signalling *per se*. This showed that even though the positional identities were lost in late cultures, late NPCs were responsive to Shh signal.

(a)

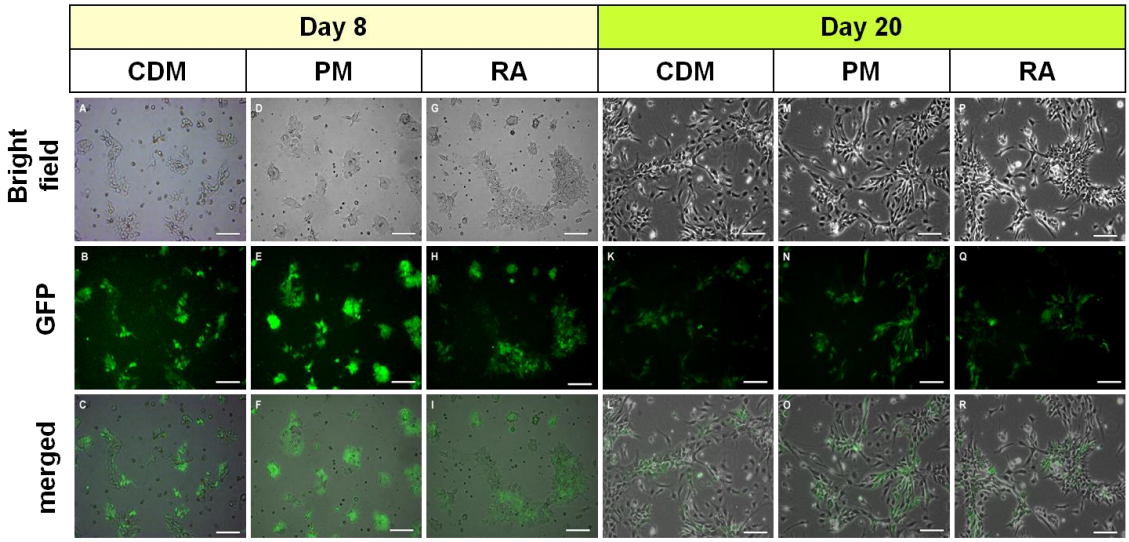

(b)

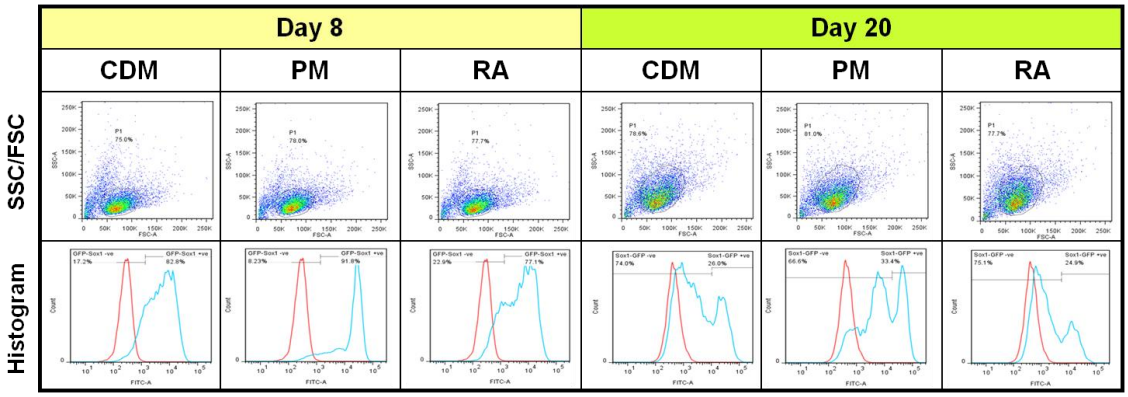

(c)

Day of sorting	CDM	PM (0.25 µM)	RA (1 µM)
Day 8	82.30	91.50	77.00
Day 20	26.00	33.40	24.90

Table 5.1 Percentage of GFP/Sox1 positive cells sorted

Figure 5.3 FACS sorting of Sox1/GFP positive and negative populations on day 8 and day 20 of neural differentiation

(a) 46C were differentiated in CDM and treated with PM (0.25 µM) and RA (1 µM). Bright field and fluorescent pictures of 46C cells on day 8 and day 20 of neural differentiation are shown. Scale bar = 100 µm

(b) 46C cells were dissociated into single cells and sorted for Sox1/GFP expression by FACS on day 8 and day 20 of neural differentiation. Cells were gated in G1, excluding clumped cells and debris. The percentage of cells included in the P1 gate is shown on the SSC/FSC plots. The fluorescent intensity of differentiated Foxg1 cells (negative control for GFP expression) (red line) and differentiated 46C cells (blue line) is shown on the histograms. Populations of cells being sorted into Sox1/GFP positive and negative are shown on the histograms.

(c) The table shows the percentage of Sox1/GFP positive and negative cells sorted on day 8 and day 20 of differentiation.

(a)

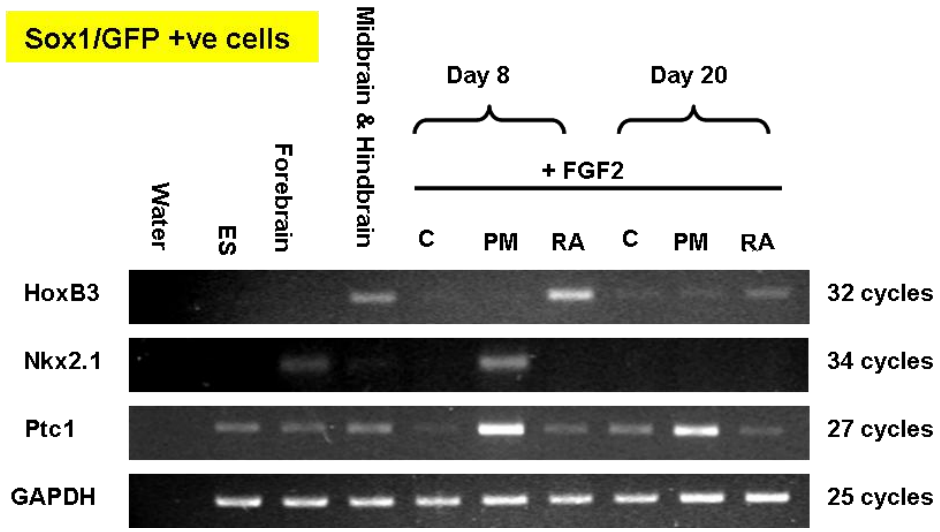

(b)

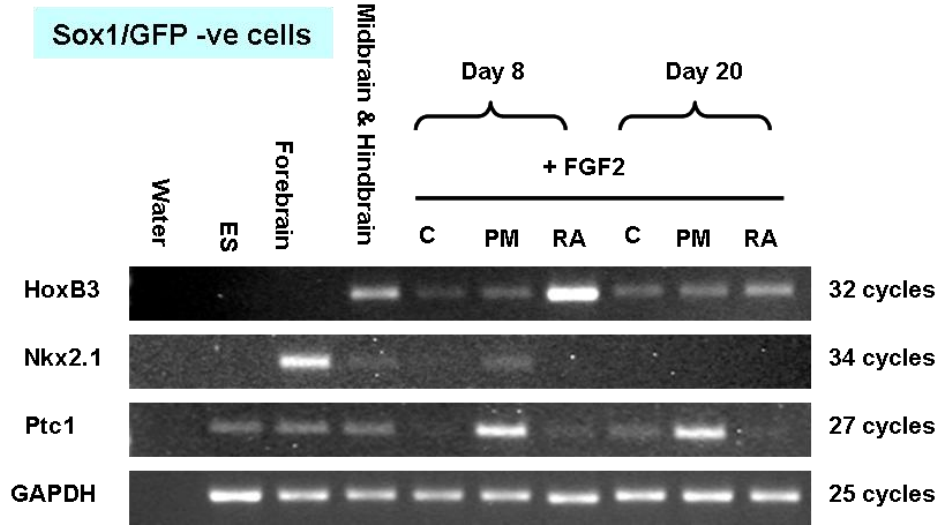

Figure 5.4 **RT-PCR analysis of PM and RA treated sample on day 8 and day 20 of differentiation**

Cells were treated with either RA (1 µM) or PM (0.25 µM) in the presence of FGF2 (20 ng/ml) added from day 4 and day 20. No RA or PM was added in CDM control (C). Sox1/GFP positive and negative populations of 46C cells were sorted on day 8 and day 20 by FACS. Expression of HoxB3, Nkx2.1 and Ptc1 were analysed by RT-PCR. Forebrain, midbrain and hindbrain were taken from E12.5 mouse embryo.

5.3 Discussion

It was observed that temporal difference in responsiveness to RA was found in early and late neural cultures (chapter 4). Late NPCs seemed to lose the ability to respond to RA, as reflected by a reduced caudalizing effect of RA and the lack of expression of a number of forebrain markers. Therefore, the question addressed by the present study was whether the change in responsiveness was due to a change in Sox1 expression over time, and if it was, whether it had any relation to the difference in responsiveness to patterning cues in early and late neural cultures.

The first investigation was to examine the percentage and intensity of Sox1/GFP expressing cells over time. The high percentage (nearly 100%) of Sox1/GFP expressing cells was maintained for the first 14 days of differentiation and decreased substantially on day 18. This observation appeared to be similar to Conti et al.'s study that Sox1/GFP expression was downregulated after 5 passages. Even though the images obtained from fluorescence microscopy clearly showed that the intensity of Sox1/GFP expressing cells decreased from day 10 to day 18, the intensity of Sox1/GFP expressing-cells obtained from flow cytometry analysis seemed to vary over time. The discrepancy could be due to the way cells were gated in the flow cytometry analysis because the data obtained can be easily affected by the negative control and also how the voltages were adjusted. Nevertheless, the data presented were the best possible representation of Sox1/GFP expression of 46C cells over time using flowjo as an analytical tool.

The next question addressed was whether Sox1 expression determines the responsiveness to patterning cues in early and late cultures. To investigate this, early and late NPCs were sorted into Sox1/GFP positive and Sox1/GFP negative populations using FACS. Contrary to the hypothesis that the expression of positional markers can be rescued in the Sox1/GFP positive population in late culture, the results showed that both the Sox1/GFP positive and Sox1/GFP negative populations responded to RA and PM by expressing HoxB3

and Nkx2.1 respectively in early cultures but not in late cultures. The expression pattern revealed by RT-PCR analysis (Fig. 5.4) showed that Sox1 did not seem to have any effect on the acquisition of positional markers. This was surprising considering the importance of SoxB1 proteins in regulating neural commitment. A recent study showed that SoxB1 proteins regulate neural-specific response by binding directly to the cis-regulatory modules (CRM) of morphogen-mediatory transcription factors (Oosterveen et al., 2013). CRM are stretches of DNA where a number of transcription factors can bind and regulate the expression of other genes (Davidson, 2010). The authors discovered that class II genes expressed in the ventral neural tube (Nkx2.2, Nkx6.1, Nkx6.2 and Olig2) can be induced in the limb bud by forced expression of both SoxB1 and Smo, but not SoxB1 or Smo alone. Similar responses were observed for other target genes induced by BMP and RA signalling. Interestingly, the expression of Sox1 was a lot weaker than Sox3 in the limb bud, suggesting Sox1 might not be the only factor that determined neural specification in NPCs (Oosterveen et al., 2013). Sox1 was shown to play a role in directing cells towards a neural fate. This was based on the evidence that induced expression of Sox1 in P19 embryonal carcinoma cells obviated the requirement for RA to initiate neural differentiation (Pevny et al., 1998). However, another study suggested that while Sox1 played some part in determining neuroectodermal fate it was not necessarily the only factor involved because the action of Sox1 can be overridden by the presence of serum (Zhao et al., 2004). It would be of interest to perform CHIP analysis to find out whether SoxB1 binds to the Sox-binding sites of the CRM of lineage markers in early and late markers to find out the role of Sox1 in determining the responsiveness to morphogens *in vitro*.

The responsiveness to morphogens can be determined by the signal transduction machinery. In the case of Hh signalling, the competence of neural progenitor cells to respond to Shh is regulated by the Gli family of transcriptional regulators, Gli1, Gli2 and Gli3 and their expression is under temporal control. *In vivo* study showed that during the later

stages of telencephalic development (after E12), Gli3 plays a less important role in regulating competence to Hh signalling because Nkx2.1 expression can be maintained by Shh in a Gli3 independent manner, indicating that there is a temporal change in requirement for Gli activity (Gulacsi and Anderson, 2006). Since it was reported that the maintenance of target genes requires a different threshold of Gli activity (Dessaud et al., 2010), it would be useful to study the expression Gli proteins in early and late cultures. Other candidates for investigation would include Fused and Cos2 , which are part of a cytoplasmic protein complex and are both phosphorylated in response to active Hh signalling (Robbins et al., 1997). In addition, Cos2 was reported to accumulate in cells that were responsive to Hh signalling in Drosophila embryos (Sisson et al., 1997).

5.4 Conclusion

The overall finding in this chapter, therefore, is that that both Sox1/GFP positive and negative cells responded to RA and PM by expressing HoxB3 and Nkx2.1 respectively in early but not in late cultures, indicating that HoxB3 and Nkx2.1 expression was not dependent on Sox1 expression. Cells were responsive to PM in late cultures even though Nkx2.1 expression was downregulated because Ptc1 was being induced by PM in both early and late cultures, indicating that late neural cultures were responsive to Hh signalling.

CHAPTER 6:

GENERAL DISCUSSION

To devise appropriate strategies for producing specific neural and neuronal subtypes from ES cells, we have to understand how ES cells respond to developmental cues in acquiring neural character. At present, the mechanisms for regional specification in response to morphogens as regulated *in vitro* are not entirely clear. This study addressed this by looking at the effectiveness of using BMP inhibitors in inducing neural differentiation in ES cells and also how the lineage specification of neural progenitor cells was regulated temporally. Knowledge about lineage specification is vital for making progress with using ES cells for cell replacement therapies and drug screen studies.

6.1 BMP inhibition in neural induction of ES cells

Chapter 3 originally sought to explore the effect of BMP inhibition on the generation of neural progenitors from ES cells using newly-discovered chemical inhibitors. Such chemical inhibitors are stable and cost-effective and therefore provide useful alternatives to the use of recombinant proteins such as noggin in cell differentiation protocols and for tranference into processes which are Good Manufacturing Practice (GMP) compliant. However, the results showed that ES cells differentiated in CDM alone generated a high percentage of Sox1-expressing cells (>90%) on day 4 and day 6 of differentiation (Fig. 3.3). A high percentage of Sox1 expression is desirable because Sox1-positive cells have the potential for differentiating into functional neurons that respond to various neurotransmitters in a manner that was similar to primary central neurons (Lang et al., 2004). Owing to the high percentage of Sox1-expressing cells generated by cells cultured in CDM alone, it was difficult to assess the effects of DM or LDN treatment on Sox1/GFP expression. Cells differentiated in CDM alone expressed early neural markers (nestin and Pax6), and the presence of LDN, DM and noggin treatments can only enhance the expression of neural markers slightly (Fig. 3.13-3.16). This suggests that exogenous BMP inhibition might not be essential for mouse ES

cells neural induction. This was also observed in a recent *in vitro* study showing that noggin treatment could only produce a marginal increase of neural progenitors (Bertacchi et al., 2013). Examination of noggin null mutants has revealed that noggin is not essential for the formation of neural tissue but is required for the ventral development in the posterior neural tube (McMahon et al., 1998). Noggin and chordin double-mutants displayed reduced forebrain development and did not express anterior marker Six3 (Bachiller et al., 2000). Therefore it seems that BMP inhibition might have a stronger influence on regional specification in NPCs than on the neural conversion of ES cells. ES cells differentiated in CDM alone expressed midbrain markers (Otx2 and Irx3). In the presence of noggin, cells preferentially expressed telencephalic markers (Foxg1, Tbr1 and Emx2), and downregulated midbrain and hindbrain markers (Bertacchi et al., 2013). It would be useful to examine the effect of DM or LDN treatments and of another newly-discovered BMP inhibitor, DMH1 (Ao et al., 2012), on regional patterning of neural progenitors in future studies.

6.2 Change in responsiveness in neural progenitor cells

Chapter 4 of this study revealed that late ES cell-derived neural progenitor cells (NPCs) appeared to have a tendency to be more gliogenic as more GFAP-positive cells were found in late NPCs than early NPCs (Fig. 4.12). The underlying mechanisms that lead to the change in response in late NPCs was not entirely clear but data from several studies suggests that this could be due a progressive change in responsiveness to FGF2 and EGF2 found in NPCs *in vivo* and *in vitro* (Ciccolini, 2001, Tropepe et al., 1999). Both FGF2 and EGF are required for long-term propagation of ES cell-derived neural stem cells (Conti et al., 2005), but only primary neurospheres (generated by differentiating ES cells for 8 days) and secondary neurospheres (generated by dissociating primary neurospheres) had high expression of FGFR1 and FGFR2. In contrast, the expression of EGFR was low in primary neuropheres but

increased dramatically in secondary neurospheres. Furthermore, both primary and secondary neurospheres can be generated effectively in the presence of FGF2 alone, but the generation of tertiary neurospheres (generated by dissociating primary neurospheres) required EGF (Okada et al., 2008). *In vivo*, FGF-responsive neural stem cells are found as early as E8.5 in the anterior neural plate (Tropepe et al., 1999), and FGF2 is required to maintain neural stem cell populations in the neurogenic adult subventricular zone (SVZ) (García-González et al., 2010). EGF responsiveness is not acquired until EGF receptors are expressed at mid gestation (Tropepe et al., 1999). As a result of the differential expression of FGF and EGF receptors in neural stem cells, early NPCs (E8.5 to E11.5) found in the CNS that are FGF-responsive and not EGF-responsive have the potential to generate early-born neurons such as forebrain cholinergic and midbrain dopaminergic neurons; in contrast, late NPCs (E11.5 onwards) in the CNS are EGF-responsive and have gliogenic potential and cannot generate early-born neurons (Qian et al., 2000, Temple, 2001, Tropepe et al., 1999). Recent study revealed that the responsiveness to EGF in gliogenic NPCs is dependent on the expression of tenascin C (Tnc) (Karus et al., 2011), which is an extracellular matrix glycoprotein expressed by NPCs in the brain (von Holst et al., 2007) and the spinal cord (Karus et al., 2011). Tnc knockout mutants had a reduced number of EGF-responsive neurospheres and lower expression of EGFR in the spinal cord than wild-type between E15.5 to E18.5 (Karus et al., 2011). Furthermore, the change in responsiveness to EGF also led to an increased expression of neural patterning genes including Nkx6.1 and Nkx2.2 in the Tnc-deficient spinal cord, and caused an upregulation of Sulf1, which is a downstream target of Nkx2.2 (Genethliou et al., 2009) and has been shown to inhibit FGF signalling (Otsuki et al., 2010). Further work is needed to establish whether late NPCs in this study are more responsive to EGF than early NPCs and to establish whether the temporal change in responsiveness to FGF and EGF is related to the patterning-responsiveness potential of NPCs *in vitro*.

Thus, temporal change in the competence of cells to respond to morphogens partly accounts for the irreversible progression of NPCs from being neurogenic to gliogenic. But it is also required for the proper development of the telencephalon. The sequential appearance of the MGE followed by the LGE is the result of progressive changes in the competence of telencephalic cells to respond to Shh signalling. This is based on the finding that blocking Shh activity between E9.5 to E10.5 in telencephalic explants reduced the expression of Dlx2 (expressed in the LGE) but did not affect the expression of Nkx2.1 (expressed in the MGE). In contrast, between E10.5 to E11.5, recombinant Shh induced the expression of Dlx2 but not Nkx2.1 in telencephalic explants even at the highest concentration examined (960nM) (Kohtz et al., 1998). This, therefore, indicates that early Shh signalling induces E9.5 telencephalon to take the form of MGE while late Shh signalling induces E10.5-E11.5 telencephalon to become LGE. Beyond E11.5, telencephalic explants are unable to be ventralized by Shh (Kohtz et al., 1998). While the underlying mechanism for the temporal change in responsiveness was not entirely clear, it can be construed that competence to respond to Shh in the MGE is partly regulated by Nkx2.1 (Butt et al., 2008). After the MGE is formed (E10.5), the expression of Shh target genes Gli1 (Lee et al., 1997) and Nkx6.2 (Stenman et al., 2003) is found in areas that are away from high Shh expression (Xu et al., 2005). Conditional knockout of Nkx2.1 results in upregulation of the Shh target gene Gli1 and Nkx6.2 in the MGE (Butt et al., 2008). Therefore, although Nkx2.1 expression is dependent on Shh signalling during MGE development (Sussel et al., 1999), removing Nkx2.1 after the MGE is formed seems to enable MGE progenitors to acquire competence to respond to Shh signalling (Sousa and Fishell, 2010). Whether or not other transcription factors have similar effects on regulating competence to respond to morphogens *in vitro* awaits further enquiry.

For different regions of the central nervous system to be properly developed, having temporal limits on the responsiveness to patterning cues is necessary to prevent unwanted secondary patterning of NPCs (Allen, 2008). An example can be found in the specification of the hindbrain rhombomere boundaries, which have an RA dependency that is lost from an anterior-to-posterior sequence as development proceeds (Dupe and Lumsden, 2001). Chapter 5 of this study showed that even though positional markers expression was not induced by Shh in late NPCs, cells were nevertheless still responsive to Hh signalling because Shh target gene Ptc1 expression was found to be in equal measure in both early and late cultures. The transition from being competent to incompetent in the process of inducing positional information was not due to a reduction of neural progenitors, because the expression of nestin in late cultures was similar to early cultures (Fig. 4.8). Consistent results are found in telencephalic explant study which shows that both early (E11.5) and late (E12.5) explant cultures had comparable levels of nestin expression, even though telencephalon has lost its capacity for expressing patterning genes in response to Shh after E12.5. This indicates that the loss of competence was not due to progenitors having withdrawn from the cell cycle (Kohtz et al., 1998), and suggests that late Shh signalling is involved in maintaining neural progenitor population. Hence, removing Hh signalling from E12.5 onwards leads to a reduction in the number of progenitors found in the postnatal SVZ while the regional patterning within the telencephalon is maintained (Machold et al., 2003). In the context of embryonic development, the change in the function of imposing positional identities in NPCs by morphogens has the benefit of allowing a small number of signalling pathways to be reused for other developmental processes such as regulation of progenitor cell number in the adult hippocampus (Lai et al., 2003).

NPCs expanded for a prolonged period in cultures have not only a reduced patterning response, but also reduced survivability when transplanted into rat neonatal hippocampus. Zietlow et al. found that early passage foetal -derived human progenitors (expanded *in vitro* for 2 weeks) survive up to 12 weeks in the recipient brain whereas late passage foetal derived human progenitors (expanded *in vitro* for 20 weeks) initially form healthy-looking grafts but these grafts disappear after 4 weeks. Zietlow et al. argued that the reduced survivability of late passage cells was not due to an ageing of neural progenitors because they expressed NS cell markers (Sox2, nestin) and were able to give rise to GFAP- and β-III-tubulin-positive cells. However, they also reported that the percentage of β-III-tubulin-positive cells obtained from spontaneous differentiation decreases from 27.7% to 5.8% from early to late passage cells (Zietlow et al., 2012), suggesting that cells became less neurogenic (more gliogenic) over time. Further research to deepen understanding of the developmental potential of these temporally-restricted NS cells is required if they are to be utilised in transplantation studies.

6.3 Regulation of neural patterning by co-repressor

Experimentation carried out in the course of this study has only investigated the effect of extracellular factors on the regional specification of ES cell-derived NPCs: it did not examine the epigenetic mechanisms. Previous study has shown that both class I and II homeodomain proteins in the ventral neural tube can act as repressors by relying on the Eh1 domain to recruit Gro/TLE co-repressor to establish the correct positioning of the homeodomains. Therefore, misexpression of class II protein Nkx6.1 in the dorsal region of the neural tube caused the repression of class I protein Dbx2 (Muhr et al., 2001). Many homeodomain proteins involved in AP and DV patterning, such as the Msx and Gbx proteins, contain Eh1 domain (Smith and Jaynes, 1996), indicating the importance of the role of Gro/TLE in setting the correct spatial patterns. In the case of homeodomain proteins (such as

Pax6 and Irx3), which do not contain the Eh1 domain, repression of homeodomain proteins was believed to be mediated through the activation of intermediary repressor proteins (Muhr et al., 2001).

Since neural patterning of the ventral tube relies on some homeodomain proteins that function as repressors by recruiting Gro/TLE (Muhr et al., 2001), it would be of interest to find out if the expression of Grg5 in early and late cultures inhibits the activity of Gro/TLE (Roose et al., 1998). *In vivo*, ectopic expression of Grg5 reduced the ability of Nkx6.1 to repress Dbx2 expression, causing dorsal expansion of the domain of Nkx6.1. Similar results were obtained in another pair of class I/II proteins Pax6 and Nkx2.2, indicating that the reduction in Gro/TLE activity caused by Grg5 can deregulate the positioning of the homeodomain proteins (Muhr et al., 2001). The change in positional response was not associated with the change in responsiveness to Shh signal of ventral progenitor cells as the expression of Shh and Ptc1 was unaffected by the ectopic expression of Grg5. Another interesting gene to examine in relation to changes in responsiveness in late cultures would be the Gro/TLE gene Grg4 because it shows a spatial change in expression during embryonic development. In chick, It is uniformly expressed in the neural plate and neural tube fold (stage 10), but is expressed at a higher level in the ventral region after neural tube closure (stage 15), suggesting that Grg4 might be involved in regulating ventral patterning response (Muhr et al., 2001).

6.4 Transferability of mouse ES works to human ES works

One of the reasons for studying the neural differentiation of mouse ES cells is because they can be used as informative models for human ES and iPS cells differentiation, even though there are differences in growth factor requirements in human and mouse models. For instance, the pluripotency of mouse ES cells is dependent on the synergistic effects of

BMP and LIF (Ying et al., 2003a). In contrast, human ES and iPS cells rely on the synergistic effect of TGFβ (mediated through Smad 2/3 activation) and FGF signals to suppress BMP signalling in order to regulate the expression of Nanog and therefore to maintain pluripotency (Vallier et al., 2005, Xu et al., 2008, Vallier et al., 2009). Human ES cells differentiate into extracellular trophoblast (Xu et al., 2002, Amita et al., 2013), mesoderm (Laflamme et al., 2007) and endoderm (D'Amour et al., 2005) in response to active BMP signalling. Therefore, the dual inhibition of Smad signalling using noggin (which prevents the phosphorylation of Smad1/5/8) and SB431542 (which prevents the activation of Smad2/3) enhances neural induction in human ES cell cultures yielding a high percentage of neuroepithelial cells that can potentially be differentiated into motoneurons and dopaminergic neurons (Chambers et al., 2009). Furthermore, even though human ES cells express gp130 receptors and respond to LIF by inducing STAT3 phosphorylation and translocation to the nucleus, LIF itself cannot sustain the self-renewal of human ES Cells (Daheron et al., 2004). However, once human ES cells are converted to neural progenitors, LIF can significantly enhance their *in vitro* survival by reducing caspase-mediated apoptosis and also promote their differentiation (Majumder et al., 2012). Previous study has shown that the same neural differentiation protocol that is used to generate mouse ES cell-derived neural stem cells can be also be used to generate β-III-tubulin positive-neurons and GFAP positive-cells from human ES cells, though not as effectively as is the case in mouse cells. Therefore species-specific requirements need to be met in order to achieve more efficient neural induction and differentiation of human ES cells (Conti et al., 2005).

6.5 Experimental limitation of this study: Heterogeneity in cell cultures

Discrepancies between studies using culture systems are inevitable because different cell lines and differentiation media are used. Different cell lines derived from mouse strains with dissimilar genetic backgrounds might produce variation in the pattern of gene expression. Some genes might be more susceptible to certain components of the differentiation media. These two factors might not contribute to any detectable disparity at an early stage but might produce more significant differences in phenotypic response at a later stage (Stojkovic et al., 2004). Therefore, it is necessary to study findings reported by a variety of neural differentiation approaches carefully, noting the similarities and dissimilarities between each system.

Even when the same neural differentiation protocol is used, discrepancies can be observed between each experimental setup because heterogeneity exists within ES cell cultures, and it is difficult to identify responsive cells (Parmar and Li, 2007). Pluripotency factors are heterogeneously expressed in ES cell cultures as revealed by a 10-fold variation in the expression of Oct4 and Sox2 between individual ES cells (Tang et al., 2010). Furthermore, the level of Nanog expression fluctuates in each individual ES cell (Chambers et al., 2007) , and the fluctuating levels of Nanog can have an effect on the differentiation potential of ES cells (Abranches et al., 2013). The population of ES cells with low Nanog expression had a higher degree of readiness for differentiation (indicated by a higher expression of FGF5 (ectoderm), T-brachyury (mesoderm) and Gata6 (endoderm)) than a population of ES cells with high Nanog expression (Abranches et al., 2013). Considering that pluripotency factors are also lineage specifiers (Loh and Lim, 2011, Thomson et al., 2011), it is unsurprising that the uneven expression and fluctuations in the expression of pluripotency factors of ES cells might account for the differential developmental potential between cultures. In addition, some of the transcription factors that confer positional information are not entirely copied

by ES cell-derived cultures and this might also affect competence in the generation of site-specific neurons (Conti and Cattaneo, 2010). Furthermore, each individual ES cell possesses a unique collection of histone modifications that have different kinetics and stoichiometries in lineage-control gene loci, and hence will also influence lineage decision (Gan et al., 2007).

6.6 Conclusion

Recent progress made in the neural differentiation of ES cells has proved extremely promising. The use of ES cells-derived NPCs as a source of specific neurons for clinical applications opens up wide-ranging possibilities. This study has demonstrated that a high percentage of Sox1-positive neural progenitors was generated from ES cells in CDM alone and that the effect was slightly enhanced by the introduction of BMP inhibitors. Although newly-discovered BMP inhibitors can potentially be used as a replacement of recombinant noggin, it is necessary to consider their off-target effects.

This study has also shown that regional specification of ES cell-derived neural progenitors is determined by the temporal change in competence to respond to morphogens. *In vivo*, the dynamic change in temporal competence to morphogens is essential for regulating the correct specification of different organs and tissues (Sousa and Fishell, 2010). However, *in vitro* this seems to contribute to the gradual loss in regional identities of ES cell-derived NPCs over time, indicating that the patterning response given by NPCs is restricted temporally.

Though a better understanding of the underlying mechanism for the loss of patterning response in late NPCs is vital to further progress, it remains, at present, elusive. However, the temporal change in responsiveness to morphogens can partly explain how the patterning and growth of different tissues during embryonic development relies on the redeployment of only a small number of signalling pathways. Although SoxB1 proteins have been shown to regulate neural specific response *in vivo* (Oosterveen et al., 2013), this study indicates that the loss of regionalisation in late NPCs was not due to the downregulation of Sox1 expression.

The findings submitted in this study suggest that further work is needed to reach an understanding of this temporal change in responsiveness. Such a step would greatly increase the developmental potential of ES cell-derived NPCs. Their therapeutic application is dependent on the extent to which our knowledge of NPC patterning responses is such that they can be predicted and manipulated comprehensively and accurately.

BIBLOGRAPHY

AAKU-SARASTE, E., HELLWIG, A. & HUTTNER, W. B. 1996. Loss of occludin and functional tight junctions, but not ZO-1, during neural tube closure--remodeling of the neuroepithelium prior to neurogenesis. *Dev Biol,* 180**,** 664-79.

ABRANCHES, E., BEKMAN, E. & HENRIQUE, D. 2013. Generation and characterization of a novel mouse embryonic stem cell line with a dynamic reporter of nanog expression. *PLoS One,* 8**,** e59928.

ABU-ABED, S., DOLLE, P., METZGER, D., BECKETT, B., CHAMBON, P. & PETKOVICH, M. 2001. The retinoic acid-metabolizing enzyme, CYP26A1, is essential for normal hindbrain patterning, vertebral identity, and development of posterior structures. *Genes Dev,* 15**,** 226-40.

ALLEN, N. D. 2008. Temporal and epigenetic regulation of neurodevelopmental plasticity. *Philos Trans R Soc Lond B Biol Sci,* 363**,** 23-38.

AMITA, M., ADACHI, K., ALEXENKO, A. P., SINHA, S., SCHUST, D. J., SCHULZ, L. C., ROBERTS, R. M. & EZASHI, T. 2013. Complete and unidirectional conversion of human embryonic stem cells to trophoblast by BMP4. *Proc Natl Acad Sci U S A,* 110**,** E1212-21.

ANDERSON, R. M., LAWRENCE, A. R., STOTTMANN, R. W., BACHILIER, D. & KLINGENSMITH, J. 2002. Chordin and noggin promote organizing centers of forebrain development in the mouse. *Development,* 129**,** 4975-4987.

ANDERSON, S. A., EISENSTAT, D. D., SHI, L. & RUBENSTEIN, J. L. R. 1997. Interneuron migration from basal forebrain to neocortex: Dependence on Dlx genes. *Science,* 278**,** 474-476.

ANG, S. L., CONLON, R. A., JIN, O. & ROSSANT, J. 1994. Positive and negative signals from mesoderm regulate the expression of mouse Otx2 in ectoderm explants. *Development,* 120**,** 2979-89.

AO, A., HAO, J., HOPKINS, C. R. & HONG, C. C. 2012. DMH1, a novel BMP small molecule inhibitor, increases cardiomyocyte progenitors and promotes cardiac differentiation in mouse embryonic stem cells. *PLoS One,* 7**,** e41627.

AUBERT, J., DUNSTAN, H., CHAMBERS, I. & SMITH, A. 2002. Functional gene screening in embryonic stem cells implicates Wnt antagonism in neural differentiation. *Nat Biotechnol,* 20**,** 1240-5.

AVANTAGGIATO, V., ACAMPORA, D., TUORTO, F. & SIMEONE, A. 1996. Retinoic acid induces stage-specific repatterning of the rostral central nervous system. *Dev Biol,* 175**,** 347-57.

BACHILLER, D., KLINGENSMITH, J., KEMP, C., BELO, J. A., ANDERSON, R. M., MAY, S. R., MCMAHON, J. A., MCMAHON, A. P., HARLAND, R. M., ROSSANT, J. & DE ROBERTIS, E. M. 2000. The organizer factors Chordin and Noggin are required for mouse forebrain development. *Nature,* 403**,** 658-661.

BAI, C. B. & JOYNER, A. L. 2001. Gli1 can rescue the in vivo function of Gli2. *Development,* 128**,** 5161-5172.

BAI, C. B., STEPHEN, D. & JOYNER, A. L. 2004. All mouse ventral spinal cord patterning by hedgehog is Gli dependent and involves an activator function of Gli3. *Developmental Cell,* 6**,** 103-115.

BAIN, G., KITCHENS, D., YAO, M., HUETTNER, J. E. & GOTTLIEB, D. I. 1995. Embryonic Stem-Cells Express Neuronal Properties in-Vitro. *Developmental Biology,* 168**,** 342-357.

BAIN, G., RAY, W. J., YAO, M. & GOTTLIEB, D. I. 1996. Retinoic acid promotes neural and represses mesodermal gene expression in mouse embryonic stem cells in culture. *Biochem Biophys Res Commun,* 223**,** 691-4.

BARIBAULT, H., PRICE, J., MIYAI, K. & OSHIMA, R. G. 1993. MIDGESTATIONAL LETHALITY IN MICE LACKING KERATIN-8. *Genes & Development,* 7**,** 1191-1202.

BELO, J. A., BOUWMEESTER, T., LEYNS, L., KERTESZ, N., GALLO, M., FOLLETTIE, M. & DE ROBERTIS, E. M. 1997. Cerberus-like is a secreted factor with neutralizing activity expressed in the anterior primitive endoderm of the mouse gastrula. *Mech Dev,* 68**,** 45-57.

BERGSLAND, M., RAMSK LD, D., ZAOUTER, C., KLUM, S., SANDBERG, R. & MUHR, J. 2011. Sequentially acting Sox transcription factors in neural lineage development. *Genes & Development,* 25**,** 2453-2464.

BERGSLAND, M., WERME, M., MALEWICZ, M., PERLMANN, T. & MUHR, J. 2006. The establishment of neuronal properties is controlled by Sox4 and Sox11. *Genes Dev,* 20**,** 3475-86.

BERTACCHI, M., PANDOLFINI, L., MURENU, E., VIEGI, A., CAPSONI, S., CELLERINO, A., MESSINA, A., CASAROSA, S. & CREMISI, F. 2013. The positional identity of mouse ES cell-generated neurons is affected by BMP signaling. *Cell Mol Life Sci,* 70**,** 1095-111.

BLITZ, I. L. & CHO, K. W. 2009. Finding partners: how BMPs select their targets. *Developmental Dynamics,* 238**,** 1321-1331.

BOERGERMANN, J. H., KOPF, J., YU, P. B. & KNAUS, P. 2010. Dorsomorphin and LDN-193189 inhibit BMP-mediated Smad, p38 and Akt signalling in C2C12 cells. *International Journal of Biochemistry & Cell Biology,* 42**,** 1802-1807.

BOUHON, I. A., JOANNIDES, A., KATO, H., CHANDRAN, S. & ALLEN, N. D. 2006. Embryonic stem cell-derived neural progenitors display temporal restriction to neural patterning. *Stem Cells,* 24**,** 1908-1913.

BOUHON, I. A., KATO, H., CHANDRAN, S. & ALLEN, N. D. 2005. Neural differentiation of mouse embryonic stem cells in chemically defined medium. *Brain Research Bulletin,* 68**,** 62-75.

BRADLEY, A., EVANS, M., KAUFMAN, M. H. & ROBERTSON, E. 1984. Formation of germ-line chimaeras from embryo-derived teratocarcinoma cell lines. *Nature,* 309**,** 255-6.

BRISCOE, J., PIERANI, A., JESSELL, T. M. & ERICSON, J. 2000. A homeodomain protein code specifies progenitor cell identity and neuronal fate in the ventral neural tube. *Cell,* 101**,** 435-445.

BRISCOE, J., SUSSEL, L., SERUP, P., HARTIGAN-O'CONNOR, D., JESSELL, T. M., RUBENSTEIN, J. L. R. & ERICSON, J. 1999. Homeobox gene Nkx2.2 and specification of neuronal identity by graded Sonic hedgehog signalling. *Nature,* 398**,** 622-627.

BUECKER, C., CHEN, H. H., POLO, J. M., DAHERON, L., BU, L., BARAKAT, T. S., OKWIEKA, P., PORTER, A., GRIBNAU, J., HOCHEDLINGER, K. & GEIJSEN, N. 2010. A murine ESC-like state facilitates transgenesis and homologous recombination in human pluripotent stem cells. *Cell Stem Cell,* 6**,** 535-46.

BULFONE, A., KIM, H. J., PUELLES, L., PORTEUS, M. H., GRIPPO, J. F. & RUBENSTEIN, J. L. 1993. The mouse Dlx-2 (Tes-1) gene is expressed in spatially restricted domains of the forebrain, face and limbs in midgestation mouse embryos. *Mech Dev,* 40**,** 129-40.

BULFONE, A., SMIGA, S. M., SHIMAMURA, K., PETERSON, A., PUELLES, L. & RUBENSTEIN, J. L. R. 1995. T-BRAIN-1 - A HOMOLOG OF BRACHYURY WHOSE EXPRESSION DEFINES MOLECULARLY DISTINCT DOMAINS WITHIN THE CEREBRAL-CORTEX. *Neuron,* 15**,** 63-78.

BURKE, L. J. & BANIAHMAD, A. 2000. Co-repressors 2000. *Faseb Journal,* 14**,** 1876-1888.

BURTON, P., ADAMS, D. R., ABRAHAM, A., ALLCOCK, R. W., JIANG, Z., MCCAHILL, A., GILMOUR, J., MCABNEY, J., KANE, N. M., BAILLIE, G. S., MCKENZIE, F. R., BAKER, A. H., HOUSLAY, M. D., MOUNTFORD, J. C. & MILLIGAN, G. 2010. Identification and characterization of small-molecule ligands that maintain

pluripotency of human embryonic stem cells. *Biochem Soc Trans,* 38**,** 1058-61.

BUTT, S. J. B., SOUSA, V. H., FUCCILLO, M. V., HJERLING-LEFFLER, J., MIYOSHI, G., KIMURA, S. & FISHELL, G. 2008. The requirement of Nkx2-1 in the temporal specification of cortical interneurion subtypes. *Neuron,* 59**,** 722-732.

BYLUND, M., ANDERSSON, E., NOVITCH, B. G. & MUHR, J. 2003. Vertebrate neurogenesis is counteracted by Sox1-3 activity. *Nature Neuroscience,* 6**,** 1162-1168.

CARGNELLO, M. & ROUX, P. P. 2011. Activation and Function of the MAPKs and Their Substrates, the MAPK-Activated Protein Kinases. *Microbiology and Molecular Biology Reviews,* 75**,** 50-83.

CARNEY, R. S., COCAS, L. A., HIRATA, T., MANSFIELD, K. & CORBIN, J. G. 2009. Differential regulation of telencephalic pallial-subpallial boundary patterning by Pax6 and Gsh2. *Cereb Cortex,* 19**,** 745-59.

CARTER, N. P. & ORMEROD, M. G. 2005. Introduction to the principles of flow cytometry. *In:* ORMEROD, M. G. (ed.) *Flow cytometry, a practical approach.* 3rd ed. Reigate: Oxford University Press.

CASAROSA, S., FODE, C. & GUILLEMOT, F. 1999. Mash1 regulates neurogenesis in the ventral telencephalon. *Development,* 126**,** 525-534.

CHAMBERS, I., SILVA, J., COLBY, D., NICHOLS, J., NIJMEIJER, B., ROBERTSON, M., VRANA, J., JONES, K., GROTEWOLD, L. & SMITH, A. 2007. Nanog safeguards pluripotency and mediates germline development. *Nature,* 450**,** 1230-U8.

CHAMBERS, I. & SMITH, A. 2004. Self-renewal of teratocarcinoma and embryonic stem cells. *Oncogene,* 23**,** 7150-60.

CHAMBERS, S. M., FASANO, C. A., PAPAPETROU, E. P., TOMISHIMA, M., SADELAIN, M. & STUDER, L. 2009. Highly efficient neural conversion of human ES and iPS cells by dual inhibition of SMAD signaling. *Nature Biotechnology,* 27**,** 275-280.

CHEN, D., ZHAO, M. & MUNDY, G. R. 2004. Bone morphogenetic proteins. *Growth Factors,* 22**,** 233-41.

CHEN, J. D. & EVANS, R. M. 1995. A TRANSCRIPTIONAL CO-REPRESSOR THAT INTERACTS WITH NUCLEAR HORMONE RECEPTORS. *Nature,* 377**,** 454-457.

CHI, C. L., MARTINEZ, S., WURST, W. & MARTIN, G. R. 2003. The isthmic organizer signal FGF8 is required for cell survival in the prospective midbrain and cerebellum. *Development,* 130**,** 2633-2644.

CICCOLINI, F. 2001. Identification of two distinct types of multipotent neural precursors that appear sequentially during CNS development. *Mol Cell Neurosci,* 17**,** 895-907.

CONTI, L. & CATTANEO, E. 2010. Neural stem cell systems: physiological players or in vitro entities? *Nature Reviews Neuroscience,* 11**,** 176-187.

CONTI, L., POLLARD, S. M., GORBA, T., REITANO, E., TOSELLI, M., BIELLA, G., SUN, Y. R., SANZONE, S., YING, Q. L., CATTANEO, E. & SMITH, A. 2005. Niche-independent symmetrical self-renewal of a mammalian tissue stem cell. *Plos Biology,* 3**,** 1594-1606.

CROSSLEY, P. H. & MARTIN, G. R. 1995. THE MOUSE FGF8 GENE ENCODES A FAMILY OF POLYPEPTIDES AND IS EXPRESSED IN REGIONS THAT DIRECT OUTGROWTH AND PATTERNING IN THE DEVELOPING EMBRYO. *Development,* 121**,** 439-451.

CUNY, G. D., YU, P. B., LAHA, J. K., XING, X., LIU, J.-F., LAI, C. S., DENG, D. Y., SACHIDANANDAN, C., BLOCH, K. D. & PETERSON, R. T. 2008. Structure-activity relationship study of bone morphogenetic protein (BMP) signaling inhibitors. *Bioorganic & Medicinal Chemistry Letters,* 18**,** 4388-4392.

D'AMOUR, K. A., AGULNICK, A. D., ELIAZER, S., KELLY, O. G., KROON, E. & BAETGE, E. E. 2005. Efficient differentiation of human embryonic stem cells to definitive endoderm. *Nat Biotechnol,* 23**,** 1534-41.

DAHERON, L., OPITZ, S. L., ZAEHRES, H., LENSCH, M. W., ANDREWS, P. W., ITSKOVITZ-ELDOR, J. & DALEY, G. Q. 2004. LIF/STAT3 signaling fails to maintain self-renewal of human embryonic stem cells. *Stem Cells,* 22**,** 770-8.

DANJO, T., EIRAKU, M., MUGURUMA, K., WATANABE, K., KAWADA, M., YANAGAWA, Y., RUBENSTEIN, J. L. R. & SASAI, Y. 2011. Subregional Specification of Embryonic Stem Cell-Derived Ventral Telencephalic Tissues by Timed and Combinatory Treatment with Extrinsic Signals. *Journal of Neuroscience,* 31**,** 1919-1933.

DARNELL, J. E., JR. 1997. STATs and gene regulation. *Science,* 277**,** 1630-5.

DAVIDSON, E. H. 2010. Emerging properties of animal gene regulatory networks. *Nature,* 468**,** 911-20.

DAVIES, S. P., REDDY, H., CAIVANO, M. & COHEN, P. 2000. Specificity and mechanism of action of some commonly used protein kinase inhibitors. *Biochemical Journal,* 351**,** 95-105.

DESSAUD, E., RIBES, V., BALASKAS, N., YANG, L. L., PIERANI, A., KICHEVA, A., NOVITCH, B. G., BRISCOE, J. & SASAI, N. 2010. Dynamic Assignment and Maintenance of Positional Identity in the Ventral Neural Tube by the Morphogen Sonic Hedgehog. *Plos Biology,* 8.

DESSAUD, E., YANG, L. L., HILL, K., COX, B., ULLOA, F., RIBEIRO, A., MYNETT, A., NOVITCH, B. G. & BRISCOE, J. 2007. Interpretation of the sonic hedgehog morphogen gradient by a temporal adaptation mechanism. *Nature,* 450**,** 717-U7.

DOETSCHMAN, T. C., EISTETTER, H., KATZ, M., SCHMIDT, W. & KEMLER, R. 1985. THE INVITRO DEVELOPMENT OF BLASTOCYST-DERIVED EMBRYONIC STEM-CELL LINES - FORMATION OF VISCERAL YOLK-SAC, BLOOD ISLANDS AND MYOCARDIUM. *Journal of Embryology and Experimental Morphology,* 87**,** 27-45.

DOLLE, P., FRAULOB, V., GALLEGO-LLAMAS, J., VERMOT, J. & NIEDERREITHER, K. 2010. Fate of retinoic acid-activated embryonic cell lineages. *Dev Dyn,* 239**,** 3260-74.

DUESTER, G. 1998. Alcohol dehydrogenase as a critical mediator of retinoic acid synthesis from vitamin A in the mouse embryo. *J Nutr,* 128**,** 459S-462S.

DUPE, V. & LUMSDEN, A. 2001. Hindbrain patterning involves graded responses to retinoic acid signalling. *Development,* 128**,** 2199-208.

DURSTON, A. J., TIMMERMANS, J. P., HAGE, W. J., HENDRIKS, H. F., DE VRIES, N. J., HEIDEVELD, M. & NIEUWKOOP, P. D. 1989. Retinoic acid causes an anteroposterior transformation in the developing central nervous system. *Nature,* 340**,** 140-4.

ECHELARD, Y., EPSTEIN, D. J., ST-JACQUES, B., SHEN, L., MOHLER, J., MCMAHON, J. A. & MCMAHON, A. P. 1993. Sonic hedgehog, a member of a family of putative signaling molecules, is implicated in the regulation of CNS polarity. *Cell,* 75**,** 1417-30.

EGLEN, R. M., GILCHRIST, A. & REISINE, T. 2008. An overview of drug screening using primary and embryonic stem cells. *Comb Chem High Throughput Screen,* 11**,** 566-72.

EIRAKU, M., WATANABE, K., MATSUO-TAKASAKI, M., KAWADA, M., YONEMURA, S., MATSUMURA, M., WATAYA, T., NISHIYAMA, A., MUGURUMA, K. & SASAIL, Y. 2008. Self-Organized Formation of Polarized Cortical Tissues from ESCs and Its Active Manipulation by Extrinsic Signals. *Cell Stem Cell,* 3**,** 519-532.

ENGLUND, C., FINK, A., LAU, C., PHAM, D., DAZA, R. A. M., BULFONE, A., KOWALCZYK, T. & HEVNER, R. F. 2005. Pax6, Tbr2, and Tbr1 are expressed sequentially by radial glia, intermediate progenitor cells, and postmitotic neurons in developing neocortex. *Journal of Neuroscience,* 25**,** 247-251.

ENWRIGHT, J. F., 3RD & GRAINGER, R. M. 2000. Altered retinoid signaling in the heads of small eye mouse embryos. *Dev Biol,* 221**,** 10-22.

ERICSON, J., MUHR, J., PLACZEK, M., LINTS, T., JESSELL, T. M. & EDLUND, T. 1995. SONIC HEDGEHOG INDUCES THE DIFFERENTIATION OF VENTRAL FOREBRAIN NEURONS - A COMMON SIGNAL FOR VENTRAL PATTERNING WITHIN THE NEURAL-TUBE. *Cell,* 81**,** 747-756.

ERICSON, J., RASHBASS, P., SCHEDL, A., BRENNERMORTON, S., KAWAKAMI, A., VANHEYNINGEN, V., JESSELL, T. M. & BRISCOE, J. 1997. Pax6 controls progenitor cell identity and neuronal fate in response to graded shh signaling. *Cell,* 90**,** 169-180.

EVANS, M. J. & KAUFMAN, M. H. 1981. Establishment in Culture of Pluripotential Cells from Mouse Embryos. *Nature,* 292**,** 154-156.

FAHERTY, S., KANE, M. T. & QUINLAN, L. R. 2005. Self-renewal and differentiation of mouse embryonic stem cells as measured by Oct4 gene expression: Effects of LIF, serum-free medium, retinoic acid, and dbcAMP. *In Vitro Cellular & Developmental Biology-Animal,* 41**,** 356-363.

FENG, L., HATTEN, M. E. & HEINTZ, N. 1994. Brain lipid-binding protein (BLBP): a novel signaling system in the developing mammalian CNS. *Neuron,* 12**,** 895-908.

FERLAND, R. J., CHERRY, T. J., PREWARE, P. O., MORRISEY, E. E. & WALSH, C. A. 2003. Characterization of Foxp2 and Foxp1 mRNA and protein in the developing and mature brain. *J Comp Neurol,* 460**,** 266-79.

FODE, C., MA, Q. F., CASAROSA, S., ANG, S. L., ANDERSON, D. J. & GUILLEMOT, F. 2000. A role for neural determination genes in specifying the dorsoventral identity of telencephalic neurons. *Genes & Development,* 14**,** 67-80.

FRAICHARD, A., CHASSANDE, O., BILBAUT, G., DEHAY, C., SAVATIER, P. & SAMARUT, J. 1995. In-Vitro Differentiation of Embryonic Stem-Cells into Glial-Cells and Functional-Neurons. *Journal of Cell Science,* 108**,** 3181-3188.

FRANK-KAMENETSKY, M., ZHANG, X. M., BOTTEGA, S., GUICHERIT, O., WICHTERLE, H., DUDEK, H., BUMCROT, D., WANG, F. Y., JONES, S., SHULOK, J., RUBIN, L. L. & PORTER, J. A. 2002. Small-molecule modulators of Hedgehog signaling: identification and characterization of Smoothened agonists and antagonists. *J Biol,* 1**,** 10.

FRASCH, M., CHEN, X. & LUFKIN, T. 1995. Evolutionary-conserved enhancers direct region-specific expression of the murine Hoxa-1 and Hoxa-2 loci in both mice and Drosophila. *Development,* 121**,** 957-74.

FRIEL, R., VAN DER SAR, S. & MEE, P. J. 2005. Embryonic stem cells: understanding their history, cell biology and signalling. *Adv Drug Deliv Rev,* 57**,** 1894-903.

FUJII, H., SATO, T., KANEKO, S., GOTOH, O., FUJII-KURIYAMA, Y., OSAWA, K., KATO, S. & HAMADA, H. 1997. Metabolic inactivation of retinoic acid by a novel P450 differentially expressed in developing mouse embryos. *EMBO J,* 16**,** 4163-73.

GABAY, L., LOWELL, S., RUBIN, L. L. & ANDERSON, D. J. 2003. Deregulation of dorsoventral patterning by FGF confers trilineage differentiation capacity on CNS stem cells in vitro. *Neuron,* 40**,** 485-99.

GAN, Q., YOSHIDA, T., MCDONALD, O. G. & OWENS, G. K. 2007. Concise review: Epigenetic mechanisms contribute to pluripotency and cell lineage determination of embryonic stem cells. *Stem Cells,* 25**,** 2-9.

GARC A-GONZ LEZ, D., CLEMENTE, D., COELHO, M., ESTEBAN, P. F., SOUSSI-YANICOSTAS, N. & F., D. C. 2010. Dynamic roles of FGF-2 and Anosmin-1 in the migration of neuronal precursors from the subventricular zone during pre- and postnatal development. *Experimental Neurology,* 222**,** 285-295.

GAVALAS, A. 2002. ArRAnging the hindbrain. *Trends in Neurosciences,* 25**,** 61-4.

GENETHLIOU, N., PANAYIOTOU, E., PANAYI, H., ORFORD, M., MEAN, R., LAPATHITIS, G. & MALAS, S. 2009. Spatially distinct functions of PAX6 and NKX2.2 during gliogenesis in the ventral spinal cord. *Biochem Biophys Res Commun,* 382**,** 69-73.

GERFEN, C. R. 1992. THE NEOSTRIATAL MOSAIC - MULTIPLE LEVELS OF COMPARTMENTAL ORGANIZATION. *Trends in Neurosciences,* 15**,** 133-139.

GIGUERE, V., LYN, S., YIP, P., SIU, C. H. & AMIN, S. 1990. Molecular cloning of cDNA encoding a second cellular retinoic acid-binding protein. *Proc Natl Acad Sci U S A,* 87**,** 6233-7.

GLASS, C. K. & ROSENFELD, M. G. 2000. The coregulator exchange in transcriptional functions of nuclear receptors. *Genes & Development,* 14**,** 121-141.

GLOVER, J. C., RENAUD, J. S. & RIJLI, F. M. 2006. Retinoic acid and hindbrain patterning. *Journal of Neurobiology,* 66**,** 705-725.

GOTZ, M. & BARDE, Y. A. 2005. Radial glial cells: Defined and major intermediates between embryonic, stern cells and CNS neurons. *Neuron,* 46**,** 369-372.

GOTZ, M. & HUTTNER, W. B. 2005. The cell biology of neurogenesis. *Nat Rev Mol Cell Biol,* 6**,** 777-88.

GOTZ, M., STOYKOVA, A. & GRUSS, P. 1998. Pax6 controls radial glia differentiation in the cerebral cortex. *Neuron,* 21**,** 1031-44.

GOULD, A., ITASAKI, N. & KRUMLAUF, R. 1998. Initiation of rhombomeric HoxbL4 expression requires induction by somites and a retinoid pathway. *Neuron,* 21**,** 39-51.

GRUNZ, H. & TACKE, L. 1989. Neural differentiation of Xenopus laevis ectoderm takes place after disaggregation and delayed reaggregation without inducer. *Cell Differ Dev,* 28**,** 211-7.

GULACSI, A. & ANDERSON, S. A. 2006. Shh maintains NkK2.1 in the MGE by a Gli3-independent mechanism. *Cerebral Cortex,* 16**,** I89-I95.

GULISANO, M., BROCCOLI, V., PARDINI, C. & BONCINELLI, E. 1996. Emx1 and Emx2 show different patterns of expression during proliferation and differentiation of the developing cerebral cortex in the mouse. *Eur J Neurosci,* 8**,** 1037-50.

GUTHRIE, S. 2007. Patterning and axon guidance of cranial motor neurons. *Nat Rev Neurosci,* 8**,** 859-71.

HAEGELE, L., INGOLD, B., NAUMANN, H., TABATABAI, G., LEDERMANN, B. & BRANDNER, S. 2003. Wnt signalling inhibits neural differentiation of embryonic stem cells by controlling bone morphogenetic protein expression. *Mol Cell Neurosci,* 24**,** 696-708.

HAO, J., HO, J. N., LEWIS, J. A., KARIM, K. A., DANIELS, R. N., GENTRY, P. R., HOPKINS, C. R., LINDSLEY, C. W. & HONG, C. C. 2010. In vivo structure-activity relationship study of dorsomorphin analogues identifies selective VEGF and BMP inhibitors. *ACS Chem Biol,* 5**,** 245-53.

HAO, J., LI, T. G., QI, X., ZHAO, D. F. & ZHAO, G. Q. 2006. WNT/beta-catenin pathway up-regulates Stat3 and converges on LIF to prevent differentiation of mouse embryonic stem cells. *Dev Biol,* 290**,** 81-91.

HARDIE, D. G. & CARLING, D. 1997. The AMP-activated protein kinase--fuel gauge of the mammalian cell? *Eur J Biochem,* 246**,** 259-73.

HARTFUSS, E., GALLI, R., HEINS, N. & GOTZ, M. 2001. Characterization of CNS precursor subtypes and radial glia. *Dev Biol,* 229**,** 15-30.

HAUBENSAK, W., ATTARDO, A., DENK, W. & HUTTNER, W. B. 2004. Neurons arise in the basal neuroepithelium of the early mammalian telencephalon: A major site of neurogenesis. *Proceedings of the National Academy of Sciences of the United States of America,* 101**,** 3196-3201.

HAYASHI, T., HIRSHMAN, M. F., KURTH, E. J., WINDER, W. W. & GOODYEAR, L. J. 1998. Evidence for 5' AMP-activated protein kinase mediation of the effect of muscle contraction on glucose transport. *Diabetes,* 47**,** 1369-73.

HEINS, N., MALATESTA, P., CECCONI, F., NAKAFUKU, M., TUCKER, K. L., HACK, M. A., CHAPOUTON, P., BARDE, Y. A. & GOTZ, M. 2002. Glial cells generate neurons: the role of the transcription factor Pax6. *Nature Neuroscience,* 5**,** 308-15.

HEMMATI-BRIVANLOU, A. & MELTON, D. 1997. Vertebrate neural induction. *Annu Rev Neurosci,* 20**,** 43-60.

HEMMATI-BRIVANLOU, A. & MELTON, D. A. 1994. Inhibition of activin receptor signaling promotes neuralization in Xenopus. *Cell,* 77**,** 273-81.

HERNANDEZ, R. E., PUTZKE, A. P., MYERS, J. P., MARGARETHA, L. & MOENS, C. B. 2007. Cyp26 enzymes generate the retinoic acid response pattern necessary for hindbrain development. *Development,* 134**,** 177-187.

HEVNER, R. F., DAZA, R. A., RUBENSTEIN, J. L., STUNNENBERG, H., OLAVARRIA, J. F. & ENGLUND, C. 2003a. Beyond laminar fate: toward a molecular classification of cortical projection/pyramidal neurons. *Dev Neurosci,* 25**,** 139-51.

HEVNER, R. F., NEOGI, T., ENGLUND, C., DAZA, R. A. M. & FINK, A. 2003b. Cajal-Retzius cells in the mouse: transcription factors, neurotransmitters, and birthdays suggest a pallial origin. *Developmental Brain Research,* 141**,** 39-53.

HEVNER, R. F., SHI, L., JUSTICE, N., HSUEH, Y., SHENG, M., SMIGA, S., BULFONE, A., GOFFINET, A. M., CAMPAGNONI, A. T. & RUBENSTEIN, J. L. 2001. Tbr1 regulates differentiation of the preplate and layer 6. *Neuron,* 29**,** 353-66.

HILL, R. E., FAVOR, J., HOGAN, B. L. M., TON, C. C. T., SAUNDERS, G. F., HANSON, I. M., PROSSER, J., JORDAN, T., HASTIE, N. D. & VANHEYNINGEN, V. 1991. MOUSE SMALL EYE RESULTS FROM MUTATIONS IN A PAIRED-LIKE HOMEOBOX-CONTAINING GENE. *Nature,* 354**,** 522-525.

HITOSHI, S., SEABERG, R. M., KOSCIK, C., ALEXSON, T., KUSUNOKI, S., KANAZAWA, I., TSUJI, S. & VAN DER KOOY, D. 2004. Primitive neural stem cells from the mammalian epiblast differentiate to definitive neural stem cells under the control of Notch signaling. *Genes Dev,* 18**,** 1806-11.

HONG, C. C. & YU, P. B. 2009. Applications of small molecule BMP inhibitors in physiology and disease. *Cytokine & Growth Factor Reviews,* 20**,** 409-418.

HSIEH-LI, H. M., WITTE, D. P., SZUCSIK, J. C., WEINSTEIN, M., LI, H. & POTTER, S. S. 1995. Gsh-2, a murine homeobox gene expressed in the developing brain. *Mech Dev,* 50**,** 177-86.

IMAYOSHI, I., SHIMOGORI, T., OHTSUKA, T. & KAGEYAMA, R. 2008. Hes genes and neurogenin regulate non-neural versus neural fate specification in the dorsal telencephalic midline. *Development,* 135**,** 2531-41.

INCARDONA, J. P., GAFFIELD, W., KAPUR, R. P. & ROELINK, H. 1998. The teratogenic Veratrum alkaloid cyclopamine inhibits sonic hedgehog signal transduction. *Development,* 125**,** 3553-62.

INGHAM, P. W. & MCMAHON, A. P. 2001. Hedgehog signaling in animal development: paradigms and principles. *Genes & Development,* 15**,** 3059-87.

IRIOKA, T., WATANABE, K., MIZUSAWA, H., MIZUSEKI, K. & SASAI, Y. 2005. Distinct effects of caudalizing factors on regional specification of embryonic stem cell-derived neural precursors. *Developmental Brain Research,* 154**,** 63-70.

JESSELL, T. M. 2000. Neuronal specification in the spinal cord: Inductive signals and transcriptional codes. *Nature Reviews Genetics,* 1**,** 20-29.

KAMACHI, Y., UCHIKAWA, M. & KONDOH, H. 2000. Pairing SOX off: with partners in the regulation of embryonic development. *Trends in Genetics,* 16**,** 182-187.

KAMEI, Y., KAWADA, T., KAZUKI, R. & SUGIMOTO, E. 1993. Retinoic acid receptor gamma 2 gene expression is up-regulated by retinoic acid in 3T3-L1 preadipocytes. *Biochem J,* 293 (Pt 3)**,** 807-12.

KANZLER, B., FOREMAN, R. K., LABOSKY, P. A. & MALLO, M. 2000. BMP signaling is essential for development of skeletogenic and neurogenic cranial neural crest. *Development,* 127**,** 1095-104.

KARUS, M., DENECKE, B., FFRENCH-CONSTANT, C., WIESE, S. & FAISSNER, A. 2011. The extracellular matrix molecule tenascin C modulates expression levels and territories of key patterning genes during spinal cord astrocyte specification. *Development,* 138**,** 5321-31.

KAWASAKI, H., MIZUSEKI, K., NISHIKAWA, S., KANEKO, S., KUWANA, Y., NAKANISHI, S., NISHIKAWA, S. I. & SASAI, Y. 2000. Induction of midbrain dopaminergic neurons from ES cells by stromal cell-derived inducing activity. *Neuron,* 28**,** 31-40.

KIM, D. S., LEE, J. S., LEEM, J. W., HUH, Y. J., KIM, J. Y., KIM, H. S., PARK, I. H., DALEY, G. Q., HWANG, D. Y. & DW., K. 2010. Robust enhancement of neural differentiation from human ES and iPS cells regardless of their innate difference in differentiation propensity. *Stem Cells Reviews,* 6**,** 270-281.

KIM, M., HABIBA, A., DOHERTY, J. M., MILLS, J. C., MERCER, R. W. & HUETTNER, J. E. 2009. Regulation of mouse embryonic stem cell neural differentiation by retinoic acid. *Developmental Biology,* 328**,** 456-471.

KIM, Y. M., KIM, M. Y., KIM, H. J., ROH, G. S., KO, G. H., SEO, H. G., LEE, J. H. & CHANG, K. C. 2011. Compound C independent of AMPK inhibits ICAM-1 and VCAM-1 expression in inflammatory stimulants-activated endothelial cells in vitro and in vivo. *Atherosclerosis,* 219**,** 57-64.

KINDER, S. J., TSANG, T. E., WAKAMIYA, M., SASAKI, H., BEHRINGER, R. R., NAGY, A. & TAM, P. P. L. 2001. The organizer of the mouse gastrula is composed of a dynamic population of progenitor cells for the axial mesoderm. *Development,* 128**,** 3623-3634.

KLEINSMITH, L. J. & PIERCE, G. B., JR. 1964. MULTIPOTENTIALITY OF SINGLE EMBRYONAL CARCINOMA CELLS. *Cancer Res,* 24**,** 1544-51.

KNECHT, A. K. & BRONNER-FRASER, M. 2002. Induction of the neural crest: A multigene process. *Nature Reviews Genetics,* 3**,** 453-461.

KOHTZ, J. D., BAKER, D. P., CORTE, G. & FISHELL, G. 1998. Regionalization within the mammalian telencephalon is mediated by changes in responsiveness to Sonic Hedgehog. *Development,* 125**,** 5079-5089.

KOPP, J. L., ORMSBEE, B. D., DESLER, M. & RIZZINO, A. 2008. Small increases in the level of Sox2 trigger the differentiation of mouse embryonic stem cells. *Stem Cells,* 26**,** 903-11.

KUDO, T.-A., KANETAKA, H., MIZUNO, K., RYU, Y., MIYAMOTO, Y., NUNOME, S., ZHANG, Y., KANO, M., SHIMIZU, Y. & HAYASHI, H. 2011. Dorsomorphin stimulates neurite outgrowth in PC12 cells via activation of a protein kinase A-dependent MEK-ERK1/2 signaling pathway. *Genes to Cells,* 16**,** 1121-1132.

KUNATH, T., SABA-EL-LEIL, M. K., ALMOUSAILLEAKH, M., WRAY, J., MELOCHE, S. & SMITH, A. 2007. FGF stimulation of the Erk1/2 signalling cascade triggers transition of pluripotent embryonic stem cells from self-renewal to lineage commitment. *Development,* 134**,** 2895-902.

KUROKAWA, R., SODERSTROM, M., HORLEIN, A., HALACHMI, S., BROWN, M., ROSENFELD, M. G. & GLASS, C. K. 1995. POLARITY-SPECIFIC ACTIVITIES OF RETINOIC ACID RECEPTORS DETERMINED BY A CO-REPRESSOR. *Nature,* 377**,** 451-454.

LAFLAMME, M. A., CHEN, K. Y., NAUMOVA, A. V., MUSKHELI, V., FUGATE, J. A., DUPRAS, S. K., REINECKE, H., XU, C., HASSANIPOUR, M., POLICE, S., O'SULLIVAN, C., COLLINS, L., CHEN, Y., MINAMI, E., GILL, E. A., UENO, S., YUAN, C., GOLD, J. & MURRY, C. E. 2007. Cardiomyocytes derived from human embryonic stem cells in pro-survival factors enhance function of infarcted rat hearts. *Nat Biotechnol,* 25**,** 1015-24.

LAI, E. C. 2004. Notch signaling: control of cell communication and cell fate. *Development,* 131**,** 965-973.

LAI, K., KASPAR, B. K., GAGE, F. H. & SCHAFFER, D. V. 2003. Sonic hedgehog regulates adult neural progenitor proliferation in vitro and in vivo. *Nat Neurosci,* 6**,** 21-7.

LAMB, T. M., KNECHT, A. K., SMITH, W. C., STACHEL, S. E., ECONOMIDES, A. N., STAHL, N., YANCOPOLOUS, G. D. & HARLAND, R. M. 1993. Neural Induction by the Secreted Polypeptide Noggin. *Science,* 262**,** 713-718.

LANDER, A. D. 2007. Morpheus unbound: reimagining the morphogen gradient. *Cell,* 128**,** 245-56.

LANG, R. J., HAYNES, J. M., KELLY, J., JOHNSON, J., GREENHALGH, J., O'BRIEN, C., MULHOLLAND, E. M., BAKER, L., MUNSIE, M. & CW., P. 2004. Electrical and neurotransmitter activity of mature neurons derived from mouse embryonic stem cells by Sox-1 lineage selection and directed differentiation. *European Journal of Neuroscience,* 20**,** 3209-3221.

LAWRENCE, P. A. & STRUHL, G. 1996. Morphogens, compartments, and pattern: lessons from drosophila? *Cell,* 85**,** 951-61.

LEE, J., PLATT, K. A., CENSULLO, P. & ALTABA, A. R. I. 1997. Gli1 is a target of Sonic hedgehog that induces ventral neural tube development. *Development,* 124**,** 2537-2552.

LEE, S. H., LUMELSKY, N., STUDER, L., AUERBACH, J. M. & MCKAY, R. D. 2000. Efficient generation of midbrain and hindbrain neurons from mouse embryonic stem cells. *Nature Biotechnology,* 18**,** 675-679.

LENDAHL, U., ZIMMERMAN, L. B. & MCKAY, R. D. G. 1990. CNS STEM-CELLS EXPRESS A NEW CLASS OF INTERMEDIATE FILAMENT PROTEIN. *Cell,* 60**,** 585-595.

LEROY, P., KRUST, A., ZELENT, A., MENDELSOHN, C., GARNIER, J. M., KASTNER, P., DIERICH, A. & CHAMBON, P. 1991. Multiple isoforms of the mouse retinoic acid receptor alpha are generated by alternative splicing and differential induction by retinoic acid. *EMBO J,* 10**,** 59-69.

LEVINE, A. J. & BRIVANLOU, A. H. 2007. Proposal of a model of mammalian neural induction. *Developmental Biology,* 308**,** 247-256.

LI, H., WAGNER, E., MCCAFFERY, P., SMITH, D., ANDREADIS, A. & DRAGER, U. C. 2000. A retinoic acid synthesizing enzyme in ventral retina and telencephalon of the embryonic mouse. *Mechanisms of Development,* 95**,** 283-289.

LIAO, W. L., TSAI, H. C., WANG, H. F., CHANG, J., LU, K. M., WU, H. L., LEE, Y. C., TSAI, T. F., TAKAHASHI, H., WAGNER, M., GHYSELINCK, N. B., CHAMBON, P. & LIU, F. C. 2008. Modular patterning of structure and function of the striatum by retinoid receptor signaling. *Proceedings of the National Academy of Sciences of the United States of America,* 105**,** 6765-70.

LIAO, W. L., TSAI, H. C., WU, C. Y. & LIU, F. C. 2005a. Differential expression of RAR beta isoforms in the mouse striatum during development: A gradient of RAR beta 2 expression along the rostrocaudal axis. *Developmental Dynamics,* 233**,** 584-594.

LIAO, W. L., WANG, H. F., TSAI, H. C., CHAMBON, P., WAGNER, M., KAKIZUKA, A. K. & LIU, F. C. 2005b. Retinoid signaling competence and RAR beta-mediated gene regulation in the developing mammalian telencephalon. *Developmental Dynamics,* 232**,** 887-900.

LOH, K. M. & LIM, B. 2011. A precarious balance: pluripotency factors as lineage specifiers. *Cell Stem Cell,* 8**,** 363-9.

LOMBROSO, P. J., MURDOCH, G. & LERNER, M. 1991. Molecular characterization of a protein-tyrosine-phosphatase enriched in striatum. *Proc Natl Acad Sci U S A,* 88**,** 7242-6.

LONG, J. E., SWAN, C., LIANG, W. S., COBOS, I., POTTER, G. B. & RUBENSTEIN, J. L. R. 2009. Dlx1&2 and Mash1 Transcription Factors Control Striatal Patterning

and Differentiation Through Parallel and Overlapping Pathways. *Journal of Comparative Neurology,* 512**,** 556-572.

LOWELL, S., BENCHOUA, A., HEAVEY, B. & SMITH, A. G. 2006. Notch promotes neural lineage entry by pluripotent embryonic stem cells. *Plos Biology,* 4**,** 805-818.

LUO, T., WAGNER, E., GRUN, F. & DRAGER, U. C. 2004. Retinoic acid signaling in the brain marks formation of optic projections, maturation of the dorsal telencephalon, and function of limbic sites. *J Comp Neurol,* 470**,** 297-316.

MACHOLD, R., HAYASHI, S., RUTLIN, M., MUZUMDAR, M. D., NERY, S., CORBIN, J. G., GRITLI-LINDE, A., DELLOVADE, T., PORTER, J. A., RUBIN, L. L., DUDEK, H., MCMAHON, A. P. & FISHELL, G. 2003. Sonic hedgehog is required for progenitor cell maintenance in telencephalic stem cell niches. *Neuron,* 39**,** 937-950.

MACLEAN, G., ABU-ABED, S., DOLLE, P., TAHAYATO, A., CHAMBON, P. & PETKOVICH, M. 2001. Cloning of a novel retinoic-acid metabolizing cytochrome P450, Cyp26B1, and comparative expression analysis with Cyp26A1 during early murine development. *Mechanisms of Development,* 107**,** 195-201.

MADEN, M. 2002. Retinoid signalling in the development of the central nervous system. *Nat Rev Neurosci,* 3**,** 843-53.

MADEN, M. 2006. Retinoids and spinal cord development. *J Neurobiol,* 66**,** 726-38.

MAJUMDER, A., BANERJEE, S., HARRILL, J. A., MACHACEK, D. W., MOHAMAD, O., BACANAMWO, M., MUNDY, W. R., WEI, L., DHARA, S. K. & STICE, S. L. 2012. Neurotrophic effects of leukemia inhibitory factor on neural cells derived from human embryonic stem cells. *Stem Cells,* 30**,** 2387-99.

MALATESTA, P., HACK, M. A., HARTFUSS, E., KETTENMANN, H., KLINKERT, W., KIRCHHOFF, F. & GOTZ, M. 2003. Neuronal or glial progeny: Regional differences in radial glia fate. *Neuron,* 37**,** 751-764.

MANZANARES, M., CORDES, S., ARIZA-MCNAUGHTON, L., SADL, V., MARUTHAINAR, K., BARSH, G. & KRUMLAUF, R. 1999. Conserved and distinct roles of kreisler in regulation of the paralogous Hoxa3 and Hoxb3 genes. *Development,* 126**,** 759-769.

MARIGO, V. & TABIN, C. J. 1996. Regulation of patched by sonic hedgehog in the developing neural tube. *Proc Natl Acad Sci U S A,* 93**,** 9346-51.

MARSHALL, H., NONCHEV, S., SHAM, M. H., MUCHAMORE, I., LUMSDEN, A. & KRUMLAUF, R. 1992. Retinoic acid alters hindbrain Hox code and induces transformation of rhombomeres 2/3 into a 4/5 identity. *Nature,* 360**,** 737-41.

MARTI, E., BUMCROT, D. A., TAKADA, R. & MCMAHON, A. P. 1995a. REQUIREMENT OF 19K FORM OF SONIC HEDGEHOG FOR INDUCTION OF DISTINCT VENTRAL CELL-TYPES IN CNS EXPLANTS. *Nature,* 375**,** 322-325.

MARTI, E., TAKADA, R., BUMCROT, D. A., SASAKI, H. & MCMAHON, A. P. 1995b. DISTRIBUTION OF SONIC-HEDGEHOG PEPTIDES IN THE DEVELOPING CHICK AND MOUSE EMBRYO. *Development,* 121**,** 2537-2547.

MARTIN, G. R. 1981. Isolation of a pluripotent cell line from early mouse embryos cultured in medium conditioned by teratocarcinoma stem cells. *Proc Natl Acad Sci U S A,* 78**,** 7634-8.

MARTIN, G. R. & EVANS, M. J. 1975. Differentiation of clonal lines of teratocarcinoma cells: formation of embryoid bodies in vitro. *Proc Natl Acad Sci U S A,* 72**,** 1441-5.

MASUI, S., NAKATAKE, Y., TOYOOKA, Y., SHIMOSATO, D., YAGI, R., TAKAHASHI, K., OKOCHI, H., OKUDA, A., MATOBA, R., SHAROV, A. A., KO, M. S. H. & NIWA, H. 2007. Pluripotency governed by Sox2 via regulation of Oct3/4 expression in mouse embryonic stem cells. *Nature Cell Biology,* 9**,** 625-U26.

MATSUDA, T., NAKAMURA, T., NAKAO, K., ARAI, T., KATSUKI, M., HEIKE, T. & YOKOTA, T. 1999. STAT3 activation is sufficient to maintain an undifferentiated state of mouse embryonic stem cells. *EMBO J,* 18**,** 4261-9.

MATSUNAGA, E., ARAKI, I. & NAKAMURA, H. 2000. Pax6 defines the di-mesencephalic boundary by repressing En1 and Pax2. *Development,* 127**,** 2357-65.

MAVES, L. & KIMMEL, C. B. 2005. Dynamic and sequential patterning of the zebrafish posterior hindbrain by retinoic acid. *Dev Biol,* 285**,** 593-605.

MAYE, P., BECKER, S., KASAMEYER, E., BYRD, N. & GRABEL, L. 2000. Indian hedgehog signaling in extraembryonic endoderm and ectoderm differentiation in ES embryoid bodies. *Mechanisms of Development,* 94**,** 117-132.

MCCULLOCH, E. A. & TILL, J. E. 2005. Perspectives on the properties of stem cells. *Nat Med,* 11**,** 1026-8.

MCMAHON, J. A., TAKADA, S., ZIMMERMAN, L. B., FAN, C. M., HARLAND, R. M. & MCMAHON, A. P. 1998. Noggin-mediated antagonism of BMP signaling is required for growth and patterning of the neural tube and somite. *Genes Dev,* 12**,** 1438-52.

MELOCHE, S. & POUYSSEGUR, J. 2007. The ERK1/2 mitogen-activated protein kinase pathway as a master regulator of the G1- to S-phase transition. *Oncogene,* 26**,** 3227-3239.

MENO, C., ITO, Y., SAIJOH, Y., MATSUDA, Y., TASHIRO, K., KUHARA, S. & HAMADA, H. 1997. Two closely-related left-right asymmetrically expressed genes, lefty-1 and lefty-2: their distinct expression domains, chromosomal linkage and direct neuralizing activity in Xenopus embryos. *Genes Cells,* 2**,** 513-24.

MERRILL, G. F., KURTH, E. J., HARDIE, D. G. & WINDER, W. W. 1997. AICA riboside increases AMP-activated protein kinase, fatty acid oxidation, and glucose uptake in rat muscle. *Am J Physiol,* 273**,** E1107-12.

MIYAZONO, K. & MIYAZAWA, K. 2002. Id: a target of BMP signaling. *Sci STKE,* 2002**,** pe40.

MIZUGUCHI, R., SUGIMORI, M., TAKEBAYASHI, H., KOSAKO, H., NAGAO, M., YOSHIDA, S., NABESHIMA, Y., SHIMAMURA, K. & NAKAFUKU, M. 2001. Combinatorial roles of olig2 and neurogenin2 in the coordinated induction of pan-neuronal and subtype-specific properties of motoneurons. *Neuron,* 31**,** 757-71.

MOHAMMADI, M., FROUM, S., HAMBY, J. M., SCHROEDER, M. C., PANEK, R. L., LU, G. H., ELISEENKOVA, A. V., GREEN, D., SCHLESSINGER, J. & HUBBARD, S. R. 1998. Crystal structure of an angiogenesis inhibitor bound to the FGF receptor tyrosine kinase domain. *EMBO J,* 17**,** 5896-904.

MOHAMMADI, M., MCMAHON, G., SUN, L., TANG, C., HIRTH, P., YEH, B. K., HUBBARD, S. R. & SCHLESSINGER, J. 1997. Structures of the tyrosine kinase domain of fibroblast growth factor receptor in complex with inhibitors. *Science,* 276**,** 955-960.

MOLOTKOVA, N., MOLOTKOV, A. & DUESTER, G. 2007. Role of retinoic acid during forebrain development begins late when Raldh3 generates retinoic acid in the ventral subventricular zone. *Dev Biol,* 303**,** 601-10.

MORSHEAD, C. M., BENVENISTE, P., ISCOVE, N. N. & VAN DER KOOY, D. 2002. Hematopoietic competence is a rare property of neural stem cells that may depend on genetic and epigenetic alterations. *Nature Medicine,* 8**,** 268-273.

MUHR, J., ANDERSSON, E., PERSSON, M., JESSELL, T. M. & ERICSON, J. 2001. Groucho-mediated transcriptional repression establishes progenitor cell pattern and neuronal fate in the ventral neural tube. *Cell,* 104**,** 861-873.

NAKAMURA, T., ARAI, T., TAKAGI, M., SAWADA, T., MATSUDA, T., YOKOTA, T. & HEIKE, T. 1998. A selective switch-on system for self-renewal of embryonic stem cells using chimeric cytokine receptors. *Biochemical and Biophysical Research Communications,* 248**,** 22-27.

NIEDERREITHER, K., SUBBARAYAN, V., DOLLE, P. & CHAMBON, P. 1999. Embryonic retinoic acid synthesis is essential for early mouse post-implantation development. *Nature Genetics,* 21**,** 444-448.

NIEDERREITHER, K., VERMOT, J., SCHUHBAUR, B., CHAMBON, P. & DOLLE, P. 2000. Retinoic acid synthesis and hindbrain patterning in the mouse embryo. *Development,* 127**,** 75-85.

NIETO, M., MONUKI, E. S., TANG, H., IMITOLA, J., HAUBST, N., KHOURY, S. J., CUNNINGHAM, J., GOTZ, M. & WALSH, C. A. 2004. Expression of Cux-1 and

Cux-2 in the subventricular zone and upper layers II-IV of the cerebral cortex. *J Comp Neurol,* 479**,** 168-80.

NIETO, M., SCHUURMANS, C., BRITZ, O. & GUILLEMOT, F. 2001. Neural bHLH genes control the neuronal versus glial fate decision in cortical progenitors. *Neuron,* 29**,** 401-413.

NIETO, M. A. 2001. The early steps of neural crest development. *Mechanisms of Development,* 105**,** 27-35.

NIWA, H. 2007. How is pluripotency determined and maintained? *Development,* 134**,** 635-646.

NIWA, H., BURDON, T., CHAMBERS, I. & SMITH, A. 1998. Self-renewal of pluripotent embryonic stem cells is mediated via activation of STAT3. *Genes & Development,* 12**,** 2048-2060.

NIWA, H., MIYAZAKI, J. & SMITH, A. G. 2000. Quantitative expression of Oct-3/4 defines differentiation, dedifferentiation or self-renewal of ES cells. *Nature Genetics,* 24**,** 372-376.

NIWA, H., OGAWA, K., SHIMOSATO, D. & ADACHI, K. 2009. A parallel circuit of LIF signalling pathways maintains pluripotency of mouse ES cells. *Nature,* 460**,** 118-22.

NOCTOR, S. C., MARTINEZ-CERDENO, V., IVIC, L. & KRIEGSTEIN, A. R. 2004. Cortical neurons arise in symmetric and asymmetric division zones and migrate through specific phases. *Nature Neuroscience,* 7**,** 136-144.

NONCHEV, S., VESQUE, C., MACONOCHIE, M., SEITANIDOU, T., ARIZAMCNAUGHTON, L., FRAIN, M., MARSHALL, H., SHAM, M. H., KRUMLAUF, R. & CHARNAY, P. 1996. Segmental expression of Hoxa-2 in the hindbrain is directly regulated by Krox-20. *Development,* 122**,** 543-554.

NORDSTR M, U., MAIER, E., JESSELL, T. M. & EDLUND, T. 2006. An early role for WNT signaling in specifying neural patterns of Cdx and Hox gene expression and motor neuron subtype identity. *Plos Biology,* 4**,** 252.

NOVITCH, B. G., CHEN, A. I. & JESSELL, T. M. 2001. Coordinate regulation of motor neuron subtype identity and pan-neuronal properties by the bHLH repressor Olig2. *Neuron,* 31**,** 773-89.

OGONY, J. W., MALAHIAS, E., VADIGEPALLI, R. & ANNI, H. 2013. Ethanol Alters the Balance of Sox2, Oct4 and Nanog Expression in Distinct Subpopulations during Differentiation of Embryonic Stem Cells. *Stem Cells and Development*.

OKABE, S., FORSBERGNILSSON, K., SPIRO, A. C., SEGAL, M. & MCKAY, R. D. G. 1996. Development of neuronal precursor cells and functional postmitotic neurons from embryonic stem cells in vitro. *Mechanisms of Development,* 59**,** 89-102.

OKADA, Y., MATSUMOTO, A., SHIMAZAKI, T., ENOKI, R., KOIZUMI, A., ISHII, S., ITOYAMA, Y., SOBUE, G. & OKANO, H. 2008. Spatiotemporal Recapitulation of Central Nervous System Development by Murine Embryonic Stem Cell-Derived Neural Stem/Progenitor Cells. *Stem Cells,* 26**,** 3086-3098.

OKADA, Y., SHIMAZAKI, T., SOBUE, G. & OKANO, H. 2004. Retinoic-acid-concentration-dependent acquisition of neural cell identity during in vitro differentiation of mouse embryonic stem cells. *Developmental Biology,* 275**,** 124-142.

OOSTERVEEN, T., KURDIJA, S., ENSTERO, M., UHDE, C. W., BERGSLAND, M., SANDBERG, M., SANDBERG, R., MUHR, J. & ERICSON, J. 2013. SoxB1-driven transcriptional network underlies neural-specific interpretation of morphogen signals. *Proc Natl Acad Sci U S A*.

OTSUKI, S., HANSON, S. R., MIYAKI, S., GROGAN, S. P., KINOSHITA, M., ASAHARA, H., WONG, C. H. & LOTZ, M. K. 2010. Extracellular sulfatases support cartilage homeostasis by regulating BMP and FGF signaling pathways. *Proc Natl Acad Sci U S A,* 107**,** 10202-7.

PALING, N. R., WHEADON, H., BONE, H. K. & WELHAM, M. J. 2004. Regulation of embryonic stem cell self-renewal by phosphoinositide 3-kinase-dependent signaling. *J Biol Chem,* 279**,** 48063-70.

PAN, Y., BAI, C. B., JOYNER, A. L. & WANG, B. 2006. Sonic hedgehog signaling regulates Gli2 transcriptional activity by suppressing its processing and degradation. *Molecular and Cellular Biology,* 26**,** 3365-3377.

PAPAIOANNOU, V. E., GARDNER, R. L., MCBURNEY, M. W., BABINET, C. & EVANS, M. J. 1978. Participation of cultured teratocarcinoma cells in mouse embryogenesis. *J Embryol Exp Morphol,* 44**,** 93-104.

PARMAR, M. & LI, M. 2007. Early specification of dopaminergic phenotype during ES cell differentiation. *BMC Developmental Biology,* 7**,** 86.

PARNAVELAS, J. G. 2000. The origin and migration of cortical neurones: new vistas. *Trends Neurosci,* 23**,** 126-31.

PASCHAKI, M., SCHNEIDER, C., RHINN, M., THIBAULT-CARPENTIER, C., DEMBELE, D., NIEDERREITHER, K. & DOLLE, P. 2013. Transcriptomic analysis of murine embryos lacking endogenous retinoic Acid signaling. *PLoS One,* 8**,** e62274.

PEVNY, L. H., SOCKANATHAN, S., PLACZEK, M. & LOVELL-BADGE, R. 1998. A role for SOX1 in neural determination. *Development,* 125**,** 1967-1978.

PIERANI, A., BRENNER-MORTON, S., CHIANG, C. & JESSELL, T. M. 1999. A sonic hedgehog-independent, retinoid-activated pathway of neurogenesis in the ventral spinal cord. *Cell,* 97**,** 903-15.

PLACHTA, N., BIBEL, M., TUCKER, K. L. & BARDE, Y. A. 2004. Developmental potential of defined neural progenitors derived from mouse embryonic stem cells. *Development,* 131**,** 5449-56.

PORTEUS, M. H., BULFONE, A., LIU, J. K., PUELLES, L., LO, L. C. & RUBENSTEIN, J. L. 1994. DLX-2, MASH-1, and MAP-2 expression and bromodeoxyuridine incorporation define molecularly distinct cell populations in the embryonic mouse forebrain. *J Neurosci,* 14**,** 6370-83.

PRECIOUS, S. V. 2009. *Directed differentiation of mouse ES cells for transplantation in Huntington's disease* PhD thesis, Cardiff University.

PRICE, D. J., JARMAN, A. P., MASON, J. O. & KIND, P. C. 2011. *Building Brains: An Introduction to Neural Development,* Singapore, Wiley-Blackwell.

PUELLES, L., KUWANA, E., PUELLES, E. & RUBENSTEIN, J. L. 1999. Comparison of the mammalian and avian telencephalon from the perspective of gene expression data. *European Journal of morphology,* 37**,** 139-150.

QIAN, X. M., SHEN, Q., GODERIE, S. K., HE, W. L., CAPELA, A., DAVIS, A. A. & TEMPLE, S. 2000. Timing of CNS cell generation: A programmed sequence of neuron and glial cell production from isolated murine cortical stem cells. *Neuron,* 28**,** 69-80.

QUINN, J. C., MOLINEK, M., MARTYNOGA, B. S., ZAKI, P. A., FAEDO, A., BULFONE, A., HEVNER, R. F., WEST, J. D. & PRICE, D. J. 2007. Pax6 controls cerebral cortical cell number by regulating exit from the cell cycle and specifies cortical cell identity by a cell autonomous mechanism. *Dev Biol,* 302**,** 50-65.

RAJAII, F., BITZER, Z. T., XU, Q. & SOCKANATHAN, S. 2008. Expression of the dominant negative retinoid receptor, RAR403, alters telencephalic progenitor proliferation, survival, and cell fate specification. *Dev Biol,* 316**,** 371-82.

RALLU, M., MACHOLD, R., GAIANO, N., CORBIN, J. G., MCMAHON, A. P. & FISHELL, G. 2002. Dorsoventral patterning is established in the telencephalon of mutants lacking both Gli3 and hedgehog signaling. *Development,* 129**,** 4963-4974.

RATTNER, A., HSIEH, J. C., SMALLWOOD, P. M., GILBERT, D. J., COPELAND, N. G., JENKINS, N. A. & NATHANS, J. 1997. A family of secreted proteins contains homology to the cysteine-rich ligand-binding domain of frizzled receptors. *Proc Natl Acad Sci U S A,* 94**,** 2859-63.

REIJNTJES, S., BLENTIC, A., GALE, E. & MADEN, M. 2005. The control of morphogen signalling: regulation of the synthesis and catabolism of retinoic acid in the developing embryo. *Dev Biol,* 285**,** 224-37.

REVERSADE, B., KURODA, H., LEE, H., MAYS, A. & DE ROBERTIS, E. M. 2005. Depletion of Bmp2, Bmp4, Bmp7 and Spemann organizer signals induces massive brain formation in Xenopus embryos. *Development,* 132**,** 3381-92.

REYA, T. & CLEVERS, H. 2005. Wnt signalling in stem cells and cancer. *Nature,* 434**,** 843-850.

RHINN, M. & DOLLE, P. 2012. Retinoic acid signalling during development. *Development,* 139**,** 843-58.

RIBES, V., FRAULOB, V., PETKOVICH, M. & DOLLE, P. 2007. The oxidizing enzyme CYP26a1 tightly regulates the availability of retinoic acid in the gastrulating mouse embryo to ensure proper head development and vasculogenesis. *Dev Dyn,* 236**,** 644-53.

RIBES, V., LE ROUX, I., RHINN, M., SCHUHBAUR, B. & DOLLE, P. 2009. Early mouse caudal development relies on crosstalk between retinoic acid, Shh and Fgf signalling pathways. *Development,* 136**,** 665-76.

RICHARDSON, K. 2011. *Analysis of cell surface markers within immature bovine articular cartilage.* PhD thesis, Cardiff University.

ROBBINS, D. J., NYBAKKEN, K. E., KOBAYASHI, R., SISSON, J. C., BISHOP, J. M. & THEROND, P. P. 1997. Hedgehog elicits signal transduction by means of a large complex containing the kinesin-related protein costal2. *Cell,* 90**,** 225-34.

ROOSE, J., MOLENAAR, M., PETERSON, J., HURENKAMP, J., BRANTJES, H., MOERER, P., VAN DE WETERING, M., DESTREE, O. & CLEVERS, H. 1998. The Xenopus Wnt effector XTcf-3 interacts with Groucho-related transcriptional repressors. *Nature,* 395**,** 608-12.

ROSSANT, J. & MCBURNEY, M. W. 1982. The developmental potential of a euploid male teratocarcinoma cell line after blastocyst injection. *J Embryol Exp Morphol,* 70**,** 99-112.

RUSSELL, R. R., 3RD, LI, J., COVEN, D. L., PYPAERT, M., ZECHNER, C., PALMERI, M., GIORDANO, F. J., MU, J., BIRNBAUM, M. J. & YOUNG, L. H. 2004. AMP-activated protein kinase mediates ischemic glucose uptake and prevents postischemic cardiac dysfunction, apoptosis, and injury. *J Clin Invest,* 114**,** 495-503.

SAKAI, Y., MENO, C., FUJII, H., NISHINO, J., SHIRATORI, H., SAIJOH, Y., ROSSANT, J. & HAMADA, H. 2001. The retinoic acid-inactivating enzyme CYP26 is essential for establishing an uneven distribution of retinoic acid along the anterio-posterior axis within the mouse embryo. *Genes Dev,* 15**,** 213-25.

SANDER, M., PAYDAR, S., ERICSON, J., BRISCOE, J., BERBER, E., GERMAN, M., JESSELL, T. M. & RUBENSTEIN, J. L. R. 2000. Ventral neural patterning by Nkx homeobox genes: Nkx6.1 controls somatic motor neuron and ventral interneuron fates. *Genes & Development,* 14**,** 2134-2139.

SASAI, Y. & DEROBERTIS, E. M. 1997. Ectodermal patterning in vertebrate embryos *Developmental Biology,* 134**,** 263-266.

SASAI, Y., LU, B., STEINBEISSER, H., GEISSERT, D., GONT, L. K. & DEROBERTIS, E. M. 1994. XENOPUS CHORDIN - A NOVEL DORSALIZING FACTOR-ACTIVATED BY ORGANIZER-SPECIFIC HOMEOBOX GENES. *Cell,* 79**,** 779-790.

SASAKI, H., NISHIZAKI, Y., HUI, C., NAKAFUKU, M. & KONDOH, H. 1999. Regulation of Gli2 and Gli3 activities by an amino-terminal repression domain: implication of Gli2 and Gli3 as primary mediators of Shh signaling. *Development,* 126**,** 3915-24.

SATO, N., MEIJER, L., SKALTSOUNIS, L., GREENGARD, P. & BRIVANLOU, A. H. 2004. Maintenance of pluripotency in human and mouse embryonic stem cells through activation of Wnt signaling by a pharmacological GSK-3-specific inhibitor. *Nature Medicine,* 10**,** 55-63.

SATO, T. & JOYNER, A. L. 2009. The duration of Fgf8 isthmic organizer expression is key to patterning different tectal-isthmo-cerebellum structures. *Development,* 136**,** 3617-3626.

SCHUURMANS, C. & GUILLEMOT, F. 2002. Molecular mechanisms underlying cell fate specification in the developing telencephalon. *Current Opinion in Neurobiology,* 12**,** 26-34.

SHEN, Q., WANG, Y., DIMOS, J. T., FASANO, C. A., PHOENIX, T. N., LEMISCHKA, I. R., IVANOVA, N. B., STIFANI, S., MORRISEY, E. E. & TEMPLE, S. 2006. The timing of cortical neurogenesis is encoded within lineages of individual progenitor cells. *Nat Neurosci,* 9**,** 743-51.

SHIBATA, T., YAMADA, K., WATANABE, M., IKENAKA, K., WADA, K., TANAKA, K. & INOUE, Y. 1997. Glutamate transporter GLAST is expressed in the radial glia-astrocyte lineage of developing mouse spinal cord. *J Neurosci,* 17**,** 9212-9.

SILVA, J. & SMITH, A. 2008. Capturing pluripotency. *Cell,* 132**,** 532-536.

SIMEONE, A. 2000. Positioning the isthmic organizer where Otx2 and Gbx2meet. *Trends in Genetics,* 16**,** 237-240.

SIMEONE, A., ACAMPORA, D., GULISANO, M., STORNAIUOLO, A. & BONCINELLI, E. 1992. Nested expression domains of four homeobox genes in developing rostral brain. *Nature,* 358**,** 687-90.

SIMEONE, A., AVANTAGGIATO, V., MORONI, M. C., MAVILIO, F., ARRA, C., COTELLI, F., NIGRO, V. & ACAMPORA, D. 1995. RETINOIC ACID INDUCES STAGE-SPECIFIC ANTERO-POSTERIOR TRANSFORMATION OF ROSTRAL CENTRAL-NERVOUS-SYSTEM. *Mechanisms of Development,* 51**,** 83-98.

SINHA, S. & CHEN, J. K. 2006. Purmorphamine activates the Hedgehog pathway by targeting Smoothened. *Nat Chem Biol.,* 2**,** 29-30.

SIRBU, I. O., GRESH, L., BARRA, J. & DUESTER, G. 2005. Shifting boundaries of retinoic acid activity control hindbrain segmental gene expression. *Development,* 132**,** 2611-2622.

SISSON, J. C., HO, K. S., SUYAMA, K. & SCOTT, M. P. 1997. Costal2, a novel kinesin-related protein in the Hedgehog signaling pathway. *Cell,* 90**,** 235-45.

SMITH, A. G. 2001. Embryo-derived stem cells: Of mice and men. *Annual Review of Cell and Developmental Biology,* 17**,** 435-462.

SMITH, A. G., HEATH, J. K., DONALDSON, D. D., WONG, G. G., MOREAU, J., STAHL, M. & ROGERS, D. 1988. Inhibition of pluripotential embryonic stem cell differentiation by purified polypeptides. *Nature,* 336**,** 688-90.

SMITH, A. G. & HOOPER, M. L. 1987. Buffalo rat liver cells produce a diffusible activity which inhibits the differentiation of murine embryonal carcinoma and embryonic stem cells. *Dev Biol,* 121**,** 1-9.

SMITH, S. T. & JAYNES, J. B. 1996. A conserved region of engrailed, shared among all en-, gsc-, Nk1-, Nk2- and msh-class homeoproteins, mediates active transcriptional repression in vivo. *Development,* 122**,** 3141-50.

SMITH, W. C. & HARLAND, R. M. 1992. EXPRESSION CLONING OF NOGGIN, A NEW DORSALIZING FACTOR LOCALIZED TO THE SPEMANN ORGANIZER IN XENOPUS EMBRYOS. *Cell,* 70**,** 829-840.

SMITH, W. C., KNECHT, A. K., WU, M. & HARLAND, R. M. 1993. Secreted noggin protein mimics the spemann organizer dorsalzing Xenopus mesoderm. *Nature,* 361**,** 547-549.

SMITH, W. C., NAKSHATRI, H., LEROY, P., REES, J. & CHAMBON, P. 1991. A retinoic acid response element is present in the mouse cellular retinol binding protein I (mCRBPI) promoter. *EMBO J,* 10**,** 2223-30.

SMUKLER, S. R., RUNCIMAN, S. B., XU, S. B. & VAN DER KOOY, D. 2006. Embryonic stem cells assume a primitive neural stem cell fate in the absence of extrinsic influences. *Journal of Cell Biology,* 172**,** 79-90.

SOLTER, D. 2006. From teratocarcinomas to embryonic stem cells and beyond: a history of embryonic stem cell research. *Nat Rev Genet,* 7**,** 319-27.

SOLTER, D., SKREB, N. & DAMJANOV, I. 1970. Extrauterine growth of mouse egg-cylinders results in malignant teratoma. *Nature,* 227**,** 503-4.

SONNTAG, K. C., SIMANTOV, R., BJORKLUND, L., COOPER, O., PRUSZAK, J., KOWALKE, F., GILMARTIN, J., DING, J. X., HU, Y. P., SHEN, M. M. & ISACSON, O. 2005. Context-dependent neuronal differentiation and germ layer induction of Smad4(-/-) and Cripto(-/-) embryonic stem cells. *Molecular and Cellular Neuroscience,* 28**,** 417-429.

SOPRANO, D. R. & SOPRANO, K. J. 1995. Retinoids as teratogens. *Annu Rev Nutr,* 15**,** 111-32.

SOUSA, V. H. & FISHELL, G. 2010. Sonic hedgehog functions through dynamic changes in temporal competence in the developing forebrain. *Current Opinion in Genetics & Development,* 20**,** 391-399.

SPEMANN, H. & MANGOLD, H. 1924. The induction of embryonic predispositions by implantation of organizers foreign to the species. *Archiv Fur Mikroskopische Anatomie Und Entwicklungsmechanik,* 100**,** 599-638.

STAHL, N., FARRUGGELLA, T. J., BOULTON, T. G., ZHONG, Z., DARNELL, J. E., JR. & YANCOPOULOS, G. D. 1995. Choice of STATs and other substrates specified by modular tyrosine-based motifs in cytokine receptors. *Science,* 267**,** 1349-53.

STAVRIDIS, M. P., COLLINS, B. J. & STOREY, K. G. 2010. Retinoic acid orchestrates fibroblast growth factor signalling to drive embryonic stem cell differentiation. *Development,* 137**,** 881-890.

STAVRIDIS, M. P., LUNN, J. S., COLLINS, B. J. & STOREY, K. G. 2007. A discrete period of FGF-induced Erk1/2 signalling is required for vertebrate neural specification. *Development,* 134**,** 2889-2894.

STEMPLE, D. L. & ANDERSON, D. J. 1992. ISOLATION OF A STEM-CELL FOR NEURONS AND GLIA FROM THE MAMMALIAN NEURAL CREST. *Cell,* 71**,** 973-985.

STENMAN, J. M., WANG, B. & CAMPBELL, K. 2003. Tlx controls proliferation and patterning of lateral telencephalic progenitor domains. *Journal of Neuroscience,* 23**,** 10568-10576.

STEVENS, L. C. 1970. The development of transplantable teratocarcinomas from intratesticular grafts of pre- and postimplantation mouse embryos. *Dev Biol,* 21**,** 364-82.

STEWART, C. L., KASPAR, P., BRUNET, L. J., BHATT, H., GADI, I., KONTGEN, F. & ABBONDANZO, S. J. 1992. Blastocyst implantation depends on maternal expression of leukaemia inhibitory factor. *Nature,* 359**,** 76-9.

STOJKOVIC, M., LAKO, M., STRACHAN, T. & MURDOCH, A. 2004. Derivation, growth and applications of human embryonic stem cells. *Reproduction,* 128**,** 259-67.

STONE, D. M., HYNES, M., ARMANINI, M., SWANSON, T. A., GU, Q. M., JOHNSON, R. L., SCOTT, M. P., PENNICA, D., GODDARD, A., PHILLIPS, H., NOLL, M., HOOPER, J. E., DESAUVAGE, F. & ROSENTHAL, A. 1996. The tumour-suppressor gene patched encodes a candidate receptor for Sonic hedgehog. *Nature,* 384**,** 129-134.

STOYKOVA, A. & GRUSS, P. 1994. Roles of Pax-genes in developing and adult brain as suggested by expression patterns. *J Neurosci,* 14**,** 1395-412.

STRUBING, C., AHNERTHILGER, G., SHAN, J., WIEDENMANN, B., HESCHELER, J. & WOBUS, A. M. 1995. Differentiation of pluripotent embryonic stem-cells into the neuronal lineage in-vitro gives rise to mature inhibitory and excitatory neurons *Mechanisms of Development,* 53**,** 275-287.

STUDER, M., GAVALAS, A., MARSHALL, H., ARIZA-MCNAUGHTON, L., RIJLI, F. M., CHAMBON, P. & KRUMLAUF, R. 1998. Genetic interactions between Hoxa1 and Hoxb1 reveal new roles in regulation of early hindbrain patterning. *Development,* 125**,** 1025-1036.

STUHLMILLER, T. J. & GARCIA-CASTRO, M. I. 2012. Current perspectives of the signaling pathways directing neural crest induction. *Cellular and Molecular Life Sciences,* [Epub ahead of print].

STUHMER, T., ANDERSON, S. A., EKKER, M. & RUBENSTEIN, J. L. R. 2002. Ectopic expression of the Dlx genes induces glutamic acid decarboxylase and Dlx expression. *Development,* 129**,** 245-252.

SUDA, Y., KOKURA, K., KIMURA, J., KAJIKAWA, E., INOUE, F. & AIZAWA, S. 2010. The same enhancer regulates the earliest Emx2 expression in caudal forebrain primordium, subsequent expression in dorsal telencephalon and later expression in the cortical ventricular zone. *Development,* 137**,** 2939-49.

SUN, Y., GODERIE, S. K. & TEMPLE, S. 2005. Asymmetric distribution of EGFR receptor during mitosis generates diverse CNS progenitor cells. *Neuron,* 45**,** 873-86.

SUSSEL, L., MARIN, O., KIMURA, S. & RUBENSTEIN, J. L. R. 1999. Loss of Nkx2.1 homeobox gene function results in a ventral to dorsal molecular respecification within the basal telencephalon: evidence for a transformation of the pallidum into the striatum. *Development,* 126**,** 3359-3370.

SUZUKI, A., RAYA, A., KAWAKAMI, Y., MORITA, M., MATSUI, T., NAKASHIMA, K., GAGE, F. H., RODRIGUEZ-ESTEBAN, C. & IZPISUA BELMONTE, J. C. 2006. Nanog binds to Smad1 and blocks bone morphogenetic protein-induced differentiation of embryonic stem cells. *Proc Natl Acad Sci U S A,* 103**,** 10294-9.

SWINDELL, E. C., THALLER, C., SOCKANATHAN, S., PETKOVICH, M., JESSELL, T. M. & EICHELE, G. 1999. Complementary domains of retinoic acid production and degradation in the early chick embryo. *Dev Biol,* 216**,** 282-96.

TAIPALE, J., COOPER, M. K., MAITI, T. & BEACHY, P. A. 2002. Patched acts catalytically to suppress the activity of Smoothened. *Nature,* 418**,** 892-7.

TAKAHASHI, K., TANABE, K., OHNUKI, M., NARITA, M., ICHISAKA, T., TOMODA, K. & YAMANAKA, S. 2007. Induction of pluripotent stem cells from adult human fibroblasts by defined factors. *Cell,* 131**,** 861-872.

TAKAHASHI, K. & YAMANAKA, S. 2006. Induction of pluripotent stem cells from mouse embryonic and adult fibroblast cultures by defined factors. *Cell,* 126**,** 663-76.

TANG, F., BARBACIORU, C., BAO, S., LEE, C., NORDMAN, E., WANG, X., LAO, K. & SURANI, M. A. 2010. Tracing the derivation of embryonic stem cells from the inner cell mass by single-cell RNA-Seq analysis. *Cell Stem Cell,* 6**,** 468-78.

TEMPLE, S. 2001. The development of neural stem cells. *Nature,* 414**,** 112-117.

TEN BERGE, D., KOOLE, W., FUERER, C., FISH, M., EROGLU, E. & NUSSE, R. 2008. Wnt signaling mediates self-organization and axis formation in embryoid bodies. *Cell Stem Cell,* 3**,** 508-18.

TEO, A. K., ARNOLD, S. J., TROTTER, M. W., BROWN, S., ANG, L. T., CHNG, Z., ROBERTSON, E. J., DUNN, N. R. & VALLIER, L. 2011. Pluripotency factors regulate definitive endoderm specification through eomesodermin. *Genes Dev,* 25**,** 238-50.

THOMSON, J. A., ITSKOVITZ-ELDOR, J., SHAPIRO, S. S., WAKNITZ, M. A., SWIERGIEL, J. J., MARSHALL, V. S. & JONES, J. M. 1998. Embryonic stem cell lines derived from human blastocysts. *Science,* 282**,** 1145-1147.

THOMSON, M., LIU, S. J., ZOU, L. N., SMITH, Z., MEISSNER, A. & RAMANATHAN, S. 2011. Pluripotency factors in embryonic stem cells regulate differentiation into germ layers. *Cell,* 145**,** 875-89.

TORESSON, H., MATA DE URQUIZA, A., FAGERSTROM, C., PERLMANN, T. & CAMPBELL, K. 1999. Retinoids are produced by glia in the lateral ganglionic eminence and regulate striatal neuron differentiation. *Development,* 126**,** 1317-26.

TORESSON, H., POTTER, S. S. & CAMPBELL, K. 2000. Genetic control of dorsal-ventral identity in the telencephalon: opposing roles for Pax6 and Gsh2. *Development,* 127**,** 4361-4371.

TROPEPE, V., HITOSHI, S., SIRARD, C., MAK, T. W., ROSSANT, J. & VAN DER KOOY, D. 2001. Direct neural fate specification from embryonic stem cells: A primitive mammalian neural stem cell stage acquired through a default mechanism. *Neuron,* 30**,** 65-78.

TROPEPE, V., SIBILIA, M., CIRUNA, B. G., ROSSANT, T., WAGNER, E. F. & VAN DER KOOY, D. 1999. Distinct neural stem cells proliferate in response to EGF and FGF in the developing mouse telencephalon. *Developmental Biology,* 208**,** 166-188.

VALLIER, L., ALEXANDER, M. & PEDERSEN, R. A. 2005. Activin/Nodal and FGF pathways cooperate to maintain pluripotency of human embryonic stem cells. *Journal of Cell Science,* 118**,** 4495-4509.

VALLIER, L., TOUBOUL, T., BROWN, S., CHO, C., BILICAN, B., ALEXANDER, M., CEDERVALL, J., CHANDRAN, S., AHRLUND-RICHTER, L., WEBER, A. & PEDERSEN, R. A. 2009. Signaling pathways controlling pluripotency and early cell fate decisions of human induced pluripotent stem cells. *Stem Cells,* 27**,** 2655-66.

VAUDRY, D., STORK, P. J., LAZAROVICI, P. & EIDEN, L. E. 2002. Signaling pathways for PC12 cell differentiation: making the right connections. *Science,* 296**,** 1648-1649.

VOGT, J., TRAYNOR, R. & SAPKOTA, G. P. 2011. The specificities of small molecule inhibitors of the TGFss and BMP pathways. *Cell Signal,* 23**,** 1831-42.

VON HOLST, A., EGBERS, U., PROCHIANTZ, A. & FAISSNER, A. 2007. Neural stem/progenitor cells express 20 tenascin C isoforms that are differentially regulated by Pax6. *J Biol Chem,* 282**,** 9172-81.

VON MERING, C. & BASLER, K. 1999. Distinct and regulated activities of human Gli proteins in Drosophila. *Curr Biol,* 9**,** 1319-22.

WACLAW, R. R., WANG, B. & CAMPBELL, K. 2004. The homeobox gene Gsh2 is required for retinoid production in the embryonic mouse telencephalon. *Development,* 131**,** 4013-4020.

WADDINGTON, C. H. 1933. Induction by the primitive streak and its derivatives in the chick *The Journal of Experimental Biology,* 10**,** 38-48.

WADDINGTON, C. H. 1936. Organizers in Mammalian Development. *Nature,* 138**,** 125.

WATANABE, K., KAMIYA, D., NISHIYAMA, A., KATAYAMA, T., NOZAKI, S., KAWASAKI, H., WATANABE, Y., MIZUSEKI, K. & SASAI, Y. 2005. Directed differentiation of telencephalic precursors from embryonic stem cells. *Nature Neuroscience,* 8**,** 288-296.

WATAYA, T., ANDO, S., MUGURUMA, K., IKEDA, H., WATANABE, K., EIRAKU, M., KAWADA, M., TAKAHASHI, J., HASHIMOTO, N. & SASAI, Y. 2008. Minimization of exogenous signals in ES cell culture induces rostral hypothalamic differentiation. *Proceedings of the National Academy of Sciences of the United States of America,* 105**,** 11796-11801.

WENDLING, O., DENNEFELD, C., CHAMBON, P. & MARK, M. 2000. Retinoid signaling is essential for patterning the endoderm of the third and fourth pharyngeal arches. *Development,* 127**,** 1553-62.

WHITE, J. A., GUO, Y. D., BAETZ, K., BECKETT-JONES, B., BONASORO, J., HSU, K. E., DILWORTH, F. J., JONES, G. & PETKOVICH, M. 1996. Identification of the retinoic acid-inducible all-trans-retinoic acid 4-hydroxylase. *J Biol Chem,* 271**,** 29922-7.

WHITE, J. C., HIGHLAND, M., KAISER, M. & CLAGETT-DAME, M. 2000. Vitamin A deficiency results in the dose-dependent acquisition of anterior character and shortening of the caudal hindbrain of the rat embryo. *Dev Biol,* 220**,** 263-84.

WHITE, R. J., NIE, Q., LANDER, A. D. & SCHILLING, T. F. 2007. Complex regulation of cyp26a1 creates a robust retinoic acid gradient in the zebrafish embryo. *Plos Biology,* 5**,** 2522-2533.

WICHTERLE, H., LIEBERAM, I., PORTER, J. A. & JESSELL, T. M. 2002. Directed differentiation of embryonic stem cells into motor neurons. *Cell,* 110**,** 385-397.

WIJGERDE, M., MCMAHON, J. A., RULE, M. & MCMAHON, A. P. 2002. A direct requirement for Hedgehog signaling for normal specification of all ventral progenitor domains in the presumptive mammalian spinal cord. *Genes Dev,* 16**,** 2849-64.

WILES, M. V. & JOHANSSON, B. M. 1999. Embryonic stem cell development in a chemically defined medium. *Experimental Cell Research,* 247**,** 241-248.

WILLIAMS, R. L., HILTON, D. J., PEASE, S., WILLSON, T. A., STEWART, C. L., GEARING, D. P., WAGNER, E. F., METCALF, D., NICOLA, N. A. & GOUGH, N. M. 1988. MYELOID-LEUKEMIA INHIBITORY FACTOR MAINTAINS THE DEVELOPMENTAL POTENTIAL OF EMBRYONIC STEM-CELLS. *Nature,* 336**,** 684-687.

WILSON, L. & MADEN, M. 2005. The mechanisms of dorsoventral patterning in the vertebrate neural tube. *Dev Biol,* 282**,** 1-13.

WILSON, P. A. & HEMMATI-BRIVANLOU, A. 1995. Induction of epidermis and inhibition of neural fate by Bmp-4. *Nature,* 376**,** 331-3.

WILSON, S. I., GRAZIANO, E., HARLAND, R., JESSELL, T. M. & EDLUND, T. 2000. An early requirement for FGF signalling in the acquisition of neural cell fate in the chick embryo. *Current Biology,* 10**,** 421-429.

WILSON, S. W. & RUBENSTEIN, J. L. 2000. Induction and dorsoventral patterning of the telencephalon. *Neuron,* 28**,** 641-651.

WOLPERT, L. 1996. One hundred years of positional information. *Trends Genet,* 12**,** 359-64.

WOZNEY, J. M. & ROSEN, V. 1998. Bone morphogenetic protein and bone morphogenetic protein gene family in bone formation and repair. *Clinical orthopaedics and related research,* 346**,** 26-37.

WU, C. Y., WHYE, D., MASON, R. W. & WANG, W. 2012. Efficient differentiation of mouse embryonic stem cells into motor neurons. *J Vis Exp***,** e3813.

WU, X., DING, S., DING, Q., GRAY, N. S. & SCHULTZ, P. G. 2002. A small molecule with osteogenesis-inducing activity in multipotent mesenchymal progenitor cells. *Journal of American Chemical Society,* 124**,** 14520-14521.

WU, X., WALKER, J., ZHANG, J., DING, S. & SCHULTZ, P. G. 2004. Purmorphamine induces osteogenesis by activation of the hedgehog signaling pathway. *Chemical Biology,* 11**,** 1229-1238.

XU, L., GLASS, C. K. & ROSENFELD, M. G. 1999. Coactivator and corepressor complexes in nuclear receptor function. *Current Opinion in Genetics & Development,* 9**,** 140-147.

XU, Q., WONDERS, C. P. & ANDERSON, S. A. 2005. Sonic hedgehog maintains the identity of cortical interneuron progenitors in the ventral telencephalon. *Development,* 132**,** 4987-4998.

XU, R. H., CHEN, X., LI, D. S., LI, R., ADDICKS, G. C., GLENNON, C., ZWAKA, T. P. & THOMSON, J. A. 2002. BMP4 initiates human embryonic stem cell differentiation to trophoblast. *Nature Biotechnology,* 20**,** 1261-1264.

XU, R. H., SAMPSELL-BARRON, T. L., GU, F., ROOT, S., PECK, R. M., PAN, G., YU, J., ANTOSIEWICZ-BOURGET, J., TIAN, S., STEWART, R. & THOMSON, J. A. 2008. NANOG is a direct target of TGFbeta/activin-mediated SMAD signaling in human ESCs. *Cell Stem Cell,* 3**,** 196-206.

XUAN, S., BAPTISTA, C. A., BALAS, G., TAO, W., SOARES, V. C. & LAI, E. 1995. Winged helix transcription factor BF-1 is essential for the development of the cerebral hemispheres. *Neuron,* 6**,** 1141-1152.

YAO, J., LIU, Y., HUSAIN, J., LO, R., PALAPARTI, A., HENDERSON, J. & STIFANI, S. 1998. Combinatorial expression patterns of individual TLE proteins during cell determination and differentiation suggest non-redundant functions for mammalian homologs of Drosophila Groucho. *Dev Growth Differ,* 40**,** 133-46.

YBOT-GONZALEZ, P., GASTON-MASSUET, C., GIRDLER, G., KLINGENSMITH, J., ARKELL, R., GREENE, N. D. & COPP, A. J. 2007. Neural plate morphogenesis during mouse neurulation is regulated by antagonism of Bmp signalling. *Development,* 134**,** 3203-11.

YING, Q. L., NICHOLS, J., CHAMBERS, I. & SMITH, A. 2003a. BMP induction of Id proteins suppresses differentiation and sustains embryonic stem cell self-renewal in collaboration with STAT3. *Cell,* 115**,** 281-292.

YING, Q. L., STAVRIDIS, M., GRIFFITHS, D., LI, M. & SMITH, A. 2003b. Conversion of embryonic stem cells into neuroectodermal precursors in adherent monoculture. *Nature Biotechnology,* 21**,** 183-186.

YING, Q. L., WRAY, J., NICHOLS, J., BATLLE-MORERA, L., DOBLE, B., WOODGETT, J., COHEN, P. & SMITH, A. 2008. The ground state of embryonic stem cell self-renewal. *Nature,* 453**,** 519-U5.

YU, P. B., HONG, C. C., SACHIDANANDAN, C., BABITT, J. L., DENG, D. Y., HOYNG, S. A., LIN, H. Y., BLOCH, K. D. & PETERSON, R. T. 2008. Dorsomorphin inhibits BMP signals required for embryogenesis and iron metabolism. *Nat Chem Biol. ,* 4**,** 33-41.

YUAN, H., CORBI, N., BASILICO, C. & DAILEY, L. 1995. Developmental-specific activity of the FGF-4 enhancer requires the synergistic action of Sox2 and Oct-3. *Genes Dev,* 9**,** 2635-45.

YUN, K., POTTER, S. & RUBENSTEIN, J. L. R. 2001. Gsh2 and Pax6 play complementary roles in dorsoventral patterning of the mammalian telencephalon. *Development,* 128**,** 193-205.

ZHAO, Q., EBERSPAECHER, H., LEFEBVRE, V. & DECROMBRUGGHE, B. 1997. Parallel expression of Sox9 and Col2a1 in cells undergoing chondrogenesis. *Developmental Dynamics,* 209**,** 377-386.

ZHAO, S., NICHOLS, J., SMITH, A. G. & LI, M. 2004. SoxB transcription factors specify neuroectodermal lineage choice in ES cells. *Molecular and Cellular Neuroscience,* 27**,** 332-342.

ZHOU, G. C., MYERS, R., LI, Y., CHEN, Y. L., SHEN, X. L., FENYK-MELODY, J., WU, M., VENTRE, J., DOEBBER, T., FUJII, N., MUSI, N., HIRSHMAN, M. F., GOODYEAR, L. J. & MOLLER, D. E. 2001. Role of AMP-activated protein kinase in mechanism of metformin action. *Journal of Clinical Investigation,* 108**,** 1167-1174.

ZHUANG, Y., KIM, C. G., BARTELMEZ, S., CHENG, P., GROUDINE, M. & WEINTRAUB, H. 1992. Helix-loop-helix transcription factors E12 and E47 are not essential for skeletal or cardiac myogenesis, erythropoiesis, chondrogenesis, or neurogenesis. *Proc Natl Acad Sci U S A,* 89**,** 12132-6.

ZIETLOW, R., PRECIOUS, S. V., KELLY, C. M., DUNNETT, S. B. & ROSSER, A. E. 2012. Long-term expansion of human foetal neural progenitors leads to reduced graft viability in the neonatal rat brain. *Exp Neurol,* 235**,** 563-73.